

A PILOT STUDY ASSESSING FENTANYL DOSE REQUIREMENTS IN OPIOID-MAINTAINED INDIVIDUALS

Muhammad Imran Ahmad

Discipline of Pharmacology
School of Medical Sciences, Faculty of Health Sciences
The University of Adelaide
Australia

March 2014

A thesis submitted for the degree of Master of Philosophy at The University of Adelaide

ABSTRACT

Pain is poorly managed in the opioid-maintained population. This study aimed to find safe and efficacious doses of fentanyl for acute pain management in the opioid-tolerant using experimental pain models and link that with the baseline morphine equivalent daily dose that the patients were taking. 9 patients were enrolled in the study from the Pain Management Unit at the Royal Adelaide Hospital. The study was an open label study using an infusion pump and STANPUMP software to rapidly achieve constant estimated effect compartment fentanyl concentrations. Fentanyl effect site concentrations of 2, 4, 6 and 8 ng/ml were targeted for the first visit and 4, 8, 12 and 16 ng/ml were targeted for patients on the second visit. The infusion involved four infusion steps lasting for 30 minutes each and during each step pharmacodynamic measures were taken that consisted of electroencephalography (EEG), saccadic eye movement test (SEM), pupillometry, morphine-benzedrine group scale (MBG) and cold pain test. The subjective opioid withdrawal scale tests (SOWS) were conducted once the infusion was stopped. Using PK/PD modelling techniques within R, the concentration-effect relationships were described using zero slope, linear, E_{max} and Sigmoid E_{max} models. Our study was not able to demonstrate that the baseline morphine equivalent daily dose predicted suitable doses of fentanyl in acute pain management of the opioid-tolerant. This was probably due to the fact that the study was of insufficient sample size to detect the effect of the covariate. However, we have demonstrated that the study design was safe, informative and suitable for it to be replicated with a larger number of subjects in the future.

DECLARATION

I certify that this work contains no material which has been accepted for the award of any other degree or diploma in any university or other tertiary institution and, to the best of my knowledge and belief, contains no material previously published or written by another person, except where due reference has been made in the text.

I give consent to this copy of my thesis, when deposited in the University Library, being made available for loan and photocopying, subject to the provisions of the Copyright Act 1968.

I also give permission for the digital version of my thesis to be made available on the web, via the University's digital research repository, the Library catalogue and also through web search engines, unless permission has been granted by the University to restrict access for a period of time.

Muhammad Imran Ahmad

3 March 2014

ACKNOWLEDGEMENTS

I would like to sincerely thank my primary supervisor, Professor Paul Rolan for introducing me to the world of pharmacokinetics and pharmacodynamics. I would also like to thank Professor Richard Upton for 'inducing' me into the world of PK PD modeling. Many thanks to both of them for the guidance and support over the years.

I would like to thank Associate Professor Pamela Macintyre for her supervision during the initial years of the project and for her very helpful comments on the clinical study design.

I am indebted to the dean and management at The Royal College of Medicine Perak in Malaysia for having provided me with a paid leave to undertake this study.

I am very grateful to all staff at PARC especially Francesca Zappia and Melanie Gentgall for their guidance in ensuring the smooth-running of this study.

The recruitment for this study would have not been able to run successfully without the help of Jane Agadilis and the consultants at the Pain Management Unit of the Royal Adelaide Hospital.

I wish to thank the past and present postgraduate students and staff at the Discipline of Pharmacology especially to Jacinta Johnson, Dr Mark Hutchinson, Lauren Nicotra, Dr Liang Liu, Dr Peter Grace, Dr Daniel Barratt and Gordon Crabb for all the knowledge, skills and assistances that they have provided. I would like to thank Dr Justin Hay, Rens Batist and other staff from the CHDR, Leiden who have answered my questions about using the Neurocart over the years. I am also thankful to Dr Dylan DeLosAngeles from Flinders Medical Center and Jennifer Le Mottée from the Department of Clinical Neurophysiology, Royal Adelaide Hospital for giving me very useful insights into running the EEG. I also thank Mick Draper, Lucy Zuzolo, Brigitte Sloom and Helen Foster for teaching me better techniques to use Pubmed, Endnote and Microsoft Word.

Most importantly, I would like to thank my family and friends especially my wife, Najwa for her love and support during the entire research journey.

ABBREVIATIONS

μ	mu
μV	microvolt
δ	delta
κ	kappa
5-HT	serotonin
AC	adenylyl cyclase
AIC	Akaike information criteria
Arr3	arrestin 3
BID	twice a day
cAMP	cyclic adenosine monophosphate
CCK	cholecystokinin
CGRP	calcitonin gene-related peptide
CIP	Compact Integrated Pupillograph
COX	cyclooxygenase
CREB	cyclic adenosine monophosphate response element-binding protein
C_{target}	target effect site concentration
CV	coefficient of variation
ECG	electrocardiogram
EC_{50}	concentration at which half the maximum effect was achieved
EEG	electroencephalography
E_{max}	maximum effect
ERK	extracellular signal-regulated kinases
Fz	frontal
Cz	central
GABA	gamma-aminobutyric acid
GCP	Good Clinical Practice

GDP	guanosine diphosphate
GPCR	G protein-coupled receptors
GRK	G protein-coupled receptor kinase
GTP	guanosine triphosphate
Ht	height
ICH	International Conference on Harmonisation
IL-1 β	interleukin-1 β
IL-6	interleukin-6
MBG	Morphine-Benzedrine Group scale
MEDD	morphine-equivalent daily dose
min	minute
mm	millimetre
MOR	μ -opioid receptor
ng/ml	nanograms per millilitre
NK-1	neurokinin-1
NMDA	N-methyl-D-aspartate
NOP	nociceptin/orphanin FQ peptide receptor
OIH	opioid-induced hyperalgesia
Oz	occipital
PARC	Pain and Anaesthesia Research Clinic
PD	pharmacodynamics
PK	pharmacokinetics
Pz	parietal
QD	once a day
RVM	rostral ventral medulla
SEM	saccadic eye movement test
SOWS	subjective opioid withdrawal scale
SSRI	selective serotonin reuptake inhibitor

TID	three times a day
TLR	toll-like receptor
TRPV1	transient receptor potential vanilloid-1
VPC	visual predictive check
VLow	very low
Wt	weight

Table of Contents

ABSTRACT.....	2
DECLARATION	3
ACKNOWLEDGEMENTS	4
ABBREVIATIONS	5
LIST OF TABLES	12
LIST OF FIGURES	14
1 INTRODUCTION	16
1.1 Pain.....	16
1.2 Opioids	16
1.2.1 History and basic definitions.....	18
1.2.2 Opioid structures and pharmacokinetic data	18
1.2.3 Opioid receptor physiology.....	22
1.3 Mechanisms of Opioid-Induced Tolerance and Hyperalgesia	25
1.3.1 Tolerance and Hyperalgesia.....	25
1.3.2 Mechanisms underlying tolerance and hyperalgesia	27
1.3.3 Clinical dimensions of tolerance	32
1.4 Epidemiology of opioid use.....	33
1.5 Managing pain in the opioid-maintained.....	35
1.5.1 Concentration-targeted approach	35
1.5.2 Pharmacodynamic targeted approach.....	38
1.6 Current recommendations on the management of acute pain in the opioid-tolerant	40
1.7 Pharmacokinetic/pharmacodynamic (PK/PD) modeling	42
1.8 Measuring the Pharmacodynamic Effects of Opioids.....	44
1.8.1 EEG (Electroencephalography).....	44
1.8.2 SEM (Saccadic Eye Movement)	44
1.8.3 Pupillometry.....	44
1.8.4 Cold pain test	44
1.8.5 Subjective measures of opioid effect and withdrawal.....	44
1.9 Rationale for the study.....	45
2 STUDY DESIGN AND EXPERIMENTAL METHODS	46
2.1 Aim	46
2.2 Hypothesis.....	46
2.3 Ethics	46

2.4 Participants	46
2.4.1 Inclusion criteria.....	46
2.4.2 Exclusion criteria	46
2.4.3 Withdrawal criteria	47
2.4.4 Recruitment	49
2.4.5 Subjects who did not proceed or withdrew from the study.....	50
2.5 Study plan and design overview	51
2.6 Screening.....	51
2.7 Familiarisation session	52
2.8 Requirements Prior To Study Day	52
2.9 Requirements after Discharge on the Study Day.....	52
2.10 Testing Day Schedule	52
2.11 Pharmacokinetic parameters.....	54
2.12 Methods	55
2.12.1 Clinical conduct	55
2.12.2 EEG (Electroencephalography) and SEM (Saccadic Eye Movement).....	55
2.12.3 Pupillometry.....	57
2.12.4 Cold pain test	59
2.12.5 Subjective measures of opioid effect and withdrawal.....	61
2.12.6 Physiologic and Adverse Event Measures.....	61
2.12.7 Adverse effect monitoring	61
2.12.8 Sedation measurement.....	61
2.12.9 General modelling methods.....	62
2.12.10 Model development strategy.....	62
2.12.11 Pharmacodynamic models	63
3 RESULTS.....	69
3.1 Demography.....	69
3.2 Safety.....	70
3.3 Technical issues.....	70
3.4 Effects of fentanyl in the opioid-tolerant.....	71
3.4.1 EEG effects	71
3.4.2 Saccadic peak velocity.....	78
3.4.3 Saccadic latency	79
3.4.4 Pupillometry.....	80
3.4.5 Morphine-Benzedrine Group (MBG) Scale	81

3.4.6 Pain threshold	82
3.4.7 Pain tolerance	83
3.4.8 Subjective Opioid Withdrawal Scale (SOWS)	85
3.4.9 Sedation score.....	87
3.4.10 Nausea.....	88
3.5 Pharmacodynamics	89
3.5.1 Best model for very low frequency at Pz-Oz.....	89
3.5.2 Best model for very low frequency at Fz-Cz.....	90
3.5.3 Best model for delta Pz-Oz.....	92
3.5.4 Best model for delta Fz-Cz	93
3.5.5 Best model for theta Pz-Oz	94
3.5.6 Best model for theta Fz-Cz	95
3.5.7 Best model for alpha Pz-Oz	96
3.5.8 Best model for alpha Fz-Cz.....	96
3.5.9 Best model for beta Pz-Oz.....	96
3.5.10 Best model for beta Fz-Cz	96
3.5.11 Best model for gamma Pz-Oz.....	96
3.5.12 Best model for gamma Fz-Cz.....	97
3.5.13 Best model for average saccadic peak velocity.....	98
3.5.14 Best model for saccadic latency.....	99
3.5.15 Best model for saccadic inaccuracy	100
3.5.16 Best model for number of valid saccades	100
3.5.17 Best model for pupillometry	100
3.5.18 Best model for Morphine-Benzedrine Group (MBG) Scale.....	101
3.5.19 Best model for cold pain threshold.....	102
3.5.20 Best model for cold pain tolerance.....	102
3.5.21 Best model for Subjective Opioid Withdrawal Scale	103
4 DISCUSSION	105
4.1 Safety and Dosing.....	105
4.2 Recruitment	105
4.3 Assessment of opioid effects	105
4.4 Electroencephalography	107
4.5 Saccadic eye movement tests	108
4.6 Pupillometry.....	108
4.7 Cold pain test	109

4.8 Subjective measures of opioid effect and withdrawal.....	109
4.9 Covariate effect of MEDD on the models	109
4.10 Study Design and Implementation.....	109
4.11 Subject Selection	110
4.12 Pharmacodynamic study	110
4.13 Summary of research findings	110
4.14 Clinical implications of research findings.....	110
4.14.1 Directions for future research.....	111
5 REFERENCES	112
6 APPENDICES	121
6.1 Top models for the pharmacodynamic measures	121
6.2 Morphine Bensedrine Group Scale	142
6.3 Subjective Opioid Withdrawal Scale	143
6.4 Effects of fentanyl in the opioid-tolerant.....	144
6.5 Fentanyl doses, STANPUMP and Harvard pump 22.....	157
6.5.1 STANPUMP and Harvard pump 22.....	157
6.5.2 Fentanyl doses delivered by the STANPUMP.....	157
6.5.3 Discharge of patients	163
6.6 Relationship between plasma and effect site concentration of fentanyl.....	164

LIST OF TABLES

Table 1 Acute adverse effects of opioids	16
Table 2 Additional adverse effects of opioids with chronic use	17
Table 3 Chemical structure of phenanthrenes.....	18
Table 4 Chemical structure of benzomorphans	20
Table 5 Chemical structure of phenylpiperidines	20
Table 6 Chemical structure of diphenylheptanes	21
Table 7 Comparative pharmacokinetic data of various opioids	21
Table 8 Main opioid receptors	22
Table 9 Main opioids prescribed or supplied.....	33
Table 10 References in the literature with regards to managing pain in the opioid-tolerant.....	40
Table 11 Opioid equianalgesic doses	47
Table 12 Five half-lives of various benzodiazepines	47
Table 13 Reasons for seemingly eligible patients to not proceed to the screening stage	50
Table 14 Pharmacokinetic parameters for the fentanyl infusions.....	54
Table 15 The Royal Adelaide Hospital Sedation Score.....	61
Table 16 Linear additive models	63
Table 17 Linear proportional models.....	64
Table 18 Description of tested models for zero slope model	64
Table 19 E_{max} additive models	65
Table 20 E_{max} proportional models.....	66
Table 21 Sigmoid E_{max} additive models.....	67
Table 22 Sigmoid E_{max} proportional models.....	68
Table 23 Demographic and dosing details	69
Table 24 Sedation score readings for subject 002 during her first visit.....	87
Table 25 Sedation score readings for subject 003 during her first visit.....	87
Table 26 Sedation score readings for subject 004 during his first visit.....	87
Table 27 Sedation score readings for subject 009 during her first visit.....	87
Table 28 Sedation score readings for subject 007 during his second visit	88
Table 29 Summary of model parameters for LinearProp4 model and very low Pz-Oz.....	90
Table 30 Summary of model parameters for LinearAdd2 and very low Fz-Cz.....	91
Table 31 Summary of model parameters for LinearProp4 and delta Pz-Oz.	92
Table 32 Summary of model parameters for LinearProp2 and delta Fz-Cz.	93
Table 33 Summary of model parameters for LinearProp2 and theta Pz-Oz.....	94
Table 34 Summary of model parameters for LinearProp4 and theta Fz-Cz.....	95
Table 35 Summary of model parameters for LinearProp4 and gamma Pz-Oz.	97
Table 36 Summary of model parameters for Zero3 and saccadic peak velocity.	98
Table 37 Summary of model parameters for Zero1 and saccadic latency.....	99
Table 38 Summary of model parameters for SigmoidEmaxProp1 and pupillometry.	101
Table 39 Summary of model parameters for Zero3 and MBG scale.....	102
Table 40 Summary of model parameters for LinearProp4 and cold pain tolerance.	103
Table 41 Summary of model parameters for LinearProp2 and SOWS.....	104
Table 42 Commonly used acute models of pain in opioid studies	106
Table 43 Models inducing hyperalgesia that are commonly employed in opioid studies.....	106
Table 44 Best models for very low frequency band at Pz-Oz	121
Muhammad Imran Ahmad, MPhil Thesis, 2014	12

Table 45 Best models for very low band at Fz-Cz	122
Table 46 Best models for Delta Pz-Oz	123
Table 47 Best models for Delta Fz-Cz	124
Table 48 Best models for Theta Pz-Oz	125
Table 49 Best models for Theta Fz-Cz	126
Table 50 Best models for Alpha Pz-Oz	127
Table 51 Best models for Alpha Fz-Cz	128
Table 52 Best models for Beta Pz-Oz	129
Table 53 Best models for Beta Fz-Cz	130
Table 54 Best models for Gamma Pz-Oz	131
Table 55 Best models for Gamma Fz-Cz	132
Table 56 Best models for average saccadic peak velocity	133
Table 57 Best models for saccadic latency	134
Table 58 Best models for saccadic inaccuracy	135
Table 59 Best models for number of valid saccades	136
Table 60 Best models for pupillometry	137
Table 61 Best models for Morphine-Benzedrine Group (MBG) scale	138
Table 62 Best models for pain threshold	139
Table 63 Best models for pain tolerance	140
Table 64 Best models for Subjective Opioid Withdrawal Scale	141

LIST OF FIGURES

Figure 1 Structure of opioid receptors.....	23
Figure 2 A simplified representations of the processes involved following μ -opioid receptor activation.....	24
Figure 3 Tolerance is expressed by right-shift of the concentration versus effect relationship.	25
Figure 4 Hyperalgesia is reflected by a down-ward shift of the concentration versus effect relationship.	26
Figure 5 Morphine sulphate administration in the methadone groups.	37
Figure 6 Morphine sulphate administration in the control group.....	37
Figure 7 The relationship between plasma oxycodone and analgesia for thermal pain in the skin	42
Figure 8 A flowchart summarizing the recruitment process.	49
Figure 9 Study design	53
Figure 10 Graph showing average power in very low frequency EEG band at Pz-Oz	71
Figure 11 Average power at very low EEG band versus target effect site concentration of fentanyl..	72
Figure 12 Average power at delta Pz-Oz versus target effect site concentration of fentanyl.....	73
Figure 13 Average power of delta at Fz-Cz versus target effect site concentration of fentanyl.	74
Figure 14 Average power of theta at Pz-Oz versus target effect site concentration of fentanyl.	75
Figure 15 Average power of theta at Fz-Cz versus target effect site concentration of fentanyl.....	76
Figure 16 Average power of gamma at Pz-Oz versus target effect site concentration of fentanyl.....	77
Figure 17 The average saccadic peak velocity versus target effect site concentration of fentanyl.	78
Figure 18 Average saccadic latency versus target effect site concentration of fentanyl.	79
Figure 19 Plot of pupil size versus target effect site concentration of fentanyl.....	80
Figure 20 Morphine-Benzedrine Group (MBG) Scale versus target effect site concentration of fentanyl.	81
Figure 21 Pain threshold to cold pain test versus target effect site concentration of fentanyl.	82
Figure 22 Plot of cold pain tolerance versus time.....	83
Figure 23 Plot of cold pain tolerance versus target effect site concentration of fentanyl.	84
Figure 24 Plot of Subjective Opioid Withdrawal Scale versus time.	85
Figure 25 Plot of Subjective Opioid Withdrawal Scale versus target effect site concentration of fentanyl.	86
Figure 26 Visual predictive check for LinearProp4 model and very low Pz-Oz.....	89
Figure 27 The visual predictive check for LinearAdd2 and very low Fz-Cz.	91
Figure 28 The visual predictive check for LinearProp4 and delta Pz-Oz.....	92
Figure 29 The visual predictive check for LinearProp2 and delta Fz-Cz.....	93
Figure 30 The visual predictive check for LinearProp2 and theta Pz-Oz.....	94
Figure 31 The visual predictive check for LinearProp4 and theta Fz-Cz.	95
Figure 32 The visual predictive check for LinearProp4 and gamma Pz-Oz.	97
Figure 33 The visual predictive check for Zero3 and saccadic peak velocity.	98
Figure 34 The visual predictive check for Zero1 and saccadic latency.	99
Figure 35 The visual predictive check for SigmoidEmaxProp1 and pupillometry.....	100
Figure 36 The visual predictive check for Zero3 and MBG scale.	101
Figure 37 The visual predictive check for LinearProp4 and cold pain tolerance.	103
Figure 38 The visual predictive check for LinearProp2 and SOWS.	104
Figure 39 Graph showing average power in very low frequency band at Pz-Oz.....	144
Figure 40 Graph showing average power in very low band at Fz-Cz	144

Figure 41 Average power at delta Pz-Oz versus time.	145
Figure 42 Average power of delta at Fz-Cz versus time.....	145
Figure 43 Average power of theta at Pz-Oz versus time.....	146
Figure 44 Average power of theta at Fz-Cz versus time.	146
Figure 45 Average power of alpha at Pz-Oz versus time.	147
Figure 46 Average power of alpha at Pz-Oz versus target effect site concentration of fentanyl.....	147
Figure 47 Average power of alpha at Fz-Cz versus time.	148
Figure 48 Average power of alpha at Fz-Cz versus target effect site concentration of fentanyl.....	148
Figure 49 Average power of beta at Pz-Oz versus time.....	149
Figure 50 Average power of beta at Pz-Oz versus target effect site concentration of fentanyl.	149
Figure 51 Average power of beta at Fz-Cz versus time.....	150
Figure 52 Average power of beta at Fz-Cz versus target effect site concentration of fentanyl.	150
Figure 53 Average power of gamma at Pz-Oz versus time.	151
Figure 54 Average power of gamma at Fz-Cz versus time.....	151
Figure 55 Average power of gamma at Fz-Cz versus target effect site concentration of fentanyl.	152
Figure 56 Average saccadic peak velocity versus time	152
Figure 57 Average saccadic latency versus time.....	153
Figure 58 The average saccadic inaccuracy versus time.....	153
Figure 59 Average saccadic inaccuracy versus target effect site concentration of fentanyl.....	154
Figure 60 Number of valid saccades versus time.....	154
Figure 61 Number of valid saccades versus target effect site concentration of fentanyl.	155
Figure 62 Pupil size versus time.....	155
Figure 63 Morphine-Benzedrine Group (MBG) Scale versus time.....	156
Figure 64 Pain threshold to cold pain test versus time.....	156

1 INTRODUCTION

1.1 Pain

Pain is defined by the International Association for the Study of Pain (IASP) as “an unpleasant sensory and emotional experience associated with actual or potential tissue damage, or described in terms of such damage” (1). Pain has sensory, affective and motor components (2). Pain can be nociceptive, inflammatory or neuropathic in nature. Pain is a condition which is distressing and demotivating and can negatively impact on a person’s quality of life and productivity. It is important for health professionals to manage pain effectively.

Pain can be divided according to its duration into acute and chronic pain. Acute pain usually occurs in response to acute tissue injury. It is usually self-resolving as injury heals. Pain may become chronic either due to persisting nociceptive input as in rheumatoid arthritis or in some patients, it may persist beyond the time of healing of an injury. It is currently believed that acute pain and chronic pain are not truly distinct entities but rather a continuum of a single disease manifestation (3).

Chronic pain management may involve psychological approaches, life style changes, education and exercise. However, the principal treatment modality for many patients will be pharmacotherapy. There are various classes of drugs commonly used for pain relief. For mild pain, paracetamol and non-steroidal anti-inflammatory drugs (NSAIDs) are the usual drugs of choice. For moderate to severe pain, there are often limited treatment options. Opioids are widely used for the management of acute and chronic moderate to severe pain.

1.2 Opioids

Opioids are the current gold standard therapy for the treatment of acute pain. Opioids exert their effects by binding to the μ , δ and κ receptors in the central nervous system (CNS) and in the periphery. The opioids produce a range of effects and despite their effectiveness; their use is accompanied by a wide array of adverse effects (Table 1).

Table 1 Acute adverse effects of opioids (4-8)

Nervous system	Drowsiness, euphoria, mental clouding, nausea, respiratory depression and reduced body temperature
Cardiovascular system	Orthostatic hypotension
Respiratory system	Reduced respiratory rate and depth, cough reflex suppression
Gastrointestinal system	Constipation, increase in tone of bile duct muscle and outlets of stomach and small intestine , and loss of appetite (partially CNS)
Urinary system	Urinary retention
Endocrine system	Reduced secretion of the adrenal (cortisol), thyroid and sex hormones. Increased prolactin secretion
Immunological system	Inhibition of antibody and cellular responses. Inhibition of natural killer cell activity, cytokine expression, and phagocytic activity
Musculoskeletal system	Muscular rigidity and myoclonus

Prolonged continuous use or frequent repeated use or abuse of the drug can lead to prolongation and exaggeration of the acute effects of opioids. Adverse effects of chronic opioid use are summarized below:

Table 2 Additional adverse effects of opioids with chronic use

Nervous system	Memory impairment, mental slowing, tolerance and dependence
Gastrointestinal system	Weight changes and chronic constipation.
Endocrine system	Decreased bone density, reduced libido, and impaired sexual performance
Social	Addiction
Miscellaneous	Chronic fatigue and lethargy

1.2.1 History and basic definitions

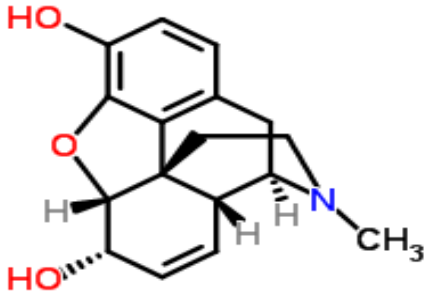
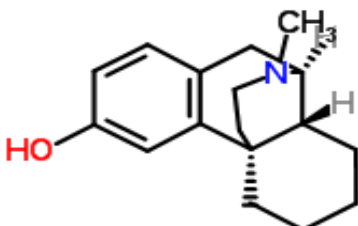

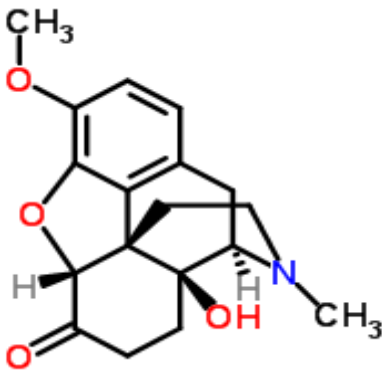
Opium is the latex excreted when an incision is made on the green capsule of *Papaver somniferum* (poppy plant) (7, 8). The main alkaloids extracted from opium are codeine, morphine, thebaine and oripavine (8). As early as 3400 BC in Mesopotamia, the opium poppy was cultivated (6). Opium was introduced to the Orient by Arab traders and it was used for treatment of dysentery (7). In 1806, Frederich Serturmer, a pharmacist's assistant isolated a pure substance from opium which he named morphine (7).

Opium contains a mixture of alkaloids from poppy seed (6). The term "opiates" refers to naturally occurring alkaloids such as morphine and codeine (6). "Opioid" is a broader term that is employed to describe all compounds that act as opioid receptor agonists (6). The term "narcotic" was once used to describe opioids but currently it is a legal term to describe drugs that are being abused (6).

1.2.2 Opioid structures and pharmacokinetic data

Morphine, the prototypical opioid consists of a benzene ring with a phenolic hydroxyl group at position 3 and an alcohol hydroxyl group at position 6 with a methyl group at the nitrogen atom (6). The hydroxyl groups at position 3 and position 6 can both be transformed to esters or ethers (6). For example, morphine that is O-methylated at position 3 becomes codeine (6) and if it is acetylated at position 3 and 6 it becomes heroin (8). There are four chemical classes of opioids:

Table 3 Chemical structure of phenanthrenes

Phenanthrenes	
Morphine 	Levorphanol 
Codeine 	Oxycodone 

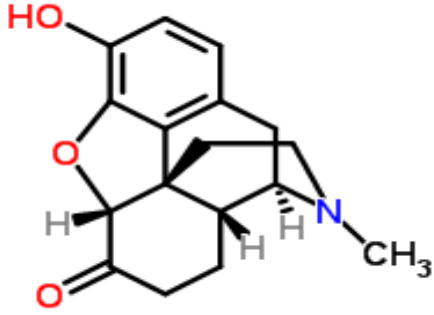
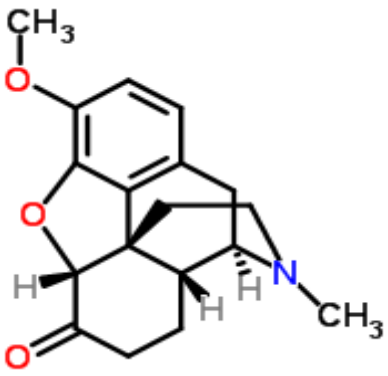
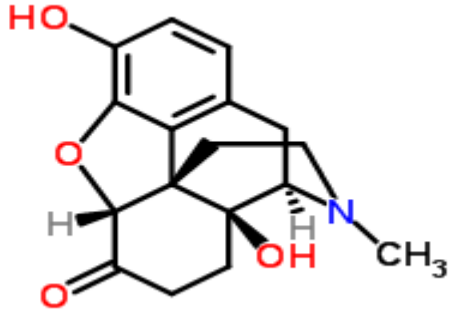
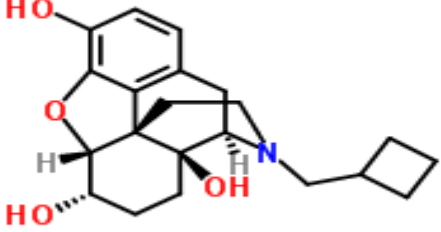
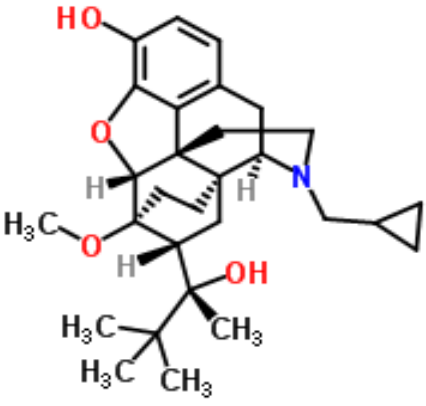
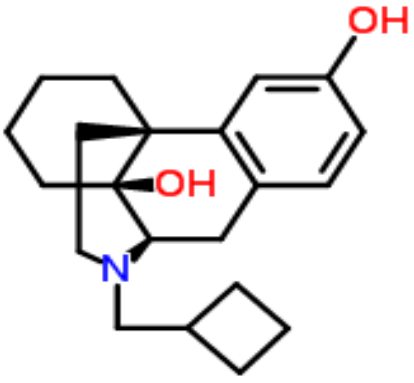
<p>Hydromorphone</p>  <p>The structure shows the morphine skeleton with a hydroxyl group (HO) at the 3-position and a methyl group (CH₃) on the nitrogen atom.</p>	<p>Hydrocodone</p>  <p>The structure shows the morphine skeleton with a methoxy group (CH₃O) at the 3-position and a methyl group (CH₃) on the nitrogen atom.</p>
<p>Oxymorphone</p>  <p>The structure shows the morphine skeleton with hydroxyl groups (HO) at the 3 and 6 positions and a methyl group (CH₃) on the nitrogen atom.</p>	<p>Nalbuphine</p>  <p>The structure shows the morphine skeleton with hydroxyl groups (HO) at the 3 and 6 positions, a cyclopropylmethyl group on the nitrogen, and a hydroxyl group (OH) at the 4-position.</p>
<p>Buprenorphine</p>  <p>The structure shows the morphine skeleton with a hydroxyl group (HO) at the 3-position, a methoxy group (H₃C-O) at the 6-position, a cyclopropylmethyl group on the nitrogen, and a tert-butyl group (C(CH₃)₃) at the 7-position.</p>	<p>Butorphanol</p>  <p>The structure shows the morphine skeleton with a hydroxyl group (OH) at the 3-position, a hydroxyl group (OH) at the 4-position, and a cyclopropylmethyl group on the nitrogen.</p>

Table 4 Chemical structure of benzomorphan

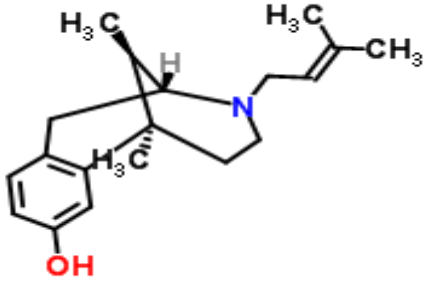
Benzomorphan	
Pentazocine	
	

Table 5 Chemical structure of phenylpiperidines

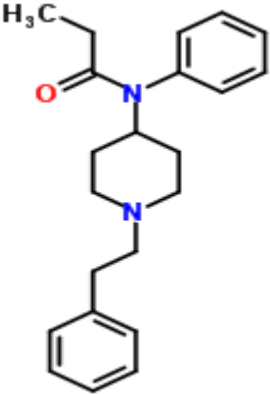
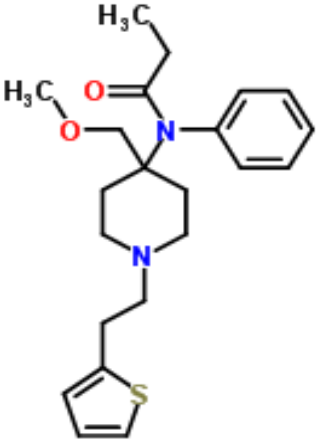
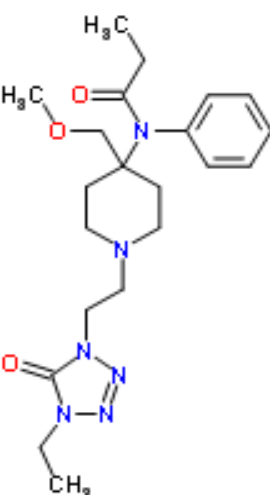
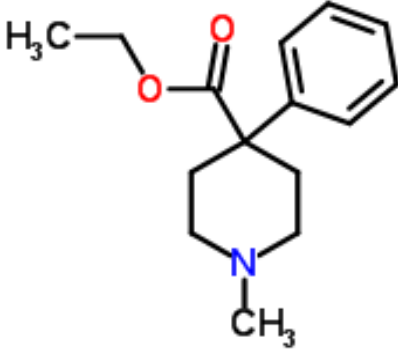
Phenylpiperidines	
Fentanyl	Sufentanil
	
Alfentanil	Meperidine
	

Table 6 Chemical structure of diphenylheptanes

Diphenylheptanes	
Propoxyphene	Methadone

As the tables above have elucidated, there is a huge variation in the physicochemical properties of opioids which affects their pharmacokinetic attributes; mainly the processes of drug absorption and distribution. The pharmacokinetic features of an opioid are of paramount importance to the clinician (Table 7). The molecular size, lipophilicity, degree of protein binding and level of ionization are the four most important dynamic factors that influence the rapidity of onset, time to peak effect, and duration of action of any drug.

Table 7 Comparative pharmacokinetic data of various opioids ((3, 6, 9-20))

Opioid	Elimination half life (min; $t_{1/2\beta}$)	Clearance (ml/kg/min)	Volume of distribution (Vd; L/kg)	Protein binding (%)	Distribution coefficient (lipophilicity)	Clinical onset of action (minute)	Active metabolites
Alfentanil	94	6.4	0.86	92	129	1	nil
Buprenorphine	1560	20	2.8	96	1217	2-5*	norbuprenorphine
Codeine	150-210	12.1	2.5-3.5	20	0.6	<60	norcodeine morphine codeine-6-glucuronide
Hydromorphone	158	14.6	2.9	8-19	1.28	5-10	hydromorphone-3-glucuronide
Fentanyl	219	13	4	84	955	2-3	nil
Methadone	50-4500	2.4	3-4	60-90	57	10-20 (iv)	nil
Morphine	177	14.7	3.2	60	1.0	5-10	morphine-3-glucuronide morphine-6-glucuronide
Oxycodone	120-180 (IR formulation)	13	2-3	45	1.64	10-15	noroxycodone oxymorphone
Pethidine	192	12.0	2.8	65-75	32	5-7	norpethidine
Remifentanyl	5-14	30-40	0.2-0.4	70	18	1	nil
Sufentanil	64	12.7	2.0	92	1727	2	desmethyلسufentanil

* The full effect however is only seen after 45 minutes
 † Not clinically significant in patients with normal renal function
 iv –intravenous, IR – immediate release

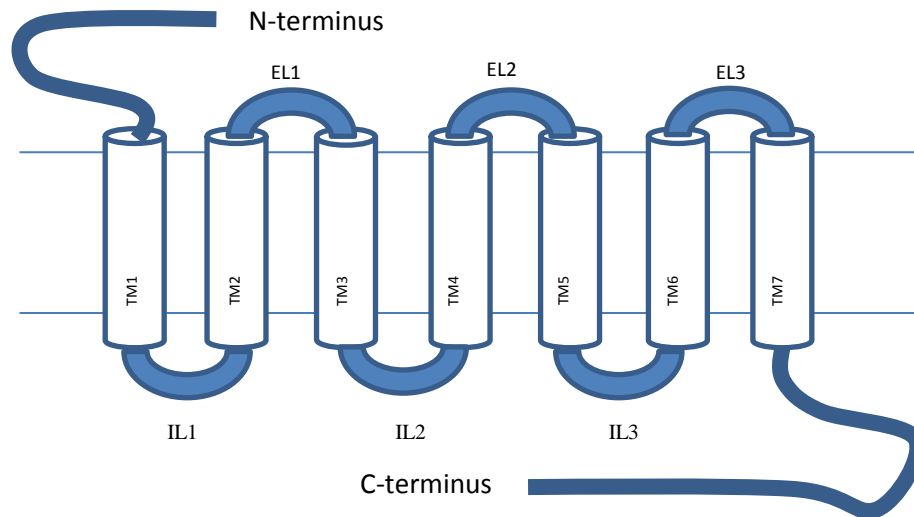
1.2.3 Opioid receptor physiology

Opioid receptors belong to a large superfamily of G protein-coupled receptors (GPCRs) (21-23). GPCRs play an important role in signal transduction. The opioid receptors are widely distributed in the brain and the spinal cord besides being expressed in various peripheral tissues including vascular, cardiac, airway/lung, gut and immune/inflammatory cells (7). Opioid receptors are activated by both opioid peptides that are made endogenously and also exogenous opioids (7). There are 4 opioid receptors: μ , δ , κ and NOP receptors (Refer Table 8). The role of each receptor is not physiologically well-defined even though all the four major receptor types play a certain role in pain modulation (26). Activation of μ -opioid receptors usually result in inhibitory actions. The μ -receptor mediates the most potent antinociceptive effects while the δ -receptor produces lesser analgesic effects. The κ -receptor is involved in dysphoria, diuresis and analgesia in peripheral tissues (24). Besides causing analgesia, opioid receptor activation also results in respiratory depression, euphoria, stimulation and suppression of hormone release and inhibition of gastrointestinal motility (21, 25).

Table 8 Main opioid receptors (For references please refer to the following articles (6, 24, 26, 27))

Receptor type	Other names	Location	Effects
Mu (μ)	MOR3, OP3	Brainstem, medial thalamus, spinal cord and peripheral nervous system	Supraspinal analgesia, respiratory depression, euphoria, sedation, reduced gastrointestinal motility and physical dependence
Kappa (κ)	KOR, OP2	Limbic & other diencephalic areas, brainstem, and spinal cord.	Spinal analgesia, sedation, dyspnoea, dependence, dysphoria, diuresis and respiratory depression
Delta (δ)	DOR, OP1	Mainly in the brain	Not well studied. Maybe causes psychotomimetic and dysphoric effects
Nociceptin/orphanin FQ peptide receptor (NOP)	ORL1	Central and peripheral nervous system	Pro- and anti-nociception, modulation of drug reward, learning, mood, anxiety, cough and parkinsonism

Each of the four major opioid receptors is controlled by its own gene. These have been mapped to chromosome 1p355-33 (δ opioid receptor), chromosome 8q11.23-21 (κ opioid receptor), chromosome 6q25-26 (μ opioid receptor), and chromosome 20q13.33 (nociceptin/orphanin FQ peptide receptor) (28). As is characteristic of GPCRs, each receptor consists of an extracellular N-terminus, 7 transmembrane helical twists, 3 extracellular loops, 3 intracellular loops and an intracellular C-terminus (6).



EL - Extracellular loop

TM - Transmembrane helix

IL - Intracellular loop

Figure 1 Structure of opioid receptors (Adapted from (29))

Opioid receptors are coupled mainly to pertussis toxin-sensitive, $G_{i/o}$ proteins (7, 29) although occasionally they couple to G_s or G_z (7). When the opioid receptor is activated, G protein α and $\beta\gamma$ subunits interact with multiple cellular effector systems (29). These interactions lead to inhibition of adenylyl cyclases and voltage-gated calcium channels while stimulating G-protein-activated inwardly K^+ channels (GIRKs), phospholipase C and protein kinase C (PKC) (29). Agonist activation of μ opioid receptors also induces phosphorylation of μ opioid receptors by G-protein-coupled receptor kinase 2 (23). This process increases the affinity of interaction with β -arrestin 2 (Arr3) which is involved in the development of opioid tolerance (see Figure 2 and section 1.3.2) (23). The protein kinases will also contribute to altered gene expression (6, 30). Inhibition of the release of pain neurotransmitters such as glutamate, substance P and Calcitonin Gene Related Peptide (CGRP) from nociceptive fibers results in analgesia (6). Opioid agonists also activate presynaptic receptors on GABA neurons causing inhibition of GABA release in ventral tegmental area (6). The inhibition allows more vigorous firing of dopaminergic neurons. The presence of extra dopamine in the nucleus accumbens results in euphoria (6).

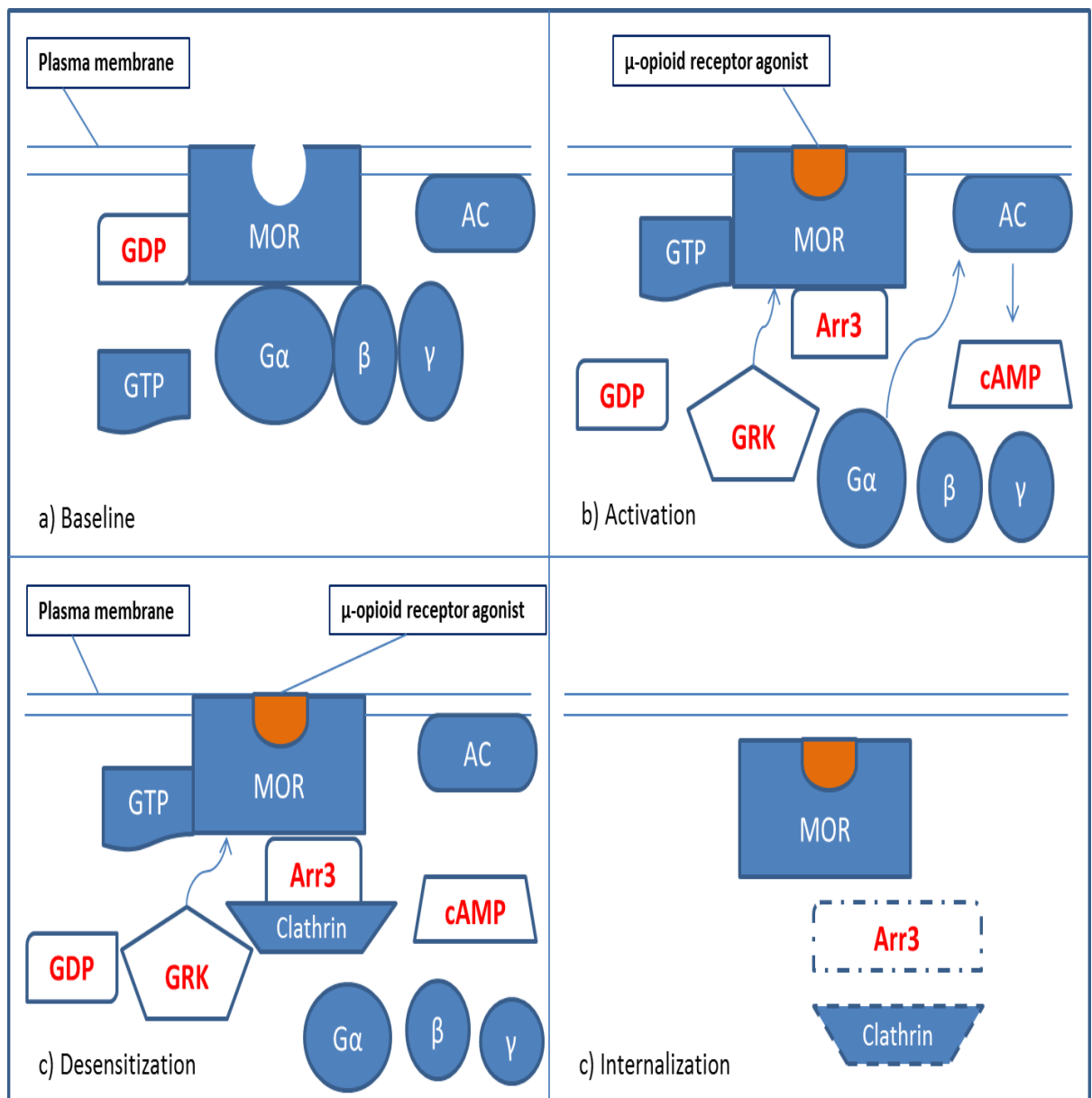


Figure 2 A simplified representations of the processes involved following μ -opioid receptor activation. Modified from (30-33). Even though opioid receptor activation, desensitization and internalization are firmly established concepts, the exact mechanisms are unclear (23). Abbreviations: MOR, μ -opioid receptor; GDP, guanosine diphosphate; GTP, guanosine triphosphate; GRK, G-protein coupled receptor kinase; Arr3, arrestin 3; AC, adenylyl cyclase; cAMP, cyclic adenosine monophosphate.

1.3 Mechanisms of Opioid-Induced Tolerance and Hyperalgesia

1.3.1 Tolerance and Hyperalgesia

Tolerance is defined as a reduction in the effects of a drug following repeated or prolonged exposure to a specific concentration of a drug (definition modified from (34)). Short term or 'acute' tolerance develops within minutes to several hours whereas long term tolerance develops during chronic drug exposure (35). Experimentally, a shift to the right in the agonist dose-response curve best demonstrates tolerance (36).

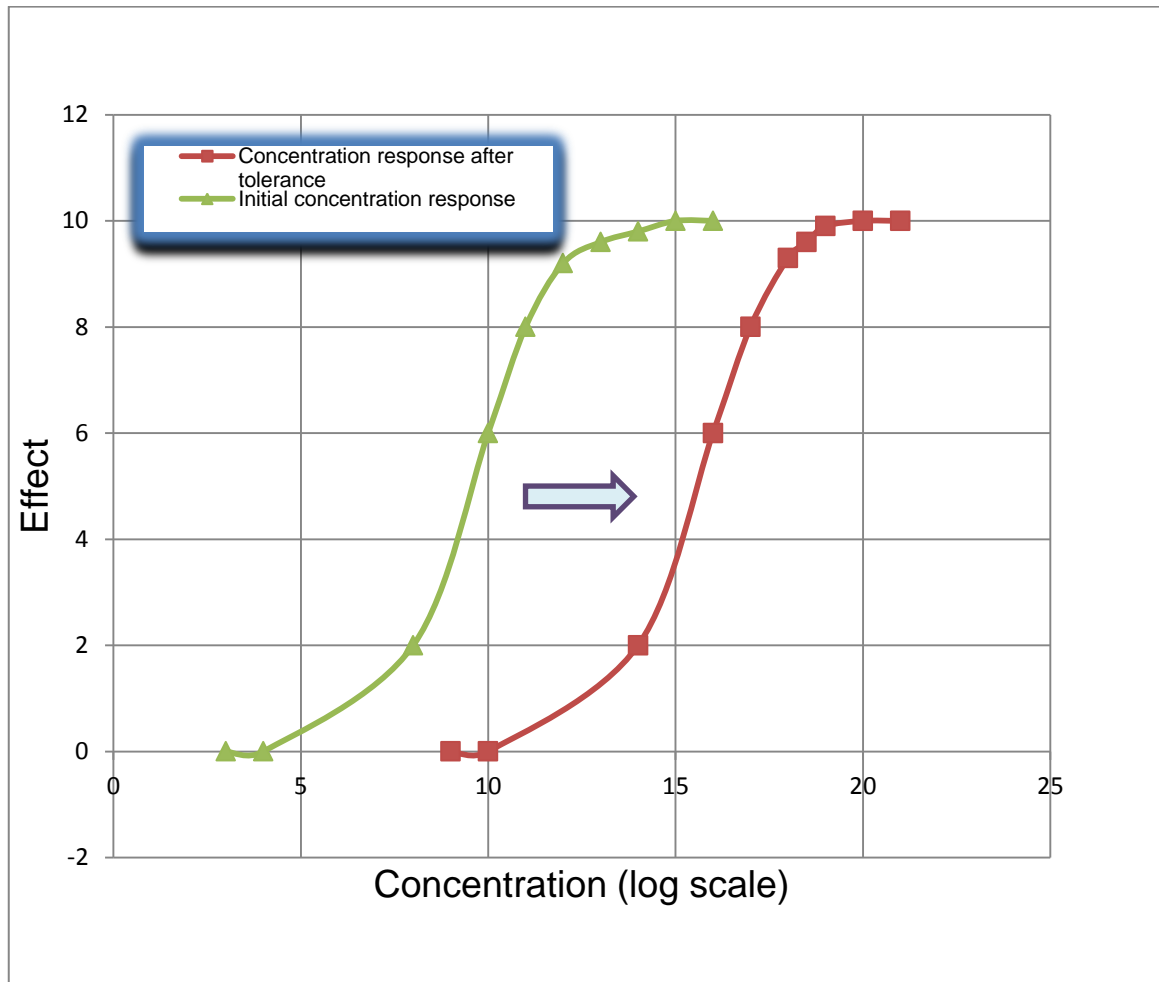


Figure 3 Tolerance is expressed by right-shift of the concentration versus effect relationship (adapted from Carroll, Angst & Clark 2004). The readings on the X and Y axis have been chosen arbitrarily.

Hyperalgesia is enhanced pain response to a noxious stimulus (37). This is different from allodynia which is a pain response to an innocuous stimulus (37). Allodynia in an individual however can accompany hyperalgesia. Hyperalgesia can be considered as either a downward shift in the dose-response curve (38) or an increase in the slope of the dose response curve (39).

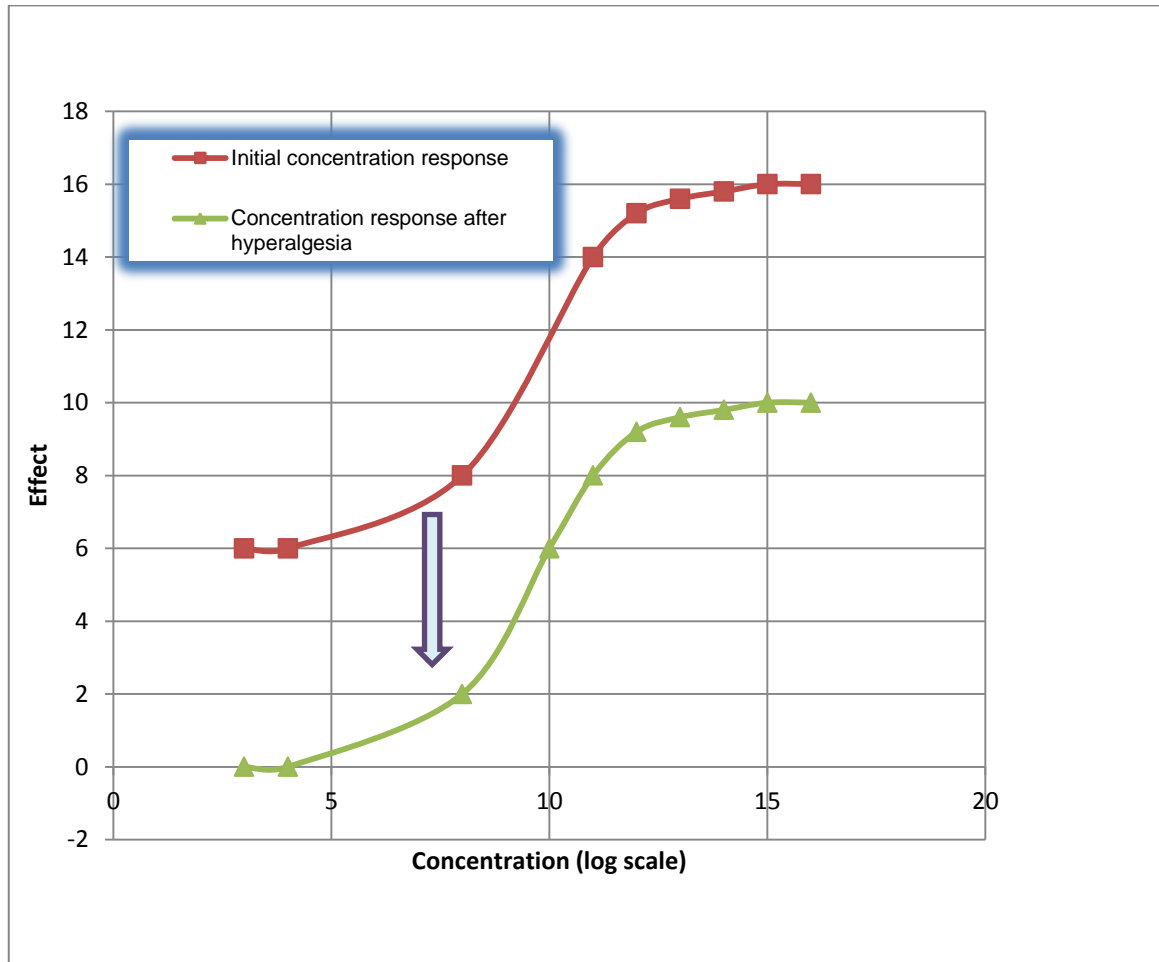


Figure 4 Hyperalgesia is reflected by a down-ward shift of the concentration versus effect relationship (adapted from Carroll, Angst & Clark 2004). The readings on the X and Y axis have been chosen rather arbitrarily.

Tolerance to opioids is characterized by a reduction in the sensitivity of antinociceptive pathways whereas hyperalgesia represents an increase in the sensitivity of the pronociceptive pathways (36). Both tolerance and hyperalgesia can appear to result in the same clinical effect which is decreased opioid effectiveness of a given dose. In the case of tolerance, full efficacy can still be achieved by giving high enough doses of a drug. However, in the presence of hyperalgesia, maximum efficacy is reduced.

1.3.2 Mechanisms underlying tolerance and hyperalgesia

The development of tolerance and opioid-induced hyperalgesia involves complex, multifactorial underlying mechanisms which are currently not fully understood. Numerous mechanisms for tolerance have been proposed with no theory integrating all the mechanisms being proposed. Tolerance involves a range of neurotransmitters (e.g. glutamate, dynorphin, substance P, cholecystokinin and nitric oxide), receptors (κ -opioid and NMDA) and intracellular signalling (adenylyl cyclase and protein kinase C) (40, 41). The mechanisms producing opioid-induced tolerance and hyperalgesia can be summarized into three categories:

- A. Alterations in primary opioid receptor systems
- B. Changes in other neurotransmitters
- C. Immune system responses

These three categories interact with each other and are not independent of each other.

- A. Alterations in primary opioid receptor systems

Receptor desensitization

The main mechanism underlying tolerance of the opioid receptors is the process of desensitization (Figure 2). Activation of the receptor by an opioid agonist induces μ -opioid receptor phosphorylation by G-protein-coupled receptor kinase 2 (23). This process is the first step in the desensitization and internalization of the μ -opioid receptor (30). This increases the affinity of interaction with Arrestin 3 (also known as Arr3, β arr-2, β -arrestin-2), a key protein for μ -opioid receptor internalization (23). The binding of Arr3 uncouples the receptor from G-protein signalling (23). This desensitization process starts the process of receptor sequestration and internalization through an Arr3- and dynamin-dependent mechanism (32). It also weakens the second messenger signalling cascade, reducing the efficacy of the opioid agonist (30). Knockout of Arr3 has provided the strongest evidence to date, that Arr3, desensitization and/or internalization mechanisms play a part in acute and chronic opioid tolerance (23). Loss of behavioural antinociceptive sensitivity to morphine (considered as acute tolerance) and development of chronic tolerance were markedly reduced in Arr3 knockout mice (42).

Dynorphin

Dynorphin plays an important role in the development of opioid-induced hyperalgesia (OIH) (43). Exposure to morphine leads to increase in cholecystokinin (CCK) activity which leads to upregulation of dynorphin in the spinal cord (44). Dynorphin is an endogenous kappa opioid receptor agonist (45). Enhanced expression of dynorphin is pronociceptive (44). Elevation of dynorphin levels in a pathological state promotes release of neurotransmitters such as calcitonin gene-related peptide (CGRP), substance P, neurokinin-1 and excitatory amino acids such as glutamate from primary afferent fibers at the dorsal root ganglion (44). Furthermore, in the hippocampus, dynorphin elicits a dose-dependent glutamate and aspartate release (44). These processes lead to creation of an abnormally sensitized pain state that manifest as tolerance to the antinociceptive properties of opioids (37).

G proteins

2 subclasses of G-proteins are related to opioids; $G_{i/o}$ and G_s . The coupling of $G_{i/o}$ to opioid receptors causes blocking of calcium channels (46). It also prevents neurons from releasing glutamate, substance P and CGRP. G_s -coupled μ -receptors on the other hand are excitatory and increase release of excitatory neurotransmitters (47). G_s -coupled μ -receptors also activate adenylyl cyclase and

protein kinase A. Chronic morphine administration enhances excitatory signalling of G_s but not the inhibitory $G_{i/o}$ (40). μ -receptors were selectively coupled to G_s proteins in the posterior horn, in the selective spinal nerve ligation model of a neuropathic pain study using lumbar spinal cord tissues from rats dosed with oxycodone (48). This action was weakened by low-dose μ -receptor antagonist, naltrexone (48). Naloxone (another μ -receptor antagonist) also prevents μ -opioid receptor coupling to G_s proteins that is enhanced by chronic opioid dosing thus preventing the build-up of analgesic tolerance and dependence (48). Furthermore, oseltamivir, a neuraminidase inhibitor similarly reduces G_s receptor coupling and reverses tolerance and hyperalgesia related to morphine in mice (49). However, this has not been tested in humans.

B. Changes in other neurotransmitters

NMDA

μ -opioid receptor stimulation causes increase in the N-methyl-D-aspartate (NMDA) receptor-mediated response (50). This occurs intracellularly through protein kinase C-mediated removal of NMDA receptor channel blockade by magnesium (50). Protein kinase C activity is further stimulated by subsequent increases in intracellular calcium (51). The stimulation of protein kinase C leads to lasting enhancement of glutamate synaptic efficiency causing a positive feedback loop (51). Continuous activation of the NMDA receptors by excitatory amino acids results in sensitization of second order neurons of the dorsal horns to noxious stimuli (44). Spinal sensitization leads to increased propagation of noxious inputs to supraspinal locations (44). This persistent process can potentially lead to hyperalgesia (44). The role of NMDA receptors in tolerance is further strengthened by the evidence that NMDA receptor blockers prevent morphine tolerance in mice and rats (52, 53). The studies in animals were supported by some clinical reports (54). The clinical report by Bell (54) demonstrated that adjuvant subcutaneous ketamine infusion improves analgesia and reduces morphine tolerance. However there has not been any randomized double blind clinical trials done using ketamine to investigate this further. With regards to dextromethorphan, at least four randomized double blind clinical trials have failed to show enhanced analgesia or reduced tolerance when combined with opioids (55-58).

Glutamate transporters

Prolonged morphine administration causes down-regulation of glutamate transporters (59). The glutamate transporters are expressed by the glia, next to the synaptic clefts (46). They function to clear glutamate from the synaptic cleft, thus diminishing NMDA activation (46). Glutamate transporters are degraded by ubiquitin/proteasome system (60). Inhibition of this process by intrathecal proteasome inhibitor, MG-132 had been shown to prevent morphine tolerance in rats (61). Whether this drug will be able to treat tolerance in humans is not yet known.

Calcitonin gene-related peptide

Calcitonin gene-related peptide (CGRP) is widely distributed in the central and peripheral nervous systems (46). It functions as excitatory neurotransmitters (46). Prostaglandin E_2 , which is released in response to inflammation stimulates the release of CGRP (62). The binding of CGRP to a G-protein coupled receptor results in activation of adenylyl cyclase and protein kinase A (46). This leads to activation of p38, extracellular signal-regulated kinases (ERK) and cAMP response element-binding protein (CREB) causing upregulation of NMDA receptors (46). It is hypothesized that CGRP exerts its role in morphine antinociceptive tolerance by regulating the expression and distribution of p38

phosphorylation in microglia (63). In rats, intrathecal treatment with BIBN4096BS (a non-peptide CGRP antagonist) have been shown to block the morphological changes associated with morphine tolerance (63). Nevertheless, the efficacy of BIBN4096BS in treating opioid-induced hyperalgesia and tolerance in humans has not been studied.

Transient receptor potential vanilloid-1 channels

Transient receptor potential vanilloid-1 (TRPV1) channels are voltage-gated channels that are activated by capsaicin (46). Opioids up-regulate the TRPV1 channels via MAPK and ERK activation (46). Blocking TRPV1 channels prevents development of morphine-associated tolerance and thermal hyperalgesia in rats (64). The effects on opioid-induced hyperalgesia and tolerance in humans have not been studied. Currently, some TRPV1 antagonists have passed Phase I studies in human volunteers successfully while others have been disappointing due to adverse effects of hyperthermia and impaired sensation of noxious heat (65).

Cyclooxygenase and prostaglandins

Both cyclooxygenase (COX) isoenzymes play a part in neuropathic pain (66). Prostaglandin E2 is a secondary messenger to NMDA receptors and nitric oxide synthase (67). In opioid withdrawal, COX-2 and protein kinase B (AKT) are both upregulated (68). Ketorolac, a COX-1 inhibitor has been shown to prevent hyperalgesia associated with withdrawal to spinal morphine in rats (69). Intrathecal nimesulide, a COX-2 inhibitor has been demonstrated to prevent and reverse morphine induced tolerance in rats (70).

CCK

Cholecystokinin (CCK) is distributed heterogeneously throughout the brain and spinal cord (71). It has been implicated as an endogenous pronociceptive agent (71). Spinal and supraspinal dosing with CCK leads to hyperalgesia and increased activity of the dorsal horn neuron (71). Morphine administration has also been shown to increase CCK levels in the cerebrospinal fluid, frontal cortex and amygdala (71). In rats, the morphine-induced increase in frontal cortex extracellular CCK can be reversed with naloxone (72). Microinjection of the CCK-2 antagonist, L-365,260 into the rostral ventral medulla (RVM) eliminates hyperaesthesia and antinociceptive tolerance to morphine (44). The specific mechanism of CCK's action is not yet known but it may act against opioid-induced inhibition of calcium influx into primary afferent neurons by bringing about movement of calcium from intracellular stores, maintaining neurotransmitter release in nociception (71).

Substance P and neurokinin-1 (NK-1) receptors

Substance P is an excitatory neurotransmitter that preferentially binds to NK-1 receptors in the dorsal horn of the spinal cord (73). Prolonged morphine administration in animals leads to increased expression of NK-1 receptor and substance P in the spinal dorsal horn (46). This is associated with hyperalgesia (73). This effect could be reversed using L-732,138 (an NK-1 antagonist) and it is not seen in NK-1 receptor knock-out mice (73).

Adenylyl cyclase

Inhibition of adenylyl cyclase by μ -receptor agonists causes reduction of cyclic AMP (46). The reduction results in hyperpolarization of neuron membranes (46). With prolonged morphine exposure, cyclic AMP returns to normal and become super-activated with withdrawal (23). This is because of changes in G-protein interactions with μ -receptors over time (46). Initially $G_{i/o}$ proteins downregulate adenylyl cyclase but with time the receptors start interacting with G_s proteins (46). This results in increase in adenylyl cyclase types I, II, IV and VIII (31). Up-regulations of the isomers

lead to increases in cyclic AMP levels causing reduction in neuron membrane potential and activation of protein kinase A (46). Morphine up-regulates certain adenylyl cyclase isomers and protein kinase A (46). Protein kinase A causes up-regulation of glucocorticoid receptors in the posterior horn (74). After cessation of morphine, glucocorticoid receptor up-regulation remains and subsequent morphine exposure causes rebounding of the expression (74). Glucocorticoid receptor upregulation is linked to tolerance to the analgesic effect of morphine (46). Preventing the activation of glucocorticoid receptors and down regulating the receptors prevents the development of tolerance to morphine in animals (46).

Serotonin and serotonin receptors

Serotonin (5-HT) in the rostral ventral medulla (RVM) plays a significant role in facilitating pain (46). In animal models of pain, serotonin depletion has been shown to protect against development of mechanical hyperalgesia and allodynia (75). In nucleus accumbens of animals, serotonin receptors have been shown to induce dopamine release which is a mechanism of morphine-associated rewarding effects (46). Granisetron and ondansetron (5-HT₃ blockers) prevents the rewarding effects of morphine in rats (76, 77). Morphine-induced hyperalgesia that was mediated by cholecystinin in the rostral ventral medulla can be blocked by spinal ondansetron (78). The use of 5-HT₃ receptor antagonist may provide a new possibility for treating hyperalgesia and tolerance associated with chronic opioid use (79). Currently, the role of 5-HT₃ receptor antagonists in managing some painful diseases such as rheumatoid arthritis and fibromyalgia seems promising (80).

Calcium channels

The expression of L- and N-type voltage-sensitive calcium channels are highest in the superficial lamina of the dorsal horn in rats treated chronically with morphine alone or combined with nimodipine (81). Both L- and N- type voltage-gated calcium channels are expressed to a greater extent in the morphine-tolerant than in the opioid-naïve animals (81). An L-type calcium channel blocker, amlodipine prevents the development of hyperalgesia and tolerance to spinal morphine analgesia in mice (82). An N-type calcium channel blocker, ziconotide improves pain that responds poorly to opioid therapy (83). Gabapentin blocks the activity of calcium channel by binding to alpha-2 and delta-1 calcium channel subunits (84). Pregabalin (a gabapentinoid) causes reduction in punctate mechanical hyperalgesia around injury sites in healthy volunteers (85). When combined with a cyclooxygenase inhibitor such as parecoxib, pregabalin causes increases in analgesic effects (85). Both gabapentin and pregabalin which were approved for use in neuropathic pain, improve the analgesic effects of opioids (46).

C. Immune system

Glial activation

Oligodendrocytes, microglia and astrocytes are the three main types of glial cells in the central nervous system (CNS) (86). All glial cells play an active role in nervous system function (86). Microglia and astrocytes also play a part in pain processing (86). Astrocytes and microglia express a range of pattern-recognition receptors including toll-like receptors (TLRs) (87, 88). Besides binding to μ -opioid receptors on neurons to produce analgesia and other effects, opioids also activate glia via the TLR4 receptor (89).

The docking of opioids onto glia leads to release of pro-inflammatory cytokines including interleukin-1 β (IL-1 β), interleukin-6 (IL-6) and tumor necrosis factor- α (TNF- α) (46, 90). IL-1 β and IL-6 are both

pronociceptive (90). IL-1 β phosphorylates NMDA receptors resulting in enhanced channel opening followed by calcium influx (89). The influx of calcium increases nitric oxide and prostaglandin E2 levels, thus boosting excitability of pain projection neurons in the spinal cord (89-91). IL-1 β also causes down-regulation of glutamate transporters leading to increase in extracellular glutamate (90, 92). The blocking of IL-1 β by interleukin-1 receptor antagonist increases morphine antinociceptive effects and shifts the dose-response curve of morphine to the left (93). In addition, minocycline (an antibiotic that inhibits microglial activation) and antibodies to tumour necrosis factor alpha also heighten the analgesic effects of morphine (94-96). These actions illustrate the importance of glial cells in the pathogenesis of opioid-induced hyperalgesia and tolerance.

1.3.3 Clinical dimensions of tolerance

Both hyperalgesia and tolerance lead to a reduction in the analgesic effectiveness of an opioid with time. As both phenomena cause inadequate analgesia, they are difficult to differentiate in a clinical setting. A number of animal studies have demonstrated the connection between tolerance and hyperalgesia implicating that opioid-induced hyperalgesia is a significant contributor to the development of tolerance (97). However, a recent study showed that patients with chronic non-radicular low-back pain maintained for one month on sustained-release morphine became tolerant to the analgesic effects of remifentanyl without developing opioid-induced hyperalgesia (98). As the study was of limited duration, in a restricted phenotype of pain population and with modest opioid doses, generalizability of this study is questionable.

Clinically, the development of tolerance towards multiple opioid effects occur at different rates (99). Tolerance towards analgesia and euphoria in animals tends to happen at a quicker rate than tolerance to respiratory depression (100). The same phenomenon has been implicated in man based on observations in methadone-maintained individuals (100). This clinically means that a patient may develop respiratory depression and sedation without attaining analgesia (99). For some patients who are chronically maintained on opioids, the ratio of drug levels that produce analgesia to the level that induces respiratory depression is high (99). As a consequence, many opioid-tolerant patients will have sedation, slurring of speech, decreased respiratory rate and need of supplemental oxygen and yet still have a high pain score (101). The opioid-maintained individuals develop tolerance to the analgesic, euphoric, sedative, respiratory depressant and nauseating effects of the opioids (102). However, they only minimally or do not develop tolerance to pupillary miosis (7).

Even though prolonged and repeated administration of an opioid will eventually lead to tolerance to its effects and cross-tolerance to the effects of other opioids, there is a wide range of variability in the degree of cross-tolerance (103). Incomplete cross tolerance is the basis for 'opioid rotation' allowing clinicians to switch between opioids while lowering the equivalent dose of the opioid (103). This allows patients who are unable to tolerate further dose escalations due to adverse reactions to regain analgesic sensitivity to the actions of another μ -opioid agonist (104).

1.4 Epidemiology of opioid use

There are three main categories of individuals who use opioids chronically. The first category is sufferers of chronic pain. The second group is those who are on opioid-substitution therapy and the third category are people who misuse or abuse opioids and then develop dependence to opioids. The distinction between the categories might not be clear at times and a person might belong to more than one group or belong to all three groups at the same time.

The rate of opioid prescription has increased in developed countries such as the United States, the United Kingdom, Canada and Australia (105, 106). In Australia, a study analysing data from the Bettering the Evaluation and Care of Health (BEACH) program involving Australian general practitioners (GPs) reported that the total prescribing rate for analgesics has been increasing over the past decade from 8.1 per 100 GP encounters in 2002-03 to 9.3 per 100 in 2011-12 (107). Extrapolation of the data for opioids suggests tripling of GP prescribed opioids from 2.13 million (108) to 7.22 million (109) over the same period. For the annual period from 2011-12, opioids accounted for nearly 7% of all medications prescribed by participating GPs in the study (109).

Data analysis from the BEACH program for the period of April 2010 to March 2011 revealed that back problem was the most frequent condition for which opioids were prescribed and 43.9% of the time, the opioids were given for chronic non-cancer conditions (110). Only about 4% of the opioids were prescribed for malignancy and about 10% were for osteoarthritis (110). The highest proportion of patients receiving opioids was from the 45-64-year-old category accounting for 37.3% of patients at opioid encounters (110). The main opioids prescribed or supplied by Australian GPs are summarized below (110):

Table 9 Main opioids prescribed or supplied

Opioids	Opioid prescriptions	Estimated number of opioid prescriptions nationally in 2010-11
Paracetamol/codeine (30 mg)	32.3%	2,130,000
Oxycodone	26.3%	1,730,000
Tramadol	16.2%	1,060,000
Buprenorphine	8.0%	530,000
Morphine sulphate	6.9%	460,000
Fentanyl	4.7%	310,000
Dextropropoxyphene/paracetamol	3.4%	220,000

Over the period of 2002-03 to 2011-12 there had been a significant increase in the prescription rate of oxycodone. It was 0.2 per 100 problems managed in 2002-03 and went up fivefold to 1.0 in 2011-12 (107). When extrapolated to a national level, there were 1.5 million extra prescriptions for oxycodone nationally in 2011-12 than there were 10 years earlier. Oxycodone is currently the 7th most commonly prescribed medication in Australia (107) reflecting the significant impact of opioids on the Australian population.

With regards to the group of people who are on pharmacotherapy for their opioid dependence, there were nearly 47,000 people in Australia on a specified day in June 2012 who received treatment for opioid dependence (111). The number of people receiving either methadone, buprenorphine or buprenorphine-naloxone for opioid dependence has nearly doubled since 1998 (from around 25,000) and New South Wales had the highest rate of people receiving opioid pharmacotherapy (111).

The increase in the rates of opioid use were not limited to opioid prescriptions for pain or opioid substitution therapy but it also involved the rate of opioid abuse in developed countries such as

Australia, the United States, the United Kingdom and Canada (105, 106). Recent studies in the USA showed that non-medical use of prescription opioids has tripled since 1990 reaching epidemic proportions (112).

It is therefore clear from these data that opioid use has been increasing in all three major groups of chronic opioid users and studies related to opioid use in humans are still very relevant to current medical practice.

1.5 Managing pain in the opioid-maintained

There is a strong evidence base for the management of acute pain in the general population (3). There are however a few populations of patients in which the management of acute pain lacks robust evidence. One of them is opioid-tolerant patients (3).

There are numerous misconceptions among health practitioners with regards to the issue of pain management of the opioid-tolerant. Many have the belief that the opioid-tolerant do not need additional analgesics for their acute pain as they are already stabilized on daily opioids (113). This is really a clear misunderstanding and studies have shown that the opioid-tolerant tend to suffer more pain than the opioid-naïve population (114).

1.5.1 Concentration-targeted approach

Several studies have been conducted here at The University of Adelaide and elsewhere with regards to attaining evidence to guide management of acute pain in the opioid-dependent. In the study by Doverly et al (115), 4 patients who had been enrolled in the South Australian Public Methadone Maintenance Program for 9 months or more were recruited. Four age-, sex- and weight-matched healthy volunteers were also recruited as controls. Methadone-maintained patients were tested on two separate occasions, 7 days apart. The study aimed at comparing the strength and duration of antinociceptive effects of morphine at 2 pseudo-steady-state plasma morphine concentrations in both groups. The study also attempted to ascertain whether the antinociceptive effects of morphine were affected by alteration in plasma methadone concentration during the interval between dosing.

The four patients who were maintained on methadone were allocated randomly into two subgroups. For the first group, the 2 subjects were tested when their methadone plasma concentration was at the putative trough level. After 7 days, they were tested when the methadone plasma level was at its putative peak. The second group was tested in reverse order. Patients who were tested during the putative trough of methadone plasma concentration were given their scheduled daily oral methadone dose 15 minutes after stopping morphine infusion. The four healthy controls were only tested on one occasion and not given methadone.

The methadone patients and the controls were given a bolus of 2.2 mg intravenous morphine sulphate followed by a constant infusion of 1.2 mg/h for one hour to achieve a target pseudo-steady-state plasma concentration of 20 ng/ml. This plasma morphine concentration is higher than the level that is needed to achieve minimum effective postoperative analgesia. After the 1 hour duration, methadone-maintained patients were given an additional bolus of 6.6 mg and the infusion rate was increased to 4.8 mg/h for 1 hour. The targeted pseudo-steady-state plasma concentration this time was 80 ng/ml. For the controls, instead of giving 6.6 mg bolus, they were given 4.95 mg of morphine. The infusion rate given was also lower than 4.8 mg/h at 3.6 mg/h, targeting 60 ng/ml pseudo-steady-state plasma concentration. This pseudo-steady-state target was chosen based on the evidence that 50 ng/ml of plasma morphine concentration can provide analgesia for moderate to severe postoperative pain. Pain induction was done using two methods; electrical stimulation via an ear lobe and cold pain test on the non-dominant arm. Pain detection and pain tolerance were the two indices used for measuring responses.

Doverly's study found that the patients maintained on methadone did not get analgesia from the morphine given even though significantly greater plasma morphine concentrations were attained compared to the control group. There were stark differences between responses of the methadone

Muhammad Imran Ahmad, MPhil Thesis, 2014

patients and controls to the cold pain test. The methadone patients manifested hyperalgesia as has been previously reported. In control subjects, the morphine plasma levels of 11 and 33 ng/ml significantly increased the antinociceptive response substantially. The cold pain test response more than doubled at 33 ng/ml illustrating the sensitivity of the test to morphine effects. The same effects were however not seen in the methadone-maintained which the authors attributed to cross-tolerance to the effects of morphine. The study also showed that methadone patients are hyperalgesic to pain induced by the cold pain test but not to pain caused by electrical stimulation. There was a difference in the pain tolerance readings between the methadone-maintained and the controls which was fourfold during the morphine dosing period (115).

The authors concluded from their study that methadone-maintained individuals are 'cross-tolerant to the antinociceptive effects of morphine at plasma concentrations which have previously been reported as being adequate for minimal to severe post-surgical pain relief.'

This study used the concentration-target approach based on plasma morphine concentrations which were antinociceptively adequate in the opioid-naïve population postoperatively. The subjects were given a different opioid to their maintenance opioid medication but the doses that were given were meant for the opioid-naïve population. This strategy was proven not to be effective in this study using cold pain test which is an experimental pain model.

Following up from Doverty's study, Athanasos conducted a study using almost similar design to Doverty's study but with higher doses of morphine. The target pseudo-steady-state plasma concentration of morphine targeted in this study was more than twice the concentration aimed for in the previous study (116). 18 methadone-maintained patients and 10 healthy non-opioid dependent subjects were enrolled into the study by Athanasos. The methadone-maintained were being maintained on methadone for at least one month prior to enrolment. The trial was a double-blind placebo-controlled study with the methadone-maintained patients being stratified into three groups according to their methadone daily requirements; 11-45mg, 46-80 mg and 81-115 mg.

The study aimed to examine whether 'very high' morphine given intravenously was able to produce antinociceptive and respiratory depressant effect in the methadone-maintained patients. It also tried to determine whether the magnitude of daily methadone doses affect responses. The participants were tested on two separate days with at least 5 days gap. They were dosed once with morphine and once with saline. The dosing was given in a random order. The patients on methadone were tested at roughly the time of trough plasma methadone concentrations (about 20 hours after last oral methadone dose). The dosing regimen in the methadone-maintained patients is summarized in Figure 5.

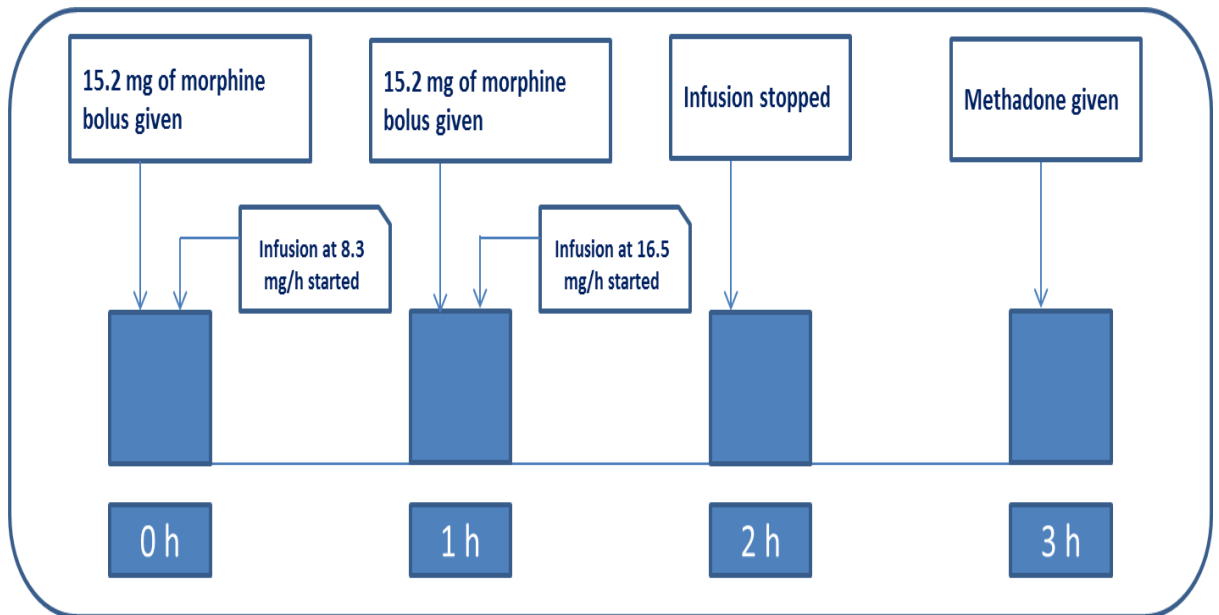


Figure 5 Morphine sulphate administration in the methadone groups. The bolus given at 0 h which was followed by an infusion attempted to achieve target pseudo-steady-state plasma concentration of 100 ng/ml. The second bolus given at 1 h was targeting 200 ng/ml pseudo-steady-state plasma concentration of morphine.

The dosing regimen for the control group is summarized in Figure 6.

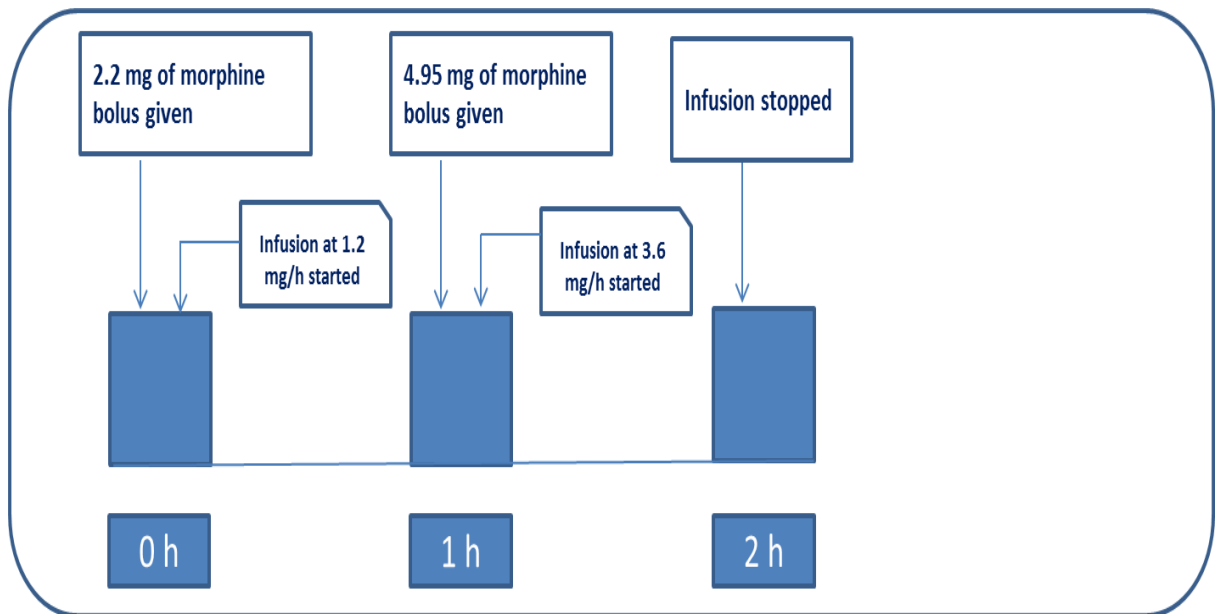


Figure 6 Morphine sulphate administration in the control group. The bolus given at 0 h which was followed by an infusion attempted to achieve target pseudo-steady-state plasma concentration of 11 ng/ml. The second bolus given at 1 h was targeting 33 ng/ml pseudo-steady state plasma concentration of morphine.

This study shows that morphine doses as high as 55 mg failed to provide antinociception for the methadone-maintained in both the electrical stimulation and cold pain tests. The high dose of morphine given in this study was 4.6 times the 12 mg dose which has been shown to be effective in healthy controls but despite that, only significant respiratory depression was demonstrated with minimal antinociception seen. What was less expected was the fact that the greatest degree of respiratory depression was found after morphine administration to the high dose methadone group.

Similar to Doverty's study, this study is based on an experimental pain paradigm which may not translate very well clinically. The study by Athanasos suggests that giving morphine in methadone-maintained patients suffering acute pain is not recommended due to minimal analgesia attained in such patients. We do not know whether we would be able to extrapolate what was seen in the methadone patients to patients who are maintained on other opioids such as morphine, buprenorphine, fentanyl, and oxycodone. The key question is whether it is possible for a person to develop tolerance to the unwanted effects of a few opioids without developing tolerance to the desirable effects of a few other opioids. It also remains uncertain if respiratory depression in the higher methadone doses group should be a concern or if more attention should be paid to sedation scores instead as a marker of morphine toxicity as studies have confirmed that assessment of sedation is a more reliable way of assessing for opioid-induced respiratory depression (3).

1.5.2 Pharmacodynamic targeted approach

Davis et al employed a pharmacodynamic (PD) targeted approach in estimating the amount of fentanyl required to provide satisfactory analgesia postoperatively in chronically opioid-consuming patients (99). The study included 19 patients scheduled for elective posterior spinal fusion who had been consuming opioids for at least 1 month before surgery.

The patients were required to cease opioid medications after midnight on the evening before operation day. No preoperative sedation was administered. Prior to induction of anaesthesia, oxygen was given while electrocardiogram, noninvasive arterial blood pressure, pulse oximetry and capnography were monitored. An intravenous fentanyl infusion of $2 \mu\text{g}\cdot\text{kg}^{-1}\cdot\text{min}^{-1}$ was initiated. The infusion rate was based on ideal body weight. No concomitant medications and no verbal or tactile stimulation were allowed during drug delivery. The infusion was given until the patients' respiratory rate becomes less than 5 per minute as measured by capnography. At that point, the infusion was stopped and propofol 1.5-2.0 mg/kg for induction of anaesthesia was administered. Using STANPUMP (a free pharmacokinetic simulation software), the fentanyl effect-site concentration at the onset of respiratory depression was estimated for each patient based on pharmacokinetic variables described by Shafer et al. (117).

Subsequently, an infusion rate was chosen to provide a fentanyl effect-site concentration (C_e) that was 30% of that associated with respiratory depression in each individual. The reason for choosing that threshold was based on existing fentanyl data which suggested that concentrations causing analgesia are about 30% of those related to respiratory depression.

After the operation and in the recovery room, the target analgesic infusion rate of fentanyl was continued. To ensure additional safety, postoperatively, only 50% of the predicted hourly analgesic requirement was given as a basal infusion. The remaining 50% was available to the patient as PCA doses on demand. Every four hours, the basal infusion rate was adjusted to maintain a demand dose rate of 2-3 per hour. The background infusion was terminated for any patient with respiratory

rate of less than 10 per minute. Oxygen was given to every patient by nasal cannula and was monitored with continuous pulse oximetry. An investigator was also assigned to observe each patient continuously for the first 24 hours postoperatively.

This method was able to provide a reliable way of providing safe and effective analgesia for the opioid-tolerant. This approach however is not practical in real clinical scenarios as the complexity of using this approach will most probably hinder it from being embraced as a standard way of providing analgesia in the opioid-tolerant. At best, it can only be used in a perioperative setting to ensure effective analgesia is delivered to an opioid-tolerant person intra- and postoperatively.

1.6 Current recommendations on the management of acute pain in the opioid-tolerant

Due to the importance of the topic, many papers and reviews have been written on the subject (3, 90, 101, 102, 113, 118-128) . Most of these reviews were focused mainly on the perioperative setting and less emphasis were given to managing acute pain in other settings such as trauma or child birth. What is clear from one of the more recent reviews is that the evidence related to acute pain management of the opioid-tolerant is constrained and were derived mainly from case series, case reports and expert opinion (90). Due to the potential adverse effects associated with opioid use, the current view with regards to managing pain in the opioid-tolerant is to resort to multimodal analgesia (101). This will block the pain transmission at multiple neuroanatomical locations and reduce dependence on opioids postoperatively (101). There are multiple levels of approach involved in the comprehensive management of acute pain in the opioid-tolerant (Table 10).

Table 10 References in the literature with regards to managing pain in the opioid-tolerant

Level and action	Reference
Preoperatively	
Early identification	(90, 122, 128-130)
Detailed history taking	(3, 90, 101, 102, 119, 122, 123, 128-130)
Education of patient	(102, 118, 119, 121, 122, 129, 131)
Reassurance that prior drug dependence will not prevent pain relief	(90, 102, 119, 121)
Management plan	(90, 102, 118, 122-124, 128, 130, 131)
Ensure usual prescribed opioids taken on surgery day	(3, 90, 102, 119, 121, 122, 124, 127-129, 131, 132)
Liaise with other healthcare professional	(90, 122, 124, 129)
Implement multimodal analgesia before surgery	(101, 102, 118, 127, 129, 133)
Avoid giving partial agonist such as pentazocine	(3, 121, 127, 133)
While nil by mouth, provide alternative analgesia e.g. background infusion	(119, 120, 128, 132)
Intraoperatively	
Replacement or continuation of baseline opioid	(101, 113, 118, 119, 124, 127, 131, 133)
Titration of additional opioid to effect	(90, 102, 118, 124, 131, 133)
Use non-opioid analgesia and adjuvant drug	(90, 102, 118, 124, 133)
Use local and regional anaesthesia	(102, 118, 127)
Postoperatively	
Provide sufficient opioids in addition to usual opioid	(90, 102, 118, 119, 121, 126, 127)
Titration of opioid to effect	(90, 101, 102, 118, 122, 128)
Pain and adverse opioid effects monitoring	(90, 101, 102, 118, 119, 131, 133)
Functional activity scores monitoring	(90, 119)
Consider PCA or intravenous boluses of opioids	(102, 118, 119, 121, 122, 127, 131, 132)
Expect need for more frequent review and dosing adjustment	(119, 122, 124, 131, 132)
Opioid rotation be kept in view	(90, 101, 121, 122, 131-133)
Use ketamine	(3, 90, 101, 102, 118, 122, 127, 132)
Use of non-opioid and adjuvant analgesic drug	(101, 102, 118, 119, 121, 122, 126, 127, 130, 133)
Give regional anaesthesia	(90, 101, 102, 118, 119, 122, 124, 127, 131-133)
Monitor for drug withdrawal	(90, 119)
Symptom management (e.g. clonidine and benzodiazepines)	(3, 90, 102, 124, 127, 128)
Liaison with other physicians and specialist teams	(90)

Discharge management	
Discussion with physician who will be prescribing opioids to patient after discharge	(3, 90, 101, 118, 122, 128, 129, 132)
Discharge management plan	(90, 101, 102, 118, 127, 128)
Consider adjuvant and nonopioid analgesics	(3, 90, 101, 122)
Keep in mind legislative constraints for opioid prescribing	(3, 90)
Consider early follow up or relevant new referral	(90, 102)

Preoperatively (or before going into labour or after a trauma), patients who are opioid-tolerant need to be identified (122, 128) and a detailed history pertaining to the medications that they are taking (including alcohol, benzodiazepines and illicit drugs), indications and dosages of those and their treatment providers need to be recorded (90). A plan that includes pain management intraoperatively/intrapartum and postoperatively/postpartum needs to be outlined.

The patient's baseline opioid should be continued on the day of surgery (90, 128). Multimodal analgesia with paracetamol, NSAIDs and gabapentinoids can be instituted (101) if there are no contraindications before surgery. During the operation, besides providing their baseline opioids, additional opioids are titrated to effect (90). Regional anaesthesia and non-opioid analgesia such as ketamine should be considered for intraoperative administration (101). Ketamine is commonly given with propofol for painful procedures done under monitored anaesthesia care (a planned procedure during which the patient undergoes local anaesthesia combined with analgesia and sedation) (101). Respiratory depression appears significantly less common when compared to propofol-opioid combinations with this regimen (101).

Postoperatively, sufficient opioids should be given in addition to the baseline opioids (90, 126, 127). Opioid-tolerant patients usually require a few times higher total daily opioid doses compared to the opioid-naïve (3, 118). One article mentioned that in the acute postoperative period, they require 200-500% increase in their opioid need after major operations (101). A switch to another opioid is also an option in some patients. Patient-controlled analgesia (PCA) or intravenous boluses of opioids are usually started postoperatively. Regional anaesthesia and use of non-opioid and adjuvant analgesic drugs merit consideration in most cases. Pain and functional activity scores need to be monitored besides observing for adverse effects and drug withdrawal. The withdrawals in this population can also be from drugs other than opioids such as alcohol, benzodiazepines or even methamphetamine (90). Clinicians should be able to identify the manifestations of withdrawal for each of the major drug classes (90) in order to manage them effectively.

Prior to discharge, discussions should be made with the physician or general practitioner who will be prescribing opioids to the patient after discharge. Timely follow up should be given for the patients to ensure proper assessment and management of their evolving pain conditions (122). Adjuvant nonopioid analgesics should be considered in addition to their opioid analgesics upon discharge (90, 101, 122).

1.7 Pharmacokinetic/pharmacodynamic (PK/PD) modeling

Due to the complexity in treating patients who are opioid-tolerant, a more sophisticated approach is required in conducting dosing studies involving the opioid-tolerant. One such approach which has been gaining popularity over the years is the PK/PD modeling approach. PK/PD modeling as its name suggests consists of pharmacokinetics and pharmacodynamics. Pharmacokinetics is the science which studies the rate processes such as absorption, distribution, metabolism and excretion of a drug (134). Pharmacokinetics (PK) describes the quantitative relationship between doses administered and dosing regimens and plasma/tissues levels of the drug while pharmacodynamics (PD) describes the relationship between plasma and/or tissue concentration(s) of the drug and the magnitude of the pharmacologic effects of the drug (134).

Pharmacokinetic/pharmacodynamic (PK/PD) modeling connects the gap between PK and PD by linking between blood concentration and effects of a drug (135). PK/PD modeling is the mathematical description of the relationships between PK and PD (134).

Drugs such as opioids exert their effects in the receptors in the Central Nervous System (CNS). Ideally the concentration of the drug should be measured at the effect site, the site of action or biophase i.e. in the CNS but in most situations this is not an option. Sampling is done usually from plasma. The shape of time profiles of concentration and effect will show delays between concentration and effect. Connecting the data in chronological order will show the appearance of a clockwise or anti-clockwise hysteresis loop, in which one plasma concentration level corresponds to more than one effect magnitude (Figure 7). For fentanyl, hysteresis is determined entirely by the biophase distribution kinetics as fentanyl binding to and dissociation from the μ -opioid receptor is fast (136).

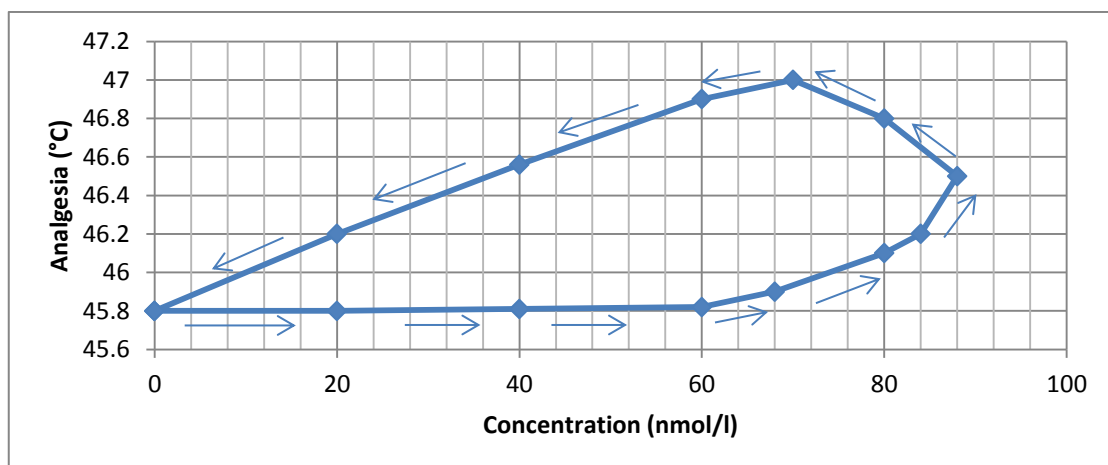


Figure 7 The relationship between plasma oxycodone and analgesia for thermal pain in the skin. Arrows indicate direction of time. (Adapted from (137)).

The hysteresis observed in concentration-effect relationships of opioids is traditionally analyzed using an effect compartment link model. This model generally reflects the delay in drug transport from plasma to the action site through the blood-brain barrier.

PK/PD modeling had led to the development of software such as STANPUMP. STANPUMP is a free program developed by Steven L. Shafer of Stanford University (117, 138) that administers certain drugs according to a three compartment pharmacokinetic model. It supports a number of infusion pumps including Harvard Pump 22 (117). This software enables a certain effect site concentration of

certain drugs to be targeted during an infusion. Using such software allows for a better correlation between predicted effect site drug concentration and pharmacological effects instead of seeing the hysteresis when correlating with the plasma concentration levels of a drug. This also allows for a high degree of accuracy and controllability of the opioid therapy (139).

The effect site is the hypothetical 'effect compartment' at the site of action that is assumed to provide the driving force for drug effect (140). The effect site concentrations are calculated using pharmacokinetic models (141) based on data from previous studies. Based on these calculations, the infusion rate is adjusted to maintain a target concentration at the drug effect site (141). Using this approach allowed a certain drug concentration to be maintained for a particular time providing time to do the necessary pharmacodynamic measurements required for the experiment.

PK/PD modeling has advanced our understanding of opioids in many ways. PK/PD modeling has strengthened our understanding of time courses of clinical effects of opioids after various dosing regimens and facilitated rational opioid selection (139). This approach provides a rational basis for designing dosing regimens and customizing opioid selection for various clinical circumstances (139). For example, Shafer and Varvel used PK/PD modeling approach to simulate plasma and effect site opioid concentrations after a bolus injection, brief infusion, or a prolonged infusion of fentanyl, alfentanil, or sufentanil used during anaesthesia (142). The simulation for the three drugs measured the relationship between the duration of infusion and recovery time after termination of the infusion. Data derived from the PK/PD analysis suggested that alfentanil is best used for operations longer than 6 to 8 hours when a rapid decline in effect site opioid concentration is desired to allow rapid recovery after stopping the infusion (142).

Another example is that from the work in PK/PD modeling we have come to know that buprenorphine acts as a full μ -opioid agonist for analgesia clinically, with no ceiling effect (143). However, there is a ceiling effect for respiratory depression caused by buprenorphine (143) and this knowledge gives clinicians the reassurance that the likelihood of this potentially fatal adverse effect is relatively lower compared to other opioids. Based on this and other facts, a recent review suggested that buprenorphine should be considered as a frontline agent in pain management (144). Unfortunately, buprenorphine is not suitable for acute pain management due to the prolonged time in reaching maximal peak analgesic effect of between 70 and 100 minutes (145).

In another PK/PD study, using spectral edge frequency from the electroencephalogram (EEG) as a measure of opioid effect, Scott and Stanski (146) found that the dose requirements for both fentanyl and alfentanil decreased approximately 50% from age 20 to age 89. No significant age-related changes in PK parameters of fentanyl and alfentanil were found (146). However, they found that brain opioid sensitivity (as determined by EEG changes) reduced significantly with age. This PK/PD approach brought to the conclusion that the decreased dose requirements for these opioids in the elderly is due to pharmacodynamic factors. Based on this study, it was confirmed that older patients are more 'sensitive' to opioids and consequently, drug regimens for such patients should be designed to achieve lower serum concentrations and to avoid accumulation of drug in body tissues that might lead to prolonged exposure to high serum concentrations.

1.8 Measuring the Pharmacodynamic Effects of Opioids

When administered to an individual, opioids can produce both desirable and undesirable effects. These effects can be measured using objective and subjective assessment methods. Some of the pharmacodynamic measures of opioids employed in previous studies and this study are briefly reviewed below.

1.8.1 EEG (Electroencephalography)

Electroencephalography (EEG) is a graphic representation of the difference in voltage between two different cerebral locations plotted over time (147). Processed EEG is a biomarker of opioid effect (148) which is objective, continuous, reproducible, non-invasive and sensitive (149).

1.8.2 SEM (Saccadic Eye Movement)

Saccades are fast, jerky eye movements that eyes make when moving from one point to another (150). Saccadic eye movements test gives an objective and sensitive measure of some centrally acting drugs (151) including opioids (150). Drugs that cause subjective feelings of sedation impairs saccadic eye movements in a dose-dependent manner (151). This quick test is easy to carry out, can be done repeatedly and is acceptable to both volunteers and patients (150). Compared to other performance measures, it has the advantage of being more sensitive to a variety of centrally acting drugs (150) and once initiated, is minimally dependent on voluntary control.

1.8.3 Pupillometry

Opioid-induced miosis is one of the most sensitive objective indicators of μ -opioid-receptor-mediated efficacy (152). The miosis induced by opioids has been demonstrated to be strictly dose-dependent with various opioids (152). It is generally accepted that opioid-induced miosis is mediated through the parasympathetic nervous system (153). Pupillometry provides an uncomplicated, cheap and quick assessment (154) of the intensity of opioid-induced miosis.

1.8.4 Cold pain test

Cold pain test is an experimental method for inducing pain in humans (155). It involves immersing the hand/forearm in cold water, inducing a slowly increasing pain that subsides quickly upon withdrawal of the limb from the water (155). This technique had been shown to be sensitive to the analgesic effects of opioids (156).

The use of experimental pain approaches such as this one allows the investigator to control the nature, localization, intensity, frequency and duration of the pain stimuli (137). This produces less variable and less confounded measure of pain which is suited for PK/PD modelling (137).

1.8.5 Subjective measures of opioid effect and withdrawal

The Morphine-Benzedrine Group (MBG) Scale and the Subjective Opioid Withdrawal Scale (SOWS) are both paper-and-pencil, 16 item scales. The MBG scale is a subscale of the Addiction Research Center Inventory (ARCI), a self-rating questionnaire for measuring typical drug effects (157). The MBG scale measures euphoric effects of drugs (157, 158).

The SOWS is not part of the ARCI but it was developed based on a set of 550 items comprising the ARCI (159). It is used for measuring the signs and symptoms of opioid withdrawal (159). The presence and intensity of opioid withdrawal symptoms were rated on a scale from 0 to 4 (0= not at all, 1= a little, 2= moderately, 3= quite a bit, 4= extremely) based on how the participants were feeling at assessment time (160). The minimum score for SOWS is 0 and the maximum is 64 (160).

This scale has been shown to be a reliable and valid measure of subjective symptoms of opioid withdrawal (160).

1.9 Rationale for the study

Evidence-based guidelines for clinicians on which agents to use, what doses should be considered and whether treatment doses are related to the dose and the pharmacological properties of the maintenance opioid are lacking, but needed. This study sought to determine the suitable doses of an opioid analgesic required in opioid-tolerant patients, which were able to overcome tolerance and hyperalgesia while maintaining an acceptable therapeutic index. The importance of this study is that it has the potential to improve acute pain management in the opioid-tolerant population.

Fentanyl was the opioid analgesic administered in this study. This drug was introduced into clinical practice in the early 1960s. It is a synthetic opioid which is lipid-soluble (161) with a (clinical) potency of 50 to 100 times that of morphine (162, 163). Fentanyl is one of the most widely used agents in the synthetic opioid family. Fentanyl has a short time to peak effect, short duration of action and minimal effects on histamine release (164). It is a pure agonist with no active metabolites (165), is suitable for use in patients with opioid tolerance and can be used outside of an intensive-care clinical environment. All these desirable characteristics have led to the use of fentanyl in this pilot study on the opioid-tolerant population.

2 STUDY DESIGN AND EXPERIMENTAL METHODS

2.1 Aim

To determine a dosing strategy that produces analgesia with an acceptable adverse effect and safety profile in opioid-dependent patients.

2.2 Hypothesis

It was hypothesized that a well-tolerated dose of fentanyl which produces demonstrable analgesia will be found and will be related to the patient's maintenance opioid dose.

2.3 Ethics

Approval for this study was given by the Research Ethics Committee of the Royal Adelaide Hospital, Adelaide, Australia (Royal Adelaide Hospital-Research Ethics Committee number 101013). The study was conducted in accordance with the ICH-GCP guidelines as adopted in Australia for research in humans.

2.4 Participants

2.4.1 Inclusion criteria

Inclusion criteria for this study were:

- i. Male or female, aged 18 to 65.
- ii. Maintained on any opioid with oral morphine equivalent daily dose (MEDD) of 60 mg and above (Table 11).
- iii. Have adequate intravenous access for drug infusion.
- iv. Currently abstaining from oral and intravenous recreational drug use.

2.4.2 Exclusion criteria

Exclusion criteria for this study were:

- i. Known positive for Hepatitis B, Hepatitis C or HIV
- ii. Contraindication to cold pain testing e.g. cardiac or vascular disease especially Raynaud's phenomenon, blood pressure problems, diabetes, epilepsy and recent serious injury.
- iii. Using a medication which affects pupil size.
- iv. Visual acuity poorer than 6/25 corrected (so that saccadic eye movements can be performed correctly).
- v. Patients with respiratory insufficiency and poor respiratory drive. The criteria will be a spirometry reading of less than 70% the predicted value and/or having resting oxygen saturation levels of less than 95% on air.
- vi. Subject is pregnant and/or lactating.
- vii. Chronic use of benzodiazepines which cannot be withheld for 5 half-lives of the benzodiazepine the patient is on (Table 12).
- viii. Known intolerance to fentanyl or other opioids.
- ix. Patients taking tramadol.
- x. Patients taking CYP3A4 inhibitors (amiodarone,azole antifungals, cimetidine, clarithromycin, cyclosporine, diltiazem, erythromycin, fluoroquinolones, grapefruit juice, HIV protease inhibitors, metronidazole, quinine, SSRIs and tacrolimus).

- xi. A positive urine test for benzodiazepines on the day of screening or testing.
- xii. A positive breathalyzer test on the day of testing.
- xiii. Creatinine clearance < 30 ml/min as estimated by Cockcroft-Gault formula.
- xiv. Patients with bradyarrhythmia.

2.4.3 Withdrawal criteria

- i. Intolerance to study medication or procedures.
- ii. Withdrawal of informed consent.

Table 11 Opioid equianalgesic doses (Adapted from (166))

Doses of opioids which are equivalent to 60 mg daily of oral morphine		
Opioid	IM/IV (mg)	Oral (mg)
morphine	20	60
hydromorphone	4	15
fentanyl	0.3	N/A
oxycodone	20	40
methadone	20	30
codeine	260	400
buprenorphine	0.8 (IV or patch)	1.6 (S/L)

Table 12 Five half-lives of various benzodiazepines (adapted from (167))

Type of Benzodiazepine	5 half-lives
alprazolam	2.5 days
bromazepam	5 days
clobazepam	13 days
clonazepam	11 days
diazepam	21 days
flunitrazepam	6 days

lorazepam	5 days
nitrazepam	10 days
oxazepam	4 days
temazepam	5 days
triazolam	10 hours

2.4.4 Recruitment

Over two thousand case notes of patients who attended the Pain (Chronic) Management Unit within the Royal Adelaide Hospital were scanned for potential eligibility into the study (see Figure 8). Candidates who appeared to be eligible for the study were sent a letter and the patient information sheet with a contact number; signed by their treating consultant. 227 customized letters were sent to the prospective participants from September 2011 to October 2012. Patients who made contact were screened over the phone to confirm suitability for the study. Seemingly suitable patients were then given a date for a screening visit. 9 patients on chronic opioid therapy were enrolled into the study.

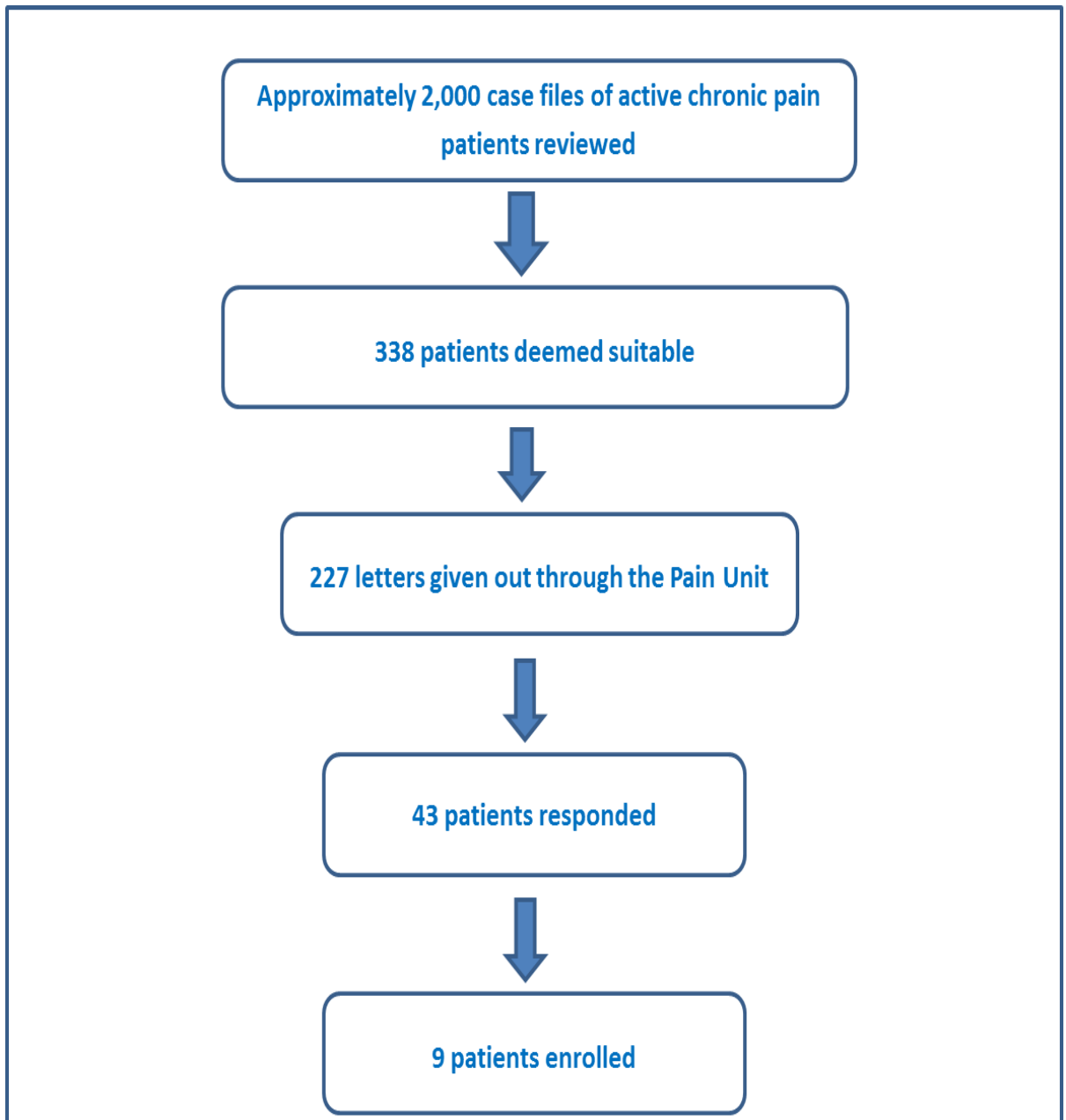


Figure 8 A flowchart summarizing the recruitment process.

2.4.5 Subjects who did not proceed or withdrew from the study

During the scanning process of the case files, a proportion of patients were not included in the list due to geographical distance between their residence and Adelaide. Patients who lived more than 50 kilometres away from the Adelaide central business district were generally not sent a letter. Not surprisingly, a significant number of patients were also on selective serotonin reuptake inhibitors (SSRIs) and they were excluded during the screening process itself as per exclusion criteria.

34 patients who were interested to participate and called the Pain and Anaesthesia Research Clinic (PARC) to express their intention to participate were not included in the study for various reasons (Table 13).

Table 13 Reasons for seemingly eligible patients to not proceed to the screening stage

Reason	Number of patients	Inclusion/Exclusion criteria
A) Drug-related issues		
Taking benzodiazepine(s) and could not withhold it for 5 half-lives of the drug	4	Exclusion vii
Taking Tramadol	1	Exclusion ix
Taking SSRI	2	Exclusion x
Doses of opioids below 60 mg MEDD	4	Inclusion ii
Actively abusing drugs	2	Inclusion iv
B) Medical conditions		
Physically challenged (paraplegia, hemiplegia and one-handedness)	3	-
Visual problems	2	Exclusion iv
Respiratory problems (Severe COPD or asthma)	1	Exclusion v
History of Hepatitis B/C/HIV infection	4	Exclusion i
C) Miscellaneous reasons		
Transportation problem	4	-
Changed circumstances	3	-
Advised by GP against participating	1	-
Change of mind	1	-
Undecided	1	-
Passed away	1	-

2.5 Study plan and design overview

The study was of a single or double session open-label non-randomized dose-escalating design.

The participants received a concentration-targeted computer-controlled intravenous infusion of fentanyl using STANPUMP. Tolerability and pharmacodynamics were assessed by adverse events, vital signs, cold pain tolerance times, computerised pupillometry, electroencephalography (EEG), eye movements test, Morphine-Benzedrine Group (MBG) Scale and the Subjective Opioid Withdrawal Scale (SOWS).

On each day of the session, the participants were instructed to take their scheduled opioid maintenance dose as usual and no dose was omitted. The fentanyl infusion was up to 4 “staircase” infusions of 30 mins, sequentially without washout. The patients were stratified into two groups.

The first group of patients were taking oral morphine equivalent daily dose (MEDD) of below 200 mg. For these participants, the target effect site concentration for the first infusion was 2 ng/ml. The subsequent steps were 4, 6 and then 8 ng/ml.

If a patient failed to achieve satisfactory analgesia during the first visit, the patient would come for a second visit. Satisfactory analgesia was defined as having a cold pain tolerance test reading twice the baseline value or reaching the absolute value of 120 seconds.

During the second visit, the target effect site concentration for the first infusion was 4 ng/ml. The subsequent steps were 8, 12 and 16 ng/ml of fentanyl at the effect site.

The second group of patients were on oral morphine equivalent daily dose (MEDD) of 200 mg and above. For these volunteers, the target effect site concentration for the first infusion was 4 ng/ml. The subsequent steps targeted 8, 12 and 16 ng/ml of fentanyl at the effect site.

If a patient in this group failed to achieve satisfactory analgesia during the first visit, the patient would come for a second visit. During the second visit, the target effect site concentration for the first infusion was 8 ng/ml. The subsequent steps targeted 16, 24 and 32 ng/ml of fentanyl at the effect site.

A battery of tests to measure the desired and undesired opioid effects were performed about 30 minutes before starting the first infusion as baseline reading and after 10 minutes of commencing each infusion step.

Participants were required to stay at the Pain and Anaesthesia Research Clinic (PARC) for 6 hours after the end of the infusion and were instructed not to drive for 24 hours after discharge from PARC. Transportation was provided for the study day. Based on simulations, it takes about only 3 hours for the concentration of fentanyl at the effect site to reach 30% of the highest level after stopping the infusion. Nevertheless, for the sake of prudence the patients were kept for another 3 hours.

2.6 Screening

Before enrolment in the study, each subject was assessed for their suitability according to the inclusion and exclusion criteria. The screening visit consisted of:

- Medical history and case note review

- Medication history
- Physical examination
- Biochemistry screen
- ECG
- Urine pregnancy test for women of child bearing potential
- Urine for benzodiazepines and other drugs of abuse
- Breathalyzer test
- Spirometry (if indicated)

Screening was to take place no more than 14 days prior to the scheduled dosing date.

2.7 Familiarisation session

Following successful screening, participants underwent a familiarisation session to accustom them to the experimental procedures of the cold pain test, EEG, saccadic eye movement recording, pupillometry, and pencil-and-paper rating scales.

2.8 Requirements Prior To Study Day

Caffeine and alcohol were restricted for 24 hours prior to each study session and until the test battery completion on the study day. The patients were also requested to have their hair washed on the night before or the morning of the test and leave it clean and dry. They were also to refrain from applying hair sprays, conditioners, oils, gels, or chemicals on the hair on the day of the test. This was done to reduce the impedance for the EEG and saccadic eye movement readings.

2.9 Requirements after Discharge on the Study Day

As a small degree of sedation could last for up to 24 hours after dosing, the volunteers were expected not to drive, cycle, operate heavy machinery or sign important documents for at least 24 hours after the study. A taxi was made available to send the participants home after the study day. They were also advised not to consume alcohol for 24 hours after the study. Recommendations were also given that a friend or relative be present to help the patient with any needs during the night after the study. The participants were allowed to go back to work 24 hours after a study day completion.

2.10 Testing Day Schedule

The study consisted of a one or two day study with identical schedule (Figure 9). Participants usually arrived at the study site at approximately 8 am in the morning. On arrival:

- i. 45 minutes before starting the infusion, urine for benzodiazepines and drugs of abuse and breathalyser for alcohol level were tested.
- ii. Baseline vital signs (blood pressure, pulse rate and respiratory rate), sedation score and pulse oximetry were then recorded.
- iii. The patient was then encouraged to go to the toilet to empty the bowel and bladder prior to starting of the study.
- iv. Electrodes were applied to the patient's scalp and face for EEG and saccadic eye movement analysis.
- v. A single indwelling venous catheter for drug administration was then inserted into the best available forearm vein in the subject's dominant arm.

30 minutes prior to starting the infusion and starting 10 minutes after the start of each infusion step the following tests were administered:

- a. EEG
- b. Saccadic eye movement (SEM) assessment (a measure of sedation to opioids)
- c. MBG scale to assess subjective opioid effect
- d. Pupillometry
- e. Cold pain tolerance test

SOWS scale was subsequently administered to detect opioid withdrawal at 15, 30 and 60 minutes after the end of the infusion.

Vital signs (blood pressure, pulse rate, respiratory rate) and sedation score were monitored at the 5th, 25th, 35th, 55th, 65th, 85th, 95th and 115th minute. At the 120th minute the readings were done once and subsequently they were done every 30 minutes until the patient was discharged. Pulse oximetry was monitored continuously except during the test batteries for 15 minutes. The vital signs, respiratory rate and pulse oximetry were monitored more frequently if clinically indicated.

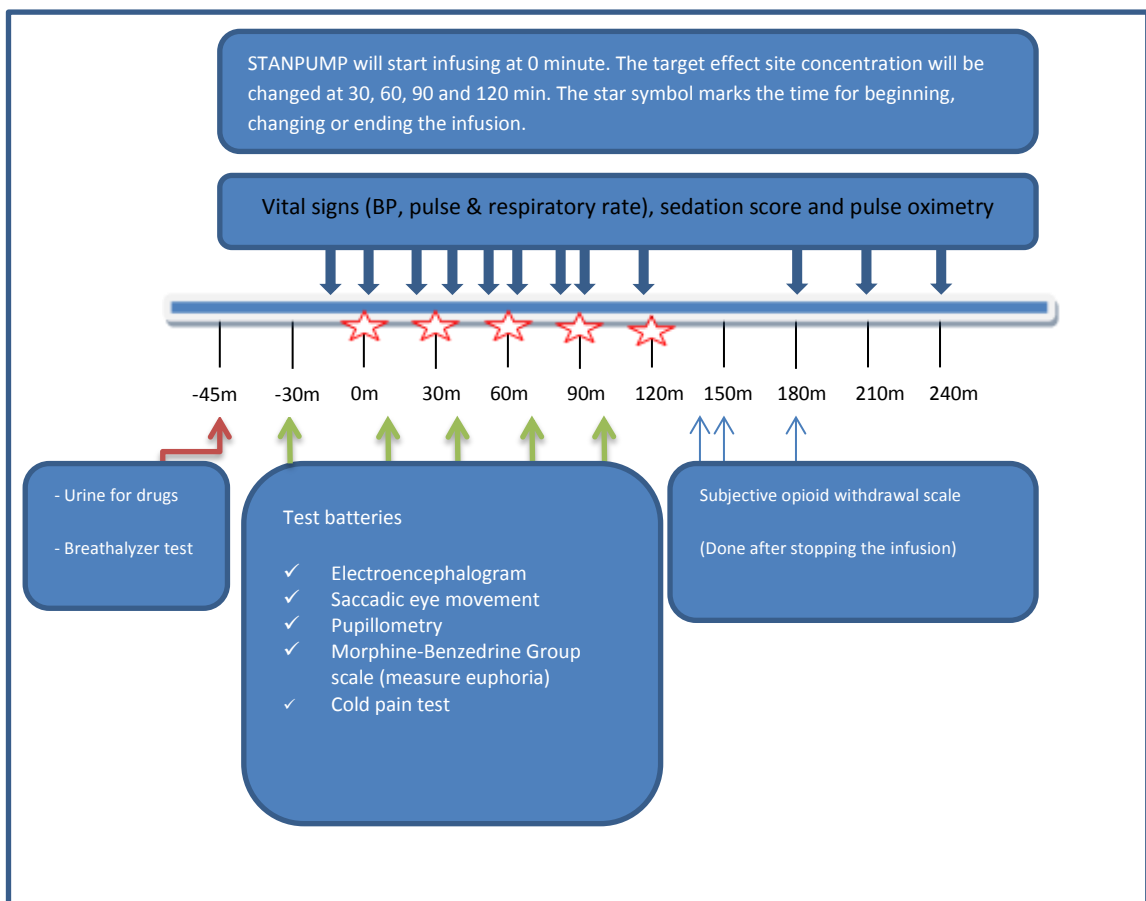


Figure 9 Study design

Dosing was ceased if:

- Satisfactory analgesia was attained demonstrated by having a cold pain tolerance test reading twice the baseline value or reaching the absolute value of 120 seconds.
- Estimated arterial oxygen saturation by pulse oximetry was persistently less than 90% for more than 1 minute which was not corrected by rousing.
- RAH sedation score of 2 or more (Refer Table 15).
- Heart rate of 45 beats per minute or less.
- Intolerable adverse effects.
- The subject wished to discontinue.
- The investigator deemed that it was in the best interest of the participant not to continue.

The subject was kept under observation for approximately a total of 9 hours for each session or longer if necessary to ensure that he or she was safe for discharge.

2.11 Pharmacokinetic parameters

For fentanyl infusions, the STANPUMP software offers three choices of pharmacokinetic parameters to choose from. We have chosen the parameters by Shafer for this study (Table 14).

Table 14 Pharmacokinetic parameters for the fentanyl infusions

V_c	6.0900 litres
k_{10}	0.0827 / minute
k_{12}	0.4710 / minute
k_{13}	0.2250 / minute
k_{21}	0.1020 / minute
k_{31}	0.0060 / minute
V_2	28.1215 litres
V_3	228.3750 litres
Cl_1	0.5036 litres / minute
Cl_2	2.8684 litres / minute
Cl_3	1.3703 litres / minute
k_{e0}	0.1470 / minute
$t_{1/2\alpha}$	0.8201 min
$t_{1/2\beta}$	17.2215 min
$t_{1/2\gamma}$	465.5648 min
$t_{1/2\alpha} k_{e0}$	4.7143 min

2.12 Methods

2.12.1 Clinical conduct

The study took place at the Pain and Anaesthesia Research Clinic (PARC) within the Royal Adelaide Hospital. Medical and nursing personnel familiar with managing complications of opioid therapy were in attendance. Equipment for intravenous drug administration and respiratory support with medications for managing opioid adverse effects (ondansetron, muscle relaxants and naloxone) were also readily available.

2.12.2 EEG (Electroencephalography) and SEM (Saccadic Eye Movement)

EEG recordings were done using gold electrodes fixed at Fz (frontal), Cz (central), Pz (parietal) and Oz (occipital) positions with the same common ground electrode as for the saccadic eye movement registration (10/20 system). EEG signals were obtained from leads Fz-Cz and Pz-Oz and a separate channel to record eye movements (for artefacts). The signals were amplified using a Grass Telefactor (F-15EB/B1) and a 15LT series Amplifier Systems (Grass Telefactor, Braintree, USA) with a time constant of 0.3 seconds and a low pass filter at 100 Hz. Data was collected and analysed using a validated Spike2 script (Cambridge Electronics Design, Cambridge, UK). Eight consecutive blocks of eight seconds were recorded per session. The analog signal was digitised using a CED 1401 Power (Cambridge Electronics Design, Cambridge, UK). For each lead, fast Fourier transform analysis was performed to obtain the sum of amplitudes in the very low (0.5-2.0 Hz), delta (2.0-4.0 Hz), theta (4.0-7.5 Hz), alpha (7.5-13.5 Hz), beta (13.5-35 Hz) and gamma (35.1-48.8 Hz) frequency ranges. The duration of EEG measurements were 64 seconds per session.

Head movements were restrained using a fixed head support or by telling the patient to not move his or her head during the test. The target consisted of a moving dot that was displayed on a computer screen. This screen was fixed at 58 cm in front of the head support. Saccadic eye movements were recorded for stimulus amplitudes of approximately 15 degrees to either side. Fifteen saccades were recorded with interstimulus intervals varying randomly between 3 and 6 seconds. The average values of latency (reaction time), saccadic peak velocity, saccadic inaccuracy (calculated as the difference between stimulus angle and corresponding saccade, expressed as a percentage of the stimulus angle) and number of valid saccades were collected for all artifact-free saccades.

Materials

- Neurocart machine (Centre for Human Drug Research, Netherlands)
- 4 gold surface electrodes (FS-E5GH-48 from Grass Technologies, West Warwick, USA)
- Blue Sensor N-00-S/25 electrodes (Ambu A/S, Ballerup, Denmark)
- Electrocaps (Easycap, Gmbh, Germany)
- Measuring tape
- Skin pen

- Nuprep Prep Gel 4 ounces tube (Weaver and Company, Aurora, Colorado, USA)
- EC2 electrolyte paste (Astro-Med, West Warwick, USA)
- Gauze
- GRASS F-EZM4A electrode impedance meter (Grass Technologies, West Warwick, USA)
- Mini electrode board F-15EB (Grass Technologies, West Warwick, USA)
- Fixomull stretch 5cm x 10 cm (BSN medical GmbH, Hamburg, Germany)

Set-up procedure

The set-up procedures were based upon the standard operating procedures (SOPs) provided by the Centre for Human Drug Research (CHDR), Netherlands.

The Neurocart machine was set up according to the CCNSETUP SOP (CHDR, Netherlands). The general setting for the procedure was in accordance with the CCNGENPR SOP.

While seating comfortably on a chair, a measuring tape was put in a straight line over the head from the nasion to the inion. The nasion is the point in the skull where the nasal bone meets the frontal bone and the inion is the most prominent projection of the occipital bone at the posteroinferior part of the skull. The total distance between the nasion and the inion was measured. The electrode locations and distances between the electrodes were then defined as 10% or 20% of the distance between the two points. A stripe was made with a skin pen on the forehead at 10% above the nasion. For example, if the total distance between the nasion and the inion in a subject was 32 cm, then a stripe will be made at 3.2 cm above the nasion. This is the frontopolar point where the earth electrode for the eye measurement was applied.

Subsequently a stripe was made at 30% of the distance from nasion to inion in the posterior direction. This is the frontal point (Fz). 20% from the frontal point is the central point (Cz) where another stripe was made. After that, another stripe on the scalp was made at 20% from the central point at the parietal point (Pz). Subsequently, 20% from the parietal point, a stripe was made at the occipital point (Oz).

The measuring tape was then placed on top of both ears and over the head of the volunteer. The distance was measured and divided by two. A stripe was made half-way on the volunteers scalp. This was repeated another three times to make it cross with the Fz, Cz, Pz and Oz marks that were made.

The electrode-box was then hung around the neck of the volunteer. Some Nuprep gel was applied on gauze. The areas next to both eyes, the frontopolar point and the four points on the scalp were scrubbed to remove layers of old cells and reduce skin resistance. Surplus gel was wiped with gauze. Two eye-electrodes were applied lateral to the outer canthi of both eyes. The ground electrode was applied 10% above the nasion.

The subject's hair was parted and exposed at the areas where EEG electrodes will be placed. The electrode cups were filled with the EC2 paste while making sure that it was filled on all sides. The

electrodes were put on the scalp at the four respective points and pressure was applied for a few seconds. The extra paste that came out of the cup was spread over the cup.

A thin tuft of hair was stretched over the cup and then rubbed with the paste coming out of the cup. Another tuft of hair was then made to cross over the cup tightly. The other ends of the electrodes were then plugged into the electrode board.

The F-EZM4A electrode impedance meter was used to check the impedance levels of all electrodes. When measuring the ISOGND lead, 6 k Ω was subtracted from the reading to get actual electrode impedance. This is in accordance with the GRASS EZM user's manual.

The resistance of each electrode was ensured to be lower than 5 k Ω . The electrodes were then attached on the shoulder of the volunteer with a plaster while ensuring that the patient was able to move his or her head freely.

After about 10 minutes of applying the EEG electrodes, a bandage (Fixomull) was applied on the four scalp locations.

Test administration

The experimenter described to the subject the purpose of the test and the procedure as follows:

We will be monitoring your brain wave activity and subsequently measure how quickly your eyes move using this computer system called Neurocart. This has been shown to be a good way to measure the effect of strong painkillers. To do this test, fine wires will be attached on top of the forehead and a little bit in front of your ears. We will apply some light paste to the skin before attaching the electrodes to have good contact and reduce resistance for proper reading of the result. The electrodes will stay in place for the study duration. The EEG test will take about two minutes. You just need to relax your whole body and close your eyes during the test. You are not allowed to talk or move during the test.

After the EEG, the eye movement test will be done which takes about two minutes. Your chin will be rested on a head support during the short duration of the test. You are required to follow the target which is a dot on the computer screen about half metres from your eyes. This painless test does not usually cause any discomfort.

2.12.3 Pupillometry

Materials

- Compact Integrated Pupillograph (CIP; AMTech Pupilknowlogy GmbH, Dossenheim, Germany)
- Table and headframe (AMTech, Dossenheim, Germany)
- Make a sign indicating a fixed point, X
- Light meter (Easy View 31, Extech Instruments, Massachusetts, USA)

Set-up procedure

1. The environmental conditions were kept constant throughout the testing especially with regards to lighting and placement of the subject during pupillometry.
2. Lighting in the room was adjusted so that the light intensity was between 3-12 lux at measurement site and there was no single source of bright light.
3. The subject was allowed to adjust to the room conditions for a minimum of 10 minutes before starting the procedure.
4. A fixed red mark, greater than 1 meter away from the subject was put up on the wall for the subject to focus on during the test. The fixed point was at about 10-20 degrees above the subject's eye level.
5. The power cable was plugged into the wall socket and the main green button was pushed.
6. The rocker switch located next to the main green switch was used to drive the table up and down.
7. The hollow rubber bellow was ensured to be attached to the magnet on the measuring head.
8. The CIP was switched on using the ON/OFF button.
9. The MODE button was pressed until AVD was displayed at the bottom of the screen.

Test administration

1. The height of the table and the chin rest was ensured to be comfortable using the rocker switch and the height-adjustable chin rest.
2. The subject was asked to move away from the head rest before the height was adjusted.
3. The subject was instructed to put the chin on the rest with the forehead against the frame.
4. The subject was instructed to focus on the mark on the wall.
5. The measuring head was lined up with the subject's right eye so that the pupil was visible using the lever on the sledge.
6. The camera was then adjusted using the X-Y-Z joystick located on the sledge. The height of the measuring head was adjusted by turning the X-Y-Z joystick clockwise or anticlockwise.
7. The horizontal dotted line was ensured to be passing through the center of the pupil and was above the two infra-red (IR) reflections.
8. The vertical lines (on the horizontal dotted line) was adjusted to ensure capture of the edge of the pupil at its widest point only and not the infra-red reflection dots, the width of the iris, or any other object.

9. Image focus was achieved by changing the distance between the CIP and the subject's eye.
10. The eye was ensured to be in sharp focus before and during the measurement by aiming for a constant green light.
11. Just prior to recording, the subject was instructed to not blink until they heard the second beep.
12. The red button located on the left of the sledge was pressed to start recording. The recording took 4 seconds and the countdown was displayed on the top right corner of the CIP screen.
13. The subject was allowed to blink again.
14. The trigger was pressed 3 times to prepare the CIP for another recording if such was required.
15. After use the CIP head frame and rubber bellow was cleaned with a dry or moist cloth.

The experimenter described to the subject the purpose of the test and the procedure as follows:

This is a pupillometer. It will take an accurate measure of the diameter (width) of your pupil, the black circle in your eye. This black bellow sits around your right eye [indicate] and you rest your chin and forehead on the frame [indicate] while I take a measurement of your pupil diameter. It is a completely painless procedure.

The basic procedure was explained as follows:

I want you to focus, with your left eye, on the fixed point on the wall behind me [indicate]. I will line up your pupil on the screen and when I have the right positioning I will warn you that I am about to take a measurement. You will hear 2 beeps, 4 seconds apart – try not to blink until you hear the second beep. Do you have any questions?

2.12.4 Cold pain test

Materials

- 2 x 20 litres plastic cylindrical containers (41 cm in depth and 29 cm in diameter)
- Digital Thermometer (Checktemp1, Hanna Instruments, USA)
- Blindfold
- Sphygmomanometer
- Digital timer (with seconds display)
- Heating immersion circulator (Julabo ED 230V/50Hz GmbH, Seelbach, Germany)
- Water pump (Unistar PS 700F, China)
- Towel

Set-up procedure

Warm water was filled into one container up to 5 cm from the top of the container. The heating immersion circulator was then immersed into the container and set at 35°C. The second container was filled with crushed ice up to 10 cm below the top of the container. Water was added until the container was filled up to 5 cm from the top. The water was stirred to ensure even mixing of the ice and water and that there were no large clumps of ice. The temperature of the water/ice combination was then checked with a digital thermometer and water or ice added as required to achieve a temperature between 0.5 and 1.5°C. The two containers were placed on a trolley 10 cm apart with the warm container on the left hand side. The water pump was placed at the bottom of the cold water container on the far side of the container (away from where the subject will stand) with the water jet facing upwards.

Test administration

The experimenter described to the subject the purpose of the test and the procedure as follows:

This is the cold pain test. It is a test of your tolerance to cold pain. Here are two water containers, one filled with warm water and one filled with ice and cold water. You will place your non-dominant hand into the warm water container for two minutes, then take it out and put it immediately into the cold water container. When your hand is in the cold water container, there are two things I will ask you to tell me: tell me when you first feel pain, then leave your hand in the cold water for as long as you can possibly tolerate the pain. Then, tell me when you feel you can no longer tolerate the pain, and remove your hand from the water. I will pass you a towel, which you may use to dry your hand. While you are completing the test you will be blindfolded, and I will inflate a blood pressure cuff on your arm just before you transfer your hand to the cold water container. This is to control for other factors that may interfere with the results. There is a water pump in the cold water container to keep the water circulating and stop the ice from clumping together. When you put your hand in each water container, immerse your hand quickly but carefully. As you will be blindfolded, I will help you transfer your hand from the warm water to the cold water. Keep your fingers straight and spread apart. Do not touch the sides or the bottom of the container and try not to move your hand around too much in the water.

I will not speak to you during the test except to give you reminder instructions. You should not speak during the test unless you have an urgent question or concern. The pain you experience from the test disappears quickly after removing your hand from the cold water, and there is no risk of permanent damage.

Every person is different in terms of his or her pain sensitivity. It is very important that we obtain an accurate and honest assessment of your pain tolerance. There is no reward for setting a record time, but please try to perform the test honestly and leave your hand in the cold water for as long as you can tolerate the pain.

The experimenter then ensured that the subject understood the instructions and enquired whether the subject had any questions before commencing the test. The subject was then seated in a comfortable chair and his/her blood pressure taken. The subject then stood in front of the containers at an appropriate distance such that the non-dominant hand could be fully immersed in the container. The temperature of the water in each container was checked with a digital thermometer, and adjusted if necessary to ensure that the temperature was within the required range (warm water: 34.5-35.5°C; cold water: 0.5-1.5°C). A blood pressure cuff was attached to the

non-dominant arm, and a blindfold placed over the eyes. With the assistance of the experimenter, the subject rapidly immersed the non-dominant hand into the warm water container. The fingers of the immersed hand were spread apart comfortably, the hand held vertically and immersed such that there was no contact with the sides of the container. The digital timer was activated as soon as the arm was immersed. At 1 minute 45 seconds, the blood pressure cuff was inflated to 20 mmHg below the diastolic pressure (baseline reading) and remained inflated for the subsequent duration of the test. At exactly 2 minutes, the subject was assisted in transferring the immersed hand to the cold water container. Another digital timer was started as soon as the hand was immersed in the cold water. The experimenter reminded the subject “Tell me when you first feel pain”. The time was recorded (in seconds from the immersion of the hand in cold water) when the subject verbally indicated the onset of pain (pain threshold). The experimenter then instructed the subject “Now leave your arm in the water as long as you can tolerate the pain”. The subject verbally indicated when the pain could no longer be tolerated (pain tolerance), the time was recorded, and the subject was assisted in removing the hand from the water. The subject was offered a towel to dry the arm, the blindfold was removed and the blood pressure cuff deflated. If a subject’s hand remained in the cold water container beyond 120 seconds from the time of immersion, he/she was asked to withdraw his/her hand and informed that beyond this point the numbness of the hand prevented continuation of the test. In these circumstances, pain tolerance was recorded as 120 seconds.

2.12.5 Subjective measures of opioid effect and withdrawal

The Morphine-Benzedrine Group (MBG) Scale and the Subjective Opioid Withdrawal Scale (SOWS) are both paper-and-pencil, 16 item scales. The two scales took approximately 3-5 minutes to complete.

2.12.6 Physiologic and Adverse Event Measures

Oxygen saturation, heart rate and blood pressure were monitored while the subject was in the clinical rooms by using an Agilent A3® (Phillips) monitor.

2.12.7 Adverse effect monitoring

As a consistent method of eliciting adverse events, the subject was asked a non-leading question as “How do you feel?” This question was asked every time the vital signs were taken.

2.12.8 Sedation measurement

The Royal Adelaide Hospital Sedation Score was used to assess sedation.

Table 15 The Royal Adelaide Hospital Sedation Score

Score	Level of Sedation	Descriptor
0	None	Awake
1	Mild	Occasionally drowsy, easy to rouse, and can stay awake once woken
2	Moderate	Constantly drowsy, still easy to rouse, unable to stay awake once woken

3	Severe	Somnolent, difficult to rouse, severe respiratory depression
S	Normally Asleep	Easy to rouse

2.12.9 General modelling methods

A mixed effect ("population") modelling approach was used (168). Population models describe the variability in drug concentration, drug effects or disease at three levels in a population: 1. Explainable variability (mechanistic models and patient-specific covariates). 2. Variability explainable by random differences between subjects. 3. Residual unexplainable variability. For the present analysis, the independent variable was the target fentanyl effect compartment concentration as programmed in STANPUMP, and the dependent variables were the various pharmacodynamic measures described above.

Population models were implemented using R software (Version 2.14.2; R Foundation for Statistical Computing, Vienna, Austria) and the SAEMIX package (version 0.96, July 1st, 2011, Emmanuelle Comets). This package implements the Stochastic Approximation Expectation Maximization algorithm in R, which is the same mixed effect modelling method implemented in the Monolix program. An important advantage of using R for the data analysis was that model fitting could be automated using scripts allowing a large number of candidate models to be tested for each pharmacodynamic metric.

2.12.10 Model development strategy

As the number of PD metrics to examine was large, a time- efficient model development strategy was needed. A standard array of models were coded and run for each PD metric. These models (given the sparseness of the data) covered the important plausible structural and covariate models that should have been considered and hence represented a rational model development strategy. The modelling approach using the SAEMIX package in R was selected specifically because it allowed running a suite of candidate models for each PD metric in an automated fashion. It should be noted that the SAEMIX package is based on Monolix 3.2, and that Monolix estimates random effects for all parameters such that optimising the random effect structure is unnecessary in a way that may be familiar to NONMEM users. We believe that similar conclusions would be reached whether SAEMIX or NONMEM software were used.

2.12.11 Pharmacodynamic models

Various models of the target concentration-effect relationship were examined for each pharmacodynamic metric.

2.12.11.1 Linear model

These models were used to test whether target fentanyl effect site concentration had any influence on the pharmacodynamic metrics (e.g. pupil size). The model was tested for whether the MEDD (morphine-equivalent daily dose) had any effect on the intercept and slope. The assumed distribution of the baseline PD metric was set to be either having a normal or log-normal distribution and the residual unexplained variability either constant (additive) or proportional.

The linear models were determined to be either additive or proportional to the baseline metric. Additive models add the drug effect to the baseline distribution while proportional models make the drug effect proportional to the baseline distribution.

Linear additive function,

$$PD_{ij} = Baseline_i + Slope_i * C_{tar,ij}$$

where PD_{ij} is the j th pharmacodynamic observation in the i th patient, $Baseline_i$ is the Baseline PD effect at 0 concentration in the i th patient, $Slope_i$ is the slope of the concentration-effect relationship in the i th patient and $C_{tar,ij}$ is the j th predicted target fentanyl concentration in the i th patient

Linear proportional function,

$$PD_{ij} = Baseline_i * (1 + Slope_i * C_{tar,ij})$$

Table 16 Linear additive models

Model name	Baseline distribution	Residual unexplained variability	MEDD on baseline	MEDD on slope
LinearAdd 1	normal	constant	no	no
LinearAdd 2	normal	proportional	no	no
LinearAdd 3	log-normal	constant	no	no
LinearAdd 4	log-normal	proportional	no	no
LinearAdd 5	normal	constant	yes	no
LinearAdd 6	normal	proportional	yes	no
LinearAdd 7	log-normal	constant	yes	no
LinearAdd 8	log-normal	proportional	yes	no
LinearAdd 9	normal	constant	no	yes
LinearAdd 10	normal	proportional	no	yes
LinearAdd 11	log-normal	constant	no	yes
LinearAdd 12	log-normal	proportional	no	yes
LinearAdd 13	normal	constant	yes	yes
LinearAdd 14	normal	proportional	yes	yes
LinearAdd 15	log-normal	constant	yes	yes
LinearAdd 16	log-normal	proportional	yes	yes

MEDD on baseline and MEDD on slope indicate should MEDD be tried as a covariate on the baseline/slope.

Table 17 Linear proportional models

Model name	Baseline distribution	Residual unexplained variability	MEDD on baseline	MEDD on slope
LinearProp 1	normal	constant	no	no
LinearProp 2	normal	proportional	no	no
LinearProp 3	log-normal	constant	no	no
LinearProp 4	log-normal	proportional	no	no
LinearProp 5	normal	constant	yes	no
LinearProp 6	normal	proportional	yes	no
LinearProp 7	log-normal	constant	yes	no
LinearProp 8	log-normal	proportional	yes	no
LinearProp 9	normal	constant	no	yes
LinearProp 10	normal	proportional	no	yes
LinearProp 11	log-normal	constant	no	yes
LinearProp 12	log-normal	proportional	no	yes
LinearProp 13	normal	constant	yes	yes
LinearProp 14	normal	proportional	yes	yes
LinearProp 15	log-normal	constant	yes	yes
LinearProp 16	log-normal	proportional	yes	yes

MEDD on baseline and MEDD on slope indicate should MEDD be tried as a covariate on the baseline/slope.

2.12.11.2 Zero slope models

These models had a linear concentration-effect relationship but the population slope was fixed to zero (no population drug effect). The models were tested to see whether baseline MEDD (morphine-equivalent daily dose) had any effect on the intercept (baseline). The assumed distributions of the baseline PD metrics were set to be either having a normal or log-normal distribution and the residual unexplained variability either constant or proportional (Table 18).

Table 18 Description of tested models for zero slope model

Model name	Baseline distribution	Residual unexplained variability	MEDD on baseline
Zero 1	normal	constant	no
Zero 2	normal	proportional	no
Zero 3	log-normal	constant	no
Zero 4	log-normal	proportional	no
Zero 5	normal	constant	yes
Zero 6	normal	proportional	yes
Zero 7	log-normal	constant	yes
Zero 8	log-normal	proportional	yes

MEDD on baseline indicates should MEDD be tried as a covariate on the baseline.

2.12.11.3 E_{max} model

The E_{max} concentration-effect relationship described maximum effect (E_{max}) and concentration at which half the maximum effect was achieved (EC_{50}). The model was tested for whether MEDD had any effect on the baseline, EC_{50} and E_{max} . The assumed distribution of the baseline PD metric was set to be either having a normal or log-normal distribution and the residual unexplained variability either constant or proportional.

The E_{max} model used was either additive or proportional to the baseline value of the metric.

E_{max} additive function,

$$PD_{ij} = Baseline_i + \frac{(Emax_i * C_{tar,ij})}{(EC50_i + C_{tar,ij})}$$

where PD_{ij} is the j th pharmacodynamic observation in the i th patient, $Baseline_i$ is the Baseline PD effect at 0 concentration in the i th patient, $Slope_i$ is the slope of the concentration-effect relationship in the i th patient and $C_{tar,ij}$ is the j th predicted target fentanyl concentration in the i th patient

E_{max} proportional function,

$$PD_{ij} = Baseline_i * (1 + \frac{(Emax_i * C_{tar,ij})}{(EC50_i + C_{tar,ij})})$$

Table 19 E_{max} additive models

Model name	Baseline distribution	Residual unexplained variability	MEDD on baseline	MEDD on EC_{50}	MEDD on E_{max}
EmaxAdd 1	normal	constant	no	no	no
EmaxAdd 2	normal	proportional	no	no	no
EmaxAdd 3	log-normal	constant	no	no	no
EmaxAdd 4	log-normal	proportional	no	no	no
EmaxAdd 5	normal	constant	yes	no	no
EmaxAdd 6	normal	proportional	yes	no	no
EmaxAdd 7	log-normal	constant	yes	no	no
EmaxAdd 8	log-normal	proportional	yes	no	no
EmaxAdd 9	normal	constant	no	yes	no
EmaxAdd 10	normal	proportional	no	yes	no
EmaxAdd 11	log-normal	constant	no	yes	no
EmaxAdd 12	log-normal	proportional	no	yes	no
EmaxAdd 13	normal	constant	no	no	yes
EmaxAdd 14	normal	proportional	no	no	yes
EmaxAdd 15	log-normal	constant	no	no	yes
EmaxAdd 16	log-normal	proportional	no	no	yes
EmaxAdd 17	normal	constant	yes	yes	yes
EmaxAdd 18	normal	proportional	yes	yes	yes
EmaxAdd 19	log-normal	constant	yes	yes	yes
EmaxAdd 20	log-normal	proportional	yes	yes	yes

MEDD on E_{max} , etc indicate should MEDD be tried as a covariate on the parameter in question.

Table 20 E_{max} proportional models

Model name	Baseline distribution	Residual unexplained variability	MEDD on baseline	MEDD on EC ₅₀	MEDD on E _{max}
E _{max} Prop 1	normal	constant	no	no	no
E _{max} Prop 2	normal	proportional	no	no	no
E _{max} Prop 3	log-normal	constant	no	no	no
E _{max} Prop 4	log-normal	proportional	no	no	no
E _{max} Prop 5	normal	constant	yes	no	no
E _{max} Prop 6	normal	proportional	yes	no	no
E _{max} Prop 7	log-normal	constant	yes	no	no
E _{max} Prop 8	log-normal	proportional	yes	no	no
E _{max} Prop 9	normal	constant	no	yes	no
E _{max} Prop 10	normal	proportional	no	yes	no
E _{max} Prop 11	log-normal	constant	no	yes	no
E _{max} Prop 12	log-normal	proportional	no	yes	no
E _{max} Prop 13	normal	constant	no	no	yes
E _{max} Prop 14	normal	proportional	no	no	yes
E _{max} Prop 15	log-normal	constant	no	no	yes
E _{max} Prop 16	log-normal	proportional	no	no	yes
E _{max} Prop 17	normal	constant	yes	yes	yes
E _{max} Prop 18	normal	proportional	yes	yes	yes
E _{max} Prop 19	log-normal	constant	yes	yes	yes
E _{max} Prop 20	log-normal	proportional	yes	yes	yes

2.12.11.4 Sigmoid E_{max} model

The sigmoid E_{max} concentration-effect relationship described the maximum effect (E_{max}), concentration at which half the maximum effect was achieved (EC₅₀) and the Hill constant. The model was tested for whether MEDD had any effect on the baseline, EC₅₀ and E_{max}. The assumed distribution of the baseline PD metric was set to be either having a normal or log-normal distribution and the residual unexplained variability either constant or proportional.

The sigmoid E_{max} model used was either additive or proportional to the baseline metric.

Sigmoid E_{max} additive function,

$$PD_{ij} = Baseline_i + \frac{(E_{max_i} * C_{tar,ij}^{hill_i})}{(EC50_i^{hill_i} + C_{tar,ij}^{hill_i})}$$

where PD_{ij} is the jth pharmacodynamic observation in the ith patient, Baseline_i is the Baseline PD effect at 0 concentration in the ith patient, Slope_i is the slope of the concentration-effect relationship in the ith patient and C_{tar,ij} is the jth predicted target fentanyl concentration in the ith patient.

Sigmoid E_{\max} proportional function,

$$PD_{ij} = Baseline_i * \left(1 + \frac{(Emax_i * C_{tar,ij}^{hill_i})}{(EC50_i^{hill_i} + C_{tar,ij}^{hill_i})}\right)$$

Table 21 Sigmoid Emax additive models

Model name	Baseline distribution	Residual unexplained variability	MEDD on baseline	MEDD on EC_{50}	MEDD on E_{\max}
SigmoidEmaxAdd 1	normal	constant	no	no	no
SigmoidEmaxAdd 2	normal	proportional	no	no	no
SigmoidEmaxAdd 3	log-normal	constant	no	no	no
SigmoidEmaxAdd 4	log-normal	proportional	no	no	no
SigmoidEmaxAdd 5	normal	constant	yes	no	no
SigmoidEmaxAdd 6	normal	proportional	yes	no	no
SigmoidEmaxAdd 7	log-normal	constant	yes	no	no
SigmoidEmaxAdd 8	log-normal	proportional	yes	no	no
SigmoidEmaxAdd 9	normal	constant	no	yes	no
SigmoidEmaxAdd 10	normal	proportional	no	yes	no
SigmoidEmaxAdd 11	log-normal	constant	no	yes	no
SigmoidEmaxAdd 12	log-normal	proportional	no	yes	no
SigmoidEmaxAdd 13	normal	constant	no	no	yes
SigmoidEmaxAdd 14	normal	proportional	no	no	yes
SigmoidEmaxAdd 15	log-normal	constant	no	no	yes
SigmoidEmaxAdd 16	log-normal	proportional	no	no	yes
SigmoidEmaxAdd 17	normal	constant	yes	yes	yes
SigmoidEmaxAdd 18	normal	proportional	yes	yes	yes
SigmoidEmaxAdd 19	log-normal	constant	yes	yes	yes
SigmoidEmaxAdd 20	log-normal	proportional	yes	yes	yes

Table 22 Sigmoid E_{max} proportional models

Model name	Baseline distribution	Residual unexplained variability	MEDD on baseline	MEDD on EC_{50}	MEDD on E_{max}
SigmoidE _{max} Prop 1	normal	constant	no	no	no
SigmoidE _{max} Prop 2	normal	proportional	no	no	no
SigmoidE _{max} Prop 3	log-normal	constant	no	no	no
SigmoidE _{max} Prop 4	log-normal	proportional	no	no	no
SigmoidE _{max} Prop 5	normal	constant	yes	no	no
SigmoidE _{max} Prop 6	normal	proportional	yes	no	no
SigmoidE _{max} Prop 7	log-normal	constant	yes	no	no
SigmoidE _{max} Prop 8	log-normal	proportional	yes	no	no
SigmoidE _{max} Prop 9	normal	constant	no	yes	no
SigmoidE _{max} Prop 10	normal	proportional	no	yes	no
SigmoidE _{max} Prop 11	log-normal	constant	no	yes	no
SigmoidE _{max} Prop 12	log-normal	proportional	no	yes	no
SigmoidE _{max} Prop 13	normal	constant	no	no	yes
SigmoidE _{max} Prop 14	normal	proportional	no	no	yes
SigmoidE _{max} Prop 15	log-normal	constant	no	no	yes
SigmoidE _{max} Prop 16	log-normal	proportional	no	no	yes
SigmoidE _{max} Prop 17	normal	constant	yes	yes	yes
SigmoidE _{max} Prop 18	normal	proportional	yes	yes	yes
SigmoidE _{max} Prop 19	log-normal	constant	yes	yes	yes
SigmoidE _{max} Prop 20	log-normal	proportional	yes	yes	yes

2.12.11.5 Final model criteria

Selection criteria for the final model were based on having coefficient of variation of fixed effect parameter values below 50%, coefficient of variation of random effect parameter values below 100%, the lowest Akaike Information Criterion (AIC) value and by passing visual inspection of the visual predictive check (VPC). VPC's are part of the standard output of the SAEMIX package. Visually, the medians of the observed data (solid red line) and the model predictions (dashed red line) have to follow each other. If they do, the confidence intervals should also concur. The distributions of the observed data will however, be generally narrower than the model predictions due to the limited data points per effect site target concentration in this study and this will be therefore regarded as acceptable.

3 RESULTS

3.1 Demography

The pilot study was conducted on 9 patients and their characteristics are described below (Table 23). Two of the participants were studied twice. A formal treatment of between occasion variability was not possible given the low number of repeated subjects, and hence these 2 repeated occasions were handled as separate subjects in the population analysis.

Table 23 Demographic and dosing details

ID	A g e	S e x	Wt	Ht	Opioid indication	Current opioid dose	M E D D	Concurrent medications	Infusion steps
001	61	F	70	180	Back pain	Oxycodone 20 mg BID	60 mg	Amitriptyline Metformin Atenolol Clonidine Venlafaxine Rabeprazole Rosuvastatin Paracetamol Sodium valproate	3
002	52	F	74.9	158	Shoulder and back pain Migraine	Methadone 35 mg QD	70 mg	Frusemide Esomeprazole Oestradiol	4
003	40	F	108	177	Back, knees and left shoulder pain	Morphine 50 mg BID Oxycodone 40 mg BID	220 mg	Gabapentin Amitriptyline Duloxetine Atorvastatin Carbimazole Lansoprazole Nicorandil	4
004	31	M	74.6	186	Arthritis secondary to Stickler's syndrome	Methadone 30 mg QD	60 mg	Warfarin	3 (2 visits)
005	59	M	82.3	182	Osteomyelitis Frontal sinusitis	Morphine 60 mg TID	180 mg	Amitriptyline Propranolol Terbutaline Salbutamol	4
006	57	M	132.5	177	Back pain	Oxycodone 20 mg BID	60 mg	Venlafaxine Telmisartan Hydrochlorothiazide Naproxen Aspirin Insulin aspart Insulin glargine Metformin	3
007	55	M	56	177	Neuropathic foot pain	Methadone 20 mg TID	120 mg	Mirtazapine Pantoprazole Atorvastatin Sodium valproate Zuclopenthixol Amitriptyline Oxazepam	4 (2 visits)
008	34	F	62.7	152.5	Right hemi-body pain with atypical CRPS of right upper limb	Oxycodone 20 mg BID	60 mg	Meloxicam Pregabalin Nortriptyline	3
009	46	F	71	165	Back pain	Hydromorphone 20 mg QD	80 mg	Indomethacin Paracetamol Rosuvastatin Metformin Salbutamol	3

								Perindopril/ amlodipine Flaxseed oil Multivitamin	
--	--	--	--	--	--	--	--	--	--

3.2 Safety

Overall, the study design proved to be safe and reasonable in achieving the wanted outcomes. The starting doses were appropriate. Starting at lower doses would have caused a delay in reaching the endpoints and beginning at higher doses might have led to intolerable adverse effects. Most of the participants only required one or two additional target effect site concentration levels in order to reach the desired endpoint. The rate of progression was reasonable. A steady manageable increase in pharmacological effects was seen throughout the study.

One patient developed mild nausea up to three hours after stopping the infusion. The patient was administered intravenous tropisetron 2 mg and the nausea resolved a few hours before discharge. Another patient complained of dry mouth which was self-resolving. Itch was the complaint of a different patient and she was given 10 mg cetirizine. The subject later admitted that the problem had been on going before the study visit.

3 participants had their oxygen saturation drop between 90-95% for less than one minute which went up after taking deep breaths and being given gentle stimulation. Four of the nine patients did not develop any level of sedation with the infusion. 3 participants developed mild sedation and one patient had mild to moderate sedation levels during the infusion. None of the participants found the study schedule too fatiguing and no one requested for a withdrawal from the study. No infusion had to be stopped before the 2nd or 3rd infusion step and no patient had to be resuscitated during the study duration.

3.3 Technical issues

There were some problematic readings with the EEG and SEM. This could have been due to either poor application of the electrodes or the patients not properly following the dot on the screen as a result of lack of motivation, boredom, fatigue or presence of other distractions in the study room. One patient gave poor readings for SEM as he was legally blind in the left eye.

Water buckets were used to conduct the cold pain test. The problem with using buckets is that the water temperature had to be monitored regularly as the temperature increases with time and cups of ice had to be added from time to time. This resulted in a more labour and time intensive experiment compared to if a circulating and cooling water bath was used.

3.4 Effects of fentanyl in the opioid-tolerant

3.4.1 EEG effects

The graphs plot average power in various band frequencies in μV (microvolt) using amplification factor of 50,000 at Pz-Oz and Fz-Cz site before and after starting fentanyl infusion.

Very low (0.5-2.0 Hz) frequency band at Pz-Oz

The average power in the 0.5-2.0 Hz frequency band of the EEG shows a general increase with an increase in the effect site concentration of fentanyl at Pz-Oz (Figure 10).

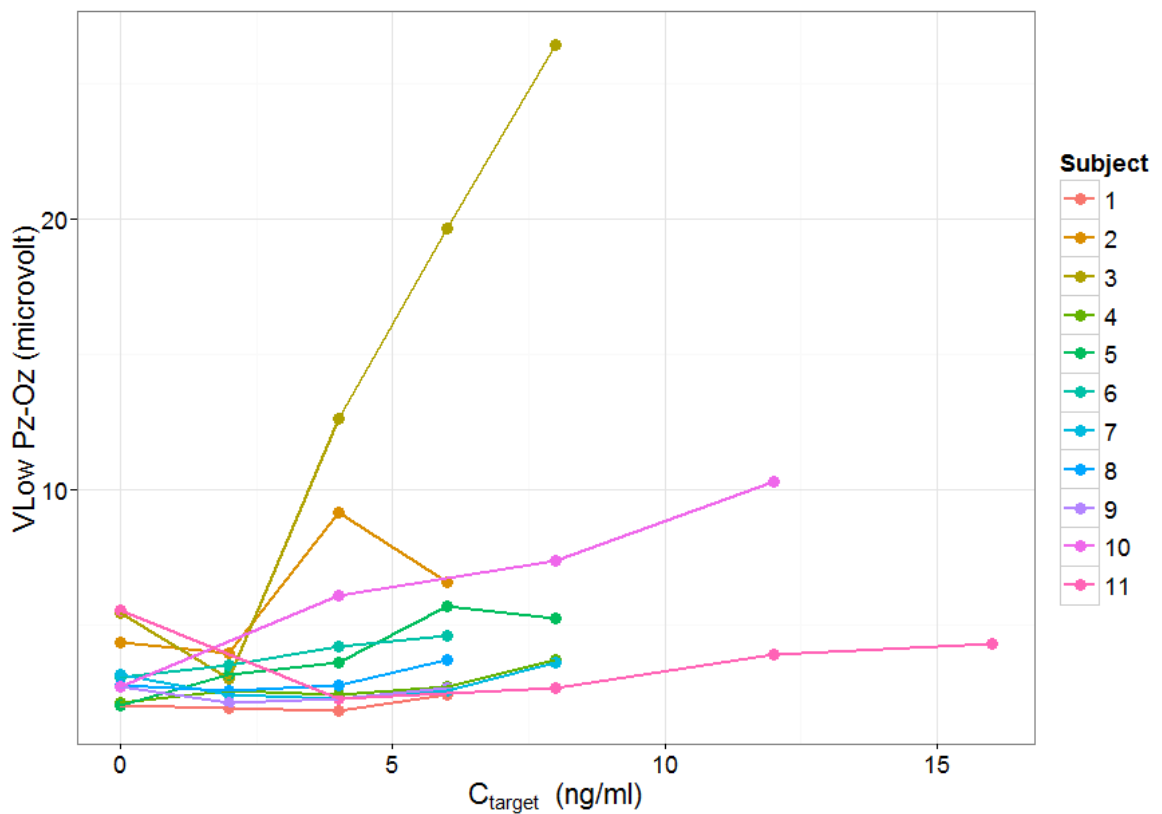


Figure 10 Graph showing average power in very low frequency EEG band (amplification factor of 50,000) at Pz-Oz site before and after starting fentanyl infusion (Time 0). C_{target} is the target effect site concentration of fentanyl.

Very low (0.5-2.0 Hz) at Fz-Cz

In the study population, the average power in the 0.5-2.0 Hz frequency band of the EEG shows a general increase with the increase in effect site concentration of fentanyl at Fz-Cz (Figure 11).

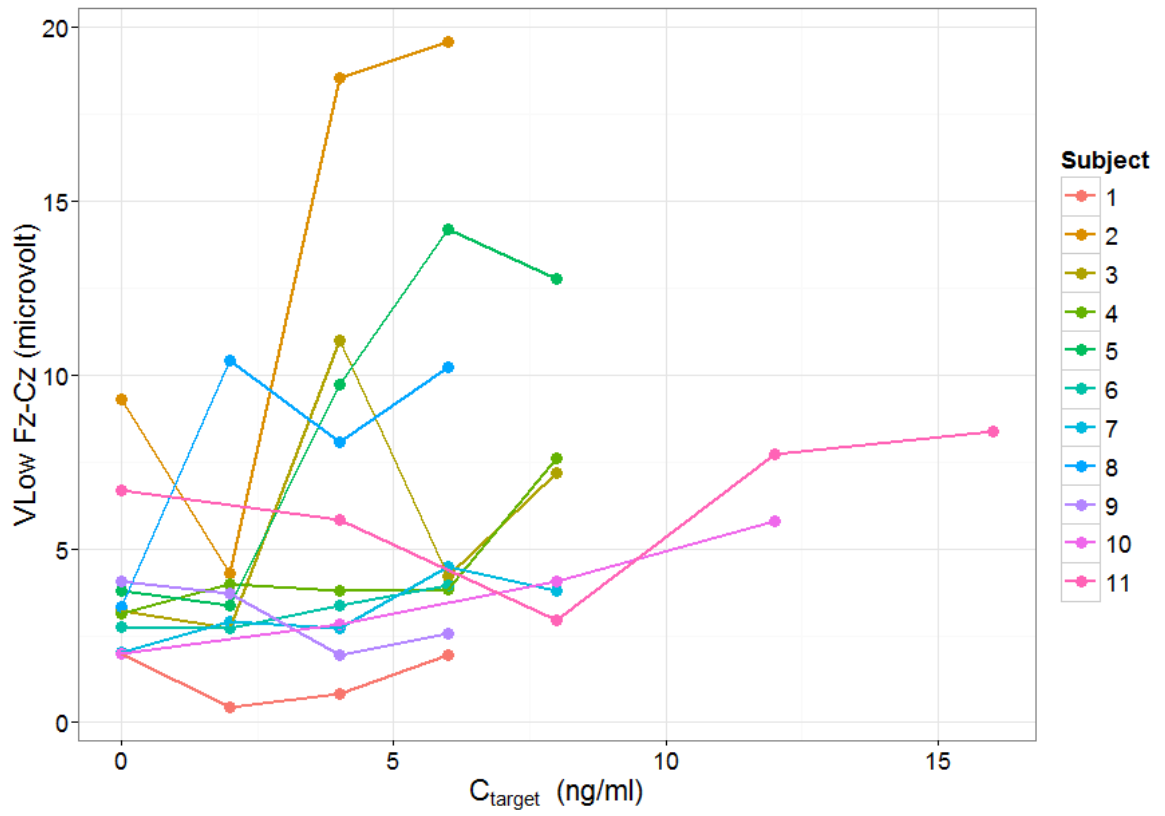


Figure 11 Average power at very low EEG band versus target effect site concentration of fentanyl.

Delta (2.0-4.0 Hz) at Pz-Oz

At Pz-Oz, the average power in the 2.0-4.0 Hz frequency band of the EEG shows a general increase with an increase in the effect site concentration of fentanyl even though the power declined from a higher reading for two subjects (Figure 12).

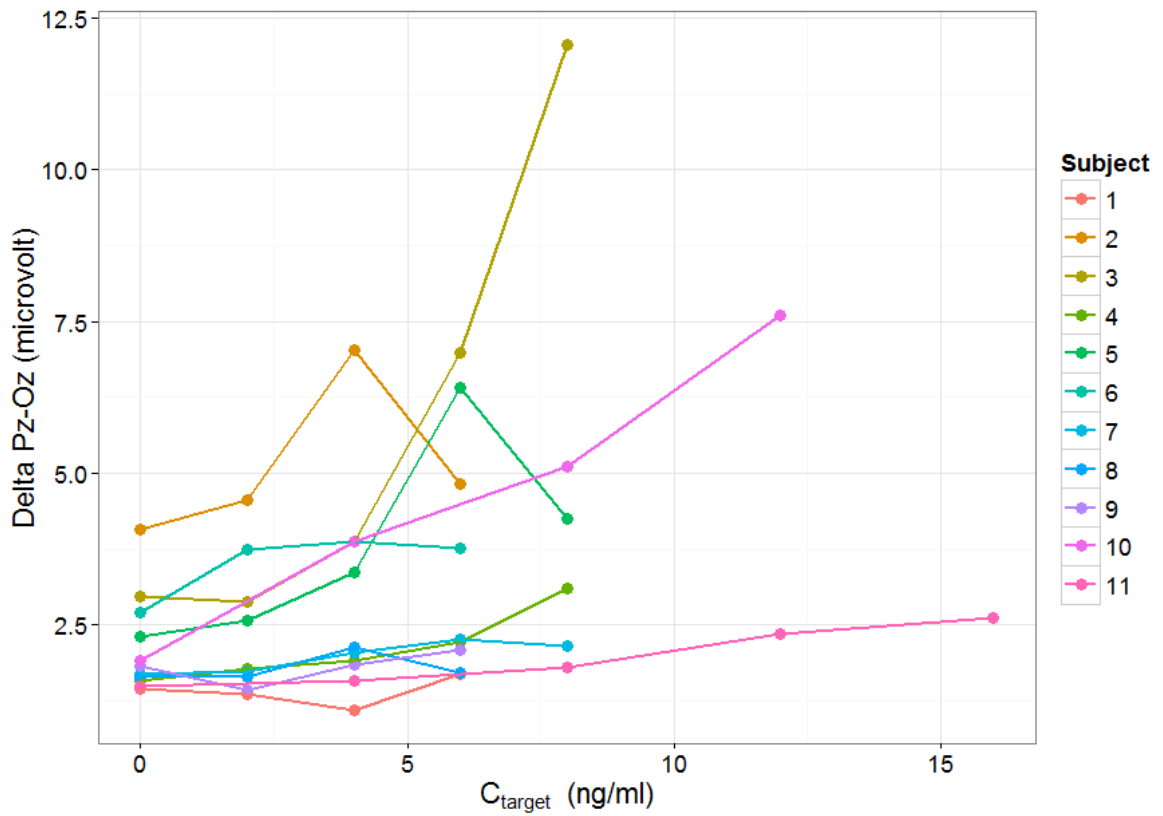


Figure 12 Average power at delta Pz-Oz versus target effect site concentration of fentanyl.

Delta (2.0-4.0 Hz) at Fz-Cz

At Fz-Cz, the average power in the 2.0-4.0 Hz frequency band of the EEG illustrates a general rise with a rise in the effect site concentration of fentanyl (Figure 13). Nearly similar to the readings of the delta band at Pz-Oz, the power decreases from a higher reading for three subjects.

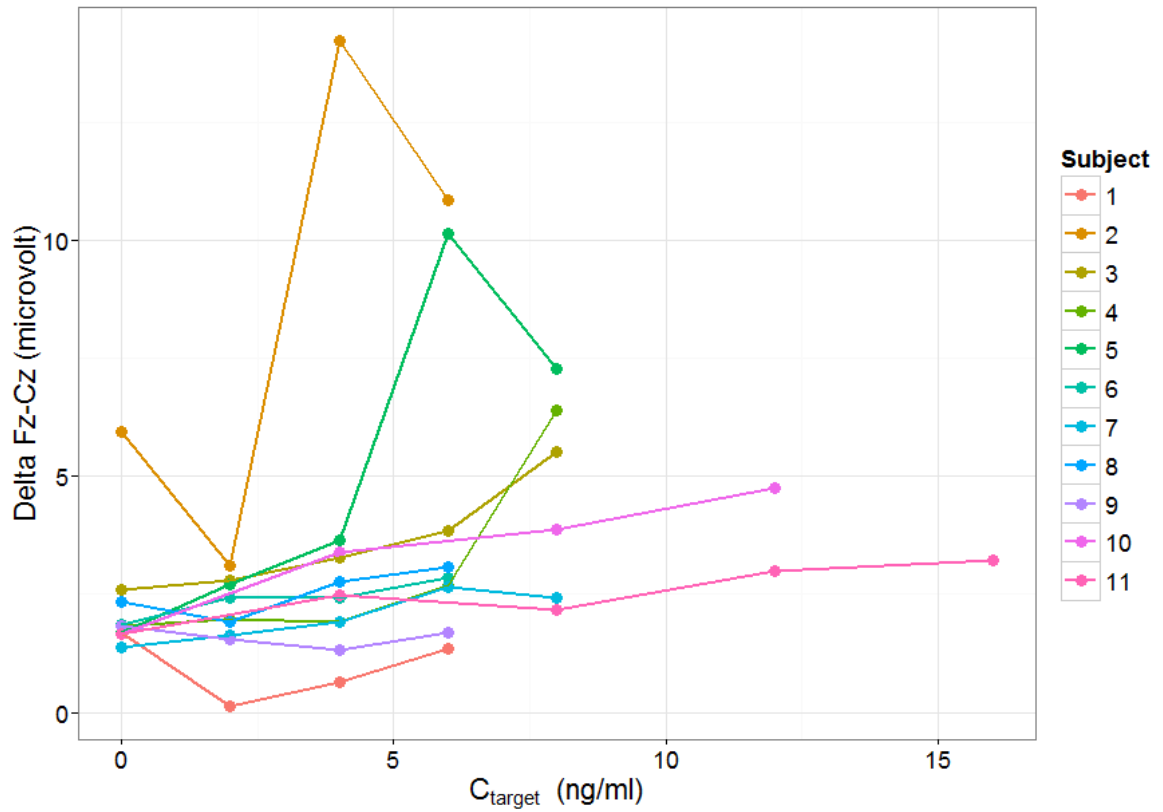


Figure 13 Average power of delta at Fz-Cz versus target effect site concentration of fentanyl.

Theta (4.0-7.5 Hz) at Pz-Oz

For most of the subjects, there is a general increasing trend in the power of the EEG band with increasing fentanyl target effect site concentration (Figure 14). Some subjects however do not consistently have an increase in their EEG power readings for this frequency band.

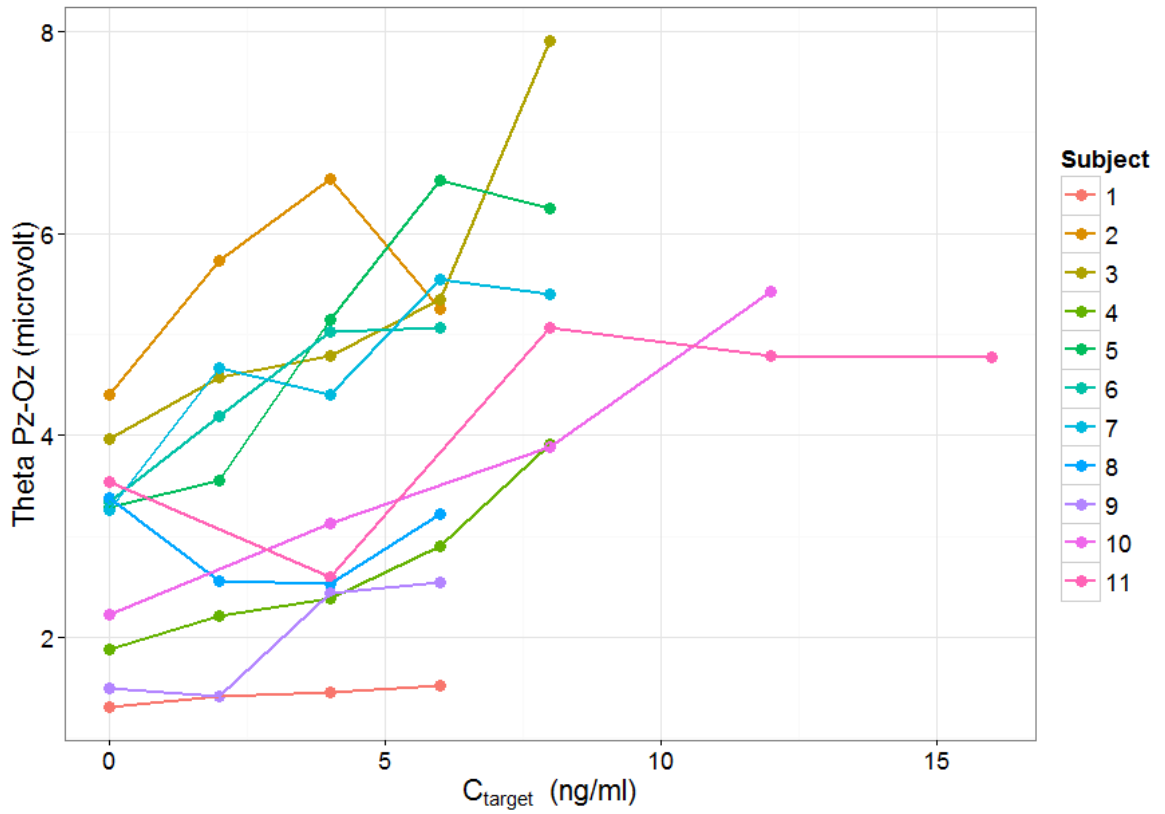


Figure 14 Average power of theta at Pz-Oz versus target effect site concentration of fentanyl.

Theta (4.0-7.5 Hz) at Fz-Cz

Two subjects have a decrease in the initial power for this EEG band but overall, there is a net increase in the values which will be demonstrated further in the best model sections of the results (Figure 15).

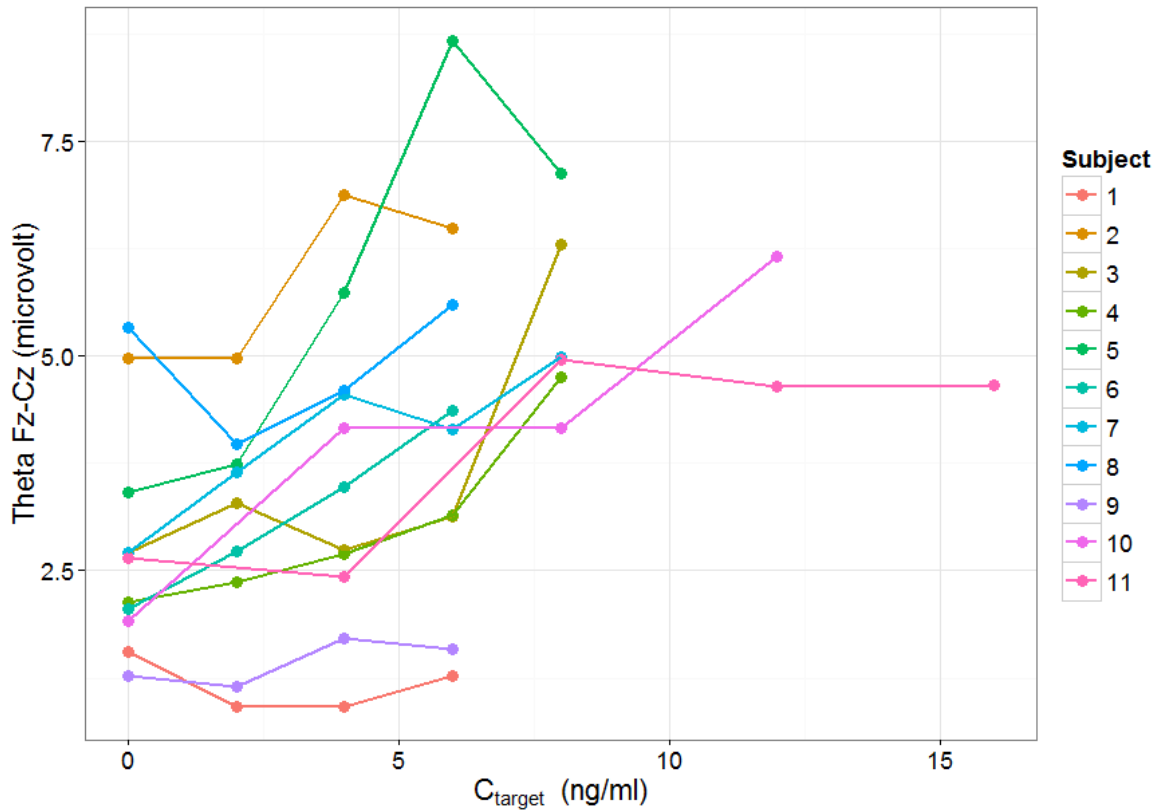


Figure 15 Average power of theta at Fz-Cz versus target effect site concentration of fentanyl.

Gamma (35.1-48.8 Hz) at Pz-Oz

At Pz-Oz, the average power of the EEG band increases steadily with time for most subjects (Figure 16). One subject however shows a declining reading with increasing effect site concentration.

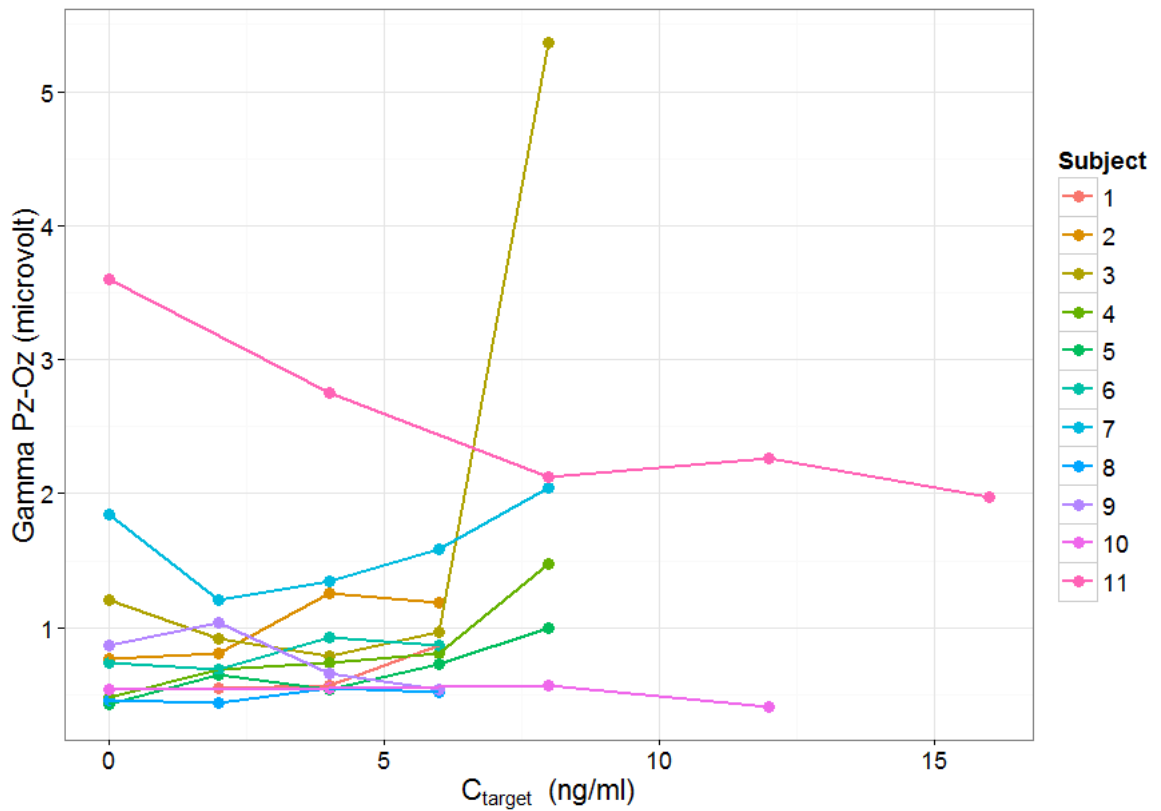


Figure 16 Average power of gamma at Pz-Oz versus target effect site concentration of fentanyl.

3.4.2 Saccadic peak velocity

Due to reasons mentioned in the discussion segment, the Neurocart did not record any readings for subject number 10 in all the saccadic eye movement metrics. This is the reason why it is not being displayed in graphs in section 3.4.2 to 3.4.5.

In this study, there are no significant changes in saccadic peak velocity recorded with increasing doses of fentanyl (Figure 17).

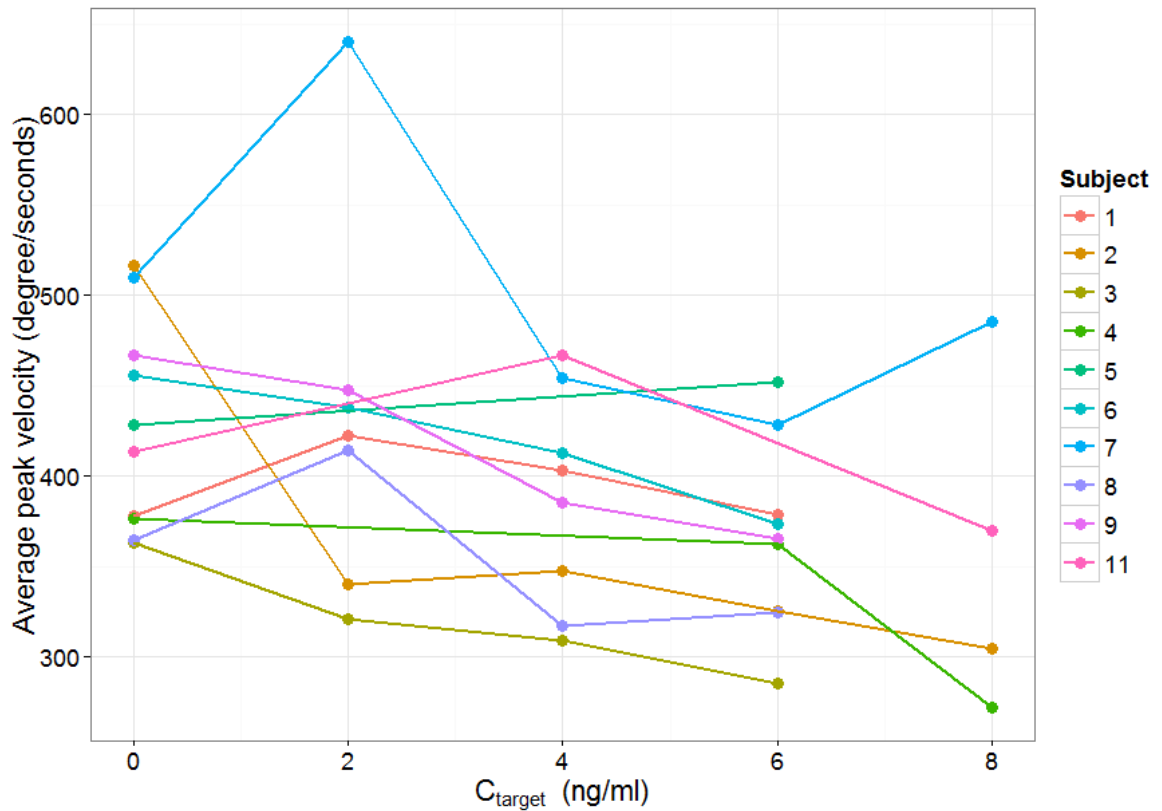


Figure 17 The average saccadic peak velocity versus target effect site concentration of fentanyl.

3.4.3 Saccadic latency

The saccadic reaction time or latency does not demonstrate any significant changes with higher doses of fentanyl at the effect site (Figure 18).

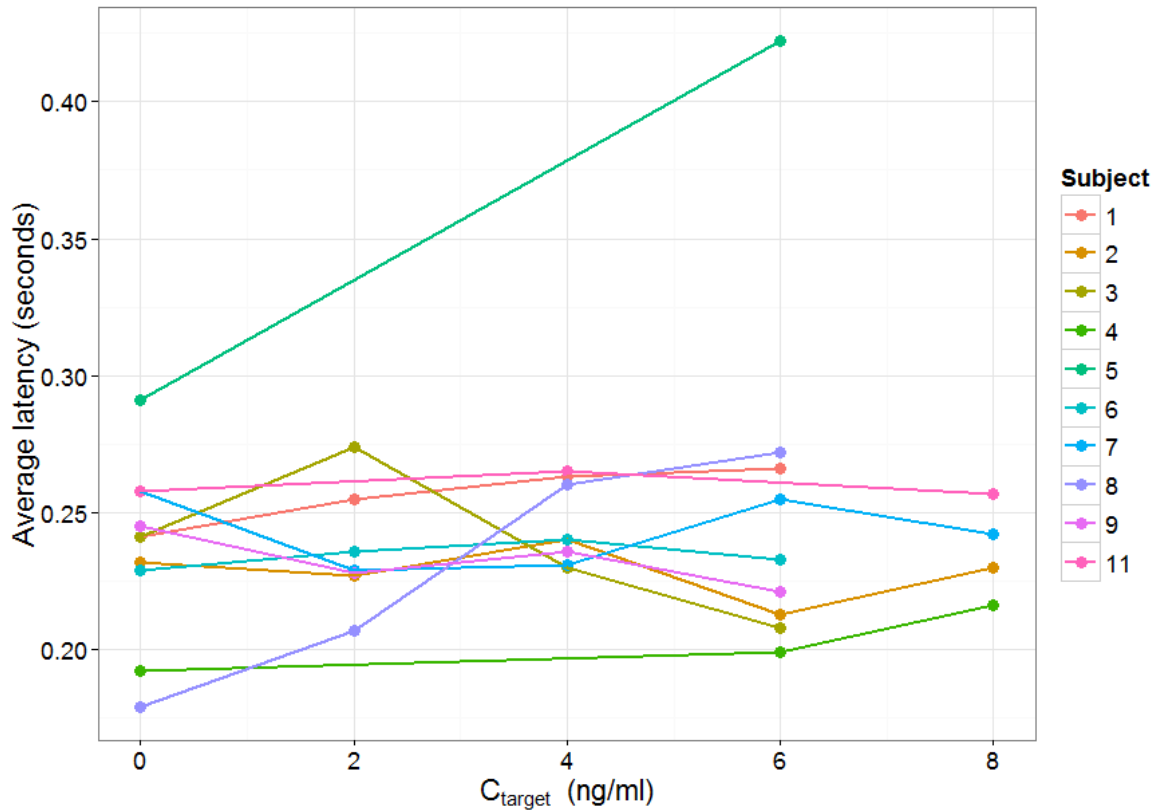


Figure 18 Average saccadic latency versus target effect site concentration of fentanyl.

3.4.4 Pupillometry

As expected, the pupil size metric decreases nicely with increasing target effect site concentration of fentanyl (Figure 19).

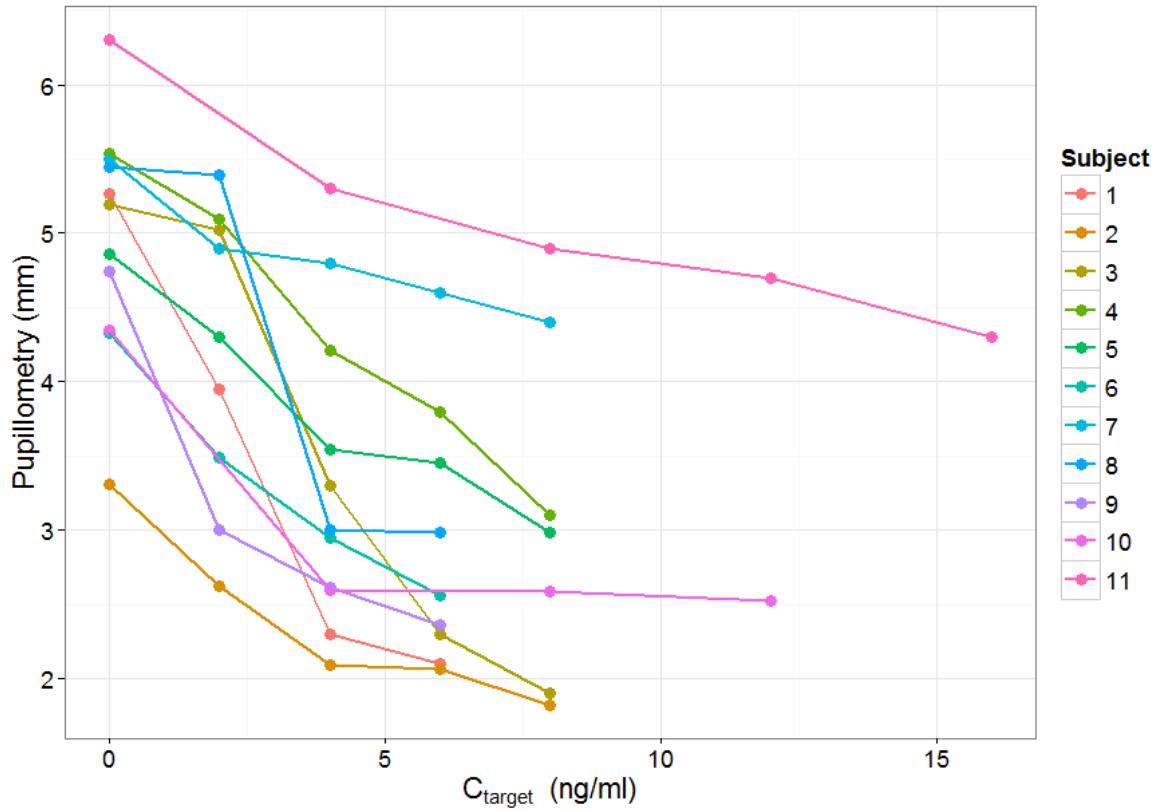


Figure 19 Plot of pupil size versus target effect site concentration of fentanyl.

3.4.5 Morphine-Benzedrine Group (MBG) Scale

In this study, the MBG scale, which is a subjective measure of euphoria, does not demonstrate any increase in euphoric experiences among the study participants with increasing fentanyl doses (Figure 20).

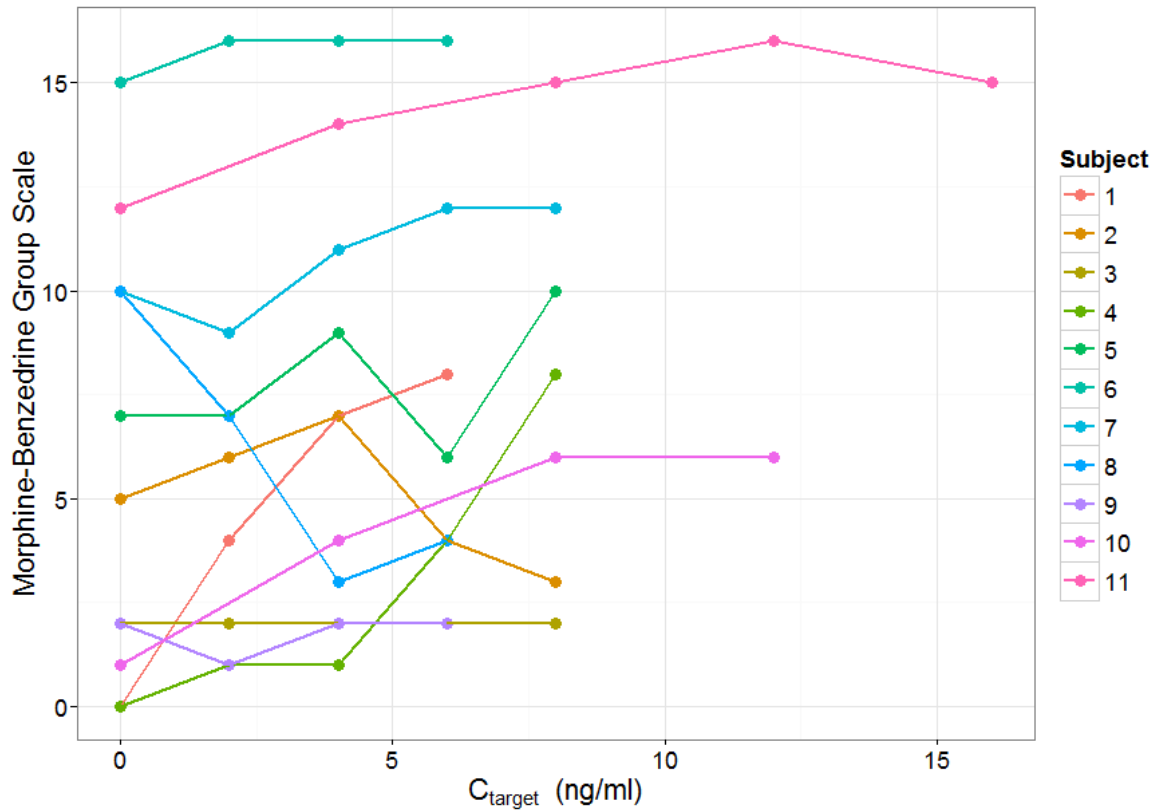


Figure 20 Morphine-Benzedrine Group (MBG) Scale versus target effect site concentration of fentanyl.

3.4.6 Pain threshold

The pain threshold does not show any consistent pattern with increasing doses of fentanyl (Figure 21). The values increase for some subjects, decrease for some and do not show any significant changes for others.

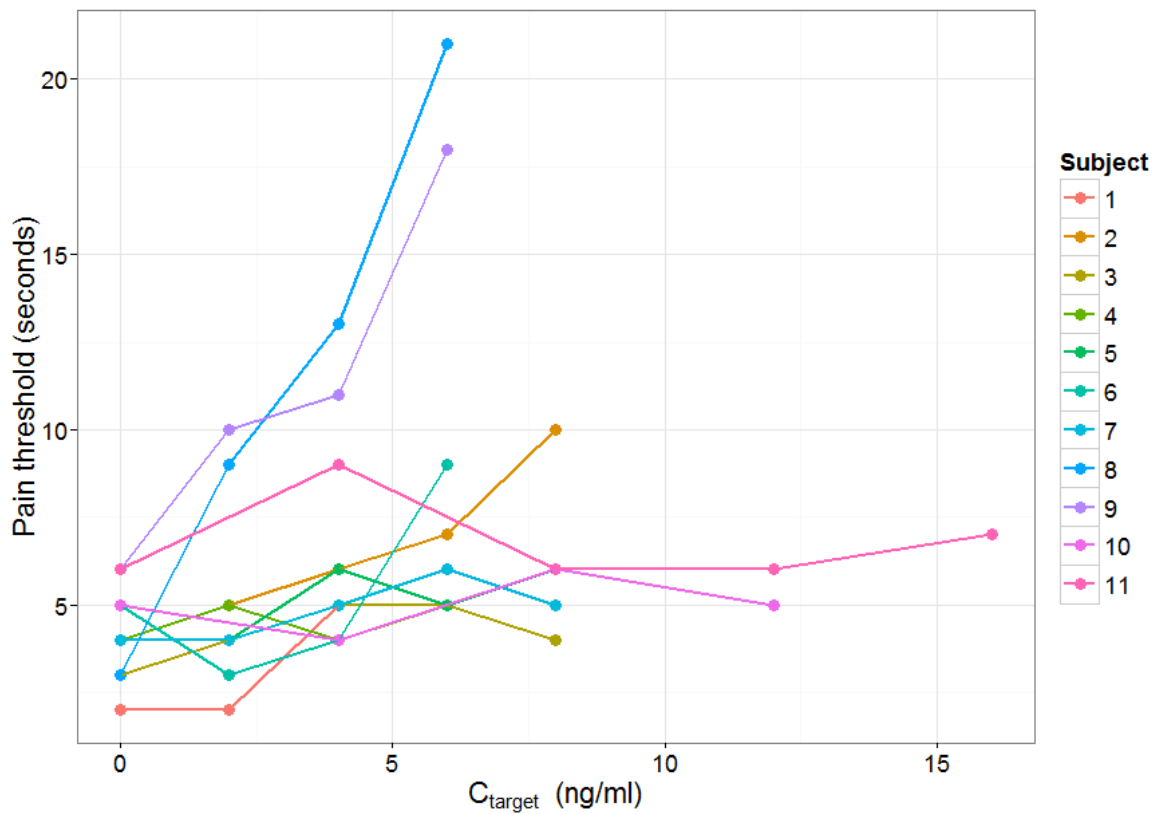


Figure 21 Pain threshold to cold pain test versus target effect site concentration of fentanyl.

3.4.7 Pain tolerance

There are increases in pain tolerance to cold pain with time in all participants (Figure 22). Similar trends are seen with increasing effect site concentrations of fentanyl (Figure 23).

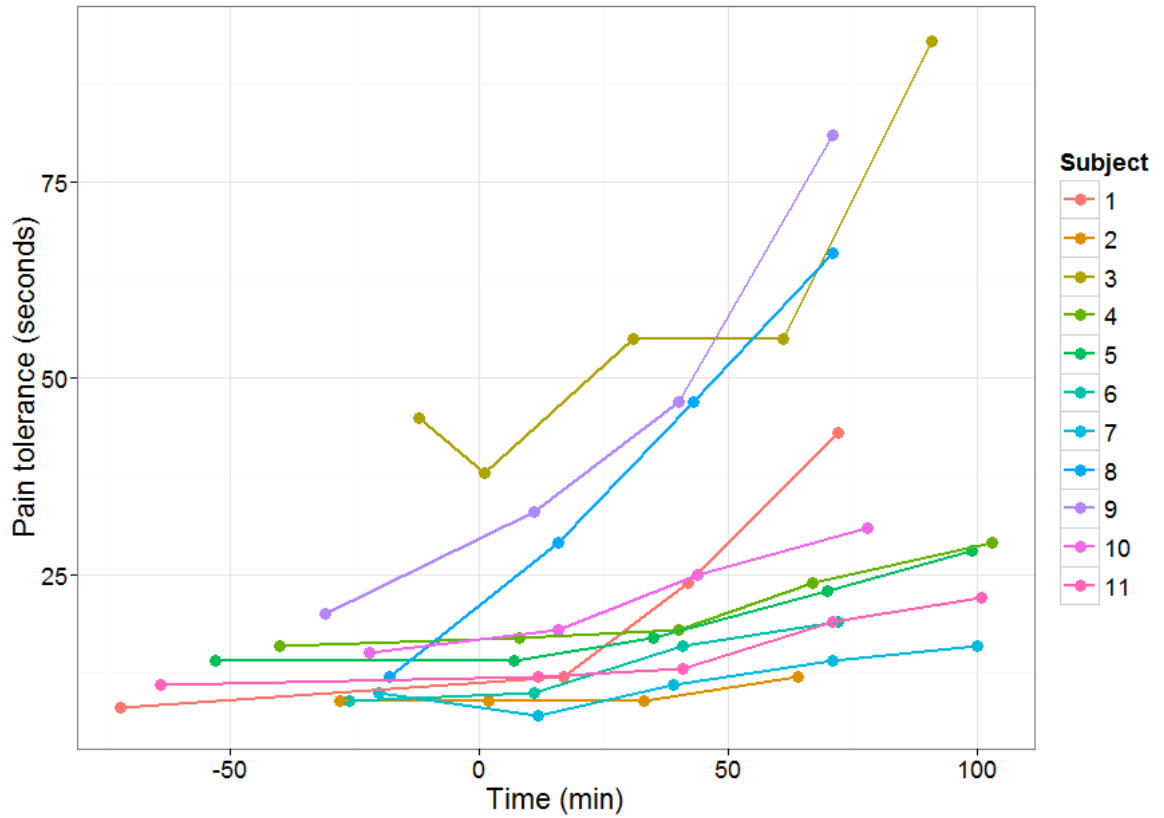


Figure 22 Plot of cold pain tolerance versus time.

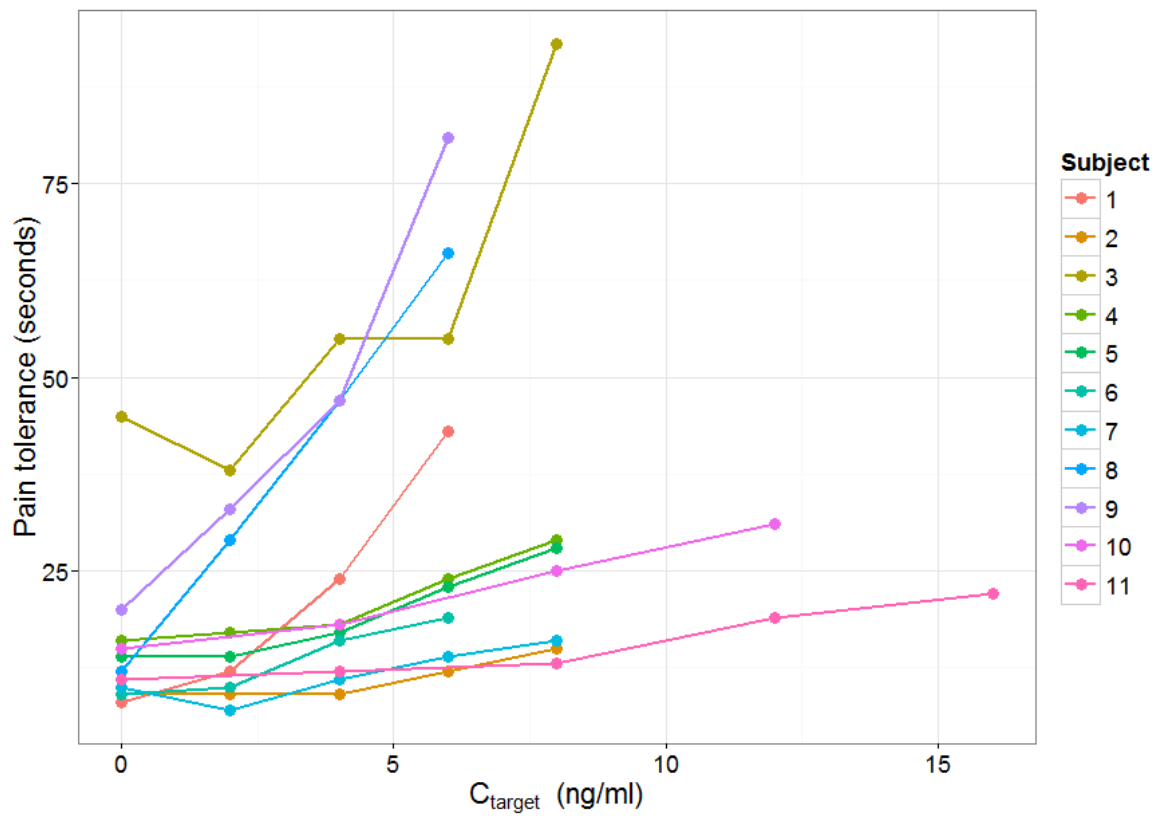


Figure 23 Plot of cold pain tolerance versus target effect site concentration of fentanyl.

3.4.8 Subjective Opioid Withdrawal Scale (SOWS)

As expected, the overall withdrawal scale readings fall steadily with time in the study population (Figure 24).

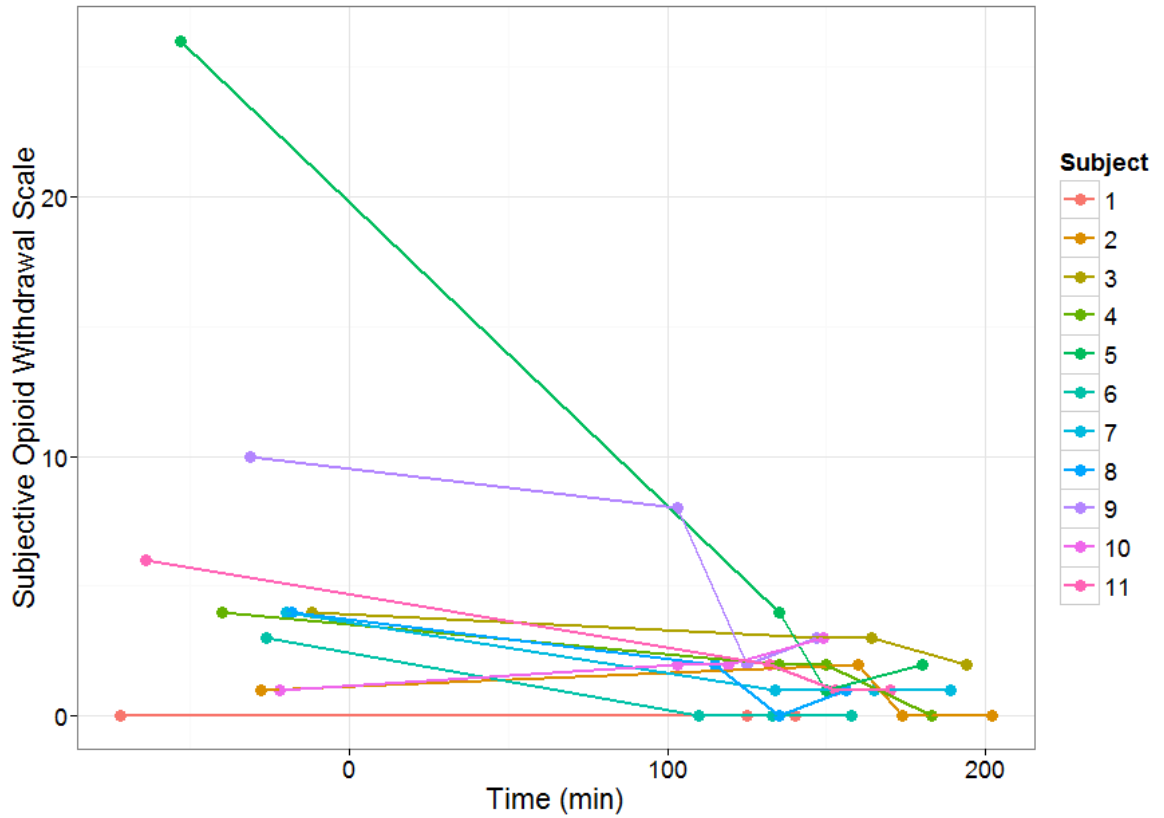


Figure 24 Plot of Subjective Opioid Withdrawal Scale versus time.

As the fentanyl doses increase, the levels of withdrawal generally decrease in the study subjects (Figure 25). For three subjects the decline is followed by a small climb in the withdrawal scale readings.

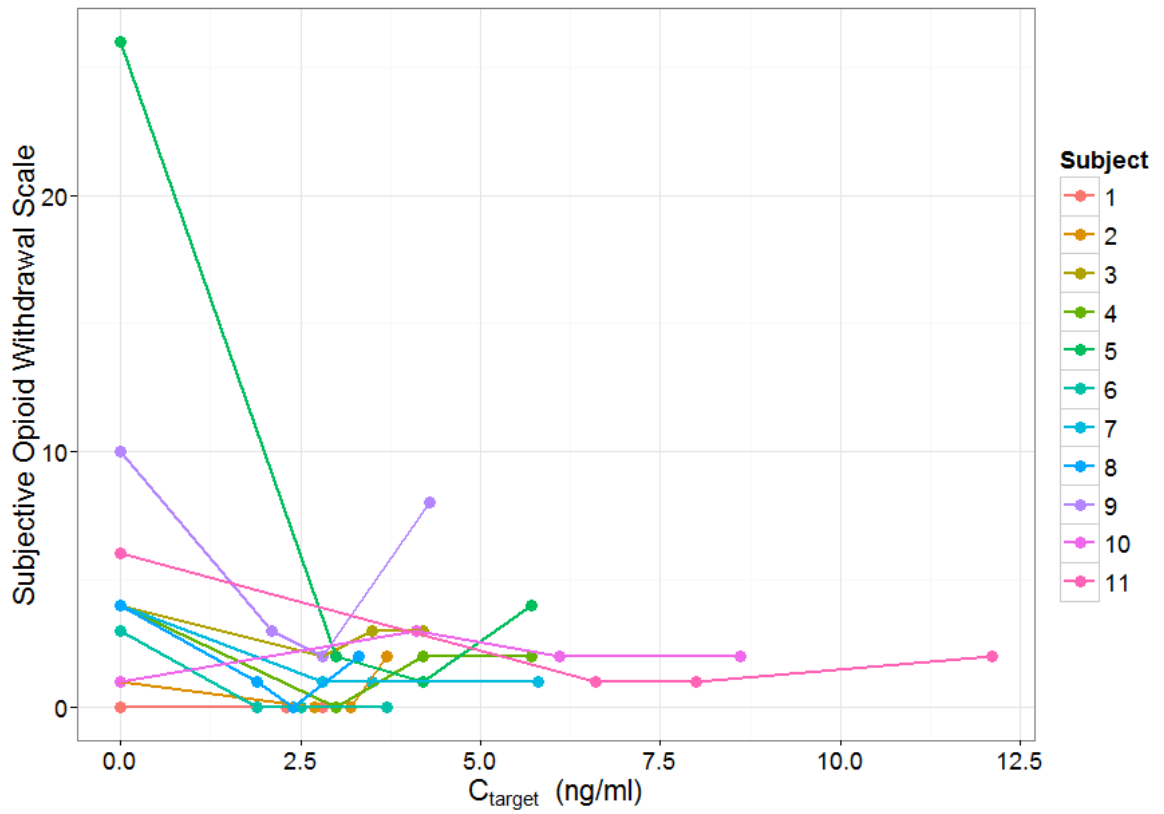


Figure 25 Plot of Subjective Opioid Withdrawal Scale versus target effect site concentration of fentanyl.

3.4.9 Sedation score

5 patients developed sedation during their study visit. Only one patient reached a sedation score of two. However that sedation level was not sustained.

Table 24 Sedation score readings for subject 002 during her first visit

002								
Predicted effect site concentration (ng/ml)	0	2	4	6	8	3.7	3.2	2.7
Time (minute)	-28	2	33	64	95	160	174	202
Sedation score	0	0	0	1	1	0	0	0

In this subject (Table 24), no sedation was demonstrated until the effect site concentration reached 6 ng/ml and it plateaued until the infusion was stopped and it then started to decline back to normal.

Table 25 Sedation score readings for subject 003 during her first visit

003								
Predicted effect site concentration (ng/ml)	0	2	4	6	8	4.2	3.5	2.8
Time (minute)	-12	1	31	61	91	149	164	194
Sedation score	0	0	0	1	1	2	1	0

The third subject (Table 25) became more sedated as the fentanyl level increased at the effect site but the sedation gradually diminished as the time from stopping the infusion increases.

Table 26 Sedation score readings for subject 004 during his first visit

004								
Predicted effect site concentration (ng/ml)	0	2	4	6	8	5.7	4.2	3
Time (minute)	-40	8	40	67	103	135	150	183
Sedation score	0	0	1	1	1	0	0	0

The fourth individual (Table 26) had a plateau in the sedation score readings and he became fully alert 15 minutes after the infusion was stopped.

Table 27 Sedation score readings for subject 009 during her first visit

009								
Predicted effect site concentration (ng/ml)	0	2	4	6	0	4.3	2.8	2.1
Time (minute)	-31	11	40	71	91	103	125	147
Sedation score	0	0	1	0	0	0	0	0

The ninth subject had very minimal sedation for a few minutes after the effect site concentration of 4 ng/ml was targeted (Table 27).

Table 28 Sedation score readings for subject 007 during his second visit

007								
Predicted effect site concentration (ng/ml)	0	4	8	12	16	12.1	8	6.6
Time (minute)	-64	12	41	71	101	132	153	170
Sedation score	0	0	0	1	0	0	0	0

The seventh subject developed a sedation score of 1 after the infusion was increased to target 12 ng/ml of fentanyl at the effect site (Table 28). This effect however was not for long.

3.4.10 Nausea

Only one patient developed nausea during the entire study. She developed nausea 33 minutes into the infusion and up to 4 hours and 30 minutes after starting the infusion. She was given 2 milligrams of intravenous tropisetron for her nausea. She recovered after the tropisetron and had no other adverse effects.

3.5 Pharmacodynamics

The top models for the pharmacodynamic measures are shown in the following pages according to the model selection criteria (see section 2.12.11.5 Final model criteria). The visual predictive check (VPC) is shown for the model that fulfils all the criteria for the model. The visual predictive check is shown only for the first visits as the second visits had very little data which could cloud the picture and result in poor predictive checks.

3.5.1 Best model for very low frequency at Pz-Oz

The best model was LinearProp4 (Figure 26). For this model, the baseline distribution was log-normal, the residual unexplained variability was proportional and MEDD was not a covariate on the intercept and slope.

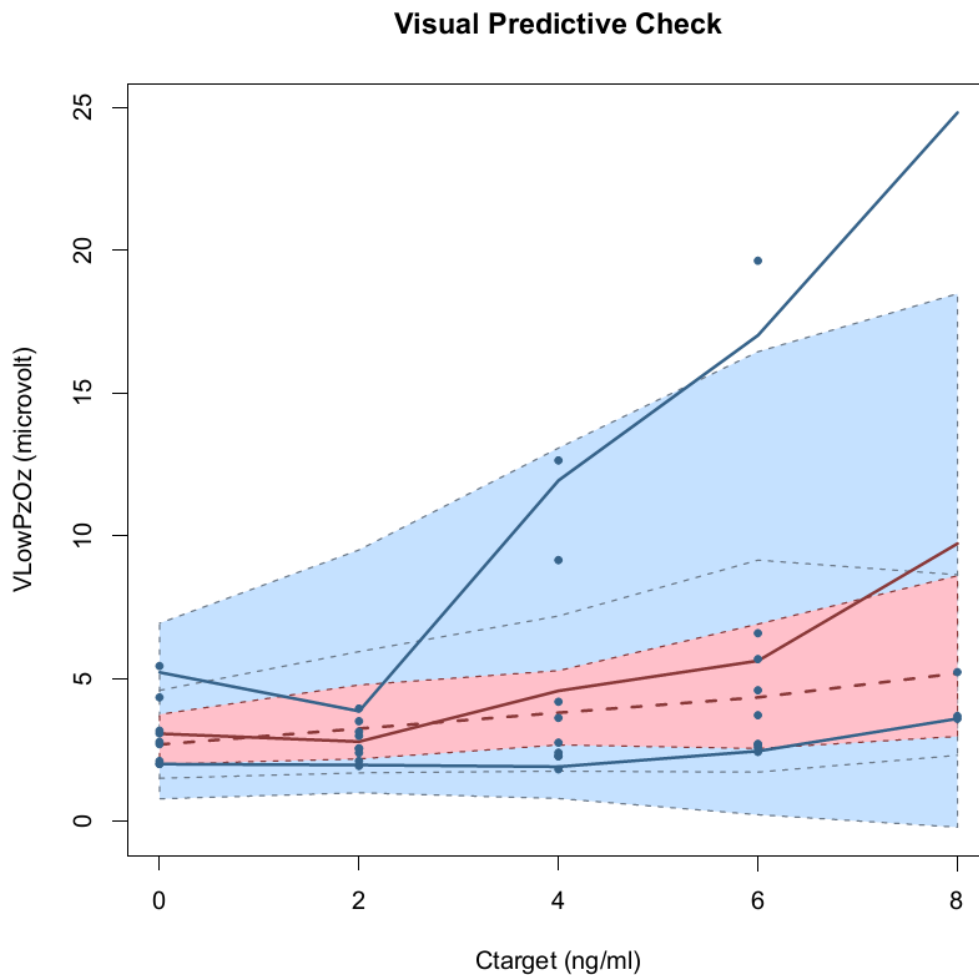


Figure 26 Visual predictive check for LinearProp4 model and very low Pz-Oz.

The estimate for the intercept was 2.83 μV and the slope was estimated to be 0.11 μV per ng/ml (Table 29).

Table 29 Summary of model parameters for LinearProp4 model and very low Pz-Oz.

Summary of model parameters for the best model				
Fixed effects				
Parameter	Estimate	Standard Errors	CV (%)	
Intercept	2.83 μV	0.333	11.8	
slope	0.11 μV per ng/ml	0.040	34.5	
b	0.23 ratio	0.011	4.9	
Variance of random effects				
	Parameter	Estimate	Standard Errors	CV (%)
intercept	omega2.intercept	0.114	0.0761	67
slope	omega2.slope	0.012	0.0069	58
CV, coefficient of variation; b, proportional residual error				

3.5.2 Best model for very low frequency at Fz-Cz

The best model was LinearAdd2 (Figure 27). For this model, the baseline distribution was normal, the residual unexplained variability was proportional and MEDD was not a covariate on the intercept and slope.

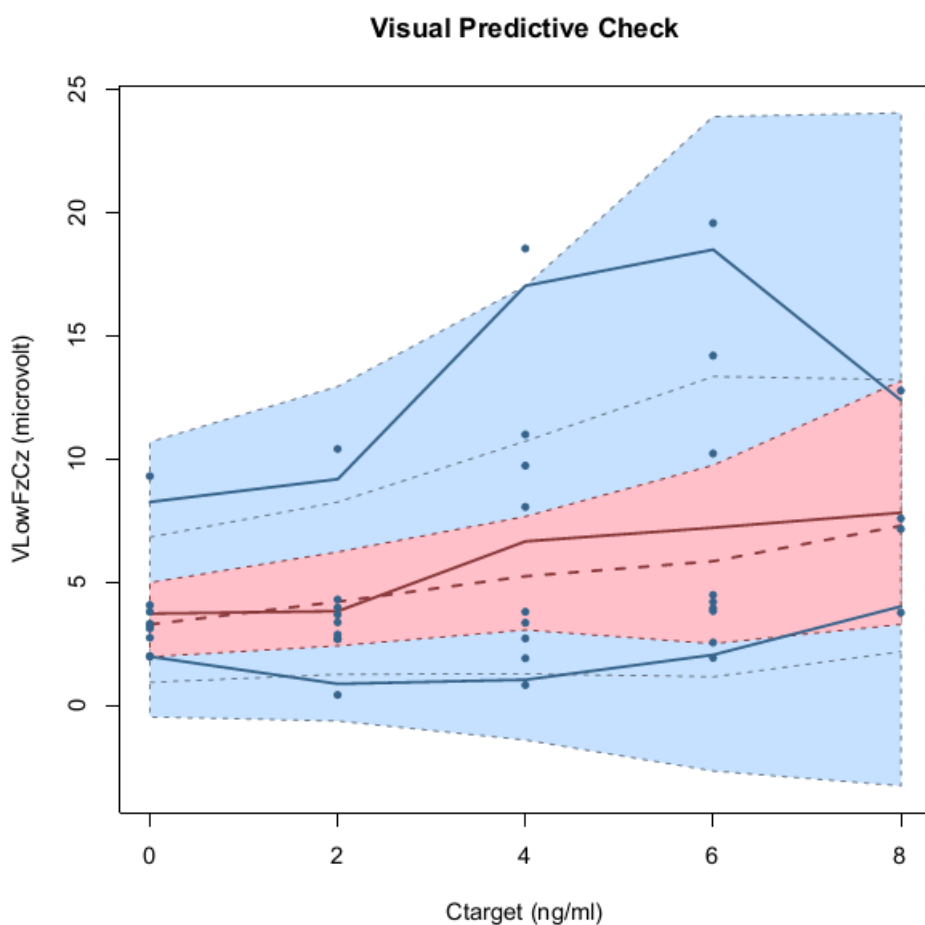


Figure 27 The visual predictive check for LinearAdd2 and very low Fz-Cz.

The estimate for the intercept was 3.80 μV and the slope was estimated to be 0.41 μV per ng/ml (Table 30).

Table 30 Summary of model parameters for LinearAdd2 and very low Fz-Cz

Summary of model parameters for the best model				
Fixed effects				
Parameter	Estimate	Standard Errors	CV (%)	
intercept	3.80 μV	0.636	16.7	
slope	0.41 μV per ng/ml	0.157	37.9	
b	0.37 ratio	0.021	5.5	
Variance of random effects				
	Parameter	Estimate	Standard Errors	CV (%)
intercept	omega2.intercept	3.06	2.61	85
slope	omega2.slope	0.17	0.11	61
CV, coefficient of variation; b, proportional residual error				

3.5.3 Best model for delta Pz-Oz

The best model was LinearProp4 (Figure 28). For this model, the baseline distribution was log-normal, the residual unexplained variability was proportional and MEDD was not a covariate on the intercept and slope.

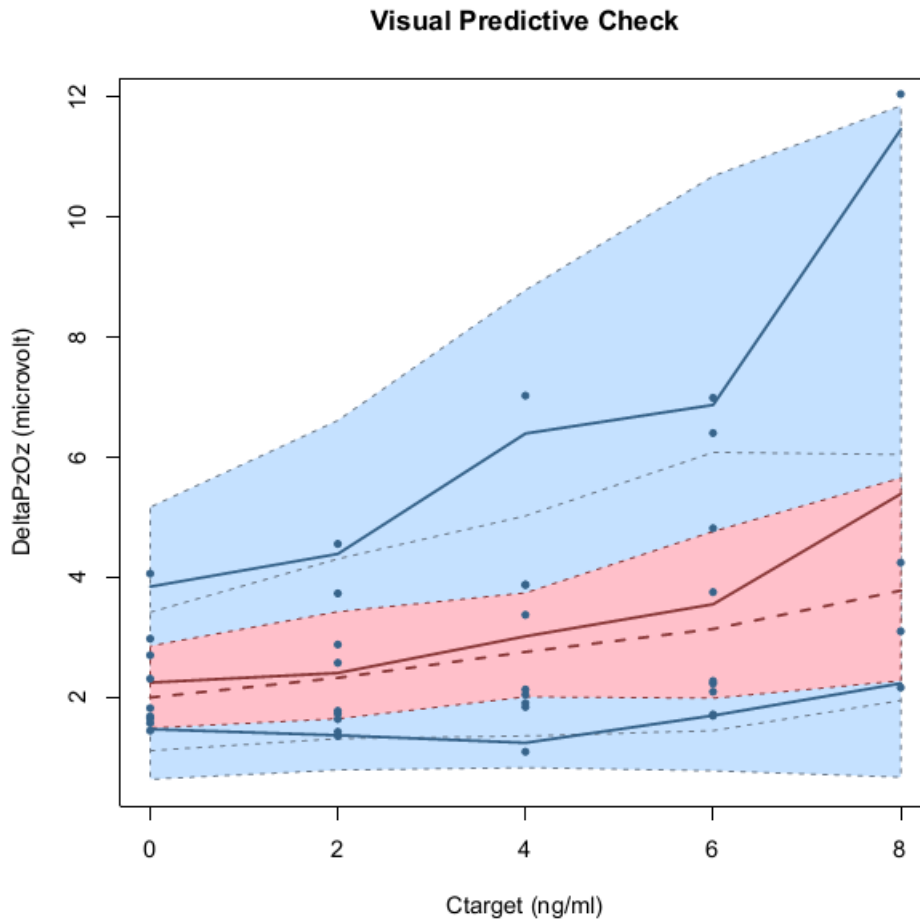


Figure 28 The visual predictive check for LinearProp4 and delta Pz-Oz.

The estimate for the intercept was 1.93 μV and the slope was estimated to be 0.11 μV per ng/ml (Table 31).

Table 31 Summary of model parameters for LinearProp4 and delta Pz-Oz.

Summary of model parameters for the best model			
Fixed effects			
Parameter	Estimate	Standard Errors	CV (%)
intercept	1.93 μV	0.218	11.3
slope	0.11 μV per ng/ml	0.030	26.5
b	0.19 ratio	0.014	7.3
Variance of random effects			

	Parameter	Estimate	Standard Errors	CV (%)
intercept	omega2.intercept	0.1154	0.0719	62
slope	omega2.slope	0.0065	0.0041	62
CV, coefficient of variation; b, proportional residual error				

3.5.4 Best model for delta Fz-Cz

The best model was LinearProp2 (Figure 29). For this model, the baseline distribution was normal, the residual unexplained variability was proportional and MEDD was not a covariate on the intercept and slope.

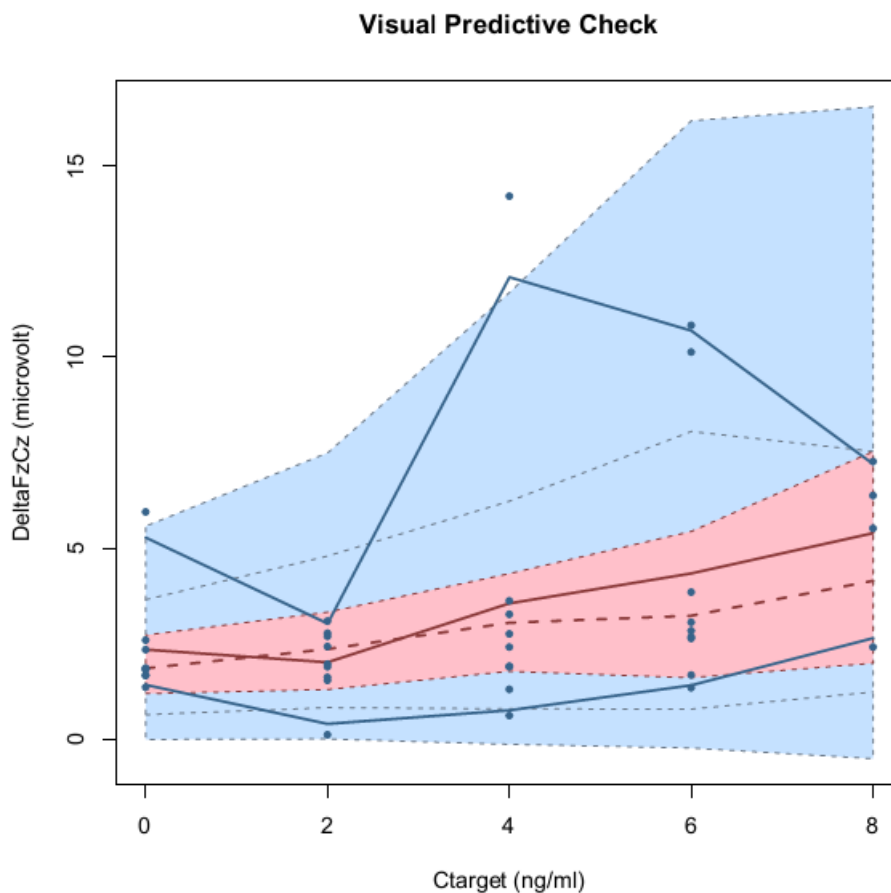


Figure 29 The visual predictive check for LinearProp2 and delta Fz-Cz.

The estimate for the intercept was 2.04 μV and the slope was estimated to be 0.13 μV per ng/ml (Table 32).

Table 32 Summary of model parameters for LinearProp2 and delta Fz-Cz.

Summary of model parameters for the best model			
Fixed effects			
Parameter	Estimate	Standard Errors	CV (%)
intercept	2.04 μV	0.299	14.7
slope	0.13 μV per ng/ml	0.044	33.3

b	0.32 ratio	0.013	3.9	
Variance of random effects				
	Parameter	Estimate	Standard Errors	CV (%)
intercept	omega2.intercept	0.67	0.453	67
slope	omega2.slope	0.01	0.008	78
CV, coefficient of variation; b, proportional residual error				

3.5.5 Best model for theta Pz-Oz

The best model was LinearProp2 (Figure 30). For this model, the baseline distribution was normal, the residual unexplained variability was proportional and MEDD was not a covariate on the intercept and slope.

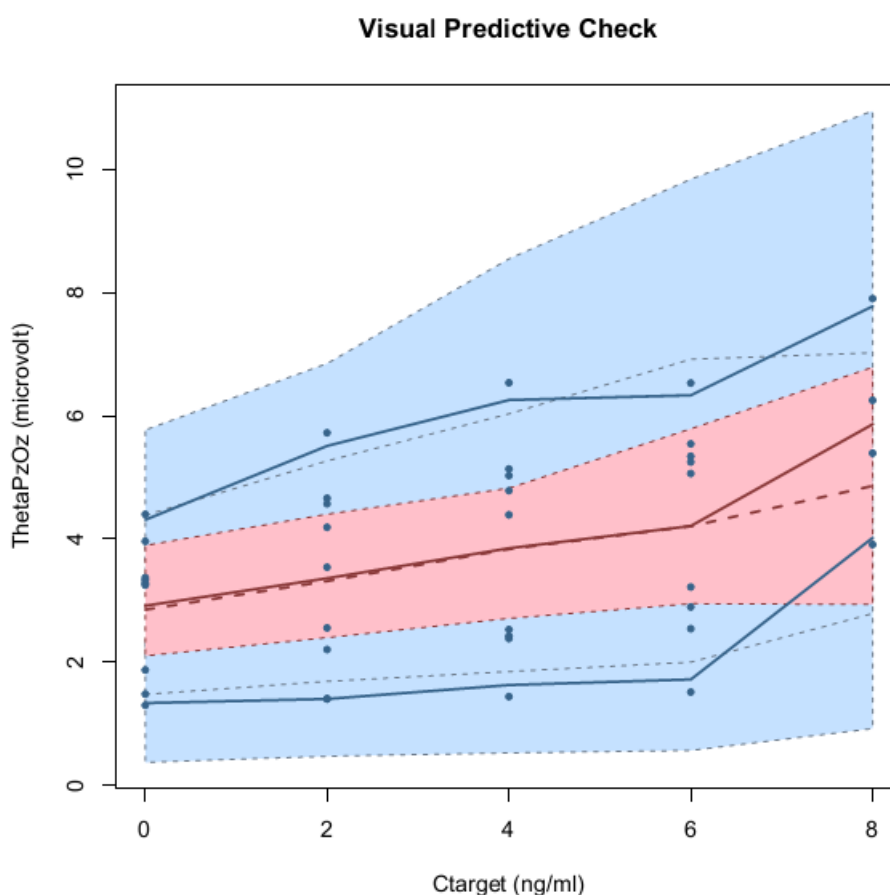


Figure 30 The visual predictive check for LinearProp2 and theta Pz-Oz.

The estimate for the intercept was 2.869 μV and the slope was estimated to be 0.081 μV per ng/ml (Table 33).

Table 33 Summary of model parameters for LinearProp2 and theta Pz-Oz.

Summary of model parameters for the best model			
Fixed effects			
Parameter	Estimate	Standard Errors	CV (%)
intercept	2.869 μV	0.315	11
slope	0.081 μV per ng/ml	0.015	19

b	0.135 ratio	0.023	17	
Variance of random effects				
	Parameter	Estimate	Standard Errors	CV (%)
intercept	omega2.intercept	0.9759	0.56612	58
slope	omega2.slope	0.0011	0.00099	90
CV, coefficient of variation; b, proportional residual error				

3.5.6 Best model for theta Fz-Cz

The best model was LinearProp4 (Figure 31). For this model, the baseline distribution was log-normal, the residual unexplained variability was proportional and MEDD was not a covariate on the intercept and slope.

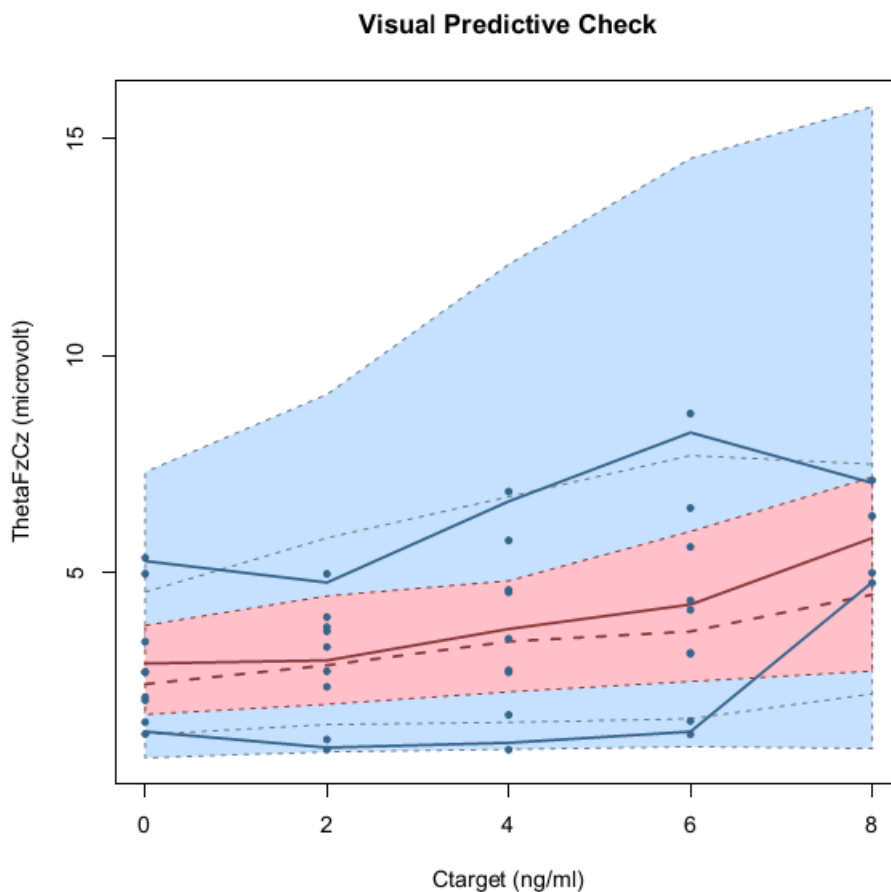


Figure 31 The visual predictive check for LinearProp4 and theta Fz-Cz.

The estimate for the intercept was 2.428 μV and the slope was estimated to be 0.097 μV per ng/ml (Table 34).

Table 34 Summary of model parameters for LinearProp4 and theta Fz-Cz.

Summary of model parameters for the best model			
Fixed effects			
Parameter	Estimate	Standard Errors	CV (%)

intercept	2.428 μV	0.329	14	
slope	0.097 μV per ng/ml	0.023	23	
b	0.186 ratio	0.023	12	
Variance of random effects				
	Parameter	Estimate	Standard Errors	CV (%)
intercept	omega2.intercept	0.1755	0.1020	58
slope	omega2.slope	0.0026	0.0023	87
CV, coefficient of variation; b, proportional residual error				

3.5.7 Best model for alpha Pz-Oz

For this metric, no model fulfilled all the model selection criteria.

3.5.8 Best model for alpha Fz-Cz

For this metric, no model fulfilled all the model selection criteria.

3.5.9 Best model for beta Pz-Oz

For this metric, no model fulfilled all the model selection criteria.

3.5.10 Best model for beta Fz-Cz

For this metric, no model fulfilled all the model selection criteria.

3.5.11 Best model for gamma Pz-Oz

The best model for this metric was LinearProp4 (Figure 32). For this model, the baseline distribution was log-normal, the residual unexplained variability was proportional and MEDD was not a covariate on the intercept and slope.

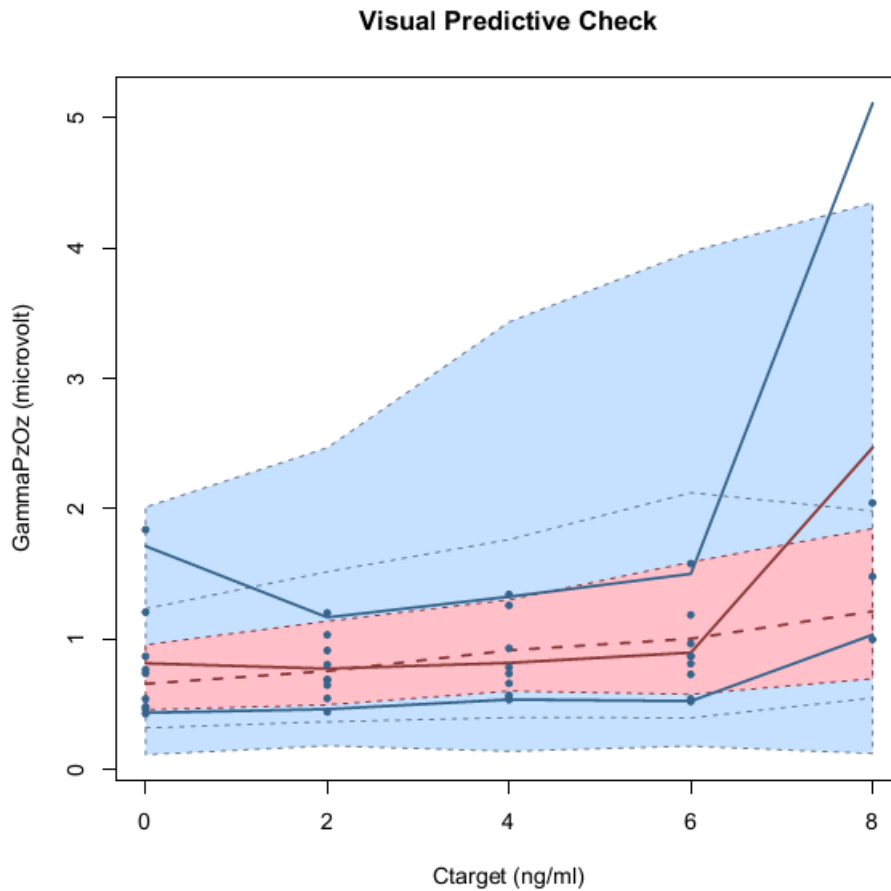


Figure 32 The visual predictive check for LinearProp4 and gamma Pz-Oz.

The estimate for the intercept was 0.772 μV and the slope was estimated to be 0.067 μV per ng/ml (Table 35).

Table 35 Summary of model parameters for LinearProp4 and gamma Pz-Oz.

Summary of model parameters for the best model				
Fixed effects				
Parameter	Estimate	Standard Errors	CV (%)	
intercept	0.772 μV	0.141	18	
slope	0.067 μV per ng/ml	0.031	46	
b	0.280 ratio	0.036	13	
Variance of random effects				
	Parameter	Estimate	Standard Errors	CV (%)
intercept	omega2.intercept	0.3131	0.1893	60
slope	omega2.slope	0.0056	0.0041	73
CV, coefficient of variation; b, proportional residual error				

3.5.12 Best model for gamma Fz-Cz

For this metric, no model fulfilled all the model selection criteria.

3.5.13 Best model for average saccadic peak velocity

The best model for this metric was Zero3 (Figure 33). For this model, the baseline distribution was log-normal, the residual unexplained variability was constant and MEDD was not a covariate on the intercept.

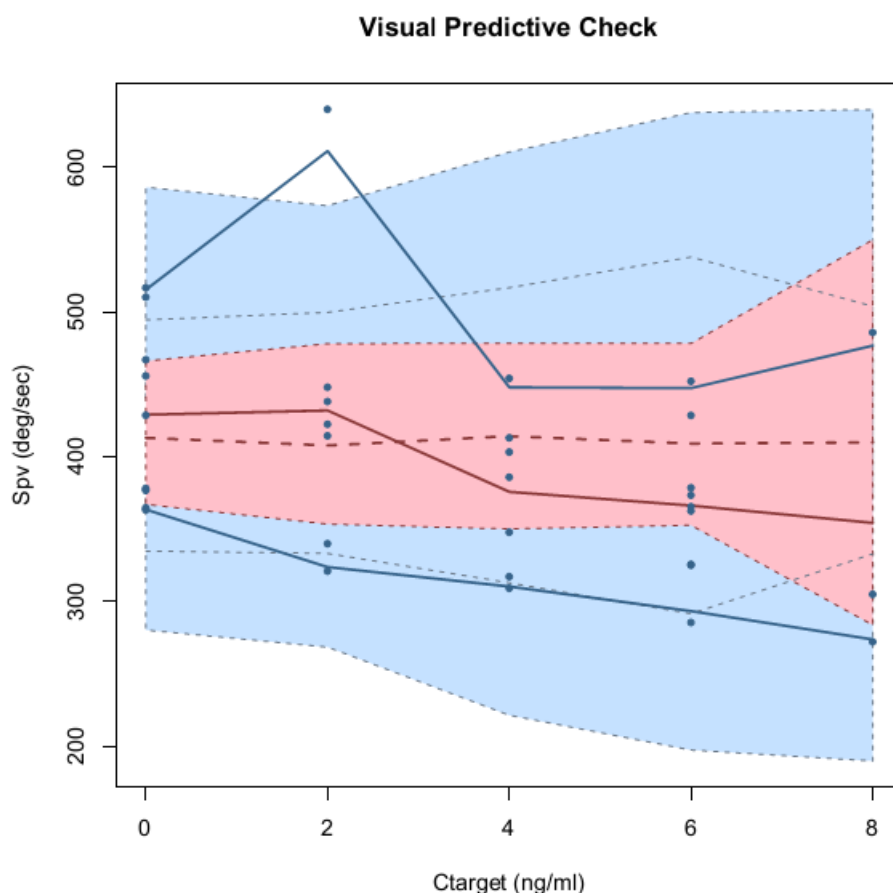


Figure 33 The visual predictive check for Zero3 and saccadic peak velocity.

The estimate for the intercept was 416 degree/second and the slope was estimated to be 0 (Table 36).

Table 36 Summary of model parameters for Zero3 and saccadic peak velocity.

Summary of model parameters for the best model				
Fixed effects				
Parameter	Estimate	Standard Errors	CV (%)	
intercept	416 deg/sec	16.8	4	
slope	0	0	Not a number	
a	47 deg/sec	7.3	16	
Variance of random effects				
	Parameter	Estimate	Standard Errors	CV (%)
intercept	omega2.intercept	0.0098	0.0075	76
slope	omega2.slope	91.4323	69.5128	76

3.5.14 Best model for saccadic latency

The best model for this metric was Zero1 (Figure 34). For this model, the baseline distribution was normal, the residual unexplained variability was constant and MEDD was not a covariate on the intercept.

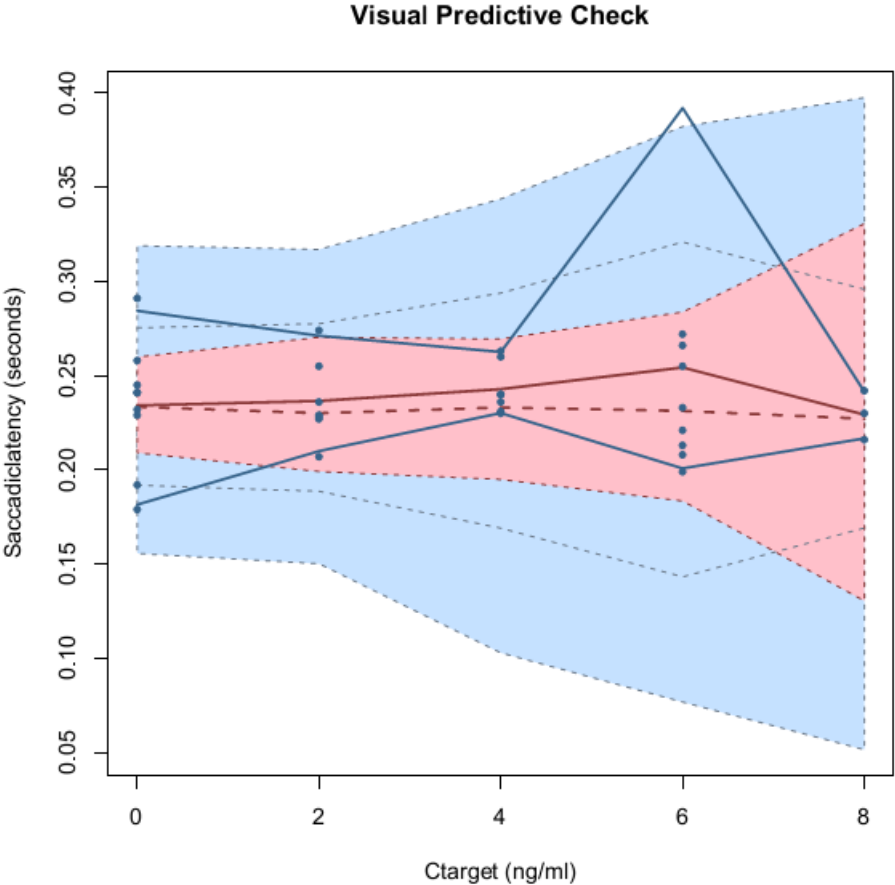


Figure 34 The visual predictive check for Zero1 and saccadic latency.

The estimate for the intercept was 0.238 seconds and the slope was estimated to be 0 (Table 37).

Table 37 Summary of model parameters for Zero1 and saccadic latency.

Summary of model parameters for the best model				
Fixed effects				
Parameter	Estimate	Standard Errors	CV (%)	
intercept	0.238 sec	0.0098	4.1	
slope	0	0	Not a number	
a	0.013 sec	0.0021	16.6	
Variance of random effects				
	Parameter	Estimate	Standard Errors	CV (%)
intercept	omega2.intercept	8.5e-04	4.4e-04	51

slope	omega2.slope	7.5e-05	3.6e-05	48
CV, coefficient of variation; a, additive residual error				

3.5.15 Best model for saccadic inaccuracy

For this metric, no model fulfilled all the model selection criteria.

3.5.16 Best model for number of valid saccades

For this metric, no model fulfilled all the model selection criteria.

3.5.17 Best model for pupillometry

The best model was SigmoidEmaxProp1 (Figure 35). For this model, the baseline distribution was normal, the residual unexplained variability was constant and MEDD was not a covariate on the intercept, EC_{50} and E_{max} .

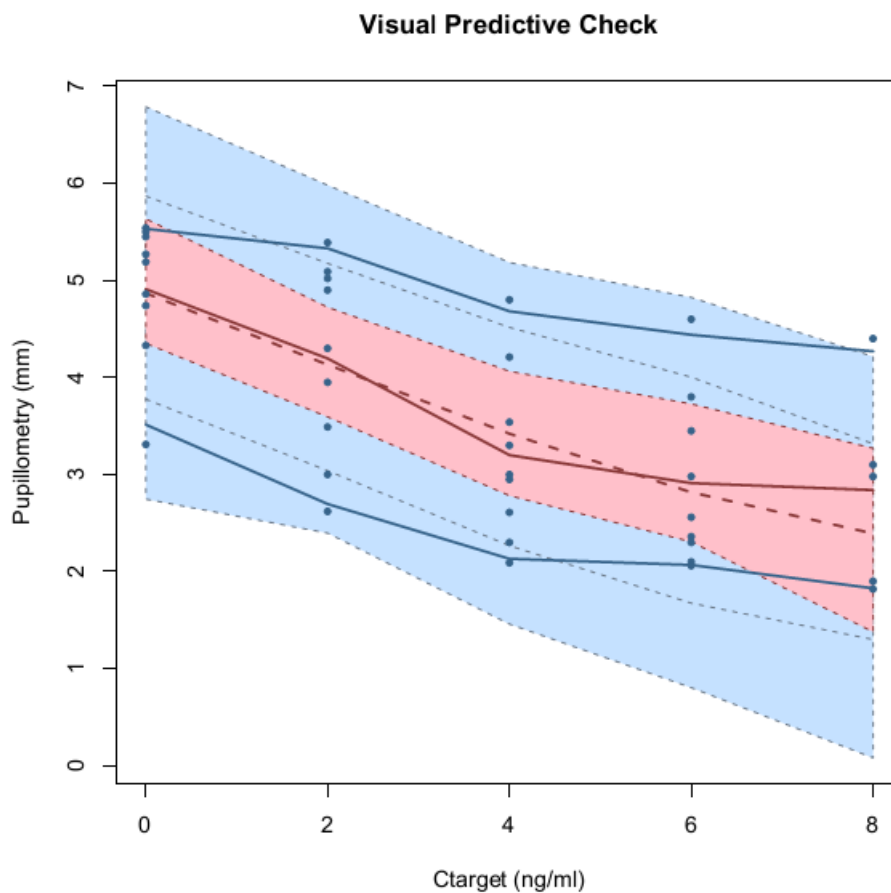


Figure 35 The visual predictive check for SigmoidEmaxProp1 and pupillometry.

The estimate for the intercept was 4.99 mm and the EC₅₀ was estimated to be 3.04 ng/ml (Table 38).

Table 38 Summary of model parameters for SigmoidEmaxProp1 and pupillometry.

Summary of model parameters for the best model				
Fixed effects				
Parameter	Estimate	Standard Errors	CV (%)	
intercept	4.99 mm	0.234	4.7	
EC ₅₀	3.04 ng/ml	0.484	15.9	
E _{max}	-0.50 mm	0.046	9.2	
hill	2.39	0.710	29.7	
a	0.11 mm	0.024	21.3	
Variance of random effects				
	Parameter	Estimate	Standard Errors	CV (%)
intercept	omega2.intercept	0.589	0.2563	44
EC ₅₀	omega2. EC ₅₀	0.165	0.1018	62
E _{max}	omega2. E _{max}	0.015	0.0085	58
hill	omega2. hill	0.744	0.3918	53
CV, coefficient of variation; a, additive residual error				

3.5.18 Best model for Morphine-Benzedrine Group (MBG) Scale

The best model for this metric was Zero3 (Figure 36). For this model, the baseline distribution was log-normal, the residual unexplained variability was constant and MEDD was not a covariate on the intercept.

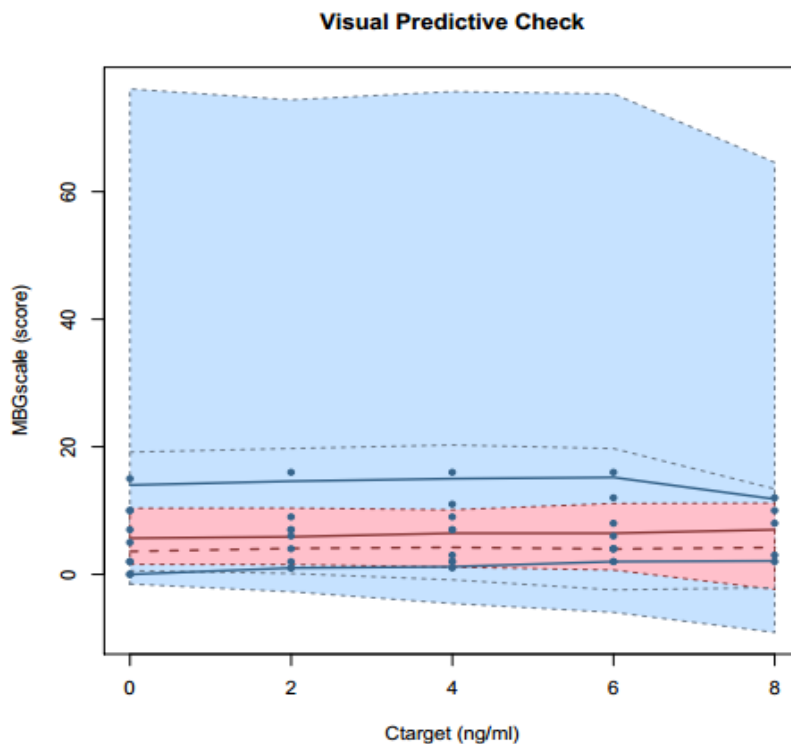


Figure 36 The visual predictive check for Zero3 and MBG scale.

The estimate for the intercept was 3.9 units and the slope was estimated to be 0 (Table 39).

Table 39 Summary of model parameters for Zero3 and MBG scale.

Summary of model parameters for the best model				
Fixed effects				
Parameter	Estimate	Standard Errors	CV (%)	
intercept	3.9 units	1.35	35	
slope	0 units per ng/ml	0	Not a number	
a	1.2 units	0.16	13	
Variance of random effects				
	Parameter	Estimate	Standard Errors	CV (%)
intercept	omega2.intercept	1.15	0.56	49
slope	omega2.slope	0.26	0.13	49
CV, coefficient of variation; a, additive residual error				

3.5.19 Best model for cold pain threshold

For this metric, no model fulfilled all the model selection criteria.

3.5.20 Best model for cold pain tolerance

The best model for this metric was LinearProp4 (Figure 37). For this model, the baseline distribution was log-normal, the residual unexplained variability was proportional and MEDD was not a covariate on the intercept and slope.

Visual Predictive Check

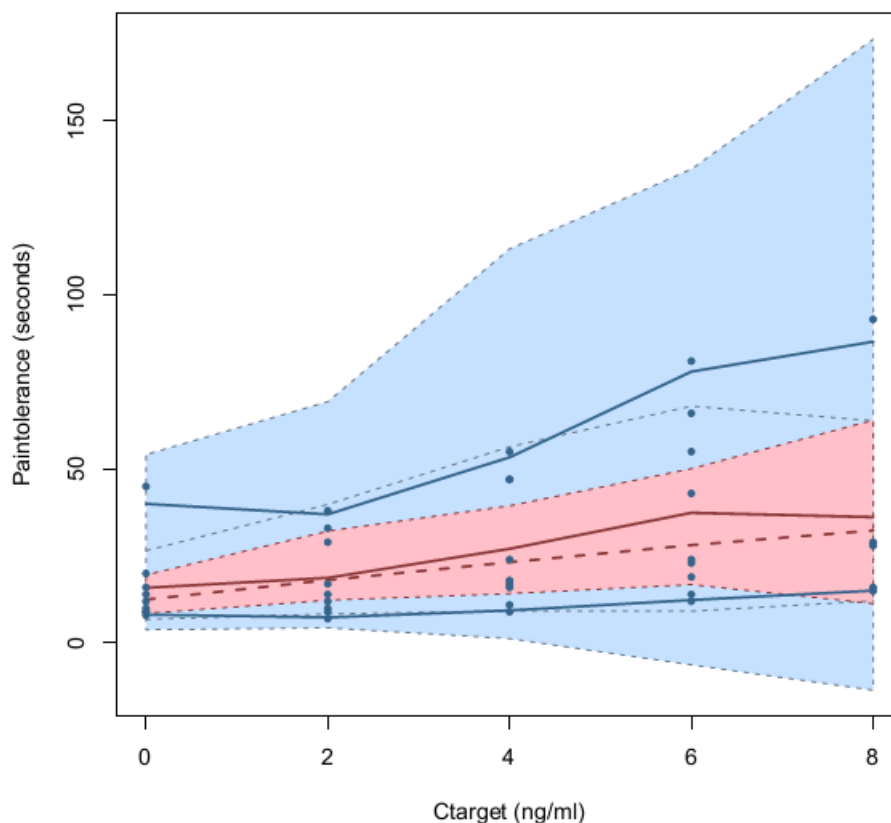


Figure 37 The visual predictive check for LinearProp4 and cold pain tolerance.

The estimate for the intercept was 12.61 seconds and the slope was estimated to be 0.22 seconds per ng/ml (Table 40).

Table 40 Summary of model parameters for LinearProp4 and cold pain tolerance.

Summary of model parameters for the best model				
Fixed effects				
Parameter	Estimate	Standard Errors	CV (%)	
intercept	12.61 sec	1.757	14	
slope	0.22 sec per ng/ml	0.062	28	
b	0.16 ratio	0.011	7	
Variance of random effects				
	Parameter	Estimate	Standard Errors	CV (%)
intercept	omega2.intercept	0.193	0.102	53
slope	omega2.slope	0.036	0.018	50
CV, coefficient of variation; b, proportional residual error				

3.5.21 Best model for Subjective Opioid Withdrawal Scale

The best model was LinearProp2 (Figure 38). For this model, the baseline distribution was normal, the residual unexplained variability was proportional and MEDD was not a covariate on the intercept and slope.

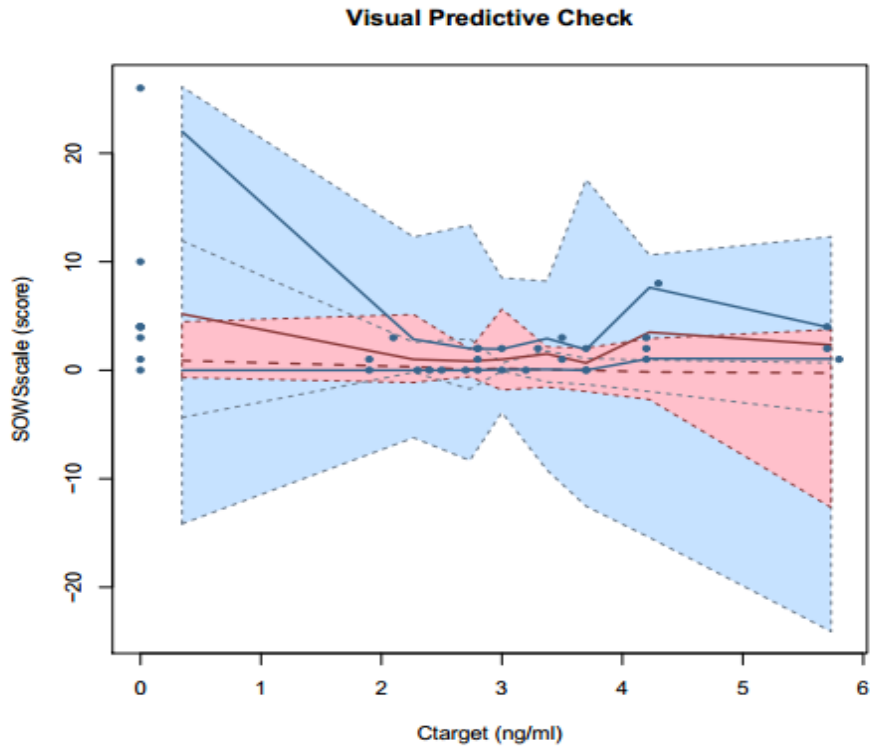


Figure 38 The visual predictive check for LinearProp2 and SOWS.

The estimate for the intercept was 2.94 units and the slope was estimated to be -0.12 units per ng/ml (Table 41).

Table 41 Summary of model parameters for LinearProp2 and SOWS.

Summary of model parameters for the best model				
Fixed effects				
Parameter	Estimate	Standard Errors	CV (%)	
intercept	2.94 units	0.879	30	
slope	-0.12 units per ng/ml	0.052	43	
b	0.94 ratio	0.056	6	
Variance of random effects				
	Parameter	Estimate	Standard Errors	CV (%)
intercept	omega2.intercept	5.081	0.034	0.68
slope	omega2.slope	0.015	0.012	82.46
CV, coefficient of variation; b, proportional residual error				

4 DISCUSSION

4.1 Safety and Dosing

Clinical pharmacology involves the quantitative analysis of drug administration and effect. In this study, we have attempted to describe the concentration-effect relationship of fentanyl in opioid-tolerant patients. An essential design feature of the study was the staircase design. This design was required in order to achieve a near steady-state plateau of the fentanyl effect site concentration allowing several pharmacodynamic measurements to be done during the interval. Furthermore, giving an infusion was deemed safer than giving multiple boluses of fentanyl.

Prior to the ethics application for the study, many discussions were conducted with regards to choosing the target effect site concentrations. Many pharmacological concentration-effect relationships demonstrate logarithmic increments but arithmetic increments were chosen in this study considering the narrow therapeutic index of fentanyl in this population. A design concern was that starting at too low doses may hinder patients from reaching the endpoints and beginning at higher doses might lead to safety issues. The estimates that were made appeared appropriate, at least for the less than 200 mg MEDD group. One patient in the above 200 mg MEDD group was supposed to be given the higher infusion regimen but she was mistakenly given the lower regimen. However, she managed to reach the endpoint in the first visit.

In essence, the study design was feasible and it involved no more than two study occasions and was safe. It is possible however that the patients who are extremely opioid-tolerant might reach the highest increment level without reaching the endpoint. The arithmetic increment in the target effect site concentration proved to be the appropriate approach.

4.2 Recruitment

The pool of patients in the Pain Management Unit of The Royal Adelaide Hospital was about 2000 and a large number of them were on opioids. However, it was difficult to find patients who suited all the inclusion and exclusion criteria. One of the main reasons that many patients were excluded from the outset was due to the fact that they were on SSRIs and the Australian Medicines Handbook (11) mentioned that the combination of SSRIs with fentanyl should be avoided or used with caution for fear of serotonin toxicity. This is probably based on at least four cases (169-171) mentioned in the literature linking co-administration of fentanyl and SSRIs with serotonin syndrome. The cases reported onsets of serotonin syndrome between 2 to 36 hours of starting fentanyl and with doses between as low as 50 micrograms intravenously to a high total of 2.54 milligrams in 36 hours. Rang et al (169) suggested that advising against this drug combination would be overcautious while Kirschner and Donovan recommended that emergency care providers be cautious and consider alternative agents in patients taking SSRIs or other serotonergic drugs (170). As the study that we were conducting was experimental in nature with no direct benefit to the patients involved, we considered that it was reasonable to exclude patients on SSRIs from the study.

4.3 Assessment of opioid effects

There are subjective and objective measures of assessing opioid effects. Subjective ways include using the MBG and SOW scales to assess euphoria and withdrawal. As the name implies, subjective tests are highly variable and environment-dependent hence the need for objective assessments.

Commonly employed objective measures for assessing opioid effects include monitoring the EEG, saccadic eye movements and pupillometry. These make up the backbone of this study.

Evaluating pain is usually problematic due to the various psychological, cognitive and social elements of the disease that come into play (172). Systemic reactions such as fever and malaise (172) further complicate the matter making pain evaluations very confounded and difficult to interpret. This has led to the use of experimental pain models in clinical trials in order to assess analgesia.

Pain models related to opioid therapy can be divided into at least two categories; acute pain models (Table 42) and models that induce hyperalgesia. Acute models such as heat stimulation of the skin activate normal physiological mechanisms through the peripheral nociceptors. Such models have traditionally been believed to not mimic pathological pain very well.

Table 42 Commonly used acute models of pain in opioid studies

Acute models
Electrical skin stimulation
Heat skin stimulation
Heat and cold skin stimulation
Intramuscular injection of hypertonic saline
Transcutaneous and intramuscular electrical stimulation
Deep pressure
Cold pressor test (cold pain test)
Tibial pressure
Skin and intramuscular repeated electrical stimulation
Pressure algometry
Short lasting radiant heat
Ischaemic pain
Nociceptive reflex test
Argon laser pain
Electrical stimulation of the teeth

Other models change the peripheral and central pain system and are believed to better reflect chronic pain processes. Such a model that induces hyperalgesia and allodynia (Table 43) include the intradermal injection of capsaicin model.

Table 43 Models inducing hyperalgesia that are commonly employed in opioid studies

Models inducing hyperalgesia
Burn injury
Repeated pinprick
Continuous electrical skin stimulation
Intradermal capsaicin
Freeze lesion
Ultraviolet radiation
Concentric and eccentric muscle contraction

In this study, we have chosen the cold pain test for pain assessments as this test had been shown to be sensitive to the analgesic effects of opioids (156).

Previous studies (173) have shown that the PD relationship for the opioid-tolerant is different from the opioid-naïve. Generally, the concentration-effect relationship for the opioid-tolerant is shifted to the right as a higher dose is needed in order to achieve the same endpoints.

In the case of cold pain tolerance, the concentration-effect relationship for the opioid-tolerant is shifted downward as opioid-dependent patients are more sensitive to the effects of cold pain and therefore have a lower cold pain tolerance reading than the opioid-naïve. This difference is however not seen with the electrical stimulation model of pain (173). These relationship patterns might not be consistently seen though, as there may be variation in responses depending on the type and doses of opioids that a patient is taking daily.

4.4 Electroencephalography

There were a few previous studies done to measure the EEG changes associated with intravenous fentanyl (146, 174-177). However, to the author's knowledge no other previous study has measured EEG changes with fentanyl without other concurrent drugs being administered even though this factor might not have any significant impact on the EEG readings. The previous studies were done in an operative setting and other drugs such as benzodiazepines, morphine and scopolamine were also given before the measurements were done. Doses of fentanyl given were within the range of 0.319 mg to 4.76 mg in one session in previous studies whereas in this study doses given were between 0.8 mg to 2.5 mg per dosing session. The montage of the electrodes and the timing for doing the EEG recordings for this study were also different from previous studies. Many studies used the EEG to measure depth of anaesthesia by measuring the 95% spectral edge. The study by Sebel et al for example started the continuous EEG recordings from before induction of anaesthesia until just before commencement of surgery and intermittently after the surgery (175). This study, on the other hand only recorded the EEG about 10 minutes after starting or changing the fentanyl infusion for about one minute. This was done to ensure that the target concentration had been reached at the effect site before doing the recordings. This consideration was not present in previous studies.

Despite the differences in methodology and EEG analysis technique employed, this study generally produced nearly similar results with previous studies namely an increase in the power of very low (0.5-2.0 Hz) and delta (2.0-4.0 Hz) bands. It should be noted that the frequency range of delta from previous studies was in the range of 0.5-3.5 Hz and not 2.0-4.0 Hz as in this study.

The best model for very low frequency (0.5-2.0 Hz) EEG band at Pz-Oz, delta (2.0-4.0 Hz) at Pz-Oz, and theta at Fz-Cz (4.0-7.5 Hz) is the Linear Proportional 4 model. This suggests that this metric could be directly related to fentanyl effect site concentrations.

The best model for very low frequency EEG band at Fz-Cz, delta at Fz-Cz and theta at Pz-Oz is the Linear Proportional 2 model.

There was no model selected for the other EEG metrics due to not fulfilling the criteria specified.

4.5 Saccadic eye movement tests

A study by Rothenberg et al published more than 30 years ago in opioid-naïve individuals reported that oral methadone reduced the accuracy of saccadic eye movement and increased their reaction time (178). They however did not see a reduction in saccadic peak velocity or increase in saccade duration. They attributed this to methadone affecting specific sensory rather than motor components of saccadic response (178).

Another study by Tedeschi et al showed that meptazinol (a mixed opioid agonist/antagonist) did not affect saccadic eye movement after a single day's treatment (4 doses of 200 mg) (179). Richens et al administered a single intramuscular injection of either meptazinol (100 mg), papaveretum (20 mg) or placebo (dextrose) followed by conducting a battery of tasks, 1 and 3 hours after drug administration in healthy volunteers. Contrary to Tedeschi's findings, their study showed that saccadic peak velocity was significantly impaired by meptazinol and papaveretum at 1 hour but only with papaveretum at 3 hours (180).

A study published in 2003 by Melichar et al in methadone-maintained participants (150) showed that the peak velocity decreased in a dose-dependent manner with 10 mg subcutaneous hydromorphone. There was also a similar decrease with 5 mg hydromorphone given subcutaneously but this was not significant (150).

A more recent study by Grace et al (181) demonstrated that opioid-tolerant patients on buprenorphine have a significantly lower baseline peak saccadic velocity compared to healthy participants. The study also illustrated that morphine reduced the peak saccadic velocity compared to placebo in healthy participants.

The present study was unable to elicit a reduction in saccadic peak velocity in all patients. This has caused skewing of the pooled data towards the zero-slope model which implies that fentanyl effect site concentration has no effect on average peak velocity. This was probably not true even though no previous studies have been done to specifically look at the effect of fentanyl on saccadic peak velocity in the opioid-tolerant.

The best model for average peak velocity was Zero 3. The best model for saccadic latency was the Zero 1 model.

There was no model selected for saccadic inaccuracy and number of valid saccades.

4.6 Pupillometry

Pupillometry provided one of the most reliable readings in this experiment. Patient cooperation required in this procedure was minimal and a clear relationship between fentanyl concentration at the effect site and pupil size was seen. Sigmoid Emax Proportional 1 model provided the best description of the data for pupil size. This was closely similar to a previous study with morphine and morphine-6-glucuronide that demonstrated that the pupil size was linked to the effect site concentrations by a sigmoid Emax model for decreasing effects (139). No previous studies have looked at the relationship between fentanyl concentration at the effect site and pupil size.

4.7 Cold pain test

Pain tolerance was related to the concentrations using a Linear Prop 4 model. No best model was determined for pain threshold.

To the author's knowledge, no previous study had been done looking at both pain tolerance and pain threshold to cold water with increasing doses of intravenous fentanyl in man. Several studies have investigated the effects of intravenous fentanyl given alone or together with other perioperative medications on different types of cold pain using various methods different from the methods used in this study (172). However, one study in methadone-maintained patients showed that there was a dose-dependent increase in cold pain tolerance with remifentanyl (182). The finding of the remifentanyl study is therefore consistent with the result of this study with regards to cold pain tolerance.

4.8 Subjective measures of opioid effect and withdrawal

The best model for Morphine-Benzedrine Group (MBG) Scale was the Zero 3 model. The lack of increasing scores on the MBG scale is consistent with a previous study conducted in healthy volunteers with intravenous fentanyl (183).

In this study, the Subjective Opioid Withdrawal Scale (SOWS) was related to the effect site concentrations using the Linear Prop 2 model. There were no previous studies done to link SOWS scores with fentanyl effect site concentration. However, Hay et al demonstrated that no statistically significant difference was found between SOWS scores at baseline and during or after remifentanyl infusion (182).

4.9 Covariate effect of MEDD on the models

This study was not able to demonstrate the covariate effect of MEDD (Morphine-equivalent daily dose) on any of the chosen models for all metrics. This was probably due to the small sample size which lowered the study power to identify covariate effects.

4.10 Study Design and Implementation

In retrospect, if the study were to be repeated, it might be useful that instead of having just one baseline saccadic eye movement test, two baseline tests be done as there seemed to be a clear learning effect with doing this test. The test results improved in most participants on the 2nd reading as the participants got used to the test.

The application of EEG electrodes should always be done after the patient has gone to the toilet and their veins cannulated as the process of cannulation and going to the toilet will usually dislodge the electrodes from its proper place giving 'noisy' readings of the EEG.

During the scrubbing process before electrodes application, one should be careful not too over scrub the skin as this will cause bleeding and may affect the readings for the EEG and saccadic eye movement tests.

4.11 Subject Selection

The participant with Stickler's syndrome should probably have not been included in the study as his left eye vision was poor and that had significantly affected the saccadic eye movements test results.

4.12 Pharmacodynamic study

For this study, venous blood samples were withdrawn for fentanyl plasma concentrations to be quantified as according to the protocol. However, due to the small sample size and the pilot nature of the study we decided that the analysis would not materially contribute to the interpretation of the study. This is primarily because venous fentanyl concentrations are known to follow a different time-course to both the arterial and effect compartment fentanyl concentrations (184). Measured venous fentanyl concentrations would not have either informed the accuracy of the STANPUMP model or confirmed effect compartment concentrations were at target values in each subject. Therefore, fentanyl assaying of the venous samples were not done.

4.13 Summary of research findings

In summary, this study design has proven to be a feasible and practical way of looking at determining the effects of MEDD (Morphine-equivalent daily dose) on the acute fentanyl requirements in the opioid-tolerant.

4.14 Clinical implications of research findings

Based on the 9 patients that we studied, we have shown that the study design was safe and feasible. Safety aspects are extremely important in this type of study as we are using a drug with a very narrow therapeutic index.

This study is pilot in nature and it was surprisingly difficult to find suitable patients for the study even though every case note in the Pain Management Unit at the Royal Adelaide Hospital was evaluated for eligibility. There is a higher pressure on doctors nowadays not to prescribe large doses of opioids which has led to the dwindling in the number of patients receiving high dose opioids and hence who are suitable for such a study. Even though the number of patients on high doses of maintenance opioids is declining, the principles of treating this cohort of patients are still important and very relevant as they still present to hospitals for acute pain management. Currently, the people who are on high maintenance doses of opioids are mainly the patients on opioid substitution programs or are abusing drugs. The illicit drug users and patients on drug substitution programs were excluded in view of difficult recruitment, poor venous access and ethical issues in giving such patients high doses of opioids.

From the study that we have conducted, fentanyl does produce analgesia in the opioid-tolerant and this could be achieved without causing gross respiratory depression. However, we were not able to link this with patients' maintenance opioid dose. We can also draw from this study that starting patients on double the dose usually needed for the opioid-naïve is a reasonable approach to dealing

with acute pain in this population. It is then also safe to increase the dose arithmetically in order to attain effective analgesia.

4.14.1 Directions for future research

A similar research design could be employed with greater number of subjects to produce better models for the metrics. These models will possibly be able to show an effect of MEDD (Morphine-equivalent daily dose) on the parameters of the models.

5 REFERENCES

1. IASP Taxonomy [internet]. Seattle: IASP Press; 1994 [cited 2013 Jul 15]. Available from: http://www.iasp-pain.org/AM/Template.cfm?Section=Pain_Definitions.
2. Katz WA, Rothenberg R. Section 3: The nature of pain: pathophysiology. *J Clin Rheumatol*. 2005;11(2 Suppl):S11-5.
3. Macintyre PE, Scott DA, Schug SA, Visser EJ, Walker SM. *Acute Pain Management : Scientific Evidence*. 3rd ed. Melbourne: ANZCA and FPM; 2010.
4. Kalant H. Opium revisited: a brief review of its nature, composition, non-medical use and relative risks. *Addiction*. 1997;92(3):267-77.
5. Chau DL, Walker V, Pai L, Cho LM. Opiates and elderly: use and side effects. *Clin Interv Aging*. 2008;3(2):273-8.
6. Trescot AM, Datta S, Lee M, Hansen H. Opioid pharmacology. *Pain Physician*. 2008;11(2 Suppl):S133-53.
7. Goodman LS, Gilman A, Brunton LL, Chabner B, Knollmann BrC. *Goodman & Gilman's the pharmacological basis of therapeutics*. 12th ed. New York: McGraw-Hill Medical; 2011.
8. Hemmings HC, Hopkins PM. *Foundations of Anesthesia: Basic Sciences for Clinical Practice*. 2nd ed. Philadelphia: Mosby 2006.
9. Yaksh T. Pharmacology and mechanisms of opioid analgesic activity. *Acta Anaesthesiol Scand*. 1997;41(1):94-111.
10. Davis MP. Buprenorphine in cancer pain. *Support Care Cancer*. 2005;13(11):878-87.
11. Australian Medicines Handbook 2013 (online). Adelaide: Australian Medicines Handbook Pty Ltd; 2013. Available from: <http://www.amh.net.au>.
12. Inturrisi CE. Clinical pharmacology of opioids for pain. *Clin J Pain*. 2002 Jul-Aug;18(4 Suppl):S3-13. PubMed PMID: 12479250. Epub 2002/12/14. eng.
13. Devlin JW, Roberts RJ. Pharmacology of commonly used analgesics and sedatives in the ICU: benzodiazepines, propofol, and opioids. *Crit Care Clin*. 2009;25(3):431-49.
14. Johansen MJ, Satterfield WC, Baze WB, Hildebrand KR, Gradert TL, Hassenbusch SJ. Continuous intrathecal infusion of hydromorphone: safety in the sheep model and clinical implications. *Pain Med*. 2004;5(1):14-25.
15. Villesen HH, Foster DJR, Upton RN, Somogyi AA, Martinez A, Grant C. Cerebral kinetics of oxycodone in conscious sheep. *J Pharm Sci*. 2006;95(8):1666-76.
16. Kharasch ED, Walker A, Whittington D, Hoffer C, Bedynek PS. Methadone metabolism and clearance are induced by nelfinavir despite inhibition of cytochrome P4503A (CYP3A) activity. *Drug Alcohol Depend*. 2009;101(3):158-68.
17. Williams DG, Hatch DJ, Howard RF. Codeine phosphate in paediatric medicine. *Br J Anaesth*. 2001 March 1, 2001;86(3):413-21.
18. Freye E, Levy JV. *Opioids in medicine: A Comprehensive Review on the Mode of Action and the use of Analgesics in Different Clinical Pain States*: Springer; 2007.
19. MIMS Australia. Australia: UBM Medica Australia; 2011.
20. *Textbook of anaesthesia*. 5th ed. Rowbotham DJ, Aitkenhead AR, Smith G, editors. Edinburgh: Churchill Livingstone Elsevier; 2009.
21. Katz N, Mazer NA. The impact of opioids on the endocrine system. *Clin J Pain*. 2009;25(2):170-5.
22. Law PY, Wong YH, Loh HH. Molecular mechanisms and regulation of opioid receptor signaling. *Annu Rev Pharmacol Toxicol*. 2000;40:389-430.
23. Christie MJ. Cellular neuroadaptations to chronic opioids: tolerance, withdrawal and addiction. *Br J Pharmacol*. 2008;154(2):384-96.
24. Janeckah A, Fichna J, Janecki T. Opioid Receptors and their Ligands. *Curr Top Med Chem*. 2004;4(1):1-17.

25. Vuong C, Van Uum SHM, O'Dell LE, Lutfy K, Friedman TC. The effects of opioids and opioid analogs on animal and human endocrine systems. *Endocr Rev.* 2010;31(1):98-132.
26. Dietis N, Rowbotham DJ, Lambert DG. Opioid receptor subtypes: Fact or artifact? *Br J Anaesth.* 2011;107(1):8-18.
27. Zöllner C, Stein C. Opioids. In: Stein C, editor. *Analgesia. Handbook of Experimental Pharmacology.* 177: Springer Berlin Heidelberg; 2007. p. 31-63.
28. Miotto K, Kaufman D, Anton B, Keith Jr DE, Evans CJ. Human opioid receptors: chromosomal mapping and mRNA localization. *NIDA Res Monogr.* 1996;161:72-82.
29. Waldhoer M, Bartlett SE, Whistler JL. Opioid receptors. *Annu Rev Biochem.* 2004;73:953-90.
30. Dumas EO, Pollack GM. Opioid tolerance development: a pharmacokinetic/pharmacodynamic perspective. *AAPS J.* 2008;10(4):537-51.
31. Taylor DA, Fleming WW. Unifying perspectives of the mechanisms underlying the development of tolerance and physical dependence to opioids. *J Pharmacol Exp Ther.* 2001;297(1):11-8.
32. Dang VC, Christie MJ. Mechanisms of rapid opioid receptor desensitization, resensitization and tolerance in brain neurons. *Br J Pharmacol.* 2012;165(6):1704-16.
33. Gurevich VV, Gurevich EV. The structural basis of arrestin-mediated regulation of G-protein-coupled receptors. *Pharmacol Ther.* 2006 Jun;110(3):465-502.
34. Lê AD, Mihic SJ, Wu PH. Alcohol tolerance. *Animal Models of Drug Addiction: Springer;* 1993. p. 95-124.
35. Morgan MM, Christie MJ. Analysis of opioid efficacy, tolerance, addiction and dependence from cell culture to human. *Br J Pharmacol.* 2011;164(4):1322-34.
36. Angst MS, Clark JD. Opioid-induced hyperalgesia: a qualitative systematic review. *Anesthesiology.* 2006;104(3):570-87.
37. Bekhit MH. Opioid-induced hyperalgesia and tolerance. *Am J Ther.* 2010;17(5):498-510.
38. Chu LF, Angst MS, Clark D. Opioid-induced hyperalgesia in humans: molecular mechanisms and clinical considerations. *Clin J Pain.* 2008;24(6):479-96.
39. Hay JL. Evaluation and treatment of opioid-induced hyperalgesia [PhD]. Adelaide: University of Adelaide; 2007.
40. Wang HY, Burns LH. G $\beta\gamma$ that interacts with adenylyl cyclase in opioid tolerance originates from a Gs protein. *J Neurobiol.* 2006;66(12):1302-10.
41. Akbari E. The role of cyclo-oxygenase inhibitors in attenuating opioid-induced tolerance, hyperalgesia, and dependence. *Med Hypotheses.* 2012;78(1):102-6.
42. Bohn LM, Gainetdinov RR, Lin FT, Lefkowitz RJ, Caron MG. Mu-opioid receptor desensitization by beta-arrestin-2 determines morphine tolerance but not dependence. *Nature.* 2000;408(6813):720-3.
43. Lee M, Silverman S, Hansen H, Patel V, Manchikanti L. A comprehensive review of opioid-induced hyperalgesia. *Pain Physician.* 2011;14(2):145-61.
44. Ossipov MH, Lai J, King T, Vanderah TW, Porreca F. Underlying mechanisms of pronociceptive consequences of prolonged morphine exposure. *Biopolymers.* 2005;80(2-3):319-24.
45. Hutchinson MR, Shavit Y, Grace PM, Rice KC, Maier SF, Watkins LR. Exploring the neuroimmunopharmacology of opioids: an integrative review of mechanisms of central immune signaling and their implications for opioid analgesia. *Pharmacol Rev.* 2011;63(3):772-810.
46. Davis MP. Opioid tolerance and hyperalgesia: Basic mechanisms and management in review. *Progress in Palliative Care.* 2011;19(2):73-86.
47. Crain SM, Shen KF. Modulation of opioid analgesia, tolerance and dependence by Gs-coupled, GM1 ganglioside-regulated opioid receptor functions. *Trends Pharmacol Sci.* 1998;19(9):358-65.
48. Largent-Milnes TM, Guo W, Wang HY, Burns LH, Vanderah TW. Oxycodone plus ultra-low-dose naltrexone attenuates neuropathic pain and associated mu-opioid receptor-Gs coupling. *J Pain.* 2008;9(8):700-13.

49. Crain SM, Shen KF. Neuraminidase inhibitor, oseltamivir blocks GM1 ganglioside-regulated excitatory opioid receptor-mediated hyperalgesia, enhances opioid analgesia and attenuates tolerance in mice. *Brain Res.* 2004;995(2):260-6.
50. Simonnet G, Rivat C. Opioid-induced hyperalgesia: abnormal or normal pain? *Neuroreport.* 2003;14(1):1-7.
51. Mao J, Price DD, Mayer DJ. Thermal hyperalgesia in association with the development of morphine tolerance in rats: roles of excitatory amino acid receptors and protein kinase C. *J Neurosci.* 1994;14(4):2301-12.
52. Mendez IA, Trujillo KA. NMDA receptor antagonists inhibit opiate antinociceptive tolerance and locomotor sensitization in rats. *Psychopharmacology (Berl).* 2008;196(3):497-509.
53. González P, Cabello P, Germany A, Norris B, Contreras E. Decrease of tolerance to, and physical dependence on morphine by, glutamate receptor antagonists. *Eur J Pharmacol.* 1997;332(3):257-62.
54. Bell RF. Low-dose subcutaneous ketamine infusion and morphine tolerance. *Pain.* 1999;83(1):101-3.
55. Heiskanen T, Härtel B, Dahl M-L, Seppälä T, Kalso E. Analgesic effects of dextromethorphan and morphine in patients with chronic pain. *Pain.* 2002;96(3):261-7.
56. Salehi M, Zargar A, Ramezani MA. Effects of Dextromethorphan on reducing methadone dosage in opium addicts undergoing methadone maintenance therapy: A double blind randomized clinical trial. *Journal of Research in Medical Sciences.* 2011;16(10):1354-60.
57. Dudgeon DJ, Bruera E, Gagnon B, Watanabe SM, Allan SJ, Warr DG, et al. A Phase III Randomized, Double-Blind, Placebo-Controlled Study Evaluating Dextromethorphan Plus Slow-Release Morphine for Chronic Cancer Pain Relief in Terminally Ill Patients. *J Pain Symptom Manage.* 2007;33(4):365-71.
58. Galer BS, Lee D, Ma T, Nagle B, Schlagheck TG. Morphidex® (morphine sulfate/dextromethorphan hydrobromide combination) in the treatment of chronic pain: Three multicenter, randomized, double-blind, controlled clinical trials fail to demonstrate enhanced opioid analgesia or reduction in tolerance. *Pain.* 2005;115(3):284-95.
59. Mao J, Sung B, Ji RR, Lim G. Chronic morphine induces downregulation of spinal glutamate transporters: implications in morphine tolerance and abnormal pain sensitivity. *J Neurosci.* 2002;22(18):8312-23.
60. Yang L, Wang S, Sung B, Lim G, Mao J. Morphine induces ubiquitin-proteasome activity and glutamate transporter degradation. *J Biol Chem.* 2008;283(31):21703-13.
61. Yang L, Wang S, Lim G, Sung B, Zeng Q, Mao J. Inhibition of the ubiquitin-proteasome activity prevents glutamate transporter degradation and morphine tolerance. *Pain.* 2008;140(3):472-8.
62. Vanderah TW. Pathophysiology of pain. *The Medical clinics of North America.* 2007;91(1):1-12.
63. Wang Z, Ma W, Chabot J-G, Quirion R. Morphological evidence for the involvement of microglial p38 activation in CGRP-associated development of morphine antinociceptive tolerance. *Peptides.* 2010;31(12):2179-84.
64. Chen Y, Geis C, Sommer C. Activation of TRPV1 contributes to morphine tolerance: Involvement of the mitogen-activated protein kinase signaling pathway. *J Neurosci.* 2008;28(22):5836-45.
65. Szallasi A, Sheta M. Targeting TRPV1 for pain relief: Limits, losers and laurels. *Expert Opin Investig Drugs.* 2012;21(9):1351-69.
66. Zeilhofer HU, Brune K. A Role for Cyclooxygenase-1 in Neuropathic Pain? *Anesthesiology.* 2003;99(5):1043-4.
67. Wong CS, Hsu MM, Chou R, Chou YY, Tung CS. Intrathecal cyclooxygenase inhibitor administration attenuates morphine antinociceptive tolerance in rats. *Br J Anaesth.* 2000;85(5):747-51.

68. Dunbar SA, Karamian I, Roberts L, Zhang J. Increased prostaglandin E2 release and activated Akt/ β -catenin signaling pathway occur after opioid withdrawal in rat spinal cord. *Anesthesiology*. 2006;105(1):154-9.
69. Dunbar SA, Karamian I, Zhang J. Ketorolac prevents recurrent withdrawal induced hyperalgesia but does not inhibit tolerance to spinal morphine in the rat. *Eur J Pain*. 2007;11(1):1-6.
70. Powell KJ, Quirion R, Jhamandas K. Inhibition of neurokinin-1-substance P receptor and prostanoid activity prevents and reverses the development of morphine tolerance in vivo and the morphine-induced increase in CGRP expression in cultured dorsal root ganglion neurons. *Eur J Neurosci*. 2003;18(6):1572-83.
71. Ossipov MH, Lai J, Vanderah TW, Porreca F. Induction of pain facilitation by sustained opioid exposure: relationship to opioid antinociceptive tolerance. *Life Sci*. 2003;73(6):783-800.
72. Becker C, Hamon M, Cesselin F, Benoliel JJ. δ 2-Opioid receptor mediation of morphine-induced CCK release in the frontal cortex of the freely moving rat. *Synapse*. 1999;34(1):47-54.
73. King T, Gardell LR, Wang R, Vardanyan A, Ossipov MH, Philip Malan Jr T, et al. Role of NK-1 neurotransmission in opioid-induced hyperalgesia. *Pain*. 2005;116(3):276-88.
74. Lim G, Wang S, Zeng Q, Sung B, Mao J. Evidence for a long-term influence on morphine tolerance after previous morphine exposure: role of neuronal glucocorticoid receptors. *Pain*. 2005;114(1-2):81-92.
75. Wei F, Dubner R, Zou S, Ren K, Bai G, Wei D, et al. Molecular depletion of descending serotonin unmasks its novel facilitatory role in the development of persistent pain. *J Neurosci*. 2010;30(25):8624-36.
76. Higgins GA, Joharchi N, Nguyen P, Sellers EM. Effect of the 5-HT₃ receptor antagonists, MDL72222 and ondansetron on morphine place conditioning. *Psychopharmacology (Berl)*. 1992;106(3):315-20.
77. Pei Q, Zetterstrom T, Leslie RA, Grahame-Smith DG. 5-HT₃ receptor antagonists inhibit morphine-induced stimulation of mesolimbic dopamine release and function in the rat. *Eur J Pharmacol*. 1993;230(1):63-8.
78. Dogrul A, Ossipov MH, Porreca F. Differential mediation of descending pain facilitation and inhibition by spinal 5HT-3 and 5HT-7 receptors. *Brain Res*. 2009;1280:52-9.
79. Liang DY, Li X, Clark JD. 5-hydroxytryptamine type 3 receptor modulates opioid-induced hyperalgesia and tolerance in mice. *Anesthesiology*. 2011;114(5):1180-9.
80. Walstab J, Rappold G, Niesler B. 5-HT₃ receptors: Role in disease and target of drugs. *Pharmacol Ther*. 2010;128(1):146-69.
81. Verma D, Gupta YK, Parashar A, Ray SB. Differential expression of L- and N-type voltage-sensitive calcium channels in the spinal cord of morphine & nimodipine treated rats. *Brain Res*. 2009;1249(0):128-34.
82. Dogrul A, Bilsky EJ, Ossipov MH, Lai J, Porreca F. Spinal L-Type Calcium Channel Blockade Abolishes Opioid-Induced Sensory Hypersensitivity and Antinociceptive Tolerance. *Anesth Analg*. 2005 December 1, 2005;101(6):1730-5.
83. Miljanich GP. Ziconotide: neuronal calcium channel blocker for treating severe chronic pain. *Curr Med Chem*. 2004;11(23):3029-40.
84. Stahl SM. Anticonvulsants and the relief of chronic pain: Pregabalin and gabapentin as α (2) δ ligands at voltage-gated calcium channels. *J Clin Psychiatry*. 2004;65(5):596-7.
85. Chizh BA, Göhring M, Tröster A, Quartey GK, Schmelz M, Koppert W. Effects of oral pregabalin and aprepitant on pain and central sensitization in the electrical hyperalgesia model in human volunteers. *Br J Anaesth*. 2007 February 1, 2007;98(2):246-54.
86. O'Callaghan JP, Miller DB. Spinal glia and chronic pain. *Metabolism*. 2010;59, Supplement 1(0):S21-S6.
87. Olson JK, Miller SD. Microglia initiate central nervous system innate and adaptive immune responses through multiple TLRs. *J Immunol*. 2004;173:3916-24.
88. Carpentier PA, Duncan DS, Miller SD. Glial toll-like receptor signaling in central nervous system infection and autoimmunity. *Brain Behav Immun*. 2008;22:140-7.

89. Milligan ED, Watkins LR. Pathological and protective roles of glia in chronic pain. *Nat Rev Neurosci.* 2009;10(1):23-36.
90. Huxtable CA, Roberts LJ, Somogyi AA, Macintyre PE. Acute pain management in opioid-tolerant patients: A growing challenge. *Anaesth Intensive Care.* 2011;39(5):804-23.
91. Watkins LR, Hutchinson MR, Rice KC, Maier SF. The "Toll" of Opioid-Induced Glial Activation: Improving the Clinical Efficacy of Opioids by Targeting Glia. *Trends Pharmacol Sci.* 2009;30(11):581-91.
92. Tawfik VL. Induction of astrocyte differentiation by propentofylline increases glutamate transporter expression in vitro: heterogeneity of the quiescent phenotype. *Glia.* 2006;54:193-203.
93. Hutchinson MR, Coats BD, Lewis SS, Zhang Y, Sprunger DB, Rezvani N, et al. Proinflammatory cytokines oppose opioid-induced acute and chronic analgesia. *Brain, Behavior, and Immunity.* 2008;22(8):1178-89.
94. Hutchinson MR, Northcutt AL, Chao LW, Kearney JJ, Zhang Y, Berkelhammer DL, et al. Minocycline suppresses morphine-induced respiratory depression, suppresses morphine-induced reward, and enhances systemic morphine-induced analgesia. *Brain, Behavior, and Immunity.* 2008;22(8):1248-56.
95. Cui Y, Liao XX, Liu W, Guo RX, Wu ZZ, Zhao CM, et al. A novel role of minocycline: Attenuating morphine antinociceptive tolerance by inhibition of p38 MAPK in the activated spinal microglia. *Brain, Behavior, and Immunity.* 2008;22(1):114-23.
96. Mika J, Wawrzczak-Bargiela A, Osikowicz M, Makuch W, Przewlocka B. Attenuation of morphine tolerance by minocycline and pentoxifylline in naive and neuropathic mice. *Brain, Behavior, and Immunity.* 2009;23(1):75-84.
97. Richebe P, Cahana A, Rivat C. Tolerance and opioid-induced hyperalgesia. Is a divorce imminent? *Pain.* 2012;153(8):1547-8.
98. Chu LF, D'Arcy N, Brady C, Zamora AK, Young CA, Kim JE, et al. Analgesic tolerance without demonstrable opioid-induced hyperalgesia: A double-blinded, randomized, placebo-controlled trial of sustained-release morphine for treatment of chronic nonradicular low-back pain. *Pain.* 2012;153(8):1583-92.
99. Davis JJ, Swenson JD, Hall RH, Dillon JD, Johnson KB, Egan TD, et al. Preoperative "fentanyl challenge" as a tool to estimate postoperative opioid dosing in chronic opioid-consuming patients. *Anesth Analg.* 2005;101(2):389-95.
100. White JM, Irvine RJ. Mechanisms of fatal opioid overdose. *Addiction.* 1999;94(7):961-80.
101. Viscomi C, Pearson JK. Perioperative Management of the Opioid-Tolerant Patient. *Advances in Anesthesia.* 2009;27(1):25-54.
102. Mitra S, Sinatra RS. Perioperative management of acute pain in the opioid-dependent patient. *Anesthesiology.* 2004;101(1):212-27.
103. Pasternak GW. Incomplete cross tolerance and multiple mu opioid peptide receptors. *Trends Pharmacol Sci.* 2001;22(2):67-70.
104. Pasternak GW. Molecular insights into μ opioid pharmacology: From the clinic to the bench. *Clin J Pain.* 2010;26(SUPPL.10):S3-S9.
105. Compton WM, Volkow ND. Major increases in opioid analgesic abuse in the United States: Concerns and strategies. *Drug Alcohol Depend.* 2006;81(2):103-7.
106. Fischer B, Rehm J. Illicit opioid use in the 21st century: witnessing a paradigm shift? *Addiction.* 2007;102(4):499-501.
107. Britt H MG, Charles J, Henderson J, Valenti L, Harrison C, Zhang C, Chambers T, Pollack A, Bayram C, O'Halloran J, & Pan Y A decade of Australian general practice activity 2002-03 to 2011-12. General practice series no. 32 Sydney: Sydney University Press 2012.
108. Britt H MG, Knox S, Charles J, Valenti L, Henderson J, Pan Y, Bayram C & Harrison C. General practice activity in Australia 2002-03. General Practice Series. Cat. no. GEP 14. . Canberra: AIHW; 2003. Available from: <http://www.aihw.gov.au/publication-detail/?id=6442467538>.
109. Britt H MG, Henderson J, Charles J, Valenti L, Harrison C, Bayram C, Zhang C, Pollack AJ, O'Halloran J, & Pan Y. . General practice activity in Australia 2011-12. General practice series no.31

Sydney: Sydney University Press 2012. Available from:

<http://purl.library.usyd.edu.au/sup/9781743320181>.

110. Harrison CM, Charles J, Henderson J, Britt H. Opioid prescribing in Australian general practice. *Med J Aust*. 2012;196(6):380-1.
111. AIHW. National opioid pharmacotherapy statistics annual data collection 2012. Canberra: AIHW; 2013.
112. Ling W, Mooney L, Hillhouse M. Prescription opioid abuse, pain and addiction: Clinical issues and implications. *Drug Alcohol Rev*. 2011;30(3):300-5.
113. Alford DP, Compton P, Samet JH. Acute pain management for patients receiving maintenance methadone or buprenorphine therapy. *Ann Intern Med*. 2006;144(2):127-34.
114. Rapp SE, Ready LB, Nessly ML. Acute pain management in patients with prior opioid consumption: A case-controlled retrospective review. *Pain*. 1995;61(2):195-201.
115. Doverty M, Somogyi AA, White JM, Bochner F, Beare CH, Menelaou A, et al. Methadone maintenance patients are cross-tolerant to the antinociceptive effects of morphine. *Pain*. 2001;93(2):155-63.
116. Athanasos P, Smith CS, White JM, Somogyi AA, Bochner F, Ling W. Methadone maintenance patients are cross-tolerant to the antinociceptive effects of very high plasma morphine concentrations. *Pain*. 2006;120(3):267-75.
117. Shafer SL, Varvel JR, Aziz N, Scott JC. Pharmacokinetics of fentanyl administered by computer-controlled infusion pump. *Anesthesiology*. 1990;73(6):1091-102.
118. Carroll IR, Angst MS, Clark JD. Management of perioperative pain in patients chronically consuming opioids. *Reg Anesth Pain Med*. 2004;29(6):576-91.
119. Kopf A, Banzhaf A, Stein C. Perioperative management of the chronic pain patient. *Best Practice and Research: Clinical Anaesthesiology*. 2005;19(1):59-76.
120. Peng PWH, Tumber PS, Gourlay D. Review article: Perioperative pain management of patients on methadone therapy. *Canadian Journal of Anesthesia*. 2005;52(5):513-23.
121. Mehta V, Langford RM. Acute pain management for opioid dependent patients. *Anaesthesia*. 2006;61(3):269-76.
122. Hadi I, Morley-Forster PK, Dain S, Horrill K, Moulin DE. Brief review: Perioperative management of the patient with chronic non-cancer pain. *Canadian Journal of Anesthesia*. 2006;53(12):1190-9.
123. Basu S, Bruce RD, Barry DT, Altice FL. Pharmacological pain control for human immunodeficiency virus-infected adults with a history of drug dependence. *J Subst Abuse Treat*. 2007;32(4):399-409.
124. Ludlow J, Christmas T, Paech MJ, Orr B. Drug abuse and dependency during pregnancy: Anaesthetic issues. *Anaesth Intensive Care*. 2007;35(6):881-93.
125. Hines S, Theodorou S, Williamson A, Fong D, Curry K. Management of acute pain in methadone maintenance therapy in-patients. *Drug Alcohol Rev*. 2008;27(5):519-23.
126. Jones HE, O'Grady K, Dahne J, Johnson R, Lemoine L, Milio L, et al. Management of acute postpartum pain in patients maintained on methadone or buprenorphine during pregnancy. *Am J Drug Alcohol Abuse*. 2009;35(3):151-6.
127. Richebé P, Beaulieu P. Perioperative pain management in the patient treated with opioids: Continuing Professional Development. *Prise en charge de la douleur périopératoire chez le patient sous opioïdes*. 2009;56(12):969-81.
128. Schug SA. Acute pain management in the opioid-tolerant patient. *Pain Management*. 2012;2(6):581.
129. Roberts DM, Meyer-Witting M. High-dose buprenorphine: Perioperative precautions and management strategies. *Anaesth Intensive Care*. 2005;33(1):17-25.
130. Bourne N. Managing acute pain in opioid tolerant patients. *J Perioper Pract*. 2008;18(11):498-503.
131. Brill S, Ginosar Y, Davidson EM. Perioperative management of chronic pain patients with opioid dependency. *Curr Opin Anaesthesiol*. 2006;19(3):325-31.

132. Marshall S, Jackson M. Acute pain management for opioid tolerant patients. Update in Anaesthesia. 2011;27(1):35-9.
133. Gordon D, Inturrisi CE, Greensmith JE, Brennan TJ, Goble L, Kerns RD. Perioperative Pain Management in the Opioid-Tolerant Individual. *J Pain*. 2008;9(5):383-7.
134. Pérez-Urizar J, Granados-Soto V, Flores-Murrieta FJ, Castaneda-Hernández G. Pharmacokinetic-pharmacodynamic modeling: Why? *Arch Med Res*. 2000;31(6):539-45.
135. Derendorf H, Meibohm B. Modeling of pharmacokinetic/pharmacodynamic (PK/PD) relationships: concepts and perspectives. *Pharm Res*. 1999;16(2):176-85.
136. Yassen A, Olofsen E, Romberg R, Sarton E, Teppema L, Danhof M, et al. Mechanism-based PK/PD modeling of the respiratory depressant effect of buprenorphine and fentanyl in healthy volunteers. *Clin Pharmacol Ther*. 2007;81(1):50-8.
137. Staahl C, Upton R, Foster DJ, Christrup LL, Kristensen K, Hansen SH, et al. Pharmacokinetic-pharmacodynamic modeling of morphine and oxycodone concentrations and analgesic effect in a multimodal experimental pain model. *J Clin Pharmacol*. 2008;48(5):619-31.
138. Shafer SL, Siegel LC, Cooke JE, Scott JC. Testing computer-controlled infusion pumps by simulation. *Anesthesiology*. 1988;68(2):261-6.
139. Lötsch J. Pharmacokinetic-Pharmacodynamic Modeling of Opioids. *J Pain Symptom Manage*. 2005;29(5, Supplement 1):90-103.
140. Wright DFB, Winter HR, Duffull SB. Understanding the time course of pharmacological effect: A PKPD approach. *Br J Clin Pharmacol*. 2011;71(6):815-23.
141. Van Poucke GE, Bravo LJB, Shafer SL. Target controlled infusions: Targeting the effect site while limiting peak plasma concentration. *IEEE Trans Biomed Eng*. 2004;51(11):1869-75.
142. Shafer SL, Varvel JR. Pharmacokinetics, pharmacodynamics, and rational opioid selection. *Anesthesiology*. 1991;74(1):53-63.
143. Pergolizzi J, Aloisi AM, Dahan A, Filitz J, Langford R, Likar R, et al. Current knowledge of buprenorphine and its unique pharmacological profile. *Pain Pract*. 2010;10(5):428-50.
144. Davis MP. Twelve Reasons for Considering Buprenorphine as a Frontline Analgesic in the Management of Pain. *J Support Oncol*. 2012;10(6):209-19.
145. Yassen A, Olofsen E, Romberg R, Sarton E, Danhof M, Dahan A. Mechanism-based pharmacokinetic-pharmacodynamic modeling of the antinociceptive effect of buprenorphine in healthy volunteers. *Anesthesiology*. 2006;104(6):1232-42.
146. Scott JC, Stanski DR. Decreased fentanyl and alfentanil dose requirements with age. A simultaneous pharmacokinetic and pharmacodynamic evaluation. *J Pharmacol Exp Ther*. 1987;240(1):159-66.
147. Olejniczak P. Neurophysiologic basis of EEG. *J Clin Neurophysiol*. 2006;23(3):186-9.
148. Egan TD, Muir KT, Hermann DJ, Stanski DR, Shafer SL. The electroencephalogram (EEG) and clinical measures of opioid potency: Defining the EEG-clinical potency relationship ('fingerprint') with application to remifentanyl. *International Journal of Pharmaceutical Medicine*. 2001;15(1):11-9.
149. Mandema JW, Danhof M. Electroencephalogram effect measures and relationships between pharmacokinetics and pharmacodynamics of centrally acting drugs. *Clin Pharmacokinet*. 1992;23(3):191-215.
150. Melichar JK, Myles JS, Eap CB, Nutt DJ. Using saccadic eye movements as objective measures of tolerance in methadone dependent individuals during the hydromorphone challenge test. *Addict Biol*. 2003;8(1):59-66.
151. Holdstock L, de Wit H. Ethanol Impairs Saccadic and Smooth Pursuit Eye Movements Without Producing Self-Reports of Sedation. *Alcoholism: Clinical and Experimental Research*. 1999;23(4):664-72.
152. Fliegert F, Kurth B, Göhler K. The effects of tramadol on static and dynamic pupillometry in healthy subjects - The relationship between pharmacodynamics, pharmacokinetics and CYP2D6 metaboliser status. *Eur J Clin Pharmacol*. 2005;61(4):257-66.

153. Knaggs RD, Crighton IM, Cobby TF, Fletcher AJP, Hobbs GJ. The Pupillary Effects of Intravenous Morphine, Codeine, and Tramadol in Volunteers. *Anesth Analg*. 2004 July 1, 2004;99(1):108-12.
154. Patil SG, Gale TJ, Stack CR, editors. Design of Novel Assessment Techniques for Opioid Dependent Patients. Engineering in Medicine and Biology Society, 2007 EMBS 2007 29th Annual International Conference of the IEEE; 2007 22-26 Aug. 2007.
155. Von Baeyer CL, Piira T, Chambers CT, Trapanotto M, Zeltzer LK. Guidelines for the cold pressor task as an experimental pain stimulus for use with children. *J Pain*. 2005;6(4):218-27.
156. Jones SF, McQuay HJ, Moore RA, Hand CW. Morphine and ibuprofen compared using the cold pressor test. *Pain*. 1988;34(2):117-22.
157. Bernard K, Penelaud PF, Mocaer E, Donazzolo Y. Absence of psychostimulant effects of a supratherapeutic dose of tianeptine: a placebo-controlled study versus methylphenidate in young healthy volunteers. *J Clin Psychopharmacol*. 2011;31(4):441-8.
158. Martin WR, Sloan JW, Sapira JD, Jasinski DR. Physiologic, subjective, and behavioral effects of amphetamine, methamphetamine, ephedrine, phenmetrazine, and methylphenidate in man. *Clin Pharmacol Ther*. 1971;12(2):245-58.
159. Handelsman L, Cochrane KJ, Aronson MJ, Ness R, Rubinstein KJ, Kanof PD. Two new rating scales for opiate withdrawal. *Am J Drug Alcohol Abuse*. 1987;13(3):293-308.
160. Dijkstra BAG, Krabbe PFM, Riezebos TGM, Van Der Staak CPF, De Jong CAJ. Psychometric evaluation of the Dutch version of the Subjective Opiate Withdrawal Scale (SOWS). *Eur Addict Res*. 2007;13(2):81-8.
161. Swenson JD, Davis JJ, Johnson KB. Postoperative care of the chronic opioid-consuming patient. *Anesthesiology Clinics of North America*. 2005;23(1):37-48.
162. Algren DA, Monteilh CP, Punja M, Schier JG, Belson M, Hepler BR, et al. Fentanyl-associated Fatalities Among Illicit Drug Users in Wayne County, Michigan (July 2005-May 2006). *J Med Toxicol*. 2013;9(1):106-15.
163. Egger CM, Duke T, Archer J, Cribb PH. Comparison of plasma fentanyl concentrations by using three transdermal fentanyl patch sizes in dogs. *Vet Surg*. 1998;27(2):159-66.
164. Fleischman RJ, Frazer DG, Daya M, Jui J, Newgard CD. Effectiveness and safety of fentanyl compared with morphine for out-of-hospital analgesia. *Prehosp Emerg Care*. 2010;14(2):167-75.
165. Davis JJ, Johnson KB, Egan TD, Vezina DP, Snell TE, Swenson JD. Preoperative Fentanyl Infusion with Pharmacokinetic Simulation for Anesthetic and Perioperative Management of an Opioid-Tolerant Patient. *Anesth Analg*. 2003;97(6):1661-2.
166. Macintyre P, Schug S. *Acute Pain Management: A Practical Guide*. 3rd ed: W.B. Saunders Company; 2007.
167. Ashton CH. Benzodiazepines: How They Work and How to Withdraw 2007 [cited 2013 July]. Available from: <http://www.benzo.org.uk/manual/bzcha01.htm#6>.
168. Mould D, Upton R. Basic concepts in population modeling, simulation, and model-based drug development. *CPT: Pharmacometrics & Systems Pharmacology*. 2012;1(9):e6.
169. Rang ST, Field J, Irving C. Serotonin toxicity caused by an interaction between fentanyl and paroxetine. *Canadian Journal of Anesthesia*. 2008;55(8):521-5.
170. Kirschner R, Donovan JW. Serotonin Syndrome Precipitated by Fentanyl During Procedural Sedation. *J Emerg Med*. 2010;38(4):477-80.
171. Ailawadhi S, Sung KW, Carlson LA, Baer MR. Serotonin syndrome caused by interaction between citalopram and fentanyl. *J Clin Pharm Ther*. 2007;32(2):199-202.
172. Staahl C, Olesen AE, Andresen T, Arendt-Nielsen L, Drewes AM. Assessing analgesic actions of opioids by experimental pain models in healthy volunteers - an updated review. *Br J Clin Pharmacol*. 2009;68(2):149-68.
173. Hay JL, White JM, Bochner F, Somogyi AA, Semple TJ, Rounsefell B. Hyperalgesia in opioid-managed chronic pain and opioid-dependent patients. *J Pain*. 2009;10(3):316-22.
174. Smith NT, Dec-Silver H, Sanford Jr TJ. EEGs during high-dose fentanyl-, sufentanil-, or morphine-oxygen anesthesia. *Anesth Analg*. 1984;63(4):386-93.

175. Sebel PS, Bovill JG, Wauquier A, Rog P. Effects of High-dose Fentanyl Anesthesia on the Electroencephalogram. *Anesthesiology*. 1981;55(3):203-11.
176. Wauquier A, Bovill JG, Sebel PS. Electroencephalographic effects of fentanyl-, sufentanil- and alfentanil anaesthesia in man. *Neuropsychobiology*. 1984;11(3):203-6.
177. Scott JC, Cooke JE, Stanski DR. Electroencephalographic quantitation of opioid effect: Comparative pharmacodynamics of fentanyl and sufentanil. *Anesthesiology*. 1991;74(1):34-42.
178. Rothenberg S, Schottenfeld S, Gross K, Selkoe D. Specific oculomotor deficit after acute methadone. *Psychopharmacology (Berl)*. 1980 March 1;67(3):221-7.
179. Tedeschi G, Smith AT, Richens A. Effect of meptazinol and ethanol on human psychomotor performance and mood ratings. *Hum Toxicol*. 1984;3(1):37-43.
180. Richens A, Allen E, Jones D, Griffiths A, Marshall R. A comparison of intramuscular meptazinol (100 mg) and papaveretum (20 mg) on human performance studies in healthy male volunteers. *Postgrad Med J*. 1983;59(Suppl. 1):19-24.
181. Grace PM, Stanford T, Gentgall M, Rolan PE. Utility of saccadic eye movement analysis as an objective biomarker to detect the sedative interaction between opioids and sleep deprivation in opioid-naive and opioid-tolerant populations. *J Psychopharmacol (Oxf)*. 2010 Nov;24(11):1631-40.
182. Hay JL, White JM, Bochner F, Somogyi AA. Antinociceptive effects of high-dose remifentanyl in male methadone-maintained patients. *Eur J Pain*. 2008;12(7):926-33.
183. Zacny JP, Lichtor JL, Zaragoza JG, De Wit H. Subjective and behavioral responses to intravenous fentanyl in healthy volunteers. *Psychopharmacology (Berl)*. 1992;107(2-3):319-26.
184. Upton RN, Foster DJR, Christrup LL, Dale O, Moksnes K, Popper L. A physiologically-based recirculatory meta-model for nasal fentanyl in man. *J Pharmacokinet Pharmacodyn*. 2012;39(5):561-76.
185. Shafer SL. STANPUMP User's Manual 1998 26 July 2010. Available from: <http://anesthesia.stanford.edu/pkpd/Documents/Forms/AllItems.aspx?RootFolder=%2fpkpd%2fDocuments%2fTarget%20Control%20Drug%20Delivery%2fSTANPUMP&FolderCTID=0x012000D855E8FE5C09E547BBC7FF1F085A203E&View={955BDAA2-728A-4457-8DE4-65820603C074}>.
186. Peng PWH, Sandler AN. A review of the use of fentanyl analgesia in the management of acute pain in adults. *Anesthesiology*. 1999;90(2):576-99.
187. Magosso E, Ursino M, Van Oostrom JH. Opioid induced respiratory depression: A mathematical model for fentanyl. *IEEE Trans Biomed Eng*. 2004;51(7):1115-28.
188. Gourlay GK, Kowalski SR, Plummer JL, Cousins MJ, Armstrong PJ. Fentanyl blood concentration-analgesic response relationship in the treatment of postoperative pain. *Anesth Analg*. 1988;67(4):329-37.

6 APPENDICES

6.1 Top models for the pharmacodynamic measures

A list of the top 31 models for most pharmacodynamic measures ranked by AIC are shown in the following pages. The best model for each metric by the model selection criteria is highlighted in bold.

Table 44 Best models for very low frequency band at Pz-Oz

No.	Very low Pz-Oz	AIC	CV(%) of fixed effects below 50	CV(%) of random effects below 100	P value	VPC	Intercept	Slope	EC50	E _{max}
1	SigmoidE _{max} Prop8	180.4	no	no	*	yes	yes	-	no	no
2	E _{max} Add8	180.9	no	no	*	yes	yes	-	no	no
3	SigmoidE _{max} Prop2	181.0	no	no		yes	no	-	no	no
4	SigmoidE _{max} Prop4	181.3	no	no		no	no	-	no	no
5	SigmoidE _{max} Prop6	181.3	no	no	**	no	yes	-	no	no
6	E _{max} Add4	181.4	no	no		no	no	-	no	no
7	LinearProp8	182.1	no	yes	**	yes	yes	no	-	-
8	E _{max} Add6	182.2	no	no	**	yes	yes	-	no	no
9	E _{max} Add16	182.8	no	no	*	yes	no	-	no	yes
10	LinearProp16	182.8	no	yes	**	yes	yes	yes	-	-
11	LinearProp12	182.9	no	yes	*	yes	no	yes	-	-
12	E _{max} Add2	183.2	no	no		yes	no	-	no	no
13	LinearProp4	183.3	yes	yes		yes	no	no	-	-
14	E _{max} Add14	183.8	no	no	*	yes	no	-	no	yes
15	SigmoidE _{max} Prop16	183.9	no	no	*	yes	no	-	no	yes
16	LinearProp6	184.4	no	yes	**	yes	yes	no	-	-
17	E _{max} Add20	184.6	no	no		yes	yes	-	yes	yes
18	LinearProp14	184.8	no	yes	*	yes	yes	yes	-	-
19	LinearProp10	184.9	no	yes	*	yes	no	yes	-	-
20	SigmoidE _{max} Prop14	184.9	no	no	*	yes	no	-	no	yes
21	LinearProp2	185.7	yes	yes		yes	no	no	-	-
22	SigmoidE _{max} Prop12	188.0	no	no		yes	no	-	yes	no
23	E _{max} Add12	190.8	no	no		yes	no	-	yes	no
24	LinearAdd12	190.8	no	yes	**	yes	no	yes	-	-
25	LinearAdd16	190.9	no	no	*	yes	yes	yes	-	-
26	LinearAdd8	191.6	no	no	**	yes	yes	no	-	-
27	LinearAdd10	192.1	no	yes	**	yes	no	yes	-	-
28	LinearAdd4	192.1	yes	yes		yes	no	no	-	-
29	LinearAdd14	192.2	no	yes	*	yes	yes	yes	-	-
30	SigmoidE _{max} Prop5	192.6	no	no	**	yes	yes	-	no	no
31	E _{max} Add10	192.8	no	no		yes	no	-	yes	no

AIC, Akaike information criteria; CV, coefficient of variation; VPC, visual predictive check; P value, P value for any of the fixed effects parameter; *, $P > 0.05$; and **, $P \leq 0.05$; Intercept, MEDD tried as a covariate on the intercept; Slope, MEDD tried as a covariate on the slope; EC50, MEDD tried as a covariate on the EC50; E_{max}, MEDD tried as a covariate on the E_{max}

Table 45 Best models for very low band at Fz-Cz

No.	Very low Fz-Cz	AIC	CV(%) of fixed effects below 50	CV(%) of random effects below 100	P value	VPC	Intercept	Slope	EC50	E _{max}
1	SigmoidE _{max} Prop2	235.5	no	no		yes	no	-	no	no
2	LinearProp2	235.7	yes	no		yes	no	no	-	-
3	LinearProp6	237.3	no	no	*	yes	yes	no	-	-
4	LinearProp10	237.4	no	no	*	yes	no	yes	-	-
5	LinearProp14	239.1	no	no	*	yes	yes	yes	-	-
6	E _{max} Add2	239.5	no	no		yes	no	-	no	no
7	E _{max} Add6	240.4	no	no	*	yes	yes	-	no	no
8	E _{max} Add14	241.2	no	no	*	yes	no	-	no	yes
9	LinearAdd2	242.0	yes	yes		yes	no	no	-	-
10	SigmoidE _{max} Prop6	242.9	no	no	*	yes	yes	-	no	no
11	LinearAdd10	243.6	no	no	*	yes	no	yes	-	-
12	LinearAdd6	243.8	no	yes	*	yes	yes	no	-	-
13	SigmoidE _{max} Prop1	244.3	no	no		yes	no	-	no	no
14	E _{max} Add18	244.8	no	no	*	yes	yes	-	yes	yes
15	SigmoidE _{max} Prop14	245.1	no	no	*	yes	no	-	no	yes
16	LinearAdd14	245.1	no	yes	*	yes	yes	yes	-	-
17	SigmoidE _{max} Prop5	246.2	no	no	*	yes	yes	-	no	no
18	Zero2	246.4	yes	yes	*	yes	no	-	-	-
19	Zero6	246.4	yes	yes		yes	yes	-	-	-
20	Zero8	248.1	no	yes	*	yes	yes	-	-	-
21	SigmoidE _{max} Prop10	251.2	no	no		yes	no	-	yes	no
22	LinearProp1	254.1	yes	yes		yes	no	no	-	-
23	SigmoidE _{max} Prop18	254.1	no	no		yes	yes	-	yes	yes
24	LinearProp5	255.8	no	yes	*	yes	yes	no	-	-
25	LinearProp9	256.2	no	no	*	yes	no	yes	-	-
26	E _{max} Add1	256.2	no	no		yes	no	-	no	no
27	E _{max} Add10	257.2	no	no		yes	no	-	yes	no
28	E _{max} Add13	257.8	no	no	*	yes	no	-	no	yes
29	E _{max} Add9	258.2	no	no	*	yes	no	-	yes	no
30	LinearProp13	258.3	no	no	*	yes	yes	yes	-	-
31	E _{max} Add5	258.7	no	no	*	yes	yes	-	no	no

Table 46 Best models for Delta Pz-Oz

No.	Delta Pz-Oz	AIC	CV(%) of fixed effects below 50	CV(%) of random effects below 100	P value	VPC	Intercept	Slope	EC50	E _{max}
1	SigmoidE _{max} Prop4	124.4	no	no		yes	no	-	no	no
2	SigmoidE _{max} Prop16	124.8	no	no	*	yes	no	-	no	yes
3	LinearProp12	124.9	no	yes	*	yes	no	yes	-	-
4	SigmoidE _{max} Prop8	125.5	no	no	*	yes	yes	-	no	no
5	LinearProp4	125.9	yes	yes		yes	no	no	-	-
6	LinearProp16	126.8	no	yes	**	yes	yes	yes	-	-
7	SigmoidE _{max} Prop2	127.2	no	no		yes	no	-	no	no
8	LinearProp8	127.4	no	yes	*	yes	yes	no	-	-
9	E _{max} Add16	127.6	no	no	*	yes	no	-	no	yes
10	LinearProp10	127.9	no	yes	*	yes	no	yes	-	-
11	E _{max} Add4	127.9	no	no		yes	no	-	no	no
12	LinearProp2	128.6	yes	yes		yes	no	no	-	-
13	SigmoidE _{max} Prop14	129.0	no	no	*	yes	no	-	no	yes
14	E _{max} Add8	129.6	no	no	*	yes	yes	-	no	no
15	LinearProp14	129.7	no	yes	*	yes	yes	yes	-	-
16	LinearProp6	130.2	no	yes	*	yes	yes	no	-	-
17	SigmoidE _{max} Prop6	130.6	no	no	*	yes	yes	-	no	no
18	LinearAdd12	130.7	no	yes	**	yes	no	yes	-	-
19	E _{max} Add10	130.9	no	no		yes	no	-	yes	no
20	E _{max} Add20	131.1	no	no	*	yes	yes	-	yes	yes
21	E _{max} Add14	131.3	no	no	*	yes	no	-	no	yes
22	E _{max} Add2	131.9	no	no		yes	no	-	no	no
23	LinearAdd4	132.1	yes	yes		yes	no	no	-	-
24	LinearAdd16	132.5	no	yes	*	yes	yes	yes	-	-
25	E _{max} Add6	133.2	no	no	*	yes	yes	-	no	no
26	LinearAdd8	133.8	no	yes	*	yes	yes	no	-	-
27	LinearAdd10	134.1	no	yes	**	yes	no	yes	-	-
28	E _{max} Add18	134.6	no	no		yes	yes	-	yes	yes
29	LinearAdd2	135.1	yes	yes		yes	no	no	-	-
30	LinearAdd14	135.9	no	yes	*	yes	yes	yes	-	-
31	LinearAdd6	136.9	no	yes	*	yes	yes	no	-	-

Table 47 Best models for Delta Fz-Cz

No.	Delta Fz-Cz	AIC	CV(%) of fixed effects below 50	CV(%) of random effects below 100	P value	VPC	Intercept	Slope	EC50	E _{max}
1	LinearProp2	173.9	yes	yes		yes	no	no	-	-
2	SigmoidE _{max} Prop2	173.9	no	no		yes	no	-	no	no
3	LinearProp10	175.2	no	yes	*	yes	no	yes	-	-
4	LinearProp6	175.8	no	yes	*	yes	yes	no	-	-
5	E _{max} Add2	176.2	no	no		yes	no	-	no	no
6	SigmoidE _{max} Prop6	176.8	no	no	*	yes	yes	-	no	no
7	LinearProp14	177.1	no	yes	*	yes	yes	yes	-	-
8	E _{max} Add14	177.5	no	no	*	yes	no	-	no	yes
9	E _{max} Add10	177.5	no	no	*	yes	no	-	yes	no
10	E _{max} Add6	178.2	no	no	*	yes	yes	-	no	no
11	SigmoidE _{max} Prop14	178.5	no	no	*	yes	no	-	no	yes
12	LinearAdd2	181.1	yes	yes		yes	no	no	-	-
13	E _{max} Add18	181.5	no	no	*	yes	yes	-	yes	yes
14	LinearAdd10	182.6	no	yes	*	yes	no	yes	-	-
15	LinearAdd6	183.1	no	yes	*	yes	yes	no	-	-
16	LinearAdd14	184.6	no	yes	*	yes	yes	yes	-	-
17	Zero2	185.2	yes	no		yes	no	-	-	-
18	Zero6	185.2	yes	no		yes	yes	-	-	-
19	SigmoidE _{max} Prop5	185.8	no	no		yes	yes	-	no	no
20	Zero8	187.1	no	yes	*	yes	yes	-	-	-
21	SigmoidE _{max} Prop18	198.3	no	no		yes	yes	-	yes	yes
22	LinearProp1	207.5	yes	no		yes	no	no	-	-
23	E _{max} Add1	208.1	no	no		yes	no	-	no	no
24	LinearProp9	209.4	no	no	*	yes	no	yes	-	-
25	E _{max} Add9	209.5	no	no	*	yes	no	-	yes	no
26	E _{max} Add13	210.0	no	no	*	yes	no	-	no	yes
27	E _{max} Add5	210.0	no	no	*	yes	yes	-	no	no
28	LinearProp5	210.2	no	no	*	yes	yes	no	-	-
29	LinearProp13	211.3	no	no	*	yes	yes	yes	-	-
30	SigmoidE _{max} Prop13	214.0	no	no	*	yes	no	-	no	yes
31	E _{max} Add17	214.1	no	no	*	yes	yes	-	yes	yes

Table 48 Best models for Theta Pz-Oz

No.	Theta Pz-Oz	AIC	CV(%) of fixed effects below 50	CV(%) of random effects below 100	P value	VPC	Intercept	Slope	EC50	E _{max}
1	LinearProp6	122.6	no	no	*	yes	yes	no	-	-
2	LinearProp2	123.1	yes	yes		yes	no	no	-	-
3	LinearAdd10	123.2	no	yes	**	yes	no	yes	-	-
4	LinearAdd14	123.4	no	yes	**	yes	yes	yes	-	-
5	LinearProp14	123.9	no	no	**	yes	yes	yes	-	-
6	LinearAdd16	123.9	no	no	**	yes	yes	yes	-	-
7	LinearAdd12	123.9	no	no	**	yes	no	yes	-	-
8	LinearProp8	124.0	no	no	**	yes	yes	no	-	-
9	LinearProp10	124.7	no	no	*	yes	no	yes	-	-
10	LinearProp16	124.8	no	yes	*	yes	yes	yes	-	-
11	LinearProp4	125.2	yes	no		yes	no	no	-	-
12	LinearAdd6	125.3	no	yes	**	yes	yes	no	-	-
13	LinearProp12	125.3	no	no	*	yes	no	yes	-	-
14	LinearAdd2	125.9	yes	yes		yes	no	no	-	-
15	LinearAdd8	126.2	no	no	**	yes	yes	no	-	-
16	LinearAdd4	126.8	no	no		yes	no	no	-	-
17	E _{max} Add2	127.2	no	no		yes	no	-	no	no
18	E _{max} Add6	127.6	no	no	**	yes	yes	-	no	no
19	E _{max} Add8	127.9	no	no	**	yes	yes	-	no	no
20	E _{max} Add10	128.6	no	no	*	yes	no	-	yes	no
21	E _{max} Add4	128.8	no	no		yes	no	-	no	no
22	SigmoidE _{max} Prop6	129.5	no	no	**	yes	yes	-	no	no
23	SigmoidE _{max} Prop2	130.6	no	no		yes	no	-	no	no
24	E _{max} Add20	131.2	no	no	*	yes	yes	-	yes	yes
25	E _{max} Add14	131.4	no	no	*	yes	no	-	no	yes
26	LinearAdd9	131.6	no	no	**	yes	no	yes	-	-
27	LinearProp5	132.0	no	no	**	yes	yes	no	-	-
28	LinearAdd13	132.1	no	no	*	yes	yes	yes	-	-
29	E _{max} Add16	132.5	no	no	*	yes	no	-	no	yes
30	LinearAdd11	132.5	no	yes	**	yes	no	yes	-	-
31	SigmoidE _{max} Prop4	132.6	no	no		yes	no	-	no	no

Table 49 Best models for Theta Fz-Cz

No.	Theta Fz-Cz	AIC	CV(%) of fixed effects below 50	CV(%) of random effects below 100	P value	VPC	Intercept	Slope	EC50	E _{max}
1	LinearProp4	145.8	yes	yes		yes	no	no	-	-
2	LinearProp2	146.1	no	yes		yes	no	no	-	-
3	LinearProp12	146.2	no	no	*	yes	no	yes	-	-
4	LinearProp10	146.5	no	no	*	yes	no	yes	-	-
5	LinearAdd12	147.0	no	no	**	yes	no	yes	-	-
6	LinearAdd4	147.2	yes	no		yes	no	no	-	-
7	LinearProp8	147.2	no	yes	*	yes	yes	no	-	-
8	LinearProp6	147.8	no	no	*	yes	yes	no	-	-
9	LinearProp16	148.0	no	no	*	yes	yes	yes	-	-
10	LinearAdd10	148.3	no	yes	*	yes	no	yes	-	-
11	LinearAdd2	148.3	yes	yes		yes	no	no	-	-
12	LinearAdd8	148.6	no	no	*	yes	yes	no	-	-
13	LinearAdd16	148.7	no	no	*	yes	yes	yes	-	-
14	LinearProp14	149.0	no	no	*	yes	yes	yes	-	-
15	LinearAdd6	150.0	no	yes	*	yes	yes	no	-	-
16	LinearAdd14	150.2	no	yes	*	yes	yes	yes	-	-
17	E _{max} Add2	150.4	no	no		yes	no	-	no	no
18	SigmoidE _{max} Prop2	150.5	no	no		yes	no	-	no	no
19	E _{max} Add8	151.4	no	no	*	yes	yes	-	no	no
20	E _{max} Add14	152.0	no	no	*	yes	no	-	no	yes
21	E _{max} Add4	152.1	no	no		yes	no	-	no	no
22	SigmoidE _{max} Prop4	152.2	no	no		yes	no	-	no	no
23	E _{max} Add16	153.2	no	no	*	yes	no	-	no	yes
24	SigmoidE _{max} Prop8	153.2	no	no	*	yes	yes	-	no	no
25	E _{max} Add6	153.5	no	no	*	yes	yes	-	no	no
26	LinearProp1	153.9	yes	no		yes	no	no	-	-
27	LinearProp9	154.2	no	no	*	yes	no	yes	-	-
28	SigmoidE _{max} Prop6	154.5	no	no	*	yes	yes	-	no	no
29	SigmoidE _{max} Prop16	154.9	no	no	*	yes	no	-	no	yes
30	LinearProp11	155.0	no	no	*	yes	no	yes	-	-
31	LinearProp3	155.1	yes	no		yes	no	no	-	-

Table 50 Best models for Alpha Pz-Oz

No.	Alpha Pz-Oz	AIC	CV(%) of fixed effects below 50	CV(%) of random effects below 100	P value	VPC	Intercept	Slope	EC50	E _{max}
1	LinearProp5	172.7	no	no	*	yes	yes	no	-	-
2	Zero1	172.8	no	no		yes	no	-	-	-
3	LinearProp3	172.9	no	no		yes	no	no	-	-
4	LinearProp7	173.0	no	no	*	yes	yes	no	-	-
5	Zero3	173.1	no	no	*	yes	no	-	-	-
6	LinearProp1	173.1	yes	no		yes	no	no	-	-
7	Zero5	173.1	no	no	*	yes	yes	-	-	-
8	Zero7	173.2	no	no	*	yes	yes	-	-	-
9	LinearProp9	173.5	no	no	**	yes	no	yes	-	-
10	LinearProp11	173.6	no	no	*	yes	no	yes	-	-
11	LinearProp13	173.9	no	no	*	yes	yes	yes	-	-
12	LinearProp15	174.1	no	no	*	yes	yes	yes	-	-
13	LinearAdd5	174.7	no	no	*	yes	yes	no	-	-
14	LinearAdd3	174.8	no	no		yes	no	no	-	-
15	LinearAdd1	174.9	no	no		yes	no	no	-	-
16	LinearAdd7	174.9	no	no	*	yes	yes	no	-	-
17	LinearAdd9	176.1	no	no	*	yes	no	yes	-	-
18	LinearAdd11	176.4	no	no	*	yes	no	yes	-	-
19	LinearAdd13	176.6	no	no	*	yes	yes	yes	-	-
20	LinearAdd15	176.8	no	no	*	yes	yes	yes	-	-
21	E _{max} Add5	176.9	no	no	*	yes	yes	-	no	no
22	E _{max} Add1	178.9	no	no		yes	no	-	no	no
23	E _{max} Add7	179.2	no	no	*	yes	yes	-	no	no
24	E _{max} Add3	179.4	no	no		yes	no	-	no	no
25	SigmoidE _{max} Prop1	180.9	no	no		yes	no	-	no	no
26	E _{max} Add9	180.9	no	no		yes	no	-	yes	no
27	E _{max} Add13	180.9	no	no		yes	no	-	no	yes
28	E _{max} Add11	181.0	no	no		yes	no	-	yes	no
29	E _{max} Add15	181.1	no	no		yes	no	-	no	yes
30	SigmoidE _{max} Prop3	183.0	no	no		yes	no	-	no	no
31	SigmoidE _{max} Prop5	183.1	no	no		yes	yes	-	no	no

Table 51 Best models for Alpha Fz-Cz

No.	Alpha Fz-Cz	AIC	CV(%) of fixed effects below 50	CV(%) of random effects below 100	P value	VPC	Intercept	Slope	EC50	E _{max}
1	Zero1	186.3	yes	no		yes	no	-	-	-
2	Zero2	186.9	yes	no		yes	no	-	-	-
3	LinearProp1	186.9	no	no		yes	no	no	-	-
4	LinearProp9	187.2	no	no	*	yes	no	yes	-	-
5	LinearAdd1	187.9	no	no		yes	no	no	-	-
6	Zero5	188.2	no	no	*	yes	yes	-	-	-
7	LinearAdd9	188.5	no	no	**	yes	no	yes	-	-
8	LinearProp2	188.7	no	no		yes	no	no	-	-
9	LinearAdd2	188.8	no	no		yes	no	no	-	-
10	Zero6	188.9	no	no	*	yes	yes	-	-	-
11	LinearProp5	189.0	no	no	*	yes	yes	no	-	-
12	Zero4	189.0	no	no		yes	no	-	-	-
13	LinearProp13	189.1	no	no	*	yes	yes	yes	-	-
14	Zero3	189.3	yes	no		yes	no	-	-	-
15	LinearProp10	189.6	no	no	*	yes	no	yes	-	-
16	LinearAdd10	189.7	no	no	*	yes	no	yes	-	-
17	LinearAdd5	189.7	no	no	*	yes	yes	no	-	-
18	LinearProp11	190.1	no	no	*	yes	no	yes	-	-
19	LinearProp3	190.3	no	no		yes	no	no	-	-
20	LinearAdd13	190.5	no	no	**	yes	yes	yes	-	-
21	LinearProp6	190.6	no	no	*	yes	yes	no	-	-
22	LinearAdd6	190.8	no	no		yes	yes	no	-	-
23	LinearAdd11	190.9	no	no	*	yes	no	yes	-	-
24	Zero8	190.9	no	no	*	yes	yes	-	-	-
25	LinearProp4	190.9	no	no		yes	no	no	-	-
26	LinearAdd3	191.0	no	no		yes	no	no	-	-
27	Zero7	191.2	no	no	*	yes	yes	-	-	-
28	LinearAdd4	191.2	no	no		yes	no	no	-	-
29	LinearAdd12	191.5	no	no	*	yes	no	yes	-	-
30	LinearProp12	191.5	no	no	*	yes	no	yes	-	-
31	LinearProp14	191.5	no	no	*	yes	yes	yes	-	-

Table 52 Best models for Beta Pz-Oz

No.	Beta Pz-Oz	AIC	CV(%) of fixed effects below 50	CV(%) of random effects below 100	P value	VPC	Intercept	Slope	EC50	E _{max}
1	SigmoidE _{max} Prop2	87.5	no	no		yes	no	-	no	no
2	SigmoidE _{max} Prop6	90.1	no	no		yes	yes	-	no	no
3	SigmoidE _{max} Prop4	90.8	no	no		yes	no	-	no	no
4	SigmoidE _{max} Prop8	90.9	no	no	*	yes	yes	-	no	no
5	SigmoidE _{max} Prop16	92.1	no	no		yes	no	-	no	yes
6	SigmoidE _{max} Prop14	92.9	no	no	*	yes	no	-	no	yes
7	E _{max} Add10	95.9	no	no		yes	no	-	yes	no
8	SigmoidE _{max} Prop7	96.3	no	no	*	yes	yes	-	no	no
9	LinearProp12	97.9	yes	no	**	yes	no	yes	-	-
10	Zero8	98.1	no	no	**	yes	yes	-	-	-
11	E _{max} Add20	98.3	no	no		yes	yes	-	yes	yes
12	Zero6	98.3	no	no	**	yes	yes	-	-	-
13	LinearProp10	98.3	yes	no	**	yes	no	yes	-	-
14	LinearAdd12	98.6	yes	no	**	yes	no	yes	-	-
15	Zero4	98.8	no	no		yes	no	-	-	-
16	LinearProp16	98.9	no	no		yes	yes	yes	-	-
17	LinearProp14	99.1	no	no	*	yes	yes	yes	-	-
18	LinearAdd16	99.7	no	no	*	yes	yes	yes	-	-
19	LinearProp6	99.8	no	no	**	yes	yes	no	-	-
20	LinearAdd6	99.9	no	no	**	yes	yes	no	-	-
21	LinearAdd8	99.9	no	no	**	yes	yes	no	-	-
22	LinearProp8	99.9	no	no	**	yes	yes	no	-	-
23	LinearAdd14	99.9	no	no	*	yes	yes	yes	-	-
24	LinearAdd10	100.2	yes	no	**	yes	no	yes	-	-
25	Zero2	100.3	yes	no	**	yes	no	-	-	-
26	LinearProp4	100.5	no	no		yes	no	no	-	-
27	SigmoidE _{max} Prop13	100.8	no	no	*	yes	no	-	no	yes
28	LinearAdd4	101.0	no	no		yes	no	no	-	-
29	SigmoidE _{max} Prop15	101.0	no	no		yes	no	-	no	yes
30	LinearProp2	101.6	no	no		yes	no	no	-	-
31	E _{max} Add16	102.5	no	no	*	yes	no	-	no	yes

Table 53 Best models for Beta Fz-Cz

No.	Beta Fz-Cz	AIC	CV(%) of fixed effects below 50	CV(%) of random effects below 100	P value	VPC	Intercept	Slope	EC50	E _{max}
1	Zero3	95.2	yes	no		yes	no	-	-	-
2	Zero1	95.2	yes	no		yes	no	-	-	-
3	LinearProp3	96.6	no	no		yes	no	no	-	-
4	LinearProp1	96.6	no	no		yes	no	no	-	-
5	Zero7	97.0	no	no	*	yes	yes	-	-	-
6	LinearAdd3	97.1	no	no		yes	no	no	-	-
7	LinearAdd1	97.1	no	no		yes	no	no	-	-
8	Zero5	97.2	no	no	*	yes	yes	-	-	-
9	LinearProp11	98.2	no	no	*	yes	no	yes	-	-
10	LinearProp9	98.3	no	no	*	yes	no	yes	-	-
11	LinearProp5	98.4	no	no	*	yes	yes	no	-	-
12	LinearProp7	98.4	no	no	*	yes	yes	no	-	-
13	LinearAdd11	98.7	no	no	*	yes	no	yes	-	-
14	LinearAdd5	98.9	no	no	*	yes	yes	no	-	-
15	LinearAdd7	98.9	no	no	*	yes	yes	no	-	-
16	LinearAdd9	98.9	no	no	*	yes	no	yes	-	-
17	SigmoidE _{max} Prop3	99.9	no	no		yes	no	-	no	no
18	LinearProp15	100.2	no	no	*	yes	yes	yes	-	-
19	LinearProp13	100.4	no	no	*	yes	yes	yes	-	-
20	LinearAdd13	100.8	no	no	*	yes	yes	yes	-	-
21	LinearAdd15	100.8	no	no	*	yes	yes	yes	-	-
22	E _{max} Add3	101.1	no	no		yes	no	-	no	no
23	E _{max} Add1	101.2	no	no		yes	no	-	no	no
24	SigmoidE _{max} Prop11	102.1	no	no		yes	no	-	yes	no
25	SigmoidE _{max} Prop9	102.4	no	no		yes	no	-	yes	no
26	SigmoidE _{max} Prop7	102.5	no	no		yes	yes	-	no	no
27	Zero2	102.9	yes	no		yes	no	-	-	-
28	E _{max} Add7	103.0	no	no		yes	yes	-	no	no
29	Zero4	103.1	yes	no		yes	no	-	-	-
30	E _{max} Add15	103.1	no	no		yes	no	-	no	yes
31	E _{max} Add11	103.1	no	no		yes	no	-	yes	no

Table 54 Best models for Gamma Pz-Oz

No.	Gamma Pz-Oz	AIC	CV(%) of fixed effects below 50	CV(%) of random effects below 100	P value	VPC	Intercept	Slope	EC50	Emax
1	SigmoidEmaxProp4	50.0	no	no		yes	no	-	no	no
2	SigmoidEmaxProp8	52.1	no	no	*	yes	yes	-	no	no
3	SigmoidEmaxProp16	55.4	no	no	*	yes	no	-	no	yes
4	SigmoidEmaxProp2	57.5	no	no		yes	no	-	no	no
5	SigmoidEmaxProp3	59.5	no	no		yes	no	-	no	no
6	SigmoidEmaxProp14	60.7	no	no	*	yes	no	-	no	yes
7	LinearProp8	63.7	no	yes	**	yes	yes	no	-	-
8	LinearProp16	64.8	no	yes	**	yes	yes	yes	-	-
9	LinearProp4	65.0	yes	yes		yes	no	no	-	-
10	EmaxAdd12	65.3	no	no		yes	no	-	yes	no
11	LinearProp12	65.3	no	yes	*	yes	no	yes	-	-
12	EmaxAdd8	67.2	no	no	**	yes	yes	-	no	no
13	LinearAdd8	67.2	no	no	**	yes	yes	no	-	-
14	LinearAdd16	67.3	no	no	*	yes	yes	yes	-	-
15	LinearAdd12	67.4	no	yes	**	yes	no	yes	-	-
16	LinearAdd4	68.4	no	no		yes	no	no	-	-
17	EmaxAdd4	68.5	no	no		yes	no	-	no	no
18	Zero8	68.9	no	no	**	yes	yes	-	-	-
19	Zero4	69.4	yes	yes		yes	no	-	-	-
20	EmaxAdd16	69.4	no	no	*	yes	no	-	no	yes
21	LinearProp6	71.5	no	no	**	yes	yes	no	-	-
22	EmaxAdd10	71.5	no	no		yes	no	-	yes	no
23	EmaxAdd18	71.9	no	no		yes	yes	-	yes	yes
24	LinearProp14	72.2	no	no	*	yes	yes	yes	-	-
25	LinearProp10	72.8	no	yes	*	yes	no	yes	-	-
26	LinearProp2	72.9	yes	yes		yes	no	no	-	-
27	LinearAdd10	74.2	no	yes	**	yes	no	yes	-	-
28	LinearAdd6	74.3	yes	no	**	yes	yes	no	-	-
29	EmaxAdd6	74.6	no	no	**	yes	yes	-	no	no
30	LinearAdd14	75.6	no	no	*	yes	yes	yes	-	-
31	EmaxAdd2	75.6	no	no		yes	no	-	no	no

Table 55 Best models for Gamma Fz-Cz

No.	Gamma Fz-Cz	AIC	CV(%) of fixed effects below 50	CV(%) of random effects below 100	P value	VPC	Intercept	Slope	EC50	E _{max}
1	Zero2	-24.8	yes	no		yes	no	-	-	-
2	Zero4	-24.7	yes	no		yes	no	-	-	-
3	LinearProp4	-23.5	no	no		yes	no	no	-	-
4	LinearAdd4	-23.5	no	no		yes	no	no	-	-
5	LinearProp2	-23.5	no	no		yes	no	no	-	-
6	LinearAdd2	-23.5	no	no		yes	no	no	-	-
7	Zero8	-23.3	no	no	*	yes	yes	-	-	-
8	Zero6	-23.2	no	no	*	yes	yes	-	-	-
9	LinearAdd12	-22.9	no	no	*	yes	no	yes	-	-
10	LinearAdd10	-22.9	no	no	*	yes	no	yes	-	-
11	LinearProp10	-22.9	no	no	*	yes	no	yes	-	-
12	LinearProp6	-22.1	no	no	*	yes	yes	no	-	-
13	LinearAdd8	-21.9	no	no	*	yes	yes	no	-	-
14	LinearAdd6	-21.8	no	no	*	yes	yes	no	-	-
15	LinearProp8	-21.7	no	no	*	yes	yes	no	-	-
16	LinearProp12	-21.4	yes	no	**	yes	no	yes	-	-
17	LinearAdd16	-21.0	no	no	*	yes	yes	yes	-	-
18	SigmoidE _{max} Prop2	-20.9	no	no		yes	no	-	no	no
19	LinearProp16	-20.8	no	no	*	yes	yes	yes	-	-
20	LinearAdd14	-20.6	no	no	*	yes	yes	yes	-	-
21	LinearProp14	-20.4	no	no	*	yes	yes	yes	-	-
22	E _{max} Add2	-19.7	no	no		yes	no	-	no	no
23	SigmoidE _{max} Prop4	-19.6	no	no		yes	no	-	no	no
24	E _{max} Add12	-19.2	no	no		yes	no	-	yes	no
25	E _{max} Add10	-19.2	no	no		yes	no	-	yes	no
26	E _{max} Add14	-19.1	no	no	*	yes	no	-	no	yes
27	E _{max} Add16	-19.1	no	no	*	yes	no	-	no	yes
28	Zero1	-18.7	yes	no		yes	no	-	-	-
29	Zero3	-18.7	yes	no		yes	no	-	-	-
30	E _{max} Add4	-18.6	no	no		yes	no	-	no	no
31	SigmoidE _{max} Prop5	-17.9	no	no	*	yes	yes	-	no	no

Table 56 Best models for average saccadic peak velocity

No.	Saccadic peak velocity	AIC	CV(%) of fixed effects below 50	CV(%) of random effects below 100	P value	VPC	Intercept	Slope	EC50	E _{max}
1	LinearAdd4	417.6	yes	no		yes	no	no	-	-
2	LinearAdd2	417.9	yes	no		yes	no	no	-	-
3	LinearProp4	418.3	yes	no		yes	no	no	-	-
4	LinearProp2	418.6	yes	no		yes	no	no	-	-
5	LinearAdd10	418.8	no	no	*	yes	no	yes	-	-
6	LinearAdd12	418.9	no	no	*	yes	no	yes	-	-
7	LinearProp10	419.0	no	no	*	yes	no	yes	-	-
8	LinearProp12	419.2	no	no	*	yes	no	yes	-	-
9	E _{max} Add4	422.4	no	no		yes	no	-	no	no
10	LinearAdd3	422.5	yes	no		yes	no	no	-	-
11	LinearAdd1	422.8	yes	no		yes	no	no	-	-
12	E _{max} Add2	422.9	no	no		yes	no	-	no	no
13	LinearProp3	423.0	yes	no		yes	no	no	-	-
14	LinearProp1	423.3	yes	no		yes	no	no	-	-
15	LinearProp11	423.4	no	no		yes	no	yes	-	-
16	LinearProp9	423.5	no	no	*	yes	no	yes	-	-
17	LinearAdd11	423.6	no	no		yes	no	yes	-	-
18	LinearAdd9	424.4	no	no	*	yes	no	yes	-	-
19	E _{max} Add16	425.8	no	no	*	yes	no	-	no	yes
20	SigmoidE _{max} Prop4	426.1	no	no		yes	no	-	no	no
21	E _{max} Add14	426.4	no	no	*	yes	no	-	no	yes
22	Zero4	426.9	yes	no		yes	no	-	-	-
23	Zero2	427.2	yes	no		yes	no	-	-	-
24	E _{max} Add3	427.3	no	no		yes	no	-	no	no
25	E _{max} Add1	427.4	no	no		yes	no	-	no	no
26	E _{max} Add10	429.2	no	no		yes	no	-	yes	no
27	E _{max} Add15	429.5	no	no	*	yes	no	-	no	yes
28	SigmoidE _{max} Prop16	429.5	no	no		yes	no	-	no	yes
29	SigmoidE _{max} Prop12	430.2	no	no	*	yes	no	-	yes	no
30	E _{max} Add13	430.9	no	no	*	yes	no	-	no	yes
31	Zero3	431.4	yes	yes		yes	no	-	-	-

Table 57 Best models for saccadic latency

No.	Saccadic latency	AIC	CV(%) of fixed effects below 50	CV(%) of random effects below 100	P value	VPC	Intercept	Slope	EC50	E _{max}
1	LinearProp6	-166.7	no	no	**	yes	yes	no	-	-
2	Zero6	-166.6	no	no	**	yes	yes	-	-	-
3	LinearProp5	-166.4	no	yes	**	yes	yes	no	-	-
4	LinearAdd6	-166.0	no	no	**	yes	yes	no	-	-
5	Zero5	-165.7	no	yes	**	yes	yes	-	-	-
6	E _{max} Add6	-165.3	no	no	**	yes	yes	-	no	no
7	LinearAdd5	-165.2	no	yes	**	yes	yes	no	-	-
8	LinearProp14	-165.1	no	no		yes	yes	yes	-	-
9	E _{max} Add5	-164.7	no	no	**	yes	yes	-	no	no
10	SigmoidE _{max} Prop6	-164.7	no	no	**	yes	yes	-	no	no
11	LinearProp13	-164.5	no	yes	*	yes	yes	yes	-	-
12	LinearAdd14	-164.1	no	no	**	yes	yes	yes	-	-
13	LinearAdd13	-163.2	no	yes	**	yes	yes	yes	-	-
14	SigmoidE _{max} Prop5	-162.7	no	no	*	yes	yes	-	no	no
15	E _{max} Add1	-161.2	no	no		yes	no	-	no	no
16	Zero2	-160.2	no	no		yes	no	-	-	-
17	LinearProp1	-160.0	no	yes		yes	no	no	-	-
18	E _{max} Add2	-159.9	no	no		yes	no	-	no	no
19	LinearProp2	-159.9	no	no		yes	no	no	-	-
20	Zero1	-159.7	yes	yes		yes	no	-	-	-
21	LinearAdd2	-159.7	no	no		yes	no	no	-	-
22	LinearAdd1	-159.2	no	yes		yes	no	no	-	-
23	SigmoidE _{max} Prop2	-158.9	no	no		yes	no	-	no	no
24	E _{max} Add14	-158.5	no	no	*	yes	no	-	no	yes
25	E _{max} Add13	-158.3	no	no	*	yes	no	-	no	yes
26	SigmoidE _{max} Prop1	-158.2	no	no		yes	no	-	no	no
27	LinearProp10	-158.1	no	no	*	yes	no	yes	-	-
28	LinearProp9	-158.0	no	yes	*	yes	no	yes	-	-
29	LinearAdd10	-157.7	no	no	*	yes	no	yes	-	-
30	LinearAdd9	-157.2	no	yes	*	yes	no	yes	-	-
31	SigmoidE _{max} Prop14	-154.9	no	no	*	yes	no	-	no	yes

Table 58 Best models for saccadic inaccuracy

No.	Saccadic inaccuracy	AIC	CV(%) of fixed effects below 50	CV(%) of random effects below 100	P value	VPC	Intercept	Slope	EC50	E _{max}
1	LinearAdd14	168.2	no	no	**	yes	yes	yes	-	-
2	LinearProp14	168.6	no	no	**	yes	yes	yes	-	-
3	LinearProp16	168.6	no	no	**	yes	yes	yes	-	-
4	LinearAdd16	168.8	no	no	**	yes	yes	yes	-	-
5	Zero4	168.9	yes	no	**	yes	no	-	-	-
6	Zero8	169.2	no	no	*	yes	yes	-	-	-
7	Zero6	169.2	no	no	**	yes	yes	-	-	-
8	Zero2	169.2	yes	no		yes	no	-	-	-
9	Zero7	169.8	no	no	**	yes	yes	-	-	-
10	Zero3	169.9	yes	no		yes	no	-	-	-
11	LinearProp15	170.1	no	no	**	yes	yes	yes	-	-
12	Zero1	170.1	yes	no		yes	no	-	-	-
13	LinearAdd13	170.3	no	no	**	yes	yes	yes	-	-
14	LinearAdd15	170.5	no	no	**	yes	yes	yes	-	-
15	LinearProp13	170.8	no	no	**	yes	yes	yes	-	-
16	LinearAdd4	171.0	no	no		yes	no	no	-	-
17	LinearAdd6	171.1	no	no	**	yes	yes	no	-	-
18	LinearProp4	171.2	no	no		yes	no	no	-	-
19	LinearAdd2	171.2	no	no		yes	no	no	-	-
20	LinearAdd8	171.2	no	no	*	yes	yes	no	-	-
21	LinearProp5	171.2	no	no	**	yes	yes	no	-	-
22	LinearProp8	171.2	no	no	*	yes	yes	no	-	-
23	Zero5	171.3	no	no	**	yes	yes	-	-	-
24	LinearProp7	171.3	no	no	*	yes	yes	no	-	-
25	LinearProp2	171.4	no	no		yes	no	no	-	-
26	LinearAdd12	171.5	no	no	*	yes	no	yes	-	-
27	LinearAdd10	171.6	no	no	**	yes	no	yes	-	-
28	LinearProp10	171.8	no	no	**	yes	no	yes	-	-
29	LinearProp12	171.9	yes	no	**	yes	no	yes	-	-
30	LinearAdd7	171.9	no	no	**	yes	yes	no	-	-
31	LinearProp3	171.9	no	no	**	yes	no	no	-	-

Table 59 Best models for number of valid saccades

No.	Number of valid saccades	AIC	CV(%) of fixed effects below 50	CV(%) of random effects below 100	P value	VPC	Intercept	Slope	EC50	E _{max}
1	LinearProp1	214.1	yes	no		yes	no	no	-	-
2	Zero2	214.3	yes	no		yes	no	-	-	-
3	LinearAdd1	214.4	yes	no		yes	no	no	-	-
4	LinearProp2	214.5	no	no		yes	no	no	-	-
5	LinearAdd3	215.3	yes	no		yes	no	no	-	-
6	Zero1	215.5	yes	no		yes	no	-	-	-
7	LinearProp3	215.5	yes	no		yes	no	no	-	-
8	LinearAdd2	215.5	no	no		yes	no	no	-	-
9	LinearProp5	215.9	no	no	*	yes	yes	no	-	-
10	LinearAdd5	216.1	no	no	*	yes	yes	no	-	-
11	LinearAdd9	216.3	no	no	*	yes	no	yes	-	-
12	Zero6	216.3	no	no	*	yes	yes	-	-	-
13	LinearProp9	216.3	no	no	*	yes	no	yes	-	-
14	LinearProp10	216.4	no	no	*	yes	no	yes	-	-
15	LinearProp6	216.5	no	no	*	yes	yes	no	-	-
16	LinearProp4	216.6	yes	no		yes	no	no	-	-
17	Zero4	216.6	yes	no		yes	no	-	-	-
18	Zero3	216.8	yes	no		yes	no	-	-	-
19	LinearAdd10	216.8	no	no	*	yes	no	yes	-	-
20	LinearAdd7	217.1	no	no	*	yes	yes	no	-	-
21	LinearAdd4	217.2	no	no	*	yes	no	no	-	-
22	Zero5	217.3	no	no	*	yes	yes	-	-	-
23	LinearProp7	217.3	no	no	*	yes	yes	no	-	-
24	SigmoidE _{max} Prop14	217.4	no	no	*	yes	no	-	no	yes
25	LinearAdd11	217.6	no	no	*	yes	no	yes	-	-
26	LinearProp11	217.8	no	no	*	yes	no	yes	-	-
27	LinearAdd13	217.8	no	no	*	yes	yes	yes	-	-
28	LinearProp13	218.1	no	no	*	yes	yes	yes	-	-
29	E _{max} Add1	218.2	no	no		yes	no	-	no	no
30	LinearProp14	218.4	no	no	*	yes	yes	yes	-	-
31	LinearProp8	218.5	no	no	*	yes	yes	no	-	-

Table 60 Best models for pupillometry

No.	Pupillometry	AIC	CV(%) of fixed effects below 50	CV(%) of random effects below 100	P value	VPC	Intercept	Slope	EC50	E _{max}
1	SigmoidE_{max}Prop1	73.8	yes	yes		yes	no	-	no	no
2	SigmoidE _{max} Prop2	75.7	no	yes		yes	no	-	no	no
3	SigmoidE _{max} Prop13	76.1	no	yes	*	yes	no	-	no	yes
4	SigmoidE _{max} Prop3	76.1	yes	yes		yes	no	-	no	no
5	SigmoidE _{max} Prop4	76.4	no	yes		yes	no	-	no	no
6	SigmoidE _{max} Prop6	76.6	no	yes	*	yes	yes	-	no	no
7	SigmoidE _{max} Prop8	77.8	no	yes	*	yes	yes	-	no	no
8	SigmoidE _{max} Prop14	78.6	no	yes	*	yes	no	-	no	yes
9	SigmoidE _{max} Prop5	96.4	no	no	*	yes	yes	-	no	no
10	E _{max} Add6	99.5	no	no	*	yes	yes	-	no	no
11	E _{max} Add5	101.3	no	no	*	yes	yes	-	no	no
12	SigmoidE _{max} Prop16	101.5	no	no	*	yes	no	-	no	yes
13	E _{max} Add1	101.8	yes	no		yes	no	-	no	no
14	E _{max} Add3	102.7	yes	no		yes	no	-	no	no
15	SigmoidE _{max} Prop7	103.7	no	no	*	yes	yes	-	no	no
16	E _{max} Add7	104.9	no	no	*	yes	yes	-	no	no
17	SigmoidE _{max} Prop15	105.4	no	no	*	yes	no	-	no	yes
18	LinearProp1	106.9	yes	yes		yes	no	no	-	-
19	LinearProp5	107.5	no	yes	*	yes	yes	no	-	-
20	LinearProp3	107.8	yes	yes		yes	no	no	-	-
21	LinearAdd1	107.9	yes	yes		yes	no	no	-	-
22	LinearProp9	108.2	no	yes	*	yes	no	yes	-	-
23	LinearAdd5	108.4	no	yes	*	yes	yes	no	-	-
24	LinearProp7	108.4	no	yes	*	yes	yes	no	-	-
25	LinearAdd3	108.5	yes	yes		yes	no	no	-	-
26	LinearProp13	109.0	no	yes	*	yes	yes	yes	-	-
27	LinearAdd7	109.1	no	yes	*	yes	yes	no	-	-
28	LinearProp11	109.1	no	yes	*	yes	no	yes	-	-
29	LinearAdd9	109.6	no	yes	*	yes	no	yes	-	-
30	LinearProp15	109.9	no	yes	*	yes	yes	yes	-	-
31	E _{max} Add2	109.9	yes	no		yes	no	-	no	no

Table 61 Best models for Morphine-Benzedrine Group (MBG) scale

No.	MBG scale	AIC	CV(%) of fixed effects below 50	CV(%) of random effects below 100	P value	VPC	Intercept	Slope	EC50	E _{max}
1	LinearAdd12	-400.5	no	no	no	no	no	no	-	-
2	LinearAdd16	-305.9	no	no	no	no	yes	yes	-	-
3	Zero3	239.4	yes	yes		yes	no	-	-	-
4	Zero1	239.6	yes	yes		yes	no	-	-	-
5	LinearAdd3	239.8	no	yes		yes	no	no	-	-
6	LinearAdd1	240.0	no	yes		yes	no	no	-	-
7	Zero7	241.1	no	yes	*	Yes	yes	-	-	-
8	Zero5	241.5	no	yes	*	yes	yes	-	-	-
9	LinearAdd7	241.5	no	yes	*	yes	yes	no	-	9
10	LinearAdd11	241.7	no	yes	*	yes	no	yes	-	-
11	LinearAdd9	241.9	no	yes	*	yes	no	yes	-	-
12	LinearAdd5	241.9	no	yes	*	yes	yes	no	-	-
13	LinearAdd15	243.5	no	yes	*	yes	yes	yes	-	-
14	LinearAdd13	243.8	no	yes	*	yes	yes	yes	-	-
15	E _{max} Add3	251.6	no	no		yes	no	-	no	no
16	LinearProp3	251.8	no	no		yes	no	no	-	-
17	LinearProp7	253.0	no	no	*	yes	yes	no	-	-
18	E _{max} Add7	253.5	no	no	*	yes	yes	-	no	no
19	SigmoidE _{max} Prop3	253.8	no	no		yes	no	-	no	no
20	LinearProp11	253.8	no	no	*	yes	no	yes	-	-
21	LinearProp1	254.0	no	yes		yes	no	no	-	-
22	LinearProp15	254.4	no	yes	*	yes	yes	yes	-	-
23	SigmoidE _{max} Prop7	255.4	no	no	*	yes	yes	-	no	no
24	LinearProp9	255.8	no	yes	*	yes	no	yes	-	-
25	LinearProp5	255.9	no	yes	*	yes	yes	no	-	-
26	LinearAdd2	256.4	no	no		yes	no	no	-	-
27	E _{max} Add15	256.5	no	no	*	yes	no	-	no	yes
28	E _{max} Add1	256.5	no	no		yes	no	-	no	no
29	Zero2	257.2	yes	yes		yes	no	-	-	-
30	LinearProp13	257.7	no	yes	*	yes	yes	yes	-	-
31	SigmoidE _{max} Prop1	257.9	no	no		yes	no	-	no	no

Table 62 Best models for pain threshold

No.	Pain threshold	AIC	CV(%) of fixed effects below 50	CV(%) of random effects below 100	P value	VPC	Intercept	Slope	EC50	E _{max}
1	E _{max} Add12	203.6	no	no	*	yes	no	-	yes	no
2	E _{max} Add10	203.8	no	no	*	yes	no	-	yes	no
3	E _{max} Add2	204.0	no	no		yes	no	-	no	no
4	E _{max} Add4	204.0	no	no		yes	no	-	no	no
5	E _{max} Add16	205.3	no	no	*	yes	no	-	no	yes
6	E _{max} Add14	205.6	no	no	*	yes	no	-	no	yes
7	E _{max} Add11	205.7	no	no	*	yes	no	-	yes	no
8	E _{max} Add6	205.8	no	no	*	yes	yes	-	no	no
9	E _{max} Add9	206.2	no	no	*	yes	no	-	yes	no
10	E _{max} Add8	206.2	no	no	*	yes	yes	-	no	no
11	E _{max} Add18	206.5	no	no	*	yes	yes	-	yes	yes
12	E _{max} Add20	206.8	no	no	*	yes	yes	-	yes	yes
13	SigmoidE _{max} Prop15	206.9	no	no	*	yes	no	-	no	yes
14	E _{max} Add3	207.0	no	no		yes	no	-	no	no
15	SigmoidE _{max} Prop9	207.2	no	no	*	yes	no	-	yes	no
16	E _{max} Add1	207.3	no	no		yes	no	-	no	no
17	SigmoidE _{max} Prop14	207.4	no	no	*	yes	no	-	no	yes
18	E _{max} Add15	207.6	no	no	*	yes	no	-	no	yes
19	E _{max} Add13	207.7	no	no	*	yes	no	-	no	yes
20	E _{max} Add19	207.8	no	no	*	yes	yes	-	yes	yes
21	SigmoidE _{max} Prop12	207.9	no	no	*	yes	no	-	yes	no
22	SigmoidE _{max} Prop4	208.2	no	no		yes	no	-	no	no
23	SigmoidE _{max} Prop1	208.3	no	no		yes	no	-	no	no
24	SigmoidE _{max} Prop16	208.5	no	no	*	yes	no	-	no	yes
25	E _{max} Add5	208.7	no	no	*	yes	yes	-	no	no
26	E _{max} Add17	208.7	no	no	*	yes	yes	-	yes	yes
27	SigmoidE _{max} Prop2	208.9	no	no		yes	no	-	no	no
28	SigmoidE _{max} Prop13	209.2	no	no	*	yes	no	-	no	yes
29	E _{max} Add7	209.3	no	no	*	yes	yes	-	no	no
30	SigmoidE _{max} Prop3	209.7	no	no		yes	no	-	no	no
31	SigmoidE _{max} Prop7	210.0	no	no	*	yes	yes	-	no	no

Table 63 Best models for pain tolerance

No.	Pain tolerance	AIC	CV(%) of fixed effects below 50	CV(%) of random effects below 100	P value	VPC	Intercept	Slope	EC50	E _{max}
1	SigmoidE _{max} Prop8	311.0	no	no	**	yes	yes	-	no	no
2	SigmoidE _{max} Prop4	312.5	no	no		yes	no	-	no	no
3	SigmoidE _{max} Prop16	314.8	no	no	*	yes	no	-	no	yes
4	SigmoidE _{max} Prop6	318.4	no	no	**	yes	yes	-	no	no
5	SigmoidE _{max} Prop2	320.6	no	no		yes	no	-	no	no
6	SigmoidE _{max} Prop14	323.0	no	no	*	yes	no	-	no	yes
7	E _{max} Add8	328.0	no	no	**	yes	yes	-	no	no
8	E _{max} Add4	329.3	no	no		yes	no	-	no	no
9	E _{max} Add12	329.8	no	no	*	yes	no	-	yes	no
10	E _{max} Add20	329.9	no	no	**	no	yes	-	yes	yes
11	E _{max} Add16	331.0	no	no	*	yes	no	-	no	yes
12	LinearProp8	332.1	no	yes	**	yes	yes	no	-	-
13	LinearProp16	332.3	no	yes	**	yes	yes	yes	-	-
14	LinearProp4	332.6	yes	yes		yes	no	no	-	-
15	LinearProp12	333.0	no	yes	*	yes	no	yes	-	-
16	LinearAdd8	333.4	no	yes	**	yes	yes	no	-	-
17	LinearAdd4	334.5	no	yes		yes	no	no	-	-
18	E _{max} Add6	334.8	no	no	**	yes	yes	-	no	no
19	LinearAdd16	335.2	no	yes	**	yes	yes	yes	-	-
20	LinearAdd12	336.4	no	yes	*	yes	no	yes	-	-
21	E _{max} Add2	336.8	no	no		yes	no	-	no	no
22	E _{max} Add18	337.0	no	no		yes	yes	-	yes	yes
23	E _{max} Add10	337.5	no	no	*	yes	no	-	yes	no
24	LinearProp6	338.4	no	yes	**	yes	yes	no	-	-
25	E _{max} Add14	338.5	no	no	*	yes	no	-	no	yes
26	SigmoidE _{max} Prop7	338.5	no	no	**	yes	yes	-	no	no
27	LinearProp14	338.8	no	yes	*	yes	yes	yes	-	-
28	LinearProp2	339.5	yes	yes		yes	no	no	-	-
29	SigmoidE _{max} Prop3	339.7	no	no		yes	no	-	no	no
30	Zero8	339.8	no	yes	**	yes	yes	-	-	-
31	LinearProp10	340.2	no	yes	*	yes	no	yes	-	-

Table 64 Best models for Subjective Opioid Withdrawal Scale

No.	Subjective Opioid Withdrawal Scale	AIC	CV(%) of fixed effects below 50	CV(%) of random effects below 100	P value	VPC	Intercept	Slope	EC50	Emax
1	SigmoidEmaxProp18	86.0	no	no		yes	yes	-	yes	yes
2	LinearProp10	93.7	no	yes	*	yes	no	yes	-	-
3	SigmoidEmaxProp2	97.6	no	no		yes	no	-	no	no
4	SigmoidEmaxProp10	98.1	no	no	*	yes	no	-	yes	no
5	LinearProp2	99.5	yes	yes		yes	no	no	-	-
6	LinearProp14	104.1	no	yes	*	yes	yes	yes	-	-
7	LinearProp6	104.6	no	yes	**	yes	yes	no	-	-
8	SigmoidEmaxProp14	106.8	no	no	*	yes	no	-	no	yes
9	SigmoidEmaxProp6	112.2	no	no	**	yes	yes	-	no	no
10	EmaxAdd14	113.8	no	no	*	yes	no	-	no	yes
11	EmaxAdd10	114.1	no	no		yes	no	-	yes	no
12	EmaxAdd2	116.7	no	no		yes	no	-	no	no
13	EmaxAdd6	116.9	no	no	**	yes	yes	-	no	no
14	EmaxAdd18	129.1	no	no		yes	yes	-	yes	yes
15	LinearAdd14	159.7	yes	no	**	yes	yes	yes	-	-
16	LinearAdd6	163.1	no	no	**	yes	yes	no	-	-
17	Zero6	168.4	no	yes	**	yes	yes	-	-	-
18	LinearAdd10	168.9	no	no	*	yes	no	yes	-	-
19	LinearAdd2	170.9	no	yes		yes	no	no	-	-
20	Zero2	178.5	yes	yes		yes	no	-	-	-
21	SigmoidEmaxProp11	207.8	no	no		yes	no	-	yes	no
22	SigmoidEmaxProp19	208.9	no	no		yes	yes	-	yes	yes
23	SigmoidEmaxProp7	213.4	no	no		yes	yes	-	no	no
24	SigmoidEmaxProp3	214.3	no	no		yes	no	-	no	no
25	SigmoidEmaxProp17	221.9	no	no		yes	yes	-	yes	yes
26	SigmoidEmaxProp1	227.4	no	no		yes	no	-	no	no
27	SigmoidEmaxProp5	228.1	no	no	**	yes	yes	-	no	no
28	SigmoidEmaxProp15	228.6	no	no	*	yes	no	-	no	yes
29	SigmoidEmaxProp13	239.7	no	no		yes	no	-	no	yes
30	LinearProp5	243.0	yes	no	**	yes	yes	no	-	-
31	LinearProp13	243.0	no	no	*	yes	yes	yes	-	-

6.2 Morphine Benzodrine Group Scale

MORPHINE BENZEDRINE GROUP SCALE (MBG) SCALE			
<p>MBG scale is used to measure euphoria. This should take approximately 1-2 minutes to complete. Instructions: answer the following statements as accurately as you can. Rate the way you have been feeling RIGHT NOW by answering True or False.</p>			
<p>Time: __ : __</p>			
		TRUE (1)	FALSE (0)
1	I would be happy all the time if I felt as I feel now		
2	I am in the mood to talk about the feeling I have		
3	I am full of energy		
4	I would be happy all the time if I felt as I do now		
5	Things around me seem more pleasing than usual		
6	I feel less discouraged than usual		
7	I feel that I will lose the contentment that I now have		
8	I feel as if something pleasant just happened to me		
9	Today I say things in the easiest possible way		
10	I feel so good that I know other people can tell it		
11	I feel more clear-headed than dreamy		
12	I can completely appreciate what others are saying when I am in this mood		
13	I feel as if I would be more popular with people today		
14	I feel a very pleasant emptiness		
15	I feel in complete harmony with the world and those around me		
16	I have a pleasant feeling in my stomach		
	Total Score __		
<p>Participant initials: _____</p>			

6.3 Subjective Opioid Withdrawal Scale

SUBJECTIVE OPIOID WITHDRAWAL SCALE (SOWS)						
Time: __ : __						
Score – Level of Symptom Check (v)						
	SYMPTOM	NOT AT ALL	A LITTLE	MODERATE	QUITE A BIT	EXTREME
1	I feel anxious					
2	I feel like yawning					
3	I am perspiring					
4	My eyes are teary					
5	My nose is running					
6	I have goosebumps					
7	I am shaking					
8	I have hot flushes					
9	I have cold flushes					
10	My bones and muscles ache					
11	I feel restless					
12	I feel nauseous					
13	I feel like vomiting					
14	My muscles twitch					
15	I have stomach cramps					
16	I feel like using now					
Total Score __						
Participant initials: _____						

6.4 Effects of fentanyl in the opioid-tolerant

6.4.1 Very low (0.5-2.0 Hz) frequency band at Pz-Oz

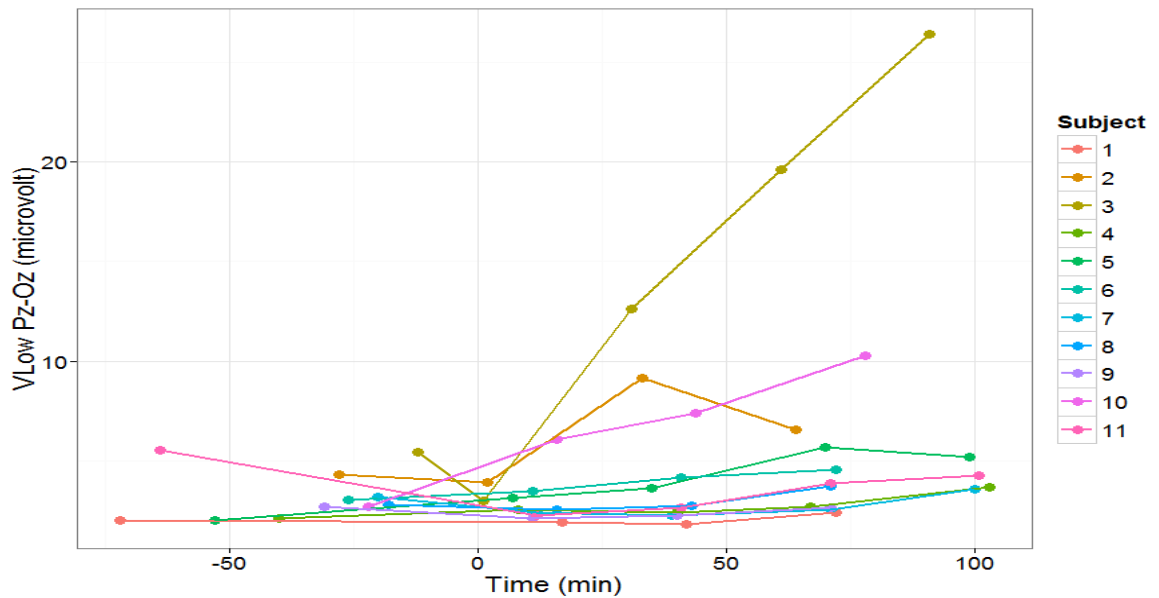


Figure 39 Graph showing average power in very low frequency EEG band using amplification factor of 50,000 at Pz-Oz site before and after starting fentanyl infusion (Time 0).

6.4.2 Very low (0.5-2.0 Hz) at Fz-Cz

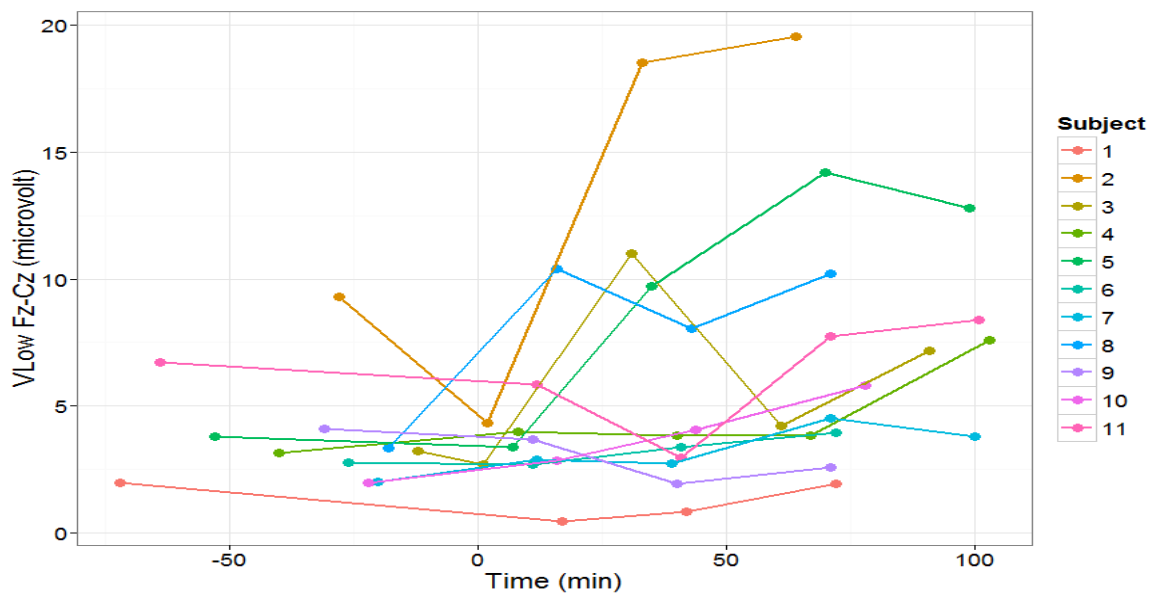


Figure 40 Graph showing average power in very low EEG band (amplification factor of 50,000) at Fz-Cz site before and after starting fentanyl infusion (Time 0).

6.4.3 Delta (2.0-4.0 Hz) at Pz-Oz

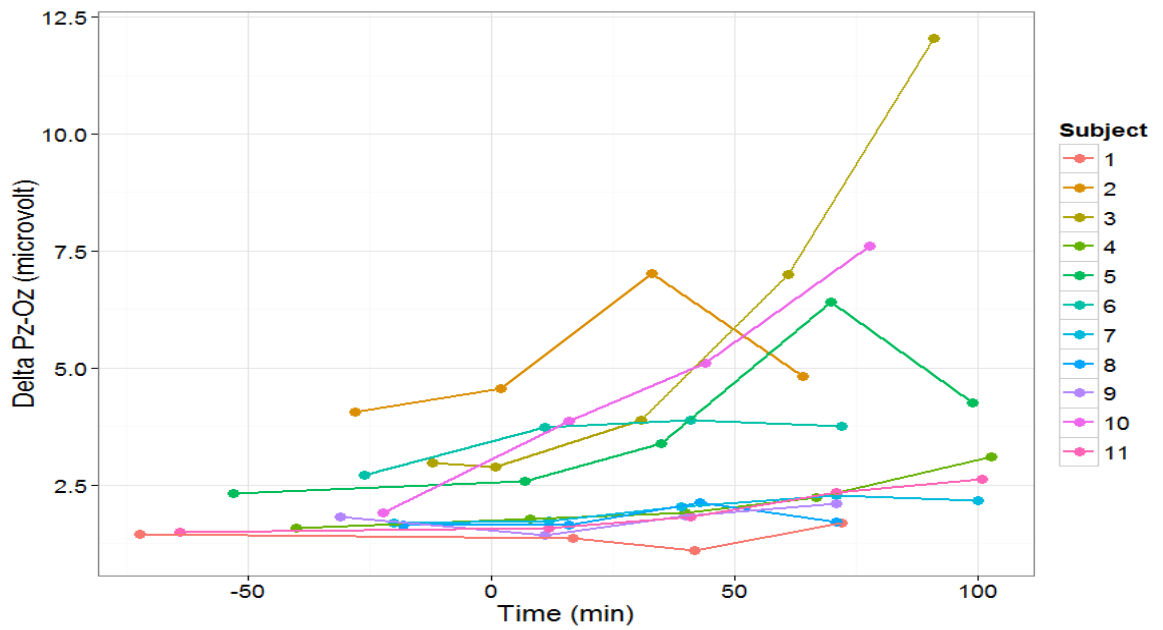


Figure 41 Average power at delta Pz-Oz versus time.

6.4.4 Delta (2.0-4.0 Hz) at Fz-Cz

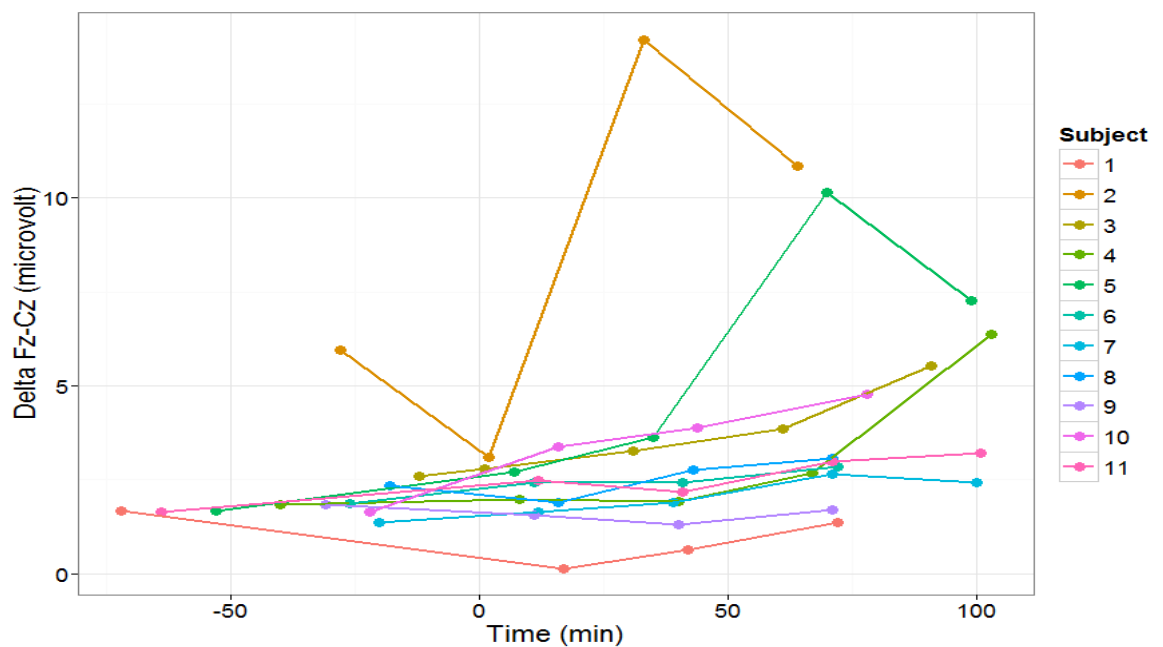


Figure 42 Average power of delta at Fz-Cz versus time

6.4.5 Theta (4.0-7.5 Hz) at Pz-Oz

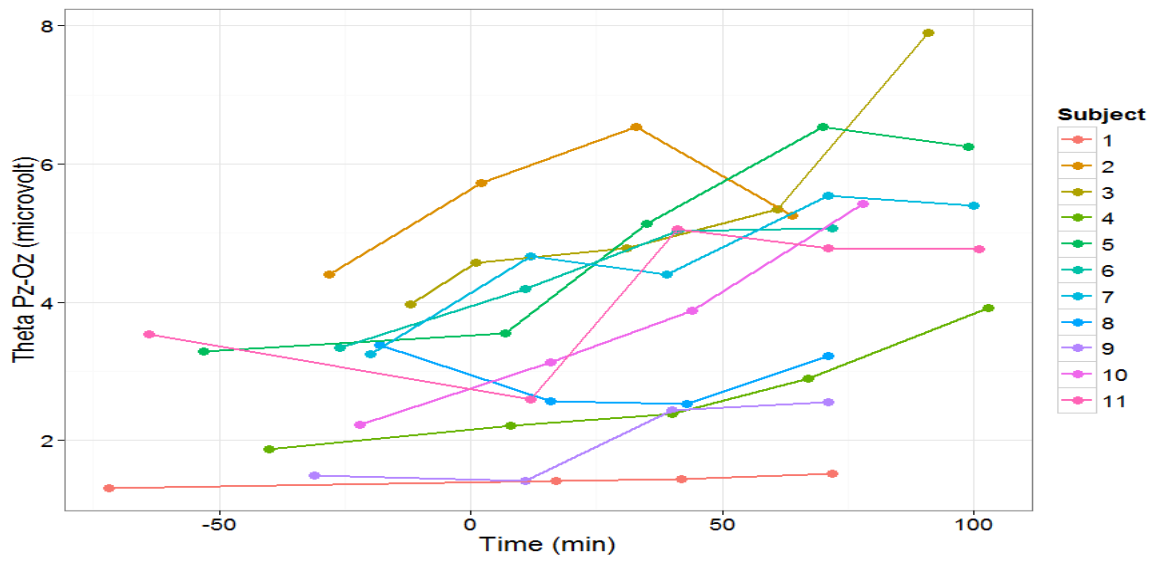


Figure 43 Average power of theta at Pz-Oz versus time.

6.4.6 Theta (4.0-7.5 Hz) at Fz-Cz

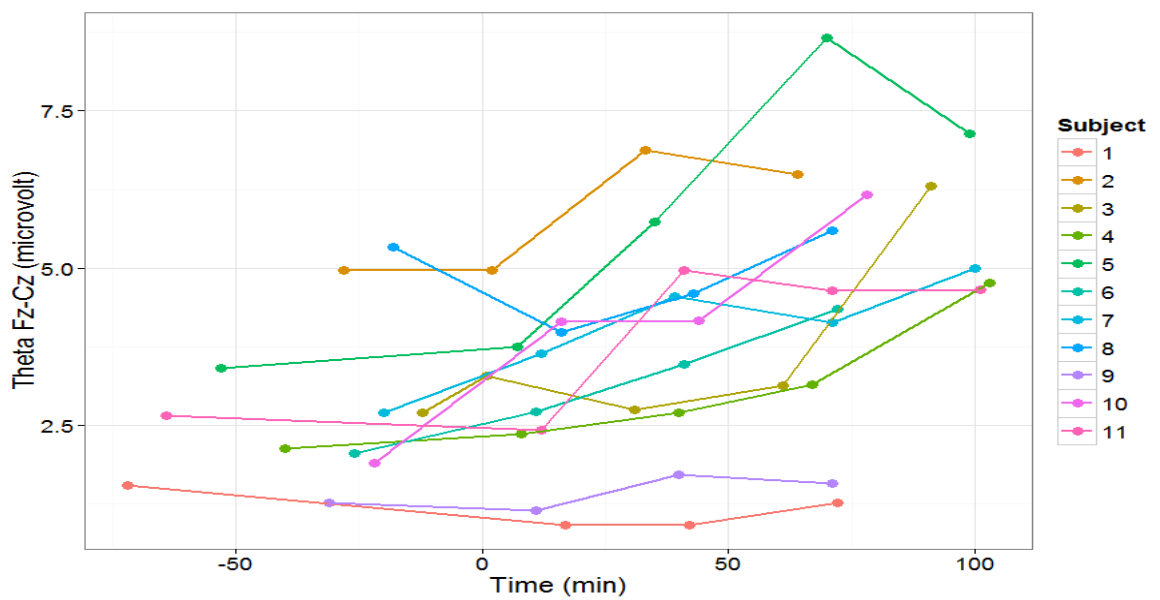


Figure 44 Average power of theta at Fz-Cz versus time.

6.4.7 Alpha (7.5-13.5 Hz) at Pz-Oz

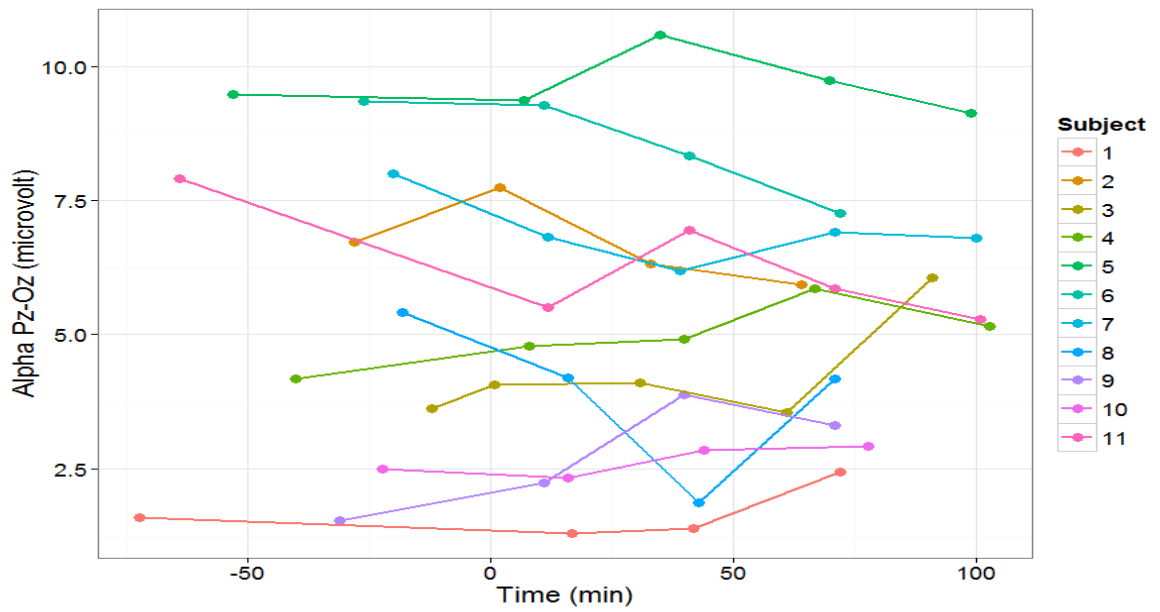


Figure 45 Average power of alpha at Pz-Oz versus time.

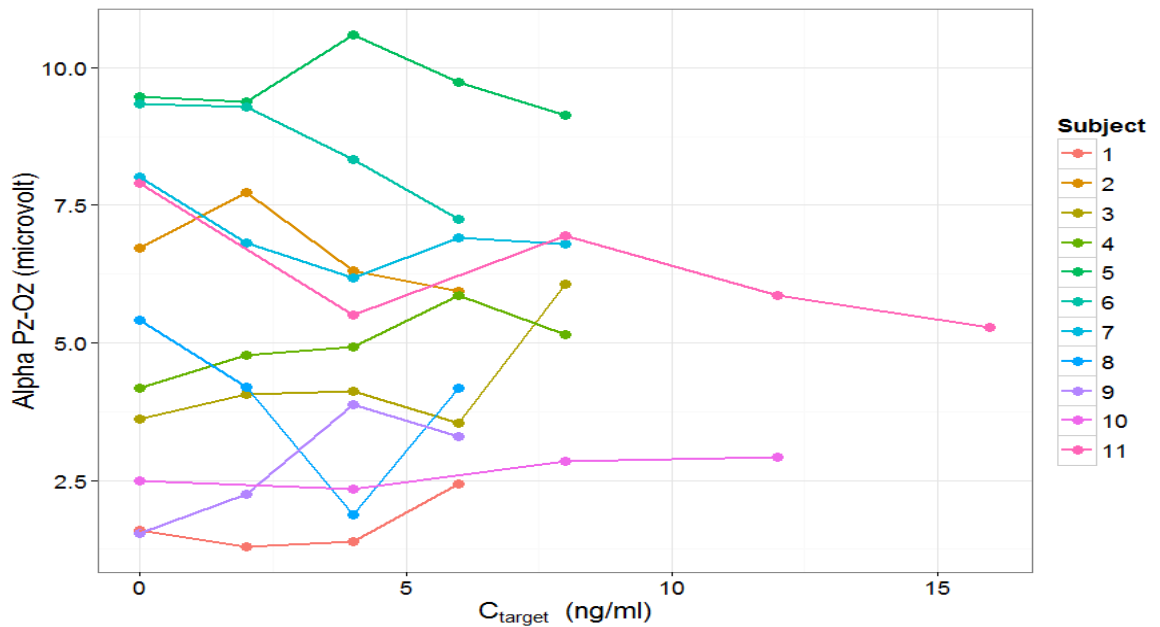


Figure 46 Average power of alpha at Pz-Oz versus target effect site concentration of fentanyl.

6.4.8 Alpha (7.5-13.5 Hz) at Fz-Cz

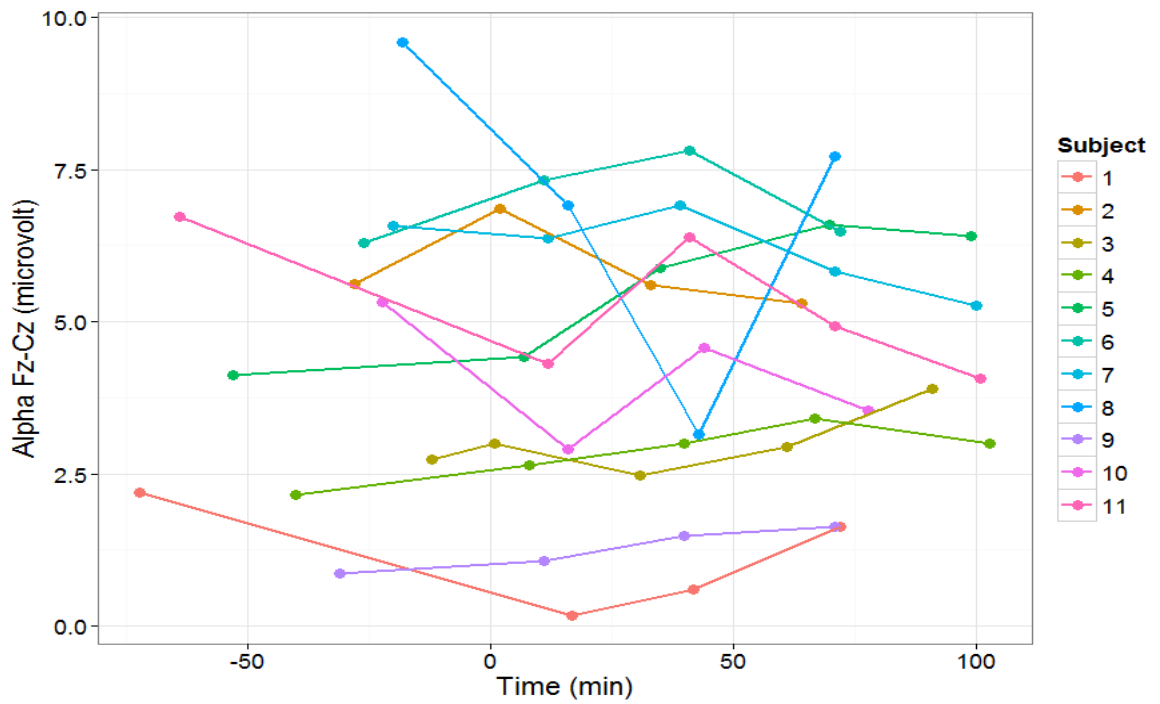


Figure 47 Average power of alpha at Fz-Cz versus time.

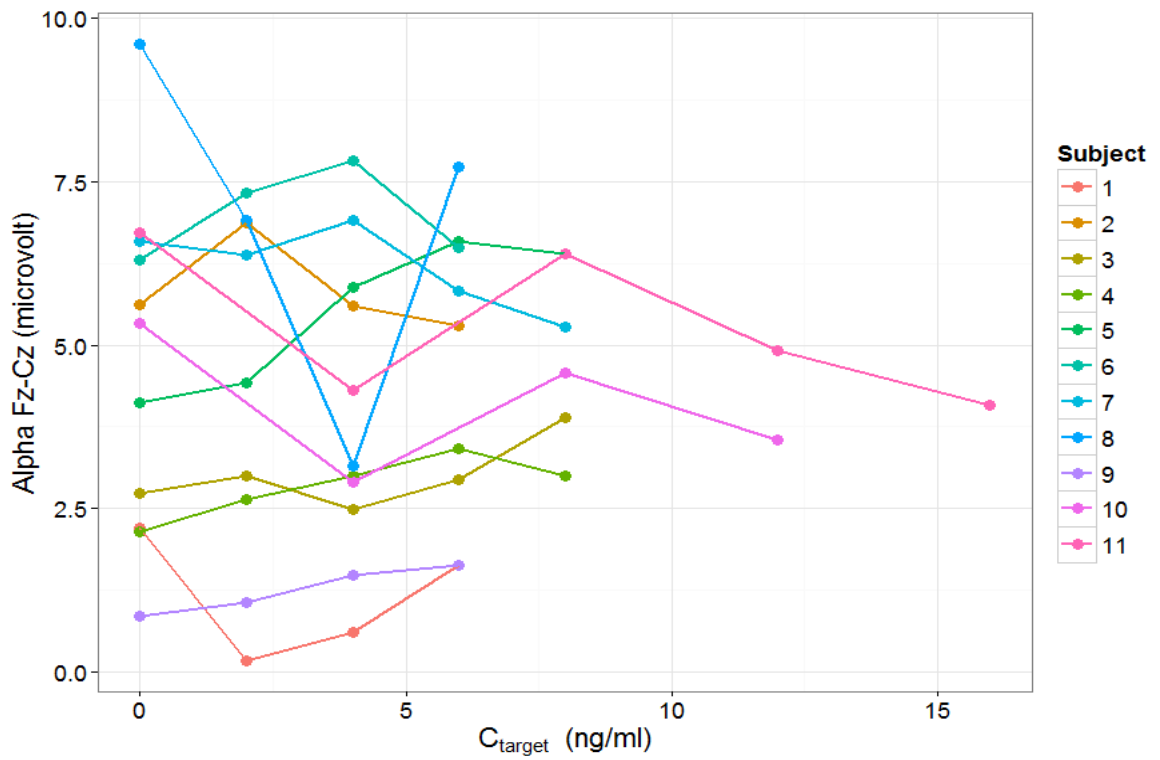


Figure 48 Average power of alpha at Fz-Cz versus target effect site concentration of fentanyl.

6.4.9 Beta (13.5-35 Hz) at Pz-Oz

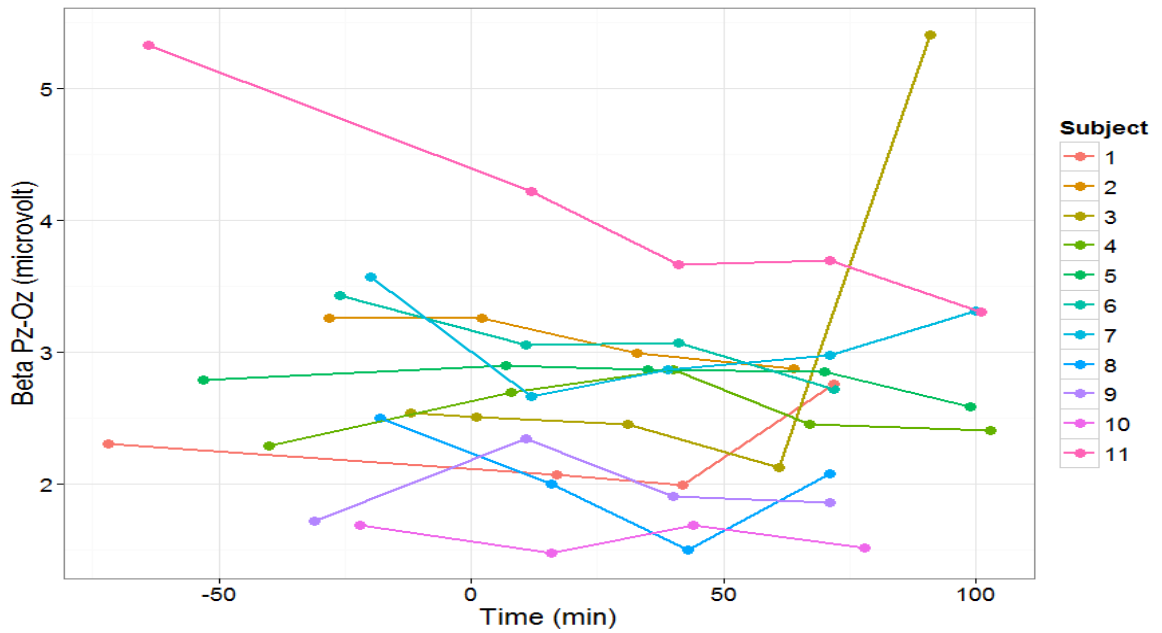


Figure 49 Average power of beta at Pz-Oz versus time.

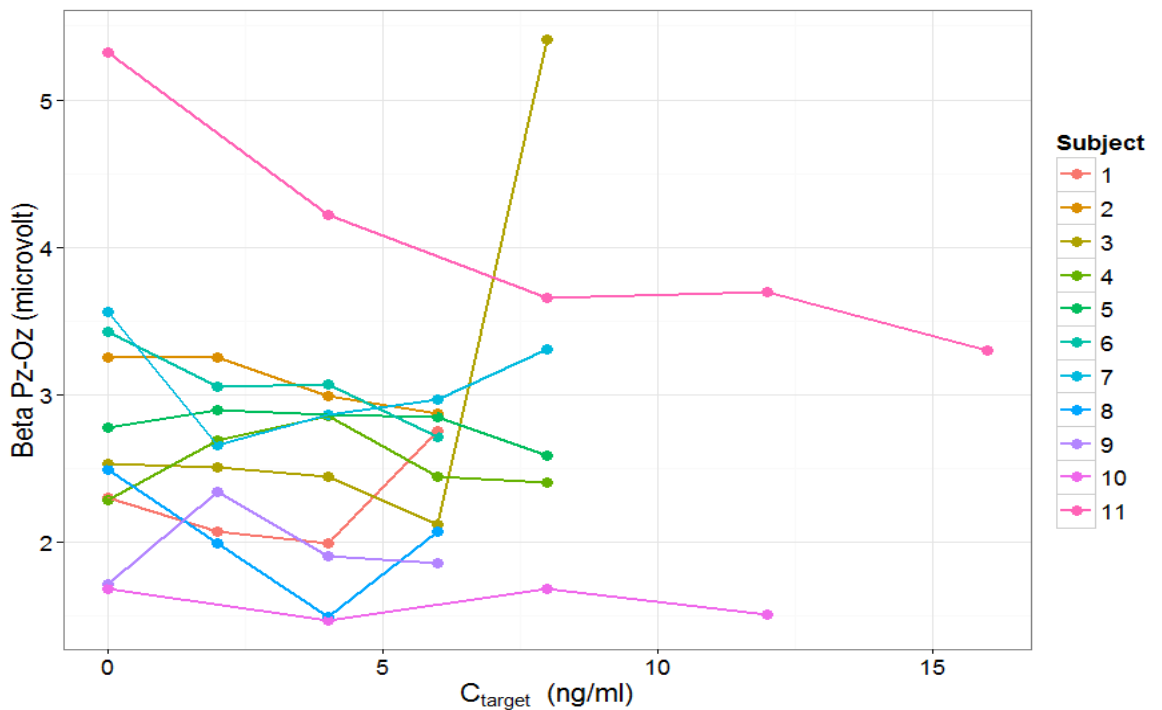


Figure 50 Average power of beta at Pz-Oz versus target effect site concentration of fentanyl.

6.4.10 Beta (13.5-35 Hz) at Fz-Cz

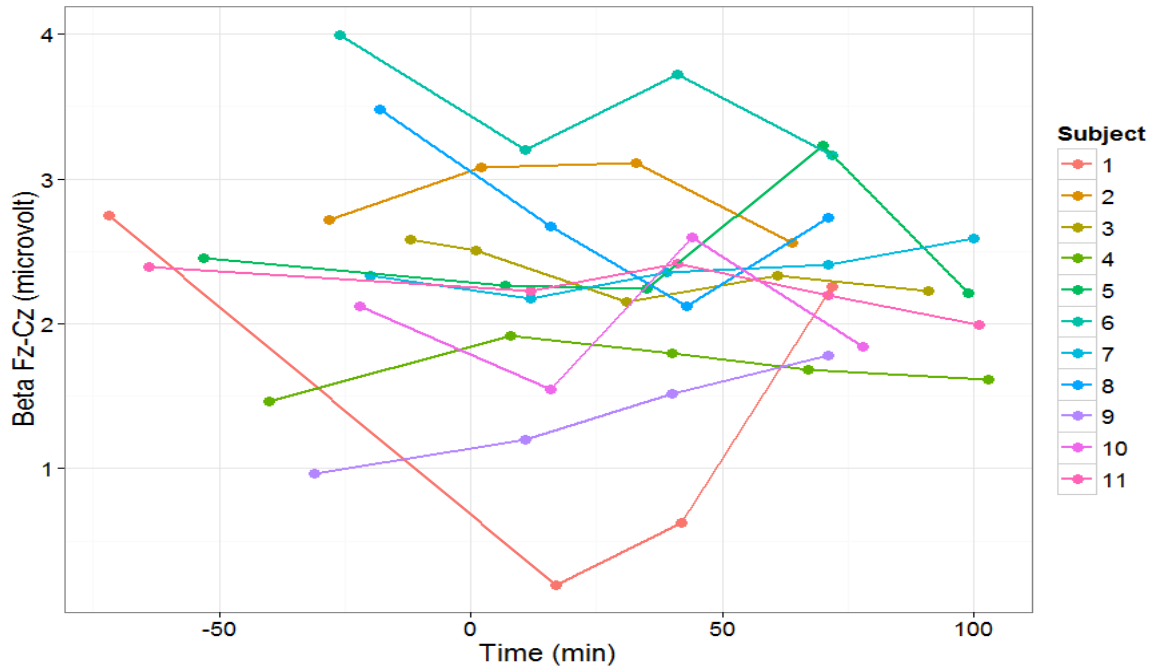


Figure 51 Average power of beta at Fz-Cz versus time.

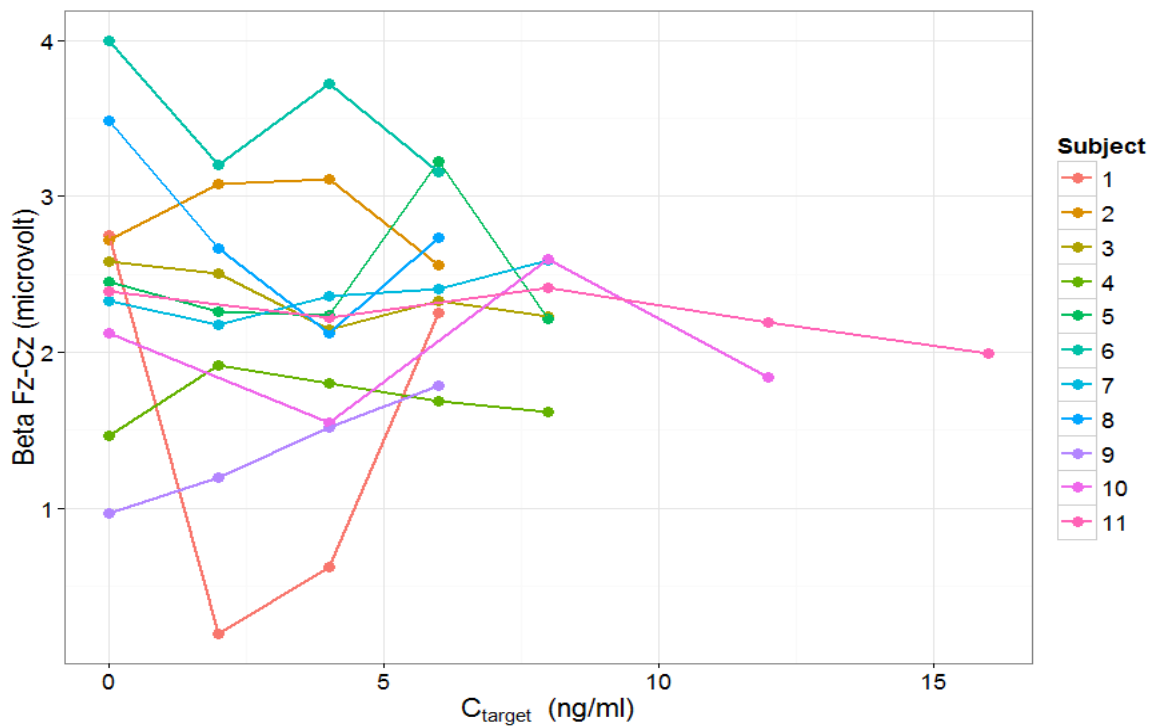


Figure 52 Average power of beta at Fz-Cz versus target effect site concentration of fentanyl.

6.4.11 Gamma (35.1-48.8 Hz) at Pz-Oz

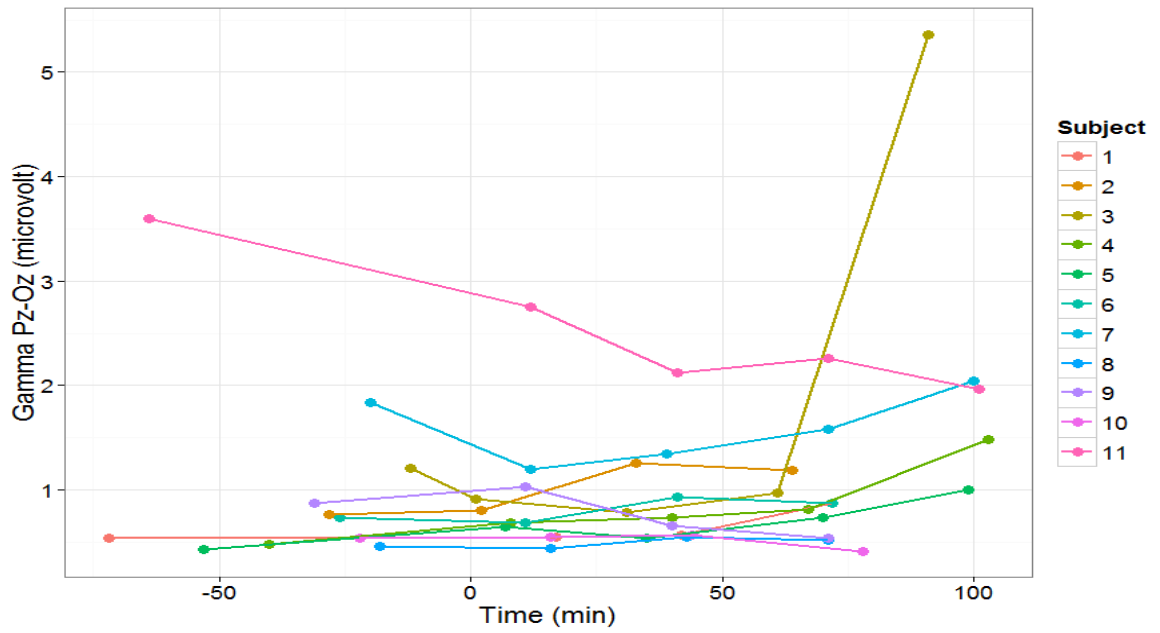


Figure 53 Average power of gamma at Pz-Oz versus time.

6.4.12 Gamma (35.1-48.8 Hz) at Fz-Cz

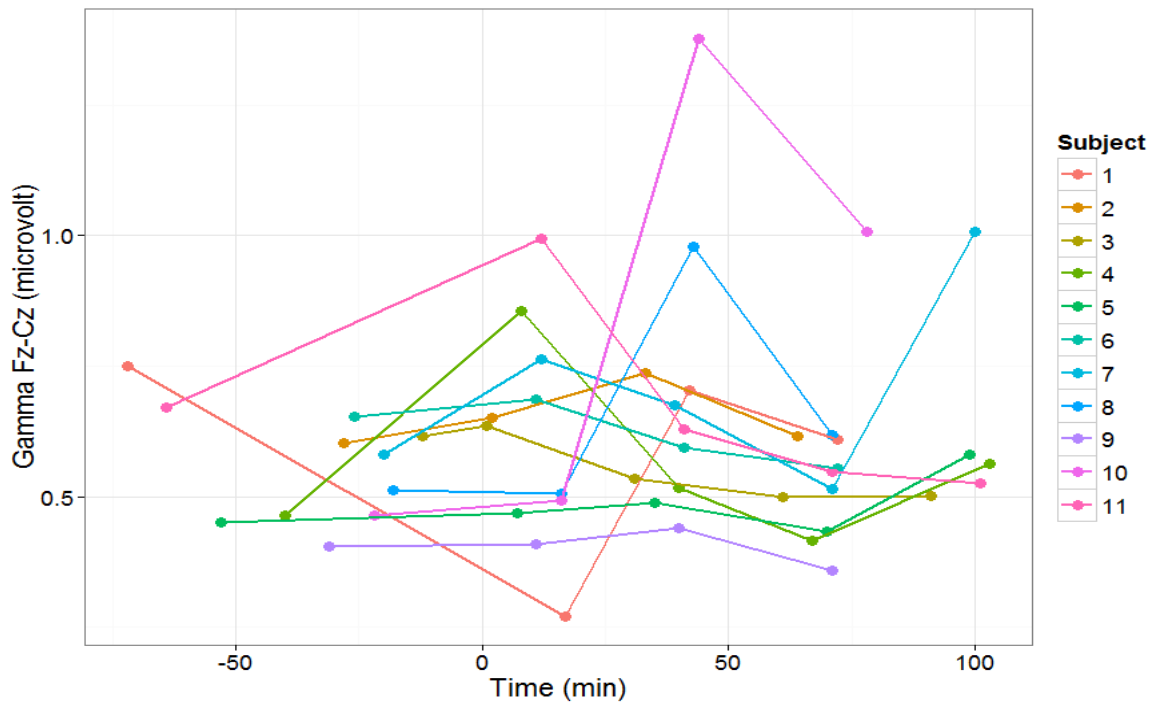


Figure 54 Average power of gamma at Fz-Cz versus time.

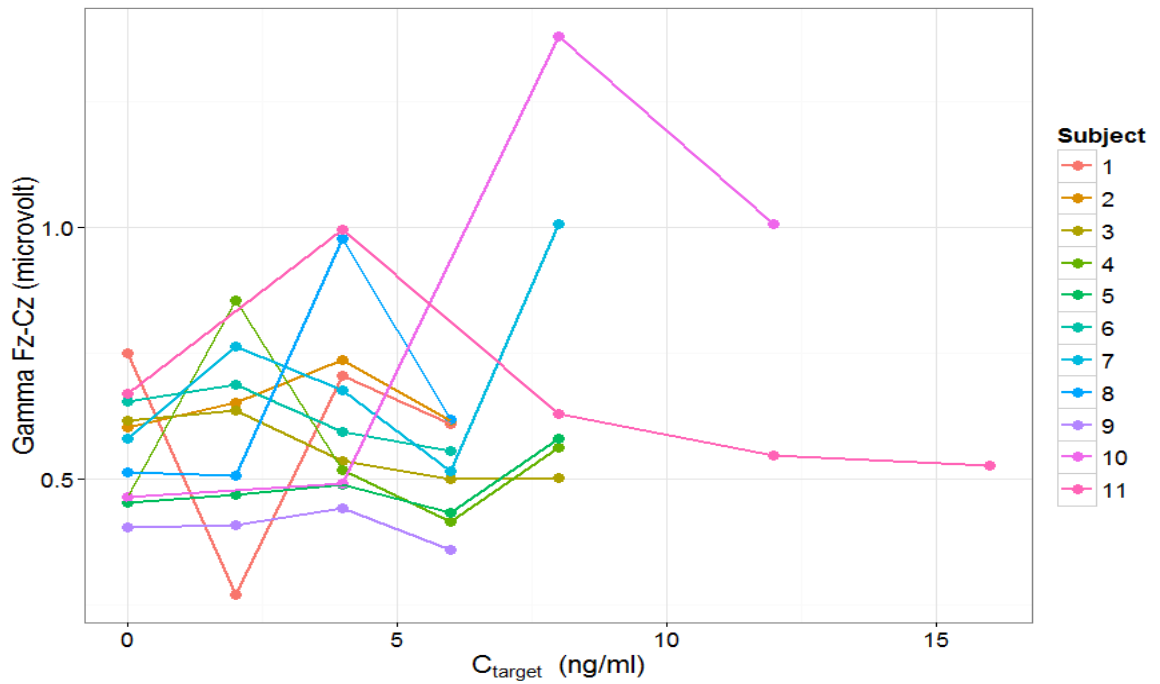


Figure 55 Average power of gamma at Fz-Cz versus target effect site concentration of fentanyl.

6.4.13 Saccadic peak velocity

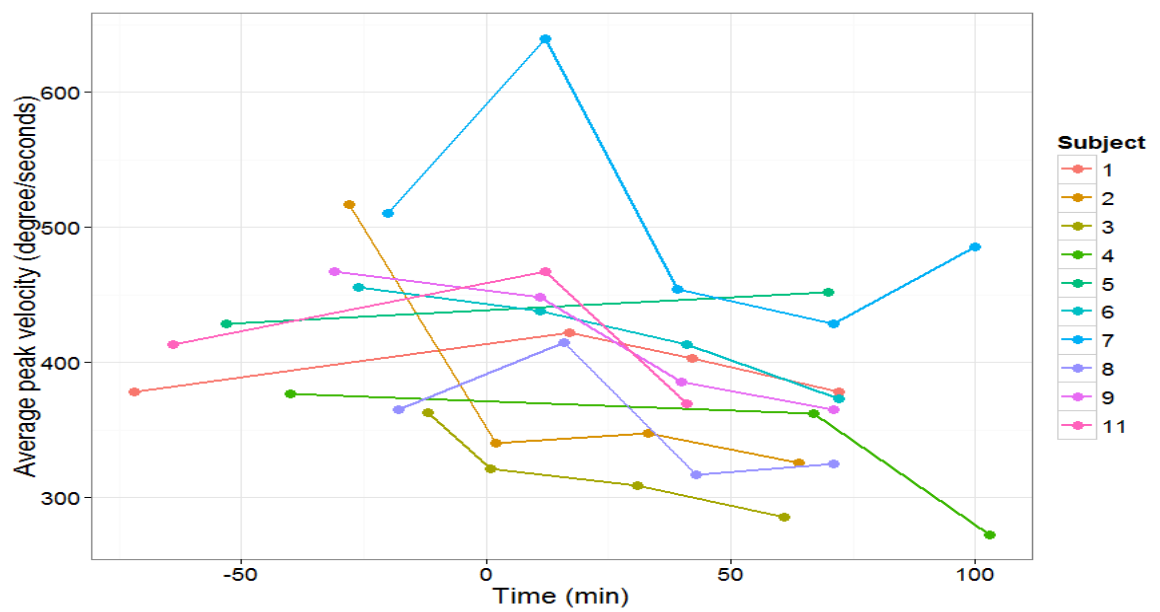


Figure 56 Average saccadic peak velocity versus time. The peak velocity is the maximum registered velocity for the saccadic eye movement.

6.4.14 Saccadic latency

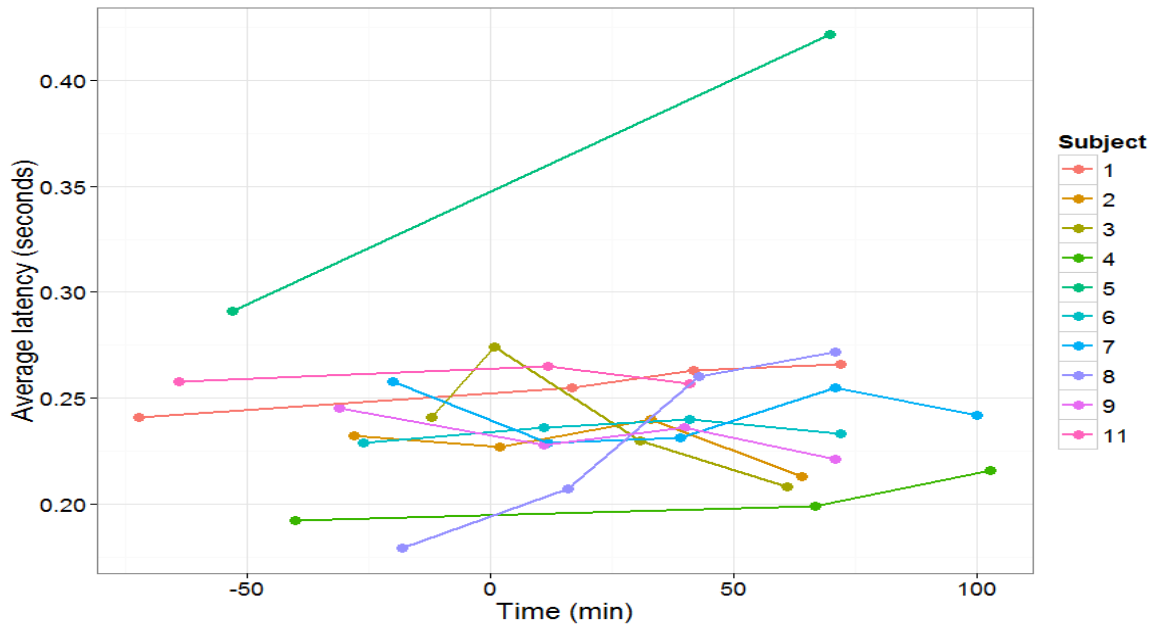


Figure 57 Average saccadic latency versus time.

6.4.15 Saccadic inaccuracy

This is the absolute value of the difference between the stimulus angle and the corresponding saccade, expressed as a percentage of the stimulus angle.

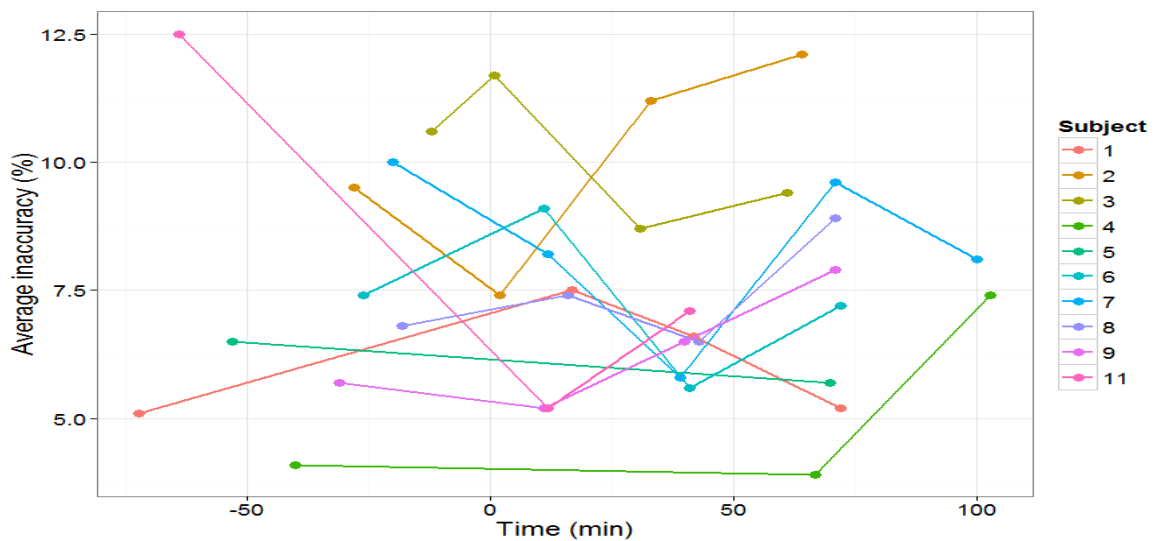


Figure 58 The average saccadic inaccuracy versus time.

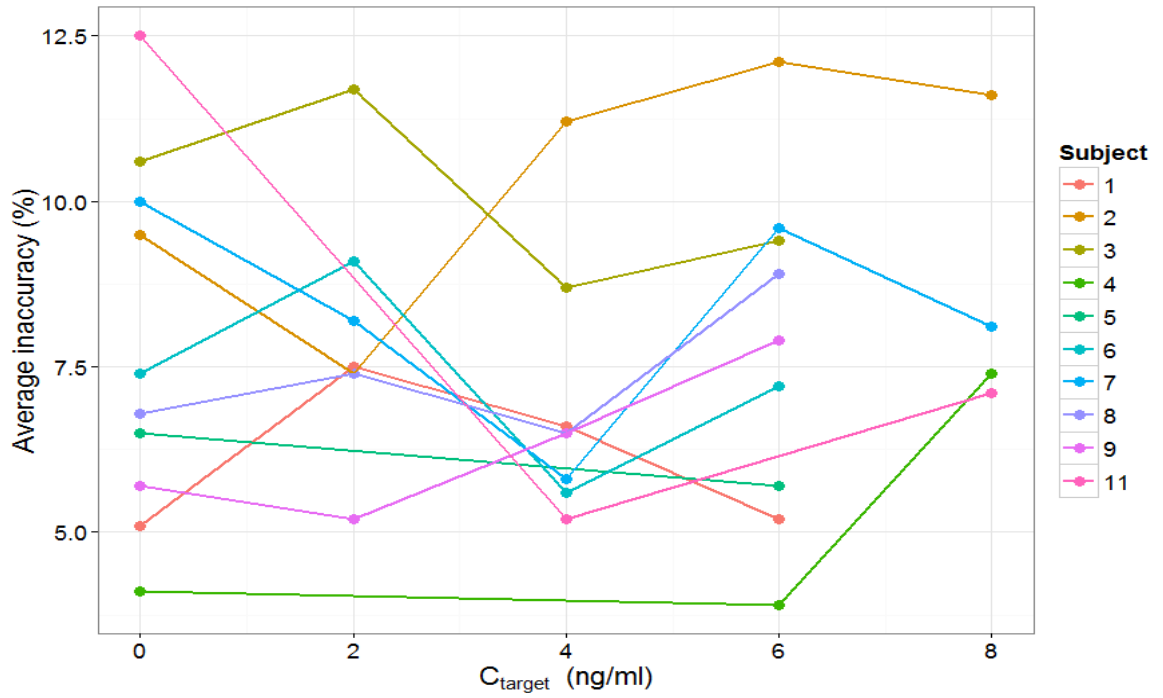


Figure 59 Average saccadic inaccuracy versus target effect site concentration of fentanyl.

6.4.16 Number of valid saccades

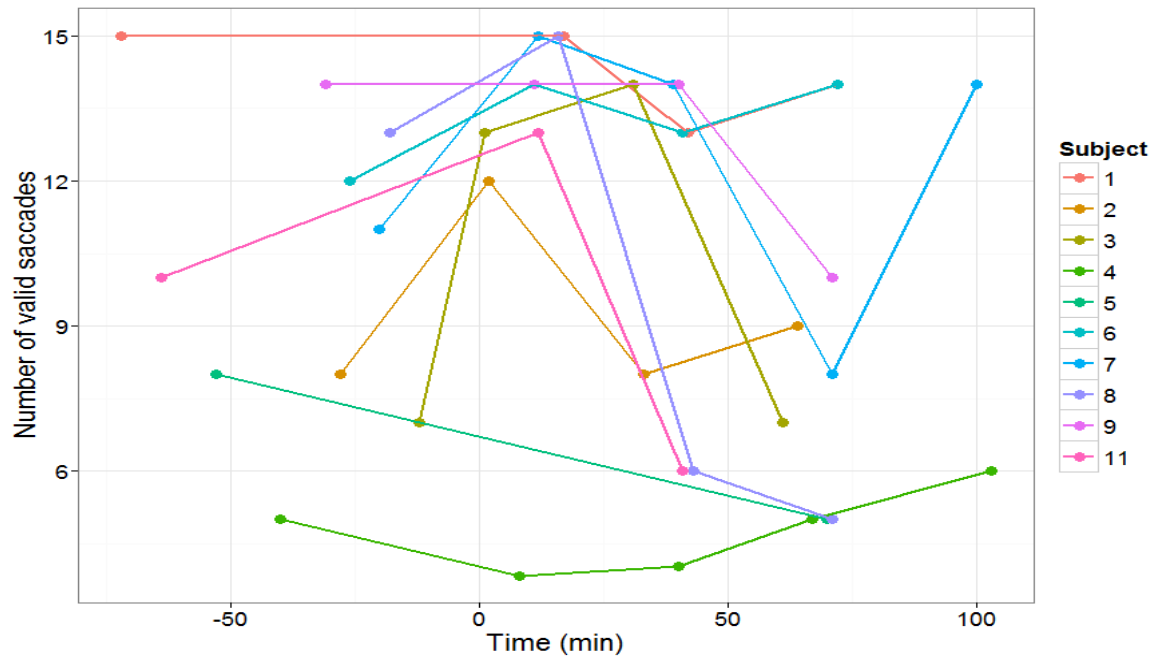


Figure 60 Number of valid saccades versus time.

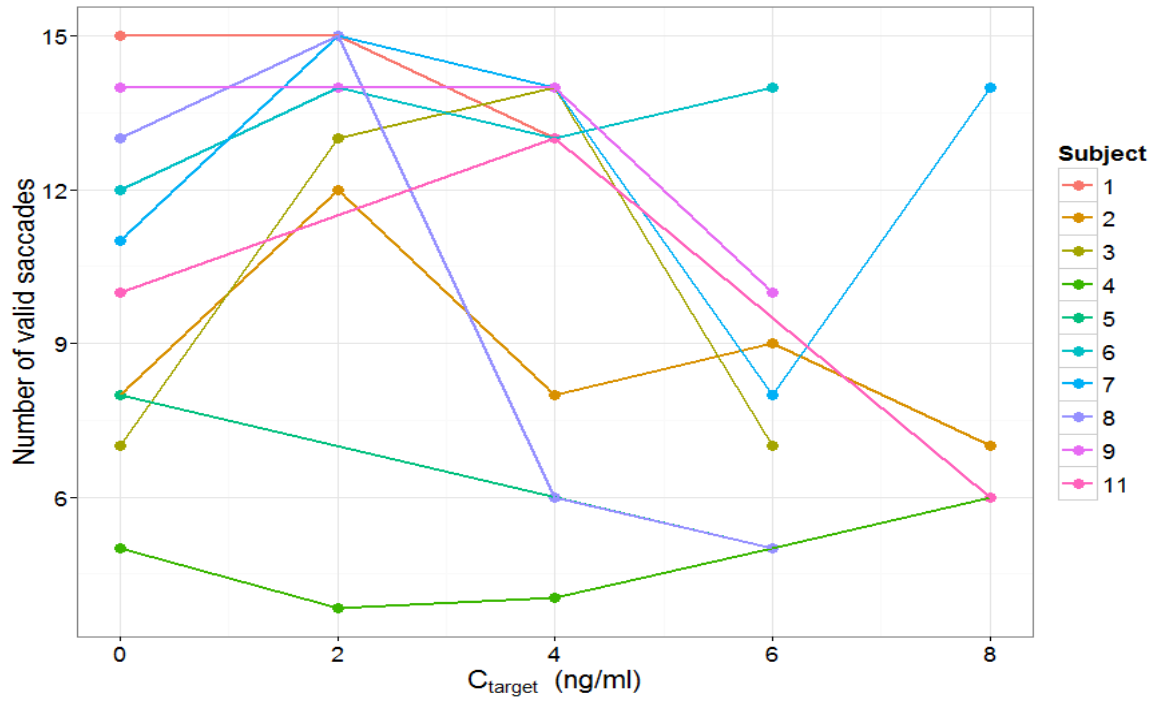


Figure 61 Number of valid saccades versus target effect site concentration of fentanyl.

6.4.17 Pupillometry

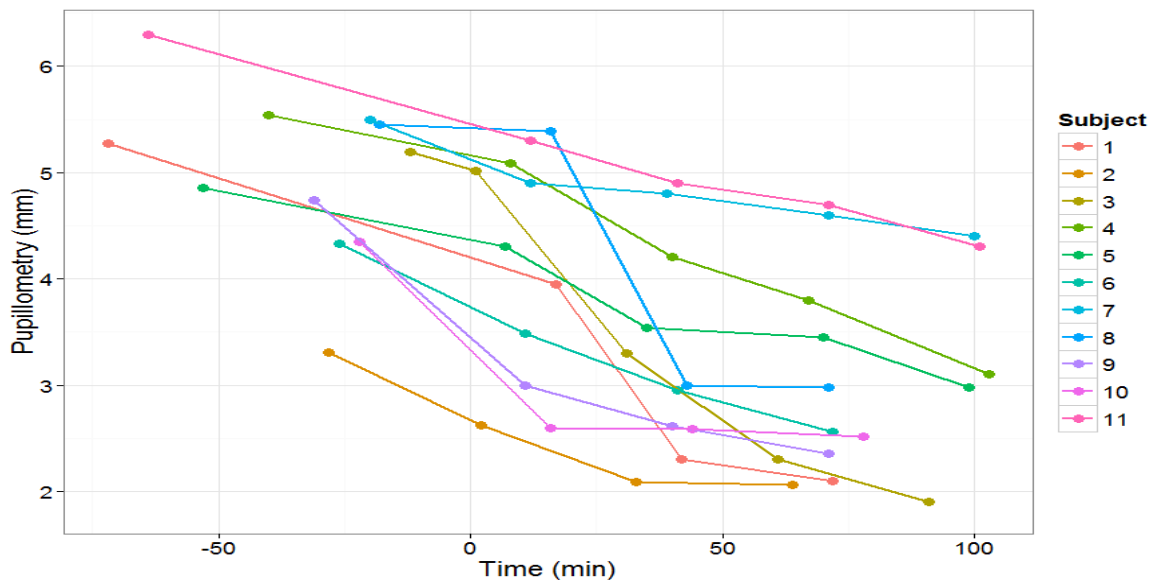


Figure 62 Pupil size versus time.

6.4.18 Morphine-Benzedrine Group (MBG) Scale

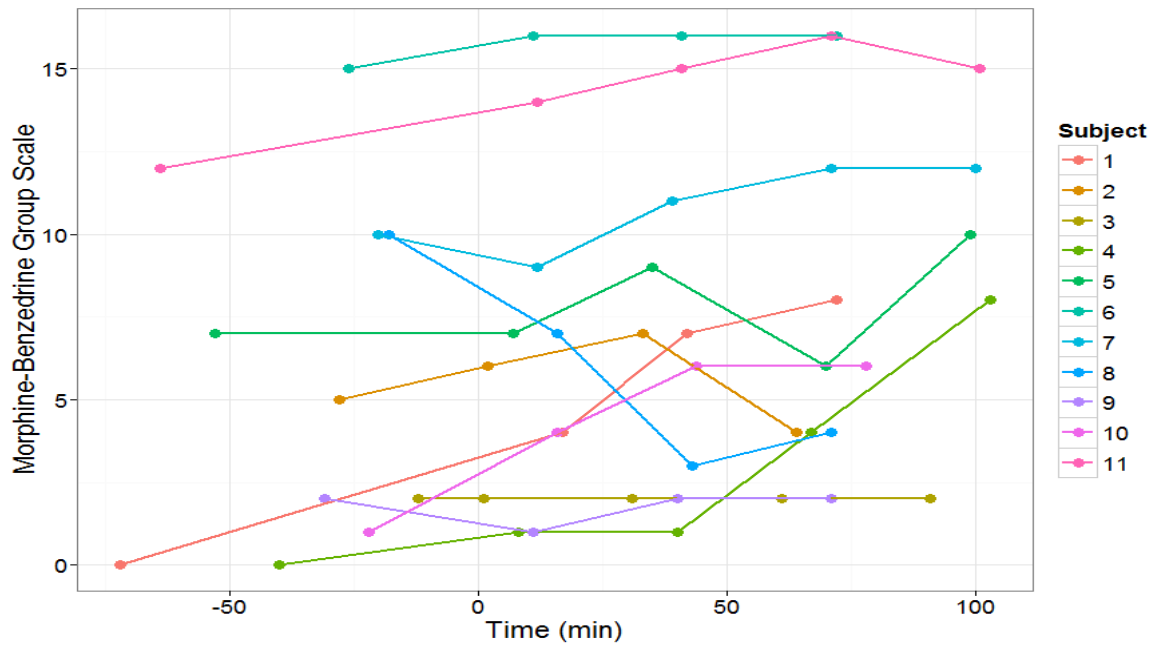


Figure 63 Morphine-Benzedrine Group (MBG) Scale versus time.

6.4.19 Pain threshold

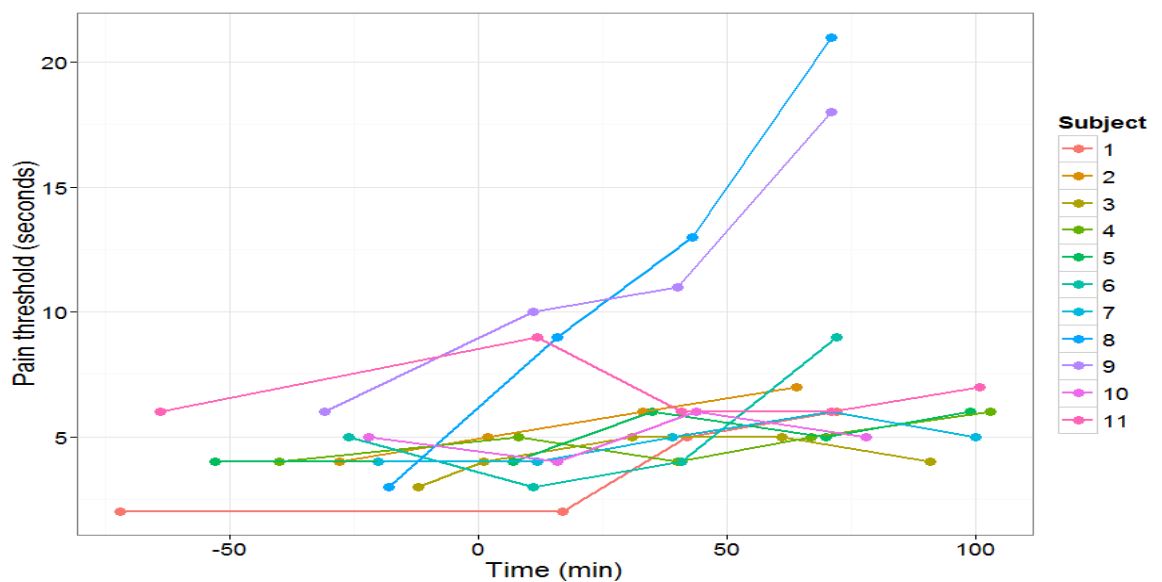


Figure 64 Pain threshold to cold pain test versus time.

6.5 Fentanyl doses, STANPUMP and Harvard pump 22

6.5.1 STANPUMP and Harvard pump 22

Fentanyl infusion rates in the study will be estimated by the computer program STANPUMP. STANPUMP is a free program developed by Steven L. Shafer of Stanford University (117, 138). It supports a number of infusion pumps including Harvard Pump 22 (117). This software will calculate the pump settings for the Harvard 22 pump which will produce a given estimated effect compartment concentration. It has been used for about 20 years by many anaesthetists in multiple clinical settings. The authors of STANPUMP themselves have used it to infuse drug for sedation in their ICU for more than two weeks (185). According to the authors, the STANPUMP has an excellent safety record and there has only been one report in 1993 of an administration error due to not knowing the rare influence of electrocautery on the Harvard Pump 22. This problem has been rectified in later versions of STANPUMP (185).

The Harvard Pump 22 is an extremely accurate research pump (185). It was invented in the 1980s by Harvard Apparatus, Massachusetts. The pump together with the software STANPUMP however is not approved for use in humans except after approval from an ethics committee (185).

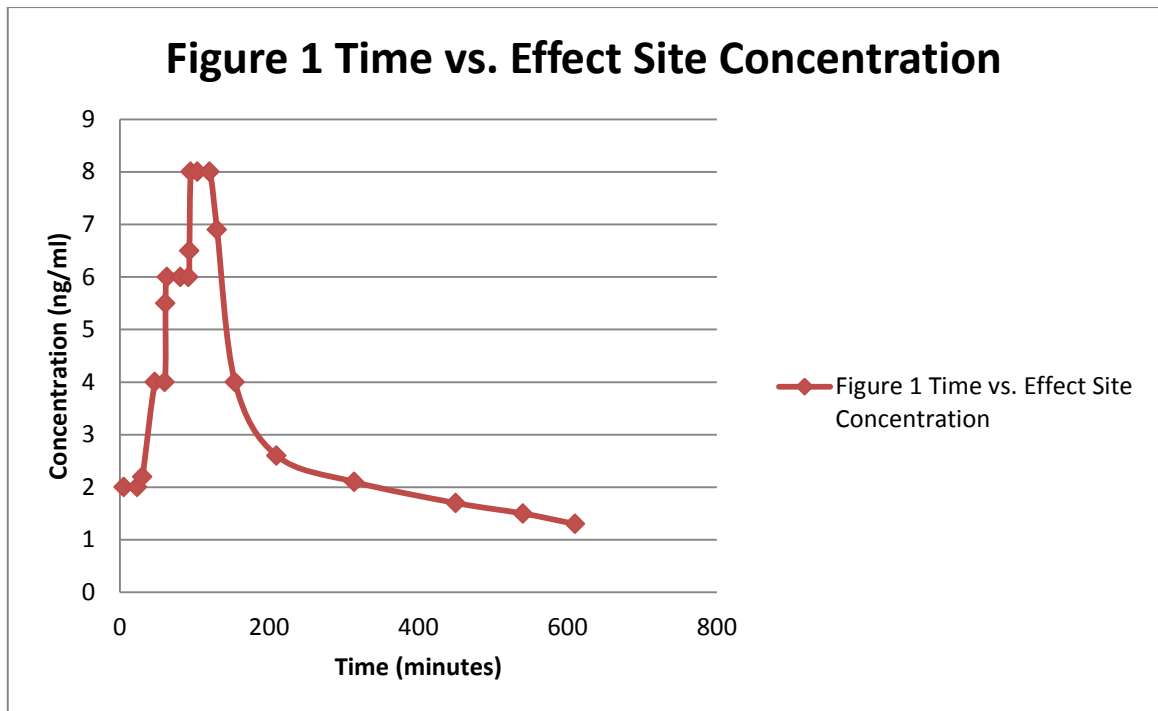
What the STANPUMP does when trying to achieve a specific effect site concentration is to give a bolus dose for a few seconds. After a few minutes of not delivering any drug, an infusion will be started in an increasing and then decreasing manner to maintain the concentration at the effect site. For the purpose of the study we will maintain a specific effect site concentration for about 25 minutes in order for us to conduct a series of tests as mentioned in the protocol. Our repeated use of the STANPUMP together with the Harvard Pump without involvement of human subjects has produced convincing results with regards to its reliability and safety.

As an added safety measure, we will record down manually the readings on the syringe every 10 minutes to ensure that a safe and reasonable amount of fentanyl is delivered to the patient via the STANPUMP.

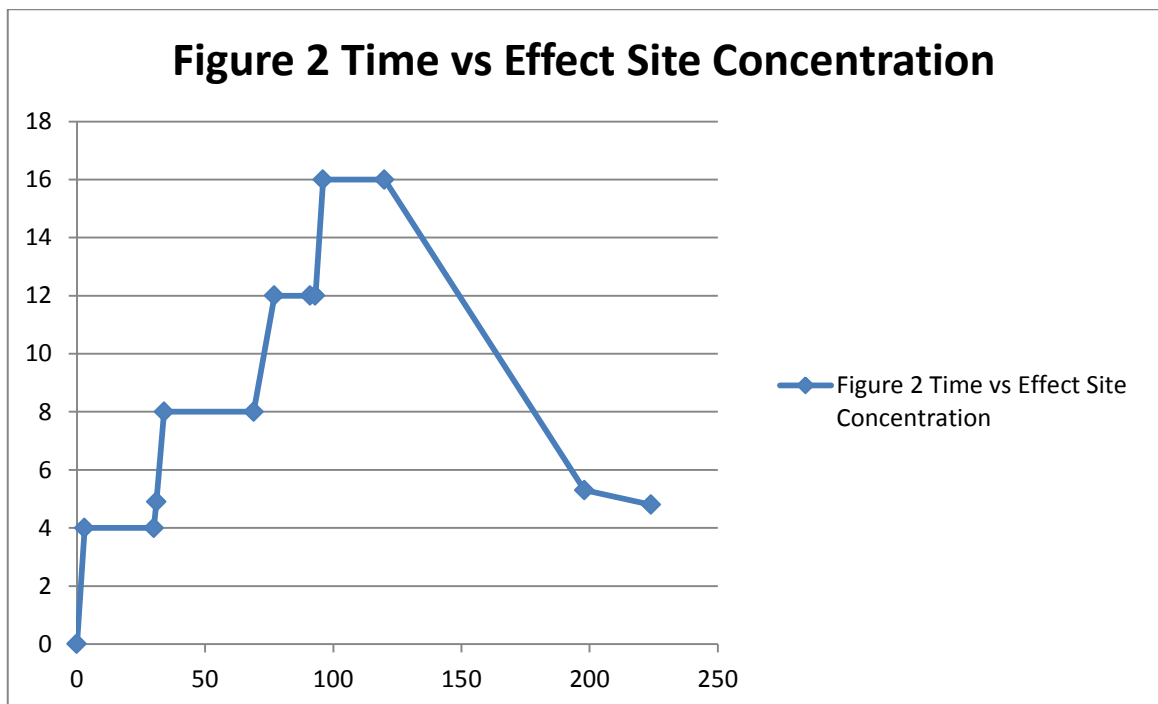
6.5.2 Fentanyl doses delivered by the STANPUMP

The pharmacokinetic parameters for fentanyl which we will be using will be the ones described by Shafer (117). Even though there is no clinically significant correlation between weight and opioid requirement (166) the weight and height of simulated patients are provided to aid conceptualization. We have ran the STANPUMP without a real patient and have discovered the following:

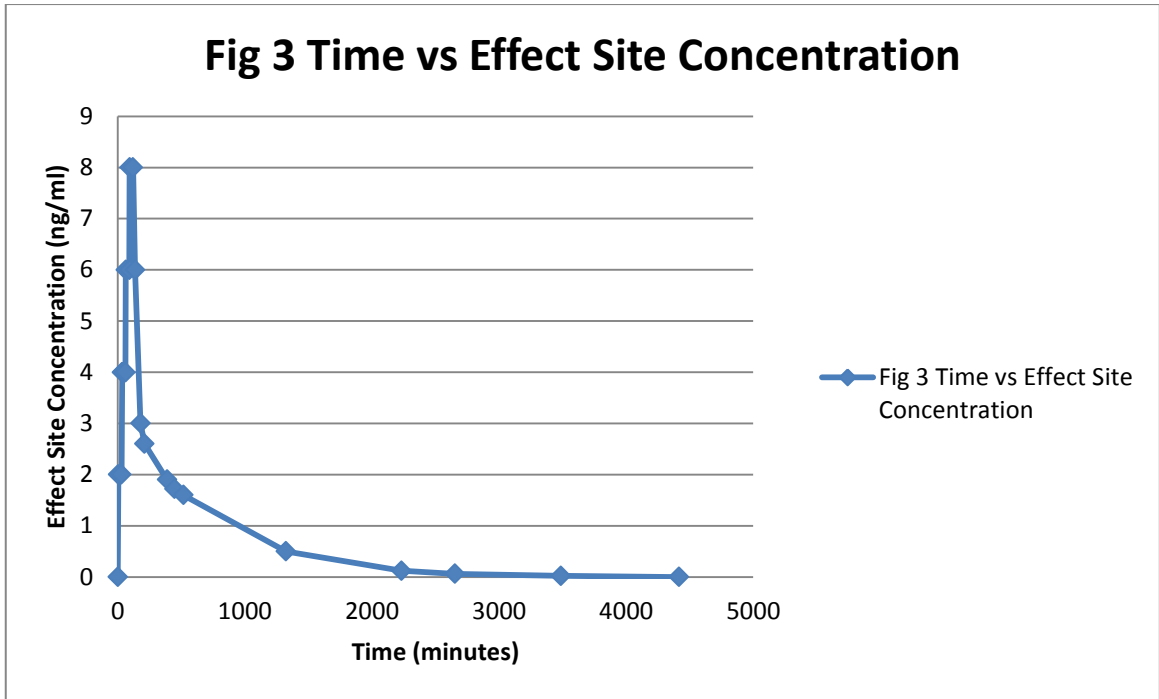
- For a 34 year old female who weighs 60 kg with a height of 175 cm, the total fentanyl delivered by the STANPUMP in achieving the 2, 4, 6 and 8 ng/ml effect site concentration was 1.3 mg or about 26 ml. As every millilitre of fentanyl injection contains 50 µg of fentanyl, the calculations given by STANPUMP was accurate. The highest infusion pump rate was 917.3 ml/hour or 12.7 µg/kg/min. Figure 1 demonstrates the changes in the effect site concentration of fentanyl with time for this subject.



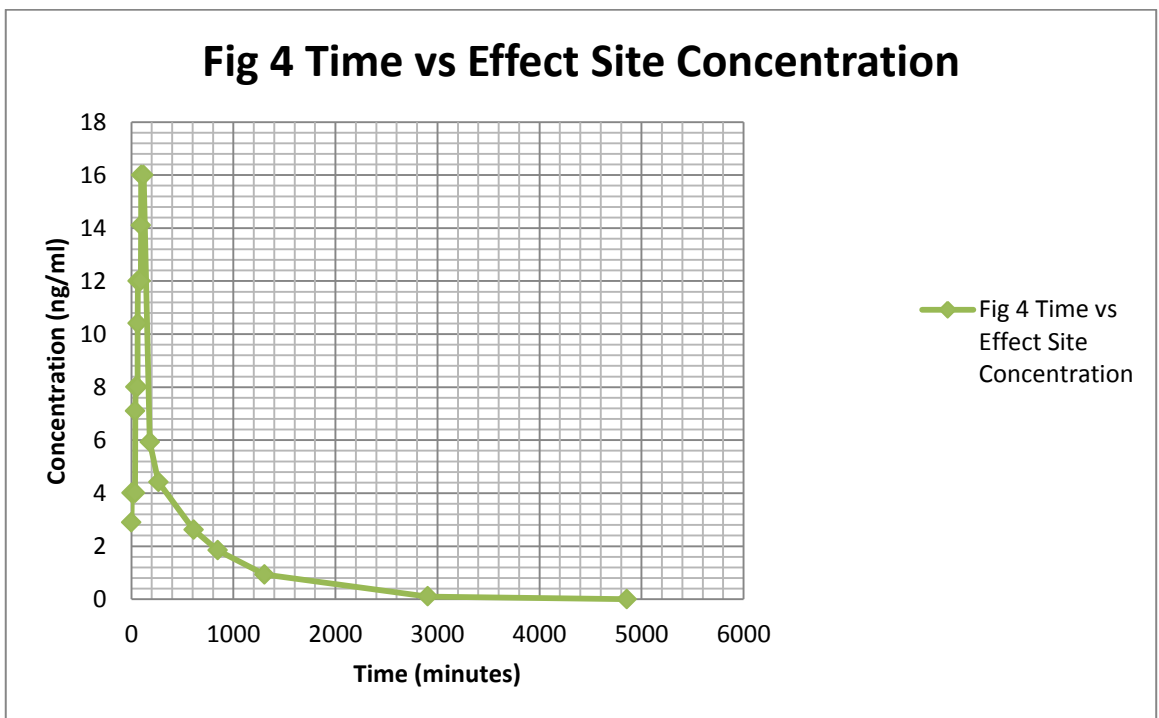
- For the same patient, when targeting 4, 8, 12 and 16 ng/ml at the effect site, the total fentanyl delivered by the STANPUMP in achieving the targets was 2.5 mg or about 50.7 ml. The highest infusion pump rate was 1838.35 ml/hour or 25.5 $\mu\text{g}/\text{kg}/\text{min}$. Figure 2 demonstrates the changes in the effect site concentration with time.



- For a 20 year old man with the same weight and height, the total fentanyl delivered by the STANPUMP in achieving the 2, 4, 6 and 8 ng/ml effect site concentration was 1.3mg or about 26 ml. The highest infusion pump rate was 917 ml/hour or 12.7 $\mu\text{g}/\text{kg}/\text{min}$. Figure 3 demonstrates the changes in the effect site concentration with time for this subject.

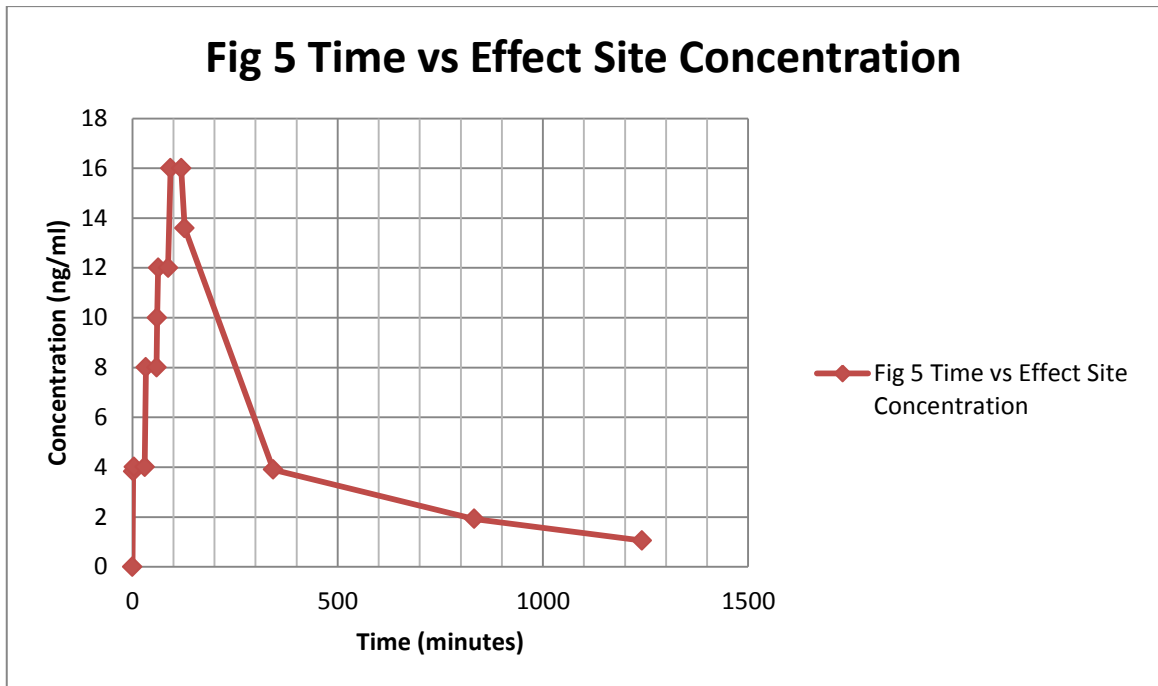


- When targeting 4, 8, 12 and 16 ng/ml at the effect site in the same 20 year old, the total fentanyl delivered by the STANPUMP in achieving the targets was 2.5 mg or about 51 ml. The highest infusion pump rate was 1836 ml/hour or 25.5 $\mu\text{g}/\text{kg}/\text{min}$. Figure 4 demonstrates the changes in the effect site concentration with time.

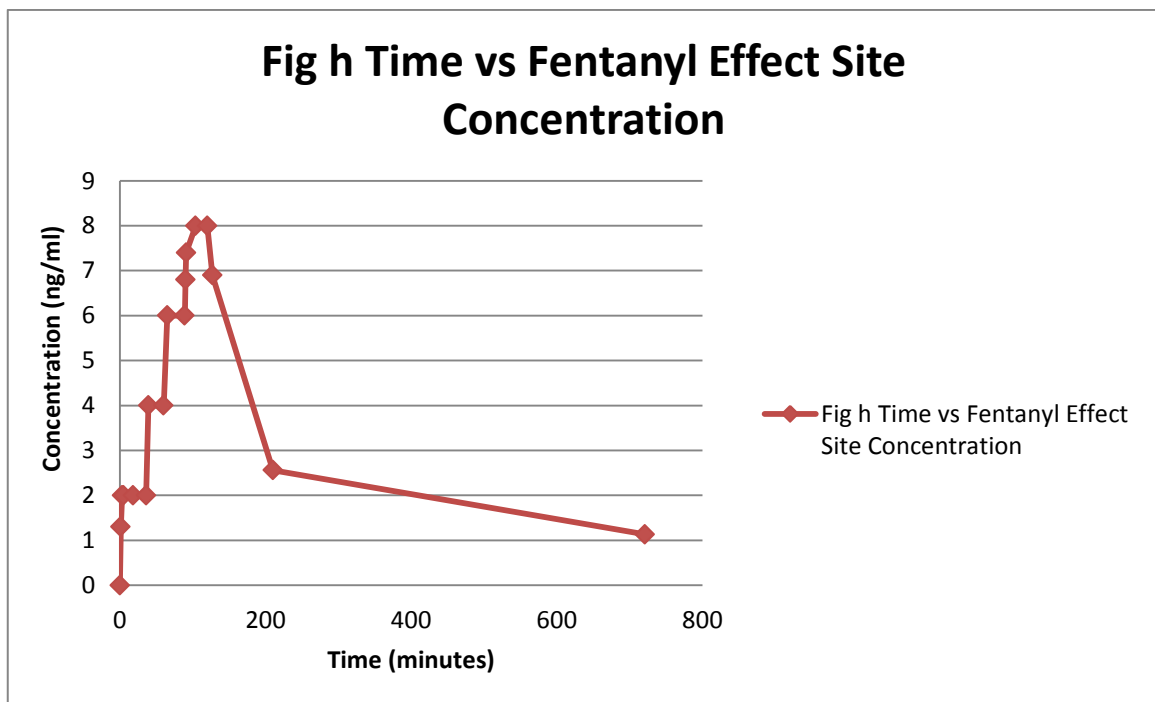


- For a 34 year old male subject who weighs 60 kg and is 175 cm tall, when targeting 4, 8, 12 and 16 ng/ml at the effect site, the total fentanyl delivered by the STANPUMP in achieving the targets was

2.6 mg or about 52.1 ml. The highest infusion pump rate was 1836ml/hour or 25.5 $\mu\text{g}/\text{kg}/\text{min}$. Figure 5 demonstrates the changes in the effect site concentration with time.

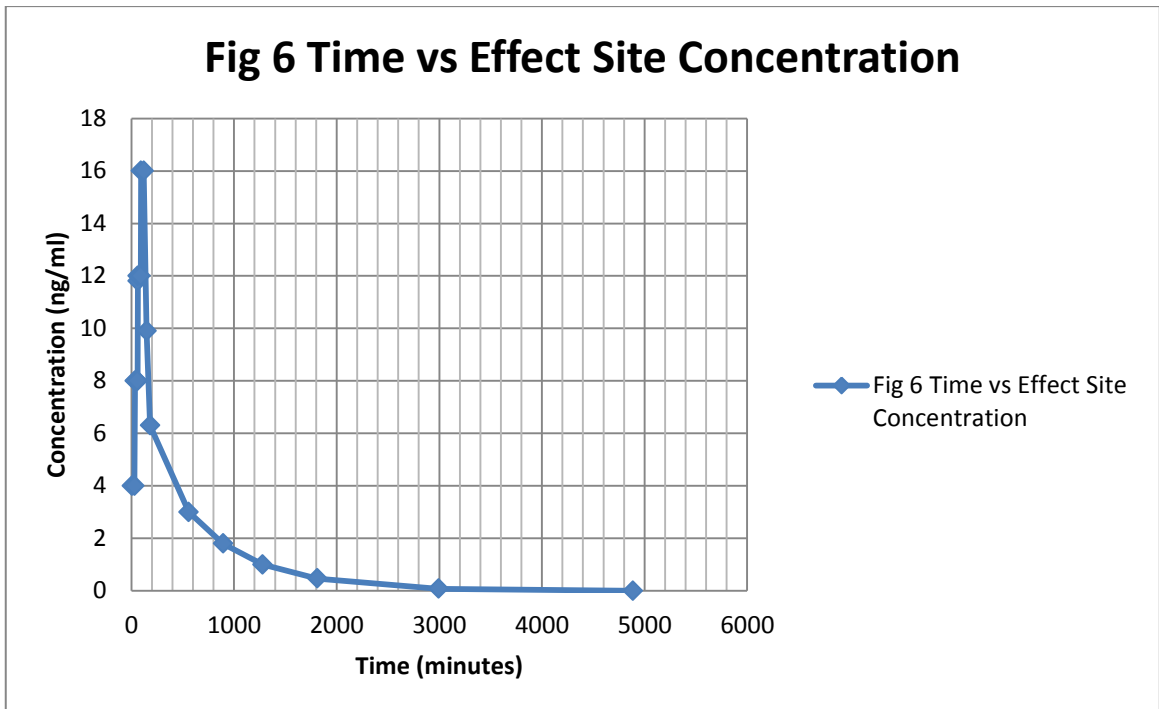


- For a 50 year old male subject who weighs 120 kg and is 175 cm tall, when targeting 2, 4, 6 and 8 ng/ml at the effect site, the total fentanyl delivered by the STANPUMP in achieving the targets was 1.3 mg or about 25 ml. The highest infusion pump rate was 919 ml/hour or 6.3 $\mu\text{g}/\text{kg}/\text{min}$. Figure h demonstrates the changes in the effect site concentration with time.

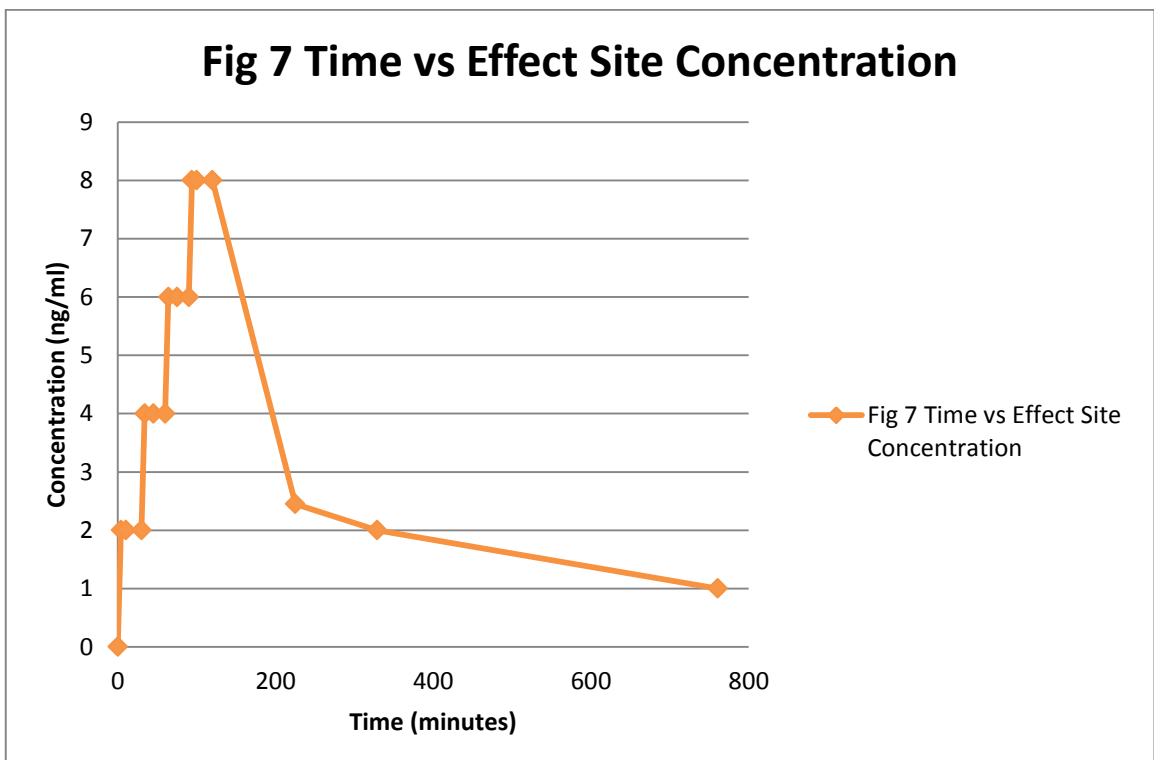


- For a 50 year old male subject who weighs 120 kg and is 175 cm tall, when targeting 4, 8, 12 and 16 ng/ml at the effect site, the total fentanyl delivered by the STANPUMP in achieving the targets was

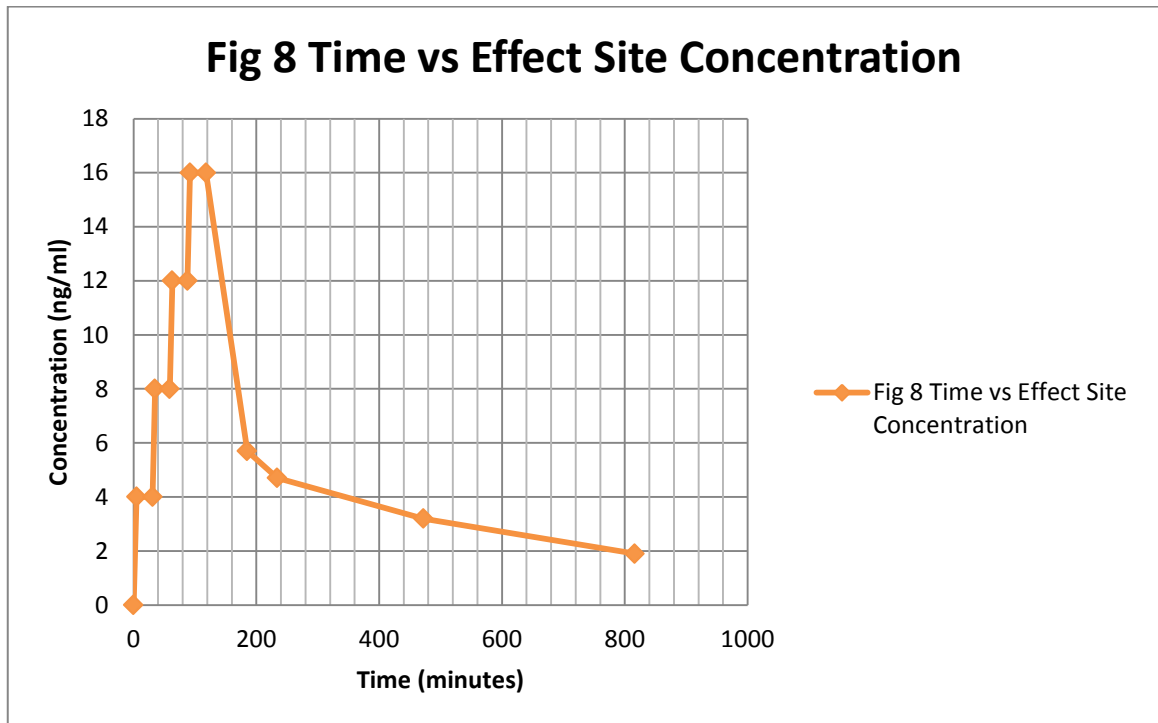
2.7 mg or about 54 ml. The highest infusion pump rate was 1838 ml/hour or 12.7 $\mu\text{g}/\text{kg}/\text{min}$. Figure 6 demonstrates the changes in the effect site concentration with time.



- For a 70 year old man with the same weight and height, the total fentanyl delivered by the STANPUMP in achieving the 2, 4, 6 and 8 ng/ml effect site concentration was 0.9 mg or about 19 ml. The highest infusion pump rate was 917.33 ml/hour or 12.7 $\mu\text{g}/\text{kg}/\text{min}$. Figure 7 demonstrates the changes in the effect site concentration with time for this subject.



- For the same patient, when targeting 4, 8, 12 and 16 ng/ml at the effect site, the total fentanyl delivered by the STANPUMP in achieving the targets was 2.6 mg or about 51.9 ml. The highest infusion pump rate was 1837 ml/hour or 25.5 $\mu\text{g}/\text{kg}/\text{min}$. Figure 8 demonstrates the changes in the effect site concentration with time.



Previously, Davis et al published in 2003 a case report regarding an opioid-tolerant patient who came in for a repeat tricuspid valve replacement (165). She was given 11 mg of fentanyl in 80 minutes. The patient showed no evidence of sedation and had a respiratory rate of 18-20 breaths/minute. Only after 24 mg of fentanyl given did the patient become unresponsive with mild rigidity in the upper extremities. Using STANPUMP, simulations of the fentanyl effect site concentration at the time of unresponsiveness was predicted to be 293 ng/ml. To provide effective analgesia during the operation and yet minimize the potential for respiratory depression, an effect site concentration 25% of that associated with unconsciousness was selected. The doses selected were able to provide safe doses of analgesia during and after the heart surgery. She was easily awakened one hour after arrival in the ICU postoperatively. The patient reported being satisfied with her quality of analgesia and denied any recall or pain associated with the operative procedure. She also commented that her experience during this perioperative course was markedly improved compared with prior surgeries. The highest total dose we are planning to give to a patient in this study is about 3 mg of fentanyl in 120 minutes which is less than one-third of the dose which showed no sedative or respiratory depression given to the opioid-tolerant patient by Davis et al.

In the opioid-naive patients, analgesic requirements of patients vary over a sixfold range for fentanyl (186). From clinical experience, the variability is higher in the opioid-tolerant. Due to this high variability we are targeting relatively low effect site concentrations of 2, 4, 6 and 8 ng/ml in the first visit.

Respiratory depression is the most important and well-known side effect of opioids (187). According to Peng et al, there is a direct concentration-effect relation between fentanyl plasma concentration (C_p) and analgesia and respiratory depression. Previously, data collected by Gourlay et al supported the concept that a relationship exists between blood fentanyl concentration and analgesic effect within each patient (188). In volunteers and patients, the range of fentanyl C_p providing analgesia without clinically significant respiratory depression is 0.6-2 ng/ml (186). Existing data for fentanyl suggest that the minimum effective plasma concentration providing analgesia is approximately 25-30% of that concentration associated with significant respiratory depression (165). Data from a 2005 study in chronic opioid-consuming patients have pointed out that effect site concentration to produce analgesia will mostly be in the range of 3-10 ng/ml (99). Based on the study we anticipate that the effect site concentrations we are targeting will be able to provide analgesia for the study population.

From the known pharmacokinetic parameters of fentanyl and based on our simulations, the concentrations at the plasma and effect site will be level in less than 5 minutes. This happens much quicker when the infusion stops and it will take less than a minute to happen. Based on this information there is little difference between the plasma and effect site concentration when it comes to the decline of fentanyl effects.

6.5.3 Discharge of patients

As for sending patients home, we plan to send them home after a 75% reduction in their highest effect site concentration. According to our simulations, this will usually take about 3 hours after stopping the infusion. However, to be extra cautious we will keep the patients for another 6 hours. This might be longer if clinically warranted. This is again driven by the data for fentanyl suggesting that the minimum effective plasma concentration providing analgesia is approximately 25%-30% of that concentration associated with significant respiratory depression.

6.6 Relationship between plasma and effect site concentration of fentanyl

Plot of plasma (C_p) and effect site (C_e) concentrations of fentanyl from the start of the STANPUMP infusion until the end of the infusion for a 40 year old female with a height of 1.77 metres and weighs 108 kilograms.

